CARACTERIZACIÓN DEL EFECTO ANTICANCEROSO E IDENTIFICACIÓN DE DIANAS MOLECULARES DE PRINCIPIOS ACTIVOS PROCEDENTES DE *Serratia marcescens*

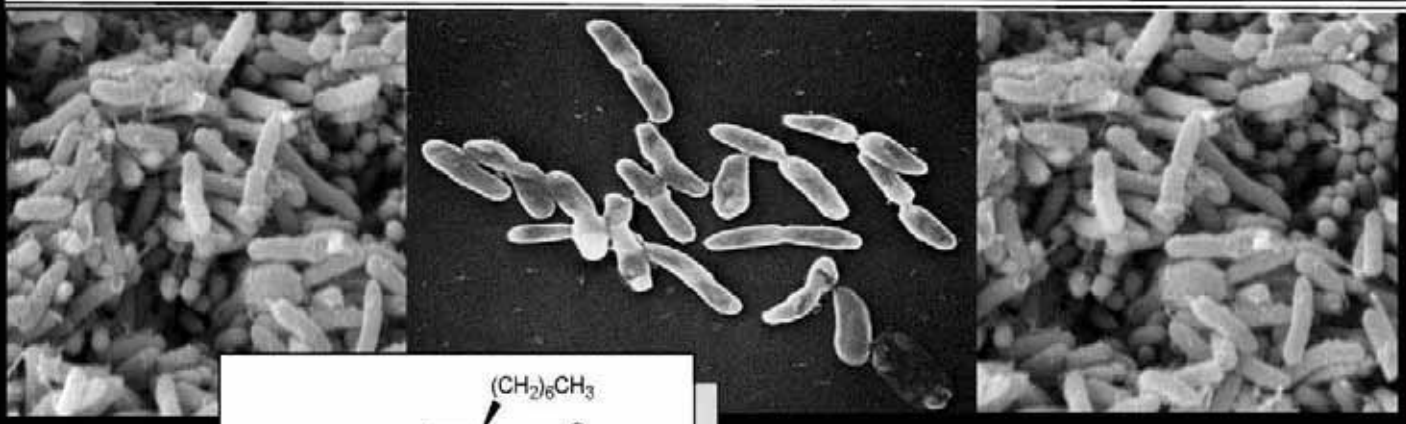

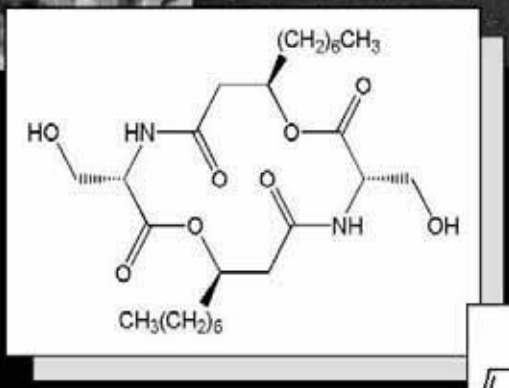

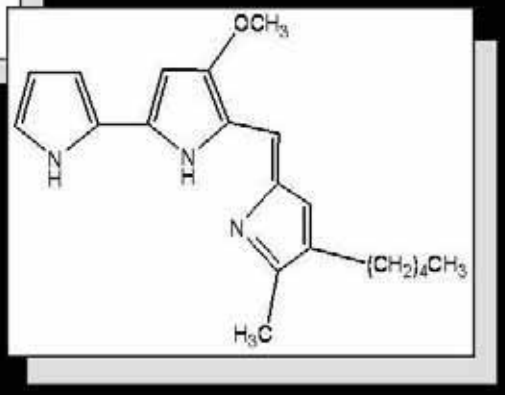

TESIS DOCTORAL

VANESSA SOTO CERRATO

2007

Facultat de Medicina

Departament de Patologia i Terapèutica Experimental

Programa de Doctorat: Biologia i Patologia Cel·lulars

Bienni 2002-2004

"CARACTERIZACIÓN DEL EFECTO ANTICANCEROSO E IDENTIFICACIÓN DE DIANAS MOLECULARES DE PRINCIPIOS ACTIVOS PROCEDENTES DE *Serratia marcescens*"

Memoria presentada por Vanessa Soto Cerrato para optar al grado de Doctor por la Universidad de Barcelona

Dr. Ricardo E. Pérez Tomás
Director

Vanessa Soto Cerrato
Doctoranda

2007

VI. RESULTADOS

1. CARACTERIZACIÓN DEL EFECTO ANTICANCEROSO DEL CICLODEPSIPÉPTIDO SERRATAMOLIDE (AT514)

Capítulo 1.1. Estudio del efecto citotóxico y citostático *in vitro* del agente anticanceroso AT514 en células de cáncer de mama.

("Soto-Cerrato V, Montaner B, Martinell M, Vilaseca M, Giralt E, Pérez-Tomás R. Cell cycle arrest and proapoptotic effects of the anticancer cyclodepsipeptide serratamolide (AT514) are independent of p53 status in breast cancer cells. Biochem Pharmacol 2005;71(1-2):32-41").

Durante la búsqueda de nuevas sustancias anticancerosas de origen natural identificamos una molécula conocida como serratamolide (AT514), la cual fue purificada de la cepa bacteriana *Serratia marcescens* 2170. Nos propusimos como objetivos analizar en detalle los efectos que pudiera tener AT514 *in vitro* sobre la viabilidad y la proliferación celular de varias líneas celulares de cáncer de mama y cáncer de ovario. Observamos una disminución en la viabilidad celular mediante el ensayo del MTT, más o menos marcada dependiendo del tipo celular, y con unos valores de concentración inhibitoria del 50% de la población celular que iban de 5,6 a 11,5 μM. Al ser analizado por citometría de flujo, observamos que en la línea celular MCF-7 dicha disminución era debida a un bloqueo del ciclo celular en la fase G_0/G_1, aunque a tiempos más largos se observaba muerte por apoptosis, mostrada por la activación de caspasas. En cambio, las células MDA-MB-231 directamente sufrían apoptosis tras el tratamiento con AT514, identificado por la presencia de cuerpos apoptóticos, la rotura del ADN por los espacios internucleosomales, modificaciones en miembros de la familia de proteínas de Bcl-2 así como por la activación de las caspasas. Por último, quisimos analizar si la proteína p53, producto del gen supresor de tumores ampliamente mutado en cánceres humanos, era necesaria para el efecto anticanceroso provocado por AT514. Los resultados mostraron que AT514 ejercía sus efectos tanto en líneas celulares con p53 funcional como mutada. Por todo ello, podemos concluir que AT514 puede producir tanto parada del ciclo celular en G_0/G_1 como muerte por apoptosis dependiendo del tipo celular y el tiempo de exposición a la droga, provocando sus efectos de forma independiente del estado de p53 confiriéndole así ventajas terapéuticas sobre otros quimioterapéuticos usados en la actualidad.

available at www.sciencedirect.com

SCIENCE DIRECT

journal homepage: www.elsevier.com/locate/biochempharm

Cell cycle arrest and proapoptotic effects of the anticancer cyclodepsipeptide serratamolide (AT514) are independent of p53 status in breast cancer cells☆

Vanessa Soto-Cerrato[a], *Beatriz Montaner*[a], *Marc Martinell*[b], *Marta Vilaseca*[c], *Ernest Giralt*[b], *Ricardo Pérez-Tomás*[a,*]

[a] *Department of Pathology and Experimental Therapeutics, Cancer Cell Biology Research Group, Universitat de Barcelona, Pavelló Central, 5a planta, LR 5101 C/Feixa Llarga s/n, E 08907 L'Hospitalet, Barcelona, Spain*

[b] *Departament de Química Orgánica, Universitat de Barcelona, Barcelona, Spain*

[c] *Laboratori d'Espectrometria de Masses, Universitat de Barcelona, Barcelona, Spain*

ARTICLE INFO

Article history:
Received 1 July 2005
Accepted 7 October 2005

Keywords:
Depsipeptide
Cell cycle arrest
Apoptosis
Caspases
p53

Abbreviations:
AT514, serratamolide
HPLC, high performance liquid chromatography
KF, Kahalalide F
MALDI, matrix-assisted laser desorption/ionization
MPLC, medium pressure liquid chromatography
MTT, 3-(4,5-dimethylthiazol-2-yl)-2,5-diphenyltetrazoliumbromide
NMR, nuclear magnetic resonance
RT-PCR, real-time quantitative polymerase chain reaction
TOF, time of flight

ABSTRACT

In a search for new anticancer agents, we have identified serratamolide (AT514), a cyclodepsipeptide from *Serratia marcescens* 2170 that induces cell cycle arrest and apoptosis in various cancer cell lines. A cell viability assay showed that the concentrations that cause 50% inhibition (IC_{50}) in human cancer cell lines range from 5.6 to 11.5 μM depending on the cell line. Flow cytometry analysis revealed that AT514 caused cell cycle arrest in G_0/G_1 or cell death, depending on the cell type and the length of time for which the cells were exposed to the drug. Subsequent studies revealed that AT514-induced cell death is caused by apoptosis, as indicated by caspases activation (8, 9, 2 and 3) and cleavage of poly (ADP-ribose) polymerase (PARP), release of cytochrome *c* and apoptosis inducing factor (AIF) from mitochondria, and the appearance of apoptotic bodies and DNA laddering. Alterations in protein levels of Bcl-2 family members might be involved in the mitochondrial disruption observed. AT514 induced p53 accumulation in wild-type p53 cells but cell death was observed in both deficient and wild-type p53 cells. Our results indicate that AT514 induces cell cycle arrest and apoptosis in breast cancer cells irrespectively of p53 status, suggesting that it might represent a potential new chemotherapeutic agent.

☆ AT514: under patent PCT WO2004/031130 A1.

* *Corresponding author*. Tel.: +34 93 4024288; fax: +34 93 4029082.
E-mail address: rperez@ub.edu (R. Pérez-Tomás).

0006-2952/$ – see front matter © 2005 Elsevier Inc. All rights reserved.
doi:10.1016/j.bcp.2005.10.020

1. Introduction

Depsipeptides are bio-oligomers composed of hydroxy and amino acids linked by amide and ester bonds. Many depsipeptides show very promising biological activities, including anticancer, antibacterial, antiviral, antifungal and anti-inflammatory properties [1]. In particular, cyclodepsipeptides (cyclic depsipeptides), such as Didemnin (A–E), Kahalalide F (KF), and FR901228 are currently under active anticancer research specifically focused on identifying their mechanism of action [2–4].

Apoptosis is a tightly regulated form of cell death in which cells actively participate in their own destruction. Drug-induced apoptosis is mainly initiated by either the activation of cell surface receptors or by directly targeting mitochondria [5]. Bcl-2 family members are responsible for integrating the apoptotic stimulus at the mitochondrial level and are involved in this cascade by either promoting (Bax, Bid) or preventing (Bcl-2, Bcl-X_L) mitochondria-dependent apoptosis [6]. This process is accompanied by the activation of aspartate-specific proteases called caspases [7]. In the receptor pathway, the initiator caspase 8 is activated, whilst in the mitochondrial pathway, cytochrome c is released into the cytoplasm and in turn caspase 9 is activated by forming a complex with Apaf-1. The tumor suppressor protein p53 or caspase 2 have been reported to activate the second pathway in response to DNA damage. Both pathways ultimately activate the effector caspases 3 or 7, which cleaves a wide range of substrates, leading to the morphological and biochemical changes that are the hallmarks of apoptosis [8]. Cells undergoing apoptosis shrink and lose their normal intercellular contacts and subsequently exhibit cytoplasmic and chromatin condensation and internucleosomal cleavage of DNA. In the final stages, cells become fragmented into small apoptotic bodies, which are then eliminated by phagocytosis.

Malfunctions of apoptosis can have health implications, as in the case of cancer. Resistance acquired by tumor cells after conventional chemotherapy is a major problem in cancer treatment. Thus, there is a need to develop new anticancer agents and therapeutic regimens for successful treatment. Consequently, the fact that apoptosis is a precisely regulated process that is frequently altered in tumor cells makes it a desirable target for the induction of cell death in cancer cells [9]. Indeed, it has already been described that most anti-tumoral agents kill tumor cells by activating apoptosis [10].

In our laboratory, during a search for new potential anticancer agents, we observed the presence of serratamolide (AT514) in cultures of the bacterial strain *Serratia marcescens* 2170 in the stationary growth phase. AT514 is a hydrophobic cyclic depsipeptide and is the main component of cell-wall lipids. It confers to bacteria wetting and spreading properties, reducing the surface tension of water and therefore increasing its adhesion to solid surfaces [11], and contributes to the virulence of *S. marcescens* [12]. In this view, given the lack of studies related to cancer therapy using AT514, we have investigated whether this molecule has cytotoxic activity against human cancer cells. We show that AT514 arrests the cell cycle at G_0/G_1 and induces apoptosis in human breast cancer cell lines. Furthermore, we describe the molecular apoptotic events triggered by this new symmetrical cyclic depsipeptide as well as its independence of the tumor suppressor protein p53. Taken together, the results of this study indicate that AT514 might represent a potential new anticancer agent since it effectively induces apoptosis in breast cancer cells irrespectively of p53 status.

2. Materials and methods

2.1. Purification and characterization of serratamolide (AT514)

AT514 (serratamolide), cyclo[(3R)-3-hydroxydecanoyl-L-seryl-(3R)-3-hydroxydecanoyl-L-seryl], was extracted by shaking *Serratia marcescens* 2170 cells with a mixture of methanol and 1 N HCl (24:1). After centrifugation (6800 × *g* for 15 min), the solvent of the supernatant was evaporated under vacuum. Atmospheric pressure liquid chromatography of the extract was performed on silica gels (pore size 60 Å) with chloroform:methanol (6:4) as solvents. The eluted fractions containing the two major products (further characterized as prodigiosin and serratamolide) were pooled and the chloroform/methanol extract was vacuum evaporated, redissolved in H_2O and lyophilized. The sample mixture was analyzed by electrospray ionization/mass spectrometry (ESI-MS) using a VG-Quattro® triple quadrupole mass spectrometer (Micromass, VG-Biotech, UK) and by matrix-assisted laser desorption (MALDI) using a Voyager delayed extraction (DE) time of flight (TOF) mass spectrometer (PerSeptive Biosystems, Framingham, USA). The product with a molecular weight (*m*/*z* 515) consistent with that expected for serratamolide was isolated from the pigmented mixture by two consecutive medium pressure liquid chromatography (MPLC) steps. MPLC was performed on a system containing a CFG® Prominent/Duramat pump, a variable wavelength LKB® Bromma 2158 UVICORD SD detector (206 nm filter), a Gilson FC 205 collector, and a Pharmacia-LKB REC 101 register. In the first step, a Lichroprep C_8 reversed-phase glass column (20 cm × 4 cm) was used with a 0–100% B linear gradient (A: 0.01 M ammonium acetate pH 7.0; B: 100% acetonitrile), 1000 ml total volume at a flow rate 240 ml/h. The eluted fractions were analyzed by HPLC (high performance liquid chromatography) on a Shimadzu LC-6A instrument with a Nucleosil® C_{18} analytical reversed-phase column (25 cm × 0.4 cm) and by MALDI-TOF. Fractions containing serratamolide were pooled, vacuum evaporated, and lyophilized. The second MPLC purification step was performed using a C_{18} reversed-phase glass column (26 cm × 2.5 cm) and a 35–55% B linear gradient (A: H_2O 0.045% trifluoroacetic acid; B: CH_3CN 0.036% trifluoroacetic acid), 800 ml total volume at a flow rate 120 ml/h. The eluted fractions were analyzed by MALDI-TOF and HPLC. A pure product (96% purity determined by HPLC) was obtained after pooling, vacuum evaporation, and lyophilization of the desired fractions. Quantification was performed by amino acid analysis on a Beckman 6300 automatic analyzer with a sulfonated-polystyrene column (25 cm × 0.4 cm, Beckman 7300/6300). The product was characterized by mass spectrometry and nuclear magnetic resonance (NMR) spectroscopy (Fig. 1A). Exact mass determination was performed by chemical ionization (CI) with methane in an AutoSpec

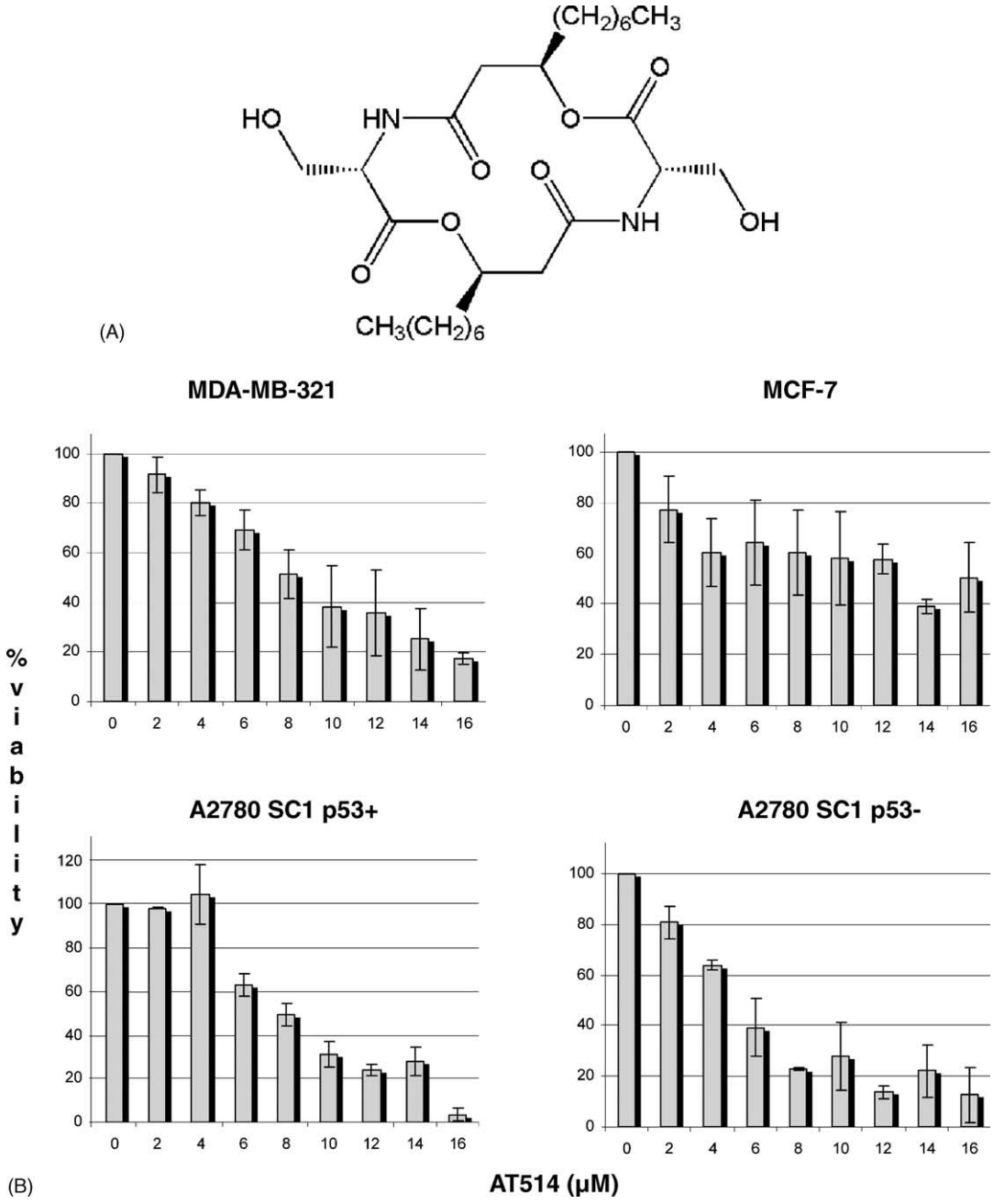

Fig. 1 – (A) Structure of serratamolide (AT514). (B) AT514 effect on cell viability after 24 h of drug exposure (from 2 to 16 μM) was analyzed by MTT assay.

magnetic sector mass spectrometer N/S-X134: *m/z* 515.335020 $(M + H)^+$. ESI-MS: *m/z* 515.2 $(M + H)^+$. MALDI-TOF: *m/z* 515.8 $(M + H)^+$, 537.8 $(M + Na)^+$, 553.8 $(M + K)^+$. ($C_{26}H_{46}N_2O_8$) requires 514.3254 (MWmonoisotopic) ^1H NMR (CD_3OH, 500 MHz, p.p.m.): 7.88 (d, 1NH), 5.28 (m, 1H), 4.47 (m, 1H), 4.07 (dd, 1H), 3.82 (dd, 1H), 2.67 (dd, 1H), 2.33 (dd, 1H), 1.66 (m, 2H), 1.3 (m, 10H), 0.89 (t, 3H). The results were in agreement with previous NMR studies [13].

2.2. *Cell lines and culture conditions*

Breast cancer cell lines MDA-MB-231 (cells with mutated p53) and MCF-7 (cells with wild-type p53) were purchased from ATCC (Rockville, MD) and cultured in DMEM:HAM F12 (1:1). The ovarian carcinoma clones from the A2780 cells were a generous gift from Dr. Karran (Cancer Research, London, UK) and were previously described [14]; the A2780 SC1 p53+ retain an intact p53 response while in the A2780 SC1 p53−, the p53 response was inhibited by introducing a dominant negative mutant p53 (p53val135). Both were cultured in DMEM. Media were purchased from Biological Industries (Beit Haemek, Israel) and supplemented with 10% heat-inactivated fetal bovine serum, 100 U/ml penicillin, 100 μg/ml streptomycin, 2 mM L-glutamine, and 50 mg/ml gentamycin (GIBCO BRL, Paisley, UK). Cells were grown in a humidified atmosphere of air containing 5% CO_2 at 37 °C.

2.3. Cell viability assay

Cell viability was determined using the MTT assay [15]. Cells were plated in triplicate wells (2×10^4 cells/well) in 100 μl of growth medium in 96-well plates and treated with increasing concentrations of AT514 (2–16 μM) or drug diluent (DMSO). Adherent cell lines were plated 24 h before treatment at a concentration of 1×10^4 cells/well. After 24 h incubation with AT514, 10 μM of MTT (Sigma Chemical Co., St. Louis, MO) was added to each well for an additional 4 h. The blue MTT formazan precipitate was then dissolved in 100 μl of *iso*-propanol: 1N HCl (24:1). The absorbance at 570 nm was measured on a multiwell plate reader. Cell viability was expressed as a percentage of control and IC_{50} represents the concentration of drug causing 50% inhibition of the increase in absorbance compared with control cells. Data are shown as the mean value ± S.E.M. of three independent experiments.

2.4. Assessment of cell cycle arrest

Cells (1×10^6) were treated with 4, 8, and 12 μM AT514 for 24 h and fixed in 70% ethanol at −20 °C overnight. Then, they were washed in PBS and incubated with 25 μl of 1 mg/ml propidium iodide (Bender MedSystems Inc., Burlingame, CA) and 5 μl of 10 mg/ml DNase free RNase (Boehringer Mannheim, Mannheim, Germany) for 30 min at 37 °C in the dark. Fluorescence was measured by flow cytometry on a FACSCalibur fitted with a 488 nm Ar laser, and data were analyzed using CellQuest Pro software (Becton Dickinson, San Jose, CA) and ModFit LT cell cycle analysis software (Verity software, Topsham, ME).

2.5. Analysis of internucleosomal DNA fragmentation

Cells (5×10^5 cells/ml) were treated with AT514 for 24 h. After washing the cells in PBS, they were lysed in 400 μl of lysis buffer (10 mM Tris–HCl pH 7.4, 1 mM EDTA, 0.2% Triton X-100) for 15 min at 4 °C. Then, cell lysates were centrifuged at 14 000 × *g* for 15 min to separate low molecular weight DNA from intact chromatin, and supernatants were treated with 0.2 mg/ml proteinase K (Sigma Chemical Co.) in a buffer containing 150 mM NaCl, 10 mM Tris–HCl pH 8.0, 40 mM EDTA, and 1% SDS, for 4 h at 37 °C. After two extractions with phenol:chloroform:*iso*-amylalcohol (25:24:1), the aqueous supernatants were precipitated with two volumes of ethanol plus 140 mM NaCl at −20 °C overnight, and recovered by centrifugation at 14 000 × *g* for 15 min at 4 °C. The DNA pellets were then washed twice in cold 70% ethanol, air-dried, and resuspended in 15 μl of TE (10 mM Tris–HCl pH 8.0, 1 mM EDTA) and treated with DNase free RNase for 1 h at 37 °C. Finally, DNA was analyzed by electrophoresis on a 1.2% agarose gel.

2.6. Hoechst staining

Cell morphology was evaluated by fluorescence microscopy following Hoechst 33342 DNA staining (Sigma Chemical Co.). Cells (2×10^5 cells/ml) were incubated in the absence (control cells) or presence of AT514 for 24 h. They were then washed in PBS and resuspended in PBS containing 2 μg/ml Hoechst 33342 and incubated for 30 min at 37 °C in the dark. After incubation, cells were washed in PBS and examined with a Carl Zeiss Jena microscope and photographed with an Olympus DP11 digital camera.

2.7. Western blot

Cells (2×10^5 cells/ml) were exposed to 4, 8, or 12 μM AT514 for 24 h. They were then washed in PBS prior to addition of a lysis buffer (85 mM Tris–HCl pH 6.8, 2% SDS, 1 μg/ml aprotinin, 1 μg/ml leupeptin, and 0.1 mM phenylmethanesulfonyl fluoride). For the measurement of cytochrome *c* and AIF release from mitochondria, lysis buffer (250 mM sucrose, 1 mM EDTA, 0.05% digitonin, 25 mM Tris pH 6.8, 1 mM dithiothreitol, 1 μg/ml leupeptin, 1 μg/ml pepstatin, 1 μg/ml aprotinin, 100 μM phenylmethanesulfonyl fluoride) was used for 30 s, lysates centrifuged at 12000 × *g* at 4°C for 3 min and the supernatants (cytosolic extract) were separated from pellets (fraction that contains mitochondria). In all cases, 50 μg protein extracts were separated by SDS-PAGE on a 15% polyacrylamide gel and transferred to Immobilon-P membranes (Millipore, Bedford, MA). Blots were blocked in 5% dry milk diluted in TBS-T (50 mM Tris–HCl pH 7.5, 150 mM NaCl, 0.1% Tween-20) for 1 h and then incubated overnight with primary antibodies. Antibodies were obtained from the following sources: cleaved caspase 3 (Cat#9661), cleaved caspase 7 (Cat#9491) and anti-Bid (Cat#2002 and 2003) were from Cell Signaling Technology (New England Biolabs, Hertfordshire, UK); anti-PARP (Cat#sc-7150), anti-procaspase 2 (Cat#sc-625), and anti-Bcl-X_L (Cat#sc-634) were from Santa Cruz biotechnologies (Santa Cruz, CA); anti-caspase 8 (Cat#559932) and anti-cytochrome *c* (Cat#556433) were from Pharmingen (BD biosciences, Palo Alto, CA); anti-Bcl-2 (Cat#OP60T) and anti-AIF (Cat#PC536) were from Oncogene Research Products (Boston MA); anti-p53 (Cat#MS-186-P1) was from Neomarkers (Fremont, CA); anti-Bax (Cat#AHP471) was from Serotec Ltd. (Oxford, UK); and anti-caspase 9 (Cat#05-572) was from Upstate (Lake Placid, NY). All primary antibodies were used according to the manufacturer's instructions. Antibody binding was detected using a secondary antibody conjugated to horseradish peroxidase (Biorad, Hertfordshire, UK) and the ECL detection kit (Amersham, Buckinghamshire, UK). Protein bands were quantified with the image analysis software program Phoretix 1-D advanced. Results were presented as normalized fold changes respect control. Normalization has been done using vinculin as a loading control.

2.8. Gene expression analysis

Cells (2×10^5 per ml) were treated with 0 (control), 4, 8, or 12 μM AT514. Total RNA extraction was performed using Ultraspec™ RNA (Biotex Laboratories, Texas, USA). The RNA pellet was washed twice in 75% ethanol, dissolved in H_2O, and cDNA synthesis was performed using random hexamers and MuLV reverse transcriptase according to the manufacturer's instructions (Applied Biosystems, Warrington, UK). The final concentration of cDNA was 1 μg in 50 μl. Each cDNA sample was analyzed for expression of Bcl-2 family members using the fluorescent TaqMan 5′ nuclease assay. Oligonucleotide primers Bcl-2 (Cat#Hs00153350_m1), Bax (Cat#Hs00180269_m1), Bcl-X_L (Cat#Hs00236329_m1), and GAPDH (Cat#Hs99999905_m1), and

probes were initially designed and synthesized as Assay-on-Demand Gene Expression Products (Applied Biosystems). The 5′ nuclease assay PCRs were performed using the ABI PRISM 7700 Sequence Detection System for thermal cycling and real-time fluorescence measurements (RT-PCR) (Applied Biosystems). Each 50 μl reaction consisted of 1X TaqMan Universal PCR MasterMix (PE Biosystems), 1X Assay-on-Demand mix containing forward primer, reverse primer, and TaqMan quantification probe (Applied Biosystems), and 100 ng cDNA template. Reaction conditions comprised an initial step of 92 °C for 10 min, then 40 cycles of 95 °C for 15 s and 60 °C for 1 min. The levels of Bcl-2 family members obtained were normalized by mRNA expression of GAPDH. The relative mRNA expression was then presented in relation to the control. Data were analyzed using "Sequence Detector Software" (SDS Version 1.9, Applied Biosystems).

3. Results

3.1. *Effect of AT514 on cell viability*

The antiproliferative effect of AT514 was determined using the MTT reduction assay in breast and ovarian tumor cell lines. Fig. 1B shows the AT514 effects on cell viability after 24 h of drug exposure ranging from 0 to 16 μM AT514. Cell viability significantly decreased in all cancer cells. In the breast cancer cell lines MCF-7 and MDA-MB-231, IC_{50} values were 11.5 ± 0.9 and 9.6 ± 1.1 μM, respectively. However, whereas MDA-MB-231 cell viability decreased more than 80%, MCF-7 viability only decreased 50% at the same doses, which could be explained not by cell death but by a cell cycle blockade. Both ovarian cancer cell lines, A2780 SC1 p53+ (p53 wild type) and A2780 SC1 p53− (in which the p53 response was inhibited by introducing a dominant negative mutant p53 (p53val135)) showed a marked decrease in cell viability. Their IC_{50} values were 8.8 ± 0.6 and 5.6 ± 0.4 μM, respectively, being wild-type p53 cells less sensitive than their mutated p53 counterparts.

3.2. *AT514 induces cell cycle arrest and delayed cell death in MCF-7*

Since AT514 induced a decrease in MCF-7 cell viability of approximately 50%, we next investigated whether this effect could be due to cell cycle arrest. Thus, we analyzed cell cycle progression by flow cytometry using propidium iodide in MCF-7 cells exposed to doses of AT514 ranging from 4 to 12 μM for 24 h. Fig. 2A shows a concentration-dependent accumulation

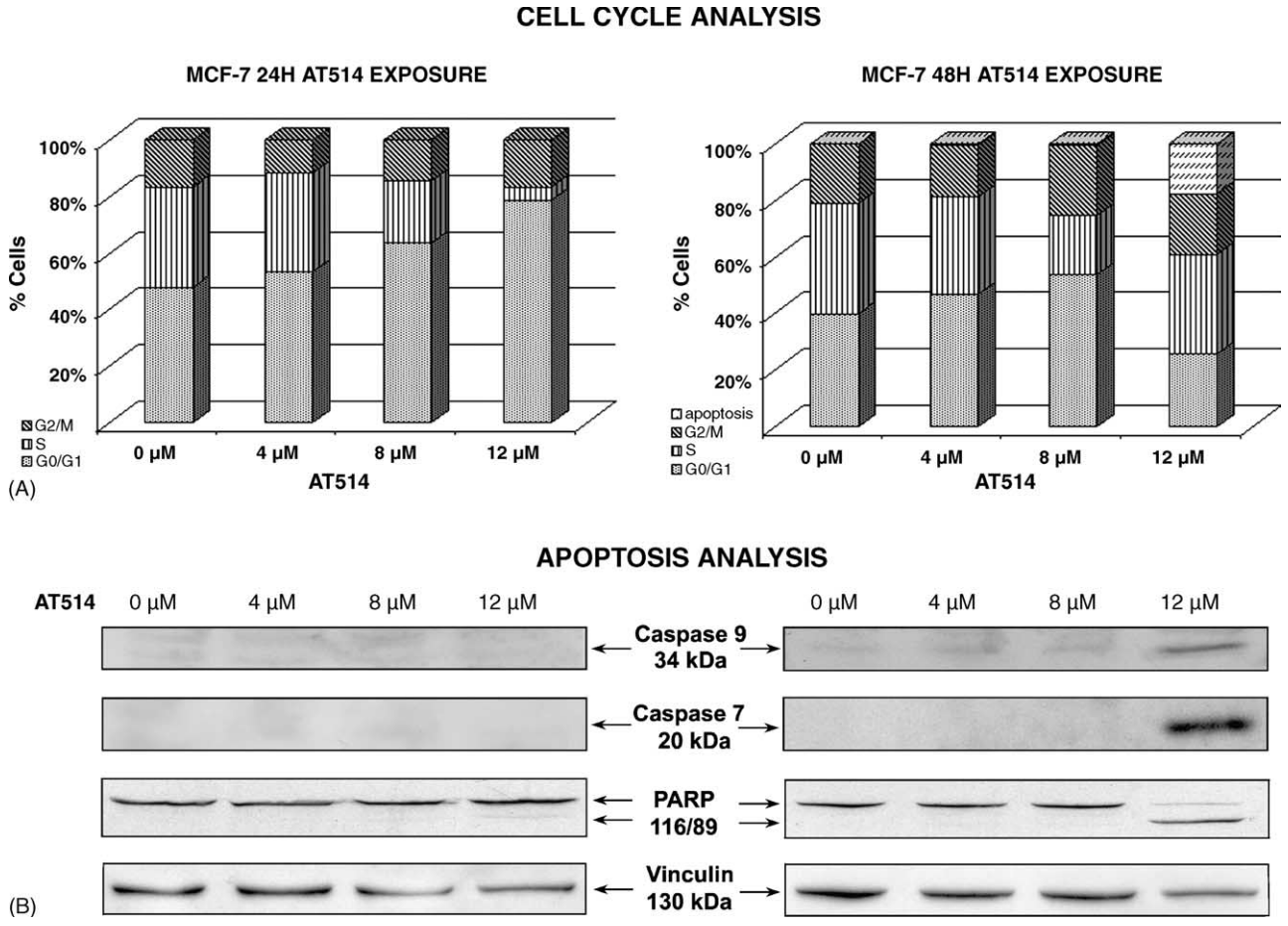

Fig. 2 – Cytostatic and cytotoxic effects of AT514. (A) AT514 induces cell cycle arrest or apoptosis depending on length of exposure in MCF-7 cells. Cells were treated with 4, 8, and 12 μM AT514 for either 24 or 48 h, incubated with propidium iodide, and analyzed by flow cytometry. (B) Apoptosis induction was analyzed by the appearance of caspase activation and PARP cleavage by western blot. Vinculin is shown as a loading control.

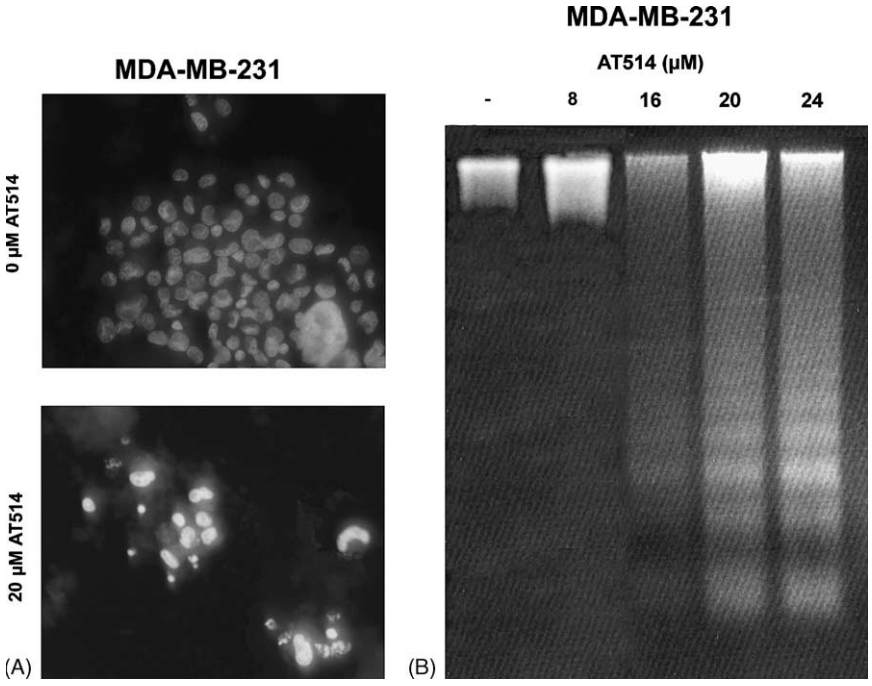

Fig. 3 – AT514 induces apoptosis in MDA-MB-231 cells after 24 h AT514 treatment. (A) Hoechst staining was used to assess nuclear condensation. (B) DNA fragmentation was visualized by analysis of DNA laddering.

of cells in G_0/G_1 (from 47.5 ± 5.5% to 78.9 ± 1.0%), whilst the percentage of cells in S phase decreased sharply. Nevertheless, after incubation with AT514 for 48 h, induction of cell death by apoptosis was detected (21 ± 4.6% at 12 μM AT514), as shown by the appearance of active caspases 9 (34 kDa) and 7 (20 kDa) and the cleaved form of the caspase substrate PARP (89 kDa) (Fig. 2B). Hence, in this cell type, the effect of AT514 depends upon the length of exposure, blocking cell cycle progression after short periods and inducing cell death after longer exposure.

3.3. AT514-induced apoptosis

In the other cell types, AT514 caused more than 80% decrease in cell viability hence it was due to cell death. In order to confirm that AT514-induced cell death was caused by apoptosis, classic morphological features of apoptosis were analyzed. The presence of nuclei condensation and apoptotic bodies was assessed using nuclear staining with Hoechst 33342 and an analysis of DNA laddering was performed to reveal internucleosomal DNA fragmentation. Both of these markers of apoptosis were present in AT514-treated MDA-MB-231 cells (Fig. 3A and B, respectively).

3.4. Caspase activation by AT514

To evaluate whether apoptosis induced by AT514 was accompanied by caspase activation, MDA-MB-231 cells were exposed to 4, 8, and 12 μM AT514 for 24 h (IC_{25}, IC_{50}, and IC_{75}, respectively) and immunoblotting studies were then performed (Fig. 4). Levels of the inactive form (procaspase) of the initiators caspase 8 and caspase 2 (55/50 and 48 kDa, respectively) decreased significantly at the higher dose, while cleaved caspase 8 (40/36 kDa) gradually appeared. Levels of the active forms of the mitochondrial pathway initiator caspase 9 (34 kDa) and the effector caspase 3 (20 kDa) also increased. This effect was especially marked at higher doses. Examination of the caspase substrate PARP (116 kDa) after AT514

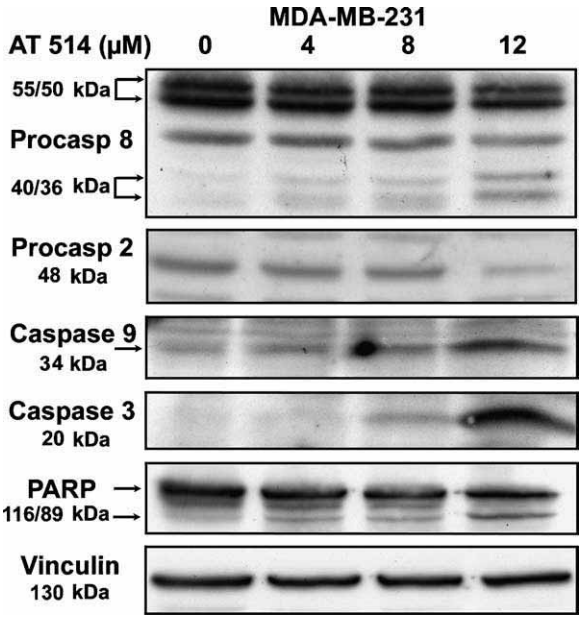

Fig. 4 – Caspase activation and PARP degradation in MDA-MB-231 cells after AT514 exposure. Cells were incubated with 4, 8, and 12 μM AT514 for 24 h and immunoblotting was performed for the inactive proform of caspases 8 and 2, the active form of caspases 9 and 3, and the caspase substrate PARP. Vinculin is shown as a loading control.

treatment showed accumulation of the cleaved product of this protein (89 kDa). Thus, caspases are clearly activated after exposure to AT514, especially at higher doses.

3.5. *Mitochondrial membrane disruption after AT514 treatment*

To further study key events in the apoptotic process, the release of apoptogenic factors, such as cytochrome c and AIF, from mitochondria into the cytosol was analyzed by Western blot (Fig. 5A). Cytochrome c and AIF protein levels were determined in the cytosolic fraction of samples treated with AT514. AIF levels showed a dose-dependent increase in response from 4 to 12 μM AT514. In contrast, cytochrome c was only detectable at higher doses of AT514, suggesting that apoptosis induced at lower doses might be mediated by AIF rather than cytochrome c.

As disruption of mitochondria is mediated by Bcl-2 family members during mitochondria-mediated apoptosis, their protein and mRNA levels were analyzed by immunoblotting and RT-PCR respectively. Levels of the antiapoptotic proteins Bcl-2 and Bcl-X_L decreased in a concentration dependent manner, while significant levels of the proapoptotic Bax protein appeared at 12 μM (Fig. 5B). The proapoptotic form of Bid (t-Bid 17 kDa) increased as disappearance of the large form (22 kDa) was observed, especially at the higher dose. mRNA levels were not significantly affected by AT514 treatment (Fig. 5C), suggesting that Bcl-2 family members are modified at the translational rather than at the transcriptional level. These AT514-induced changes may be involved in the release of apoptogenic factors from the mitochondria.

3.6. *AT514 effects are independent of p53 status*

p53 is a protein able to induce either cell cycle arrest or apoptosis in response to stress-induced DNA damage. AT514 effects were observed in both, wild type p53 (p53+) and mutant p53 (p53−) cell lines, indicating that AT514 acts independently of p53 status. However, in order to study whether exists a role for p53 on the different effects triggered by AT514, MDA-MB-231 cells (cell line with p53−), which underwent apoptosis, and MCF-7 cells (cell line with p53+), which underwent cell cycle arrest, were further analyzed. As expected, the levels of p53 protein were not increased by AT514 treatment in MDA-MB-231 (Fig. 6A). However, p53 levels were also unaltered in MCF-7 cells at the time and doses that AT514 induced cell cycle arrest, but not when it provoked apoptosis (at 12 μM for 48 h) (Fig. 6B). Moreover, p53 response to AT514 treatment was studied in wild type p53 (p53+) A2780 SC1 cells and mutated p53 (p53−) A2780 SC1 cells. IC_{25}, IC_{50} and IC_{75} concentrations were used and p53 accumulation was observed only in A2780 SC1 p53+ cells (almost two folds increase) but not in the p53 deficient clone, as expected (Fig. 6C). Although both of them underwent cell death at the higher dose (Fig. 1B), A2780 SC1 p53+ cells were less sensitive to the drug than their mutated p53 counterparts. The accumulation of functional p53 protein might be the reason why A2780 p53+ detect and react to drug damage in a different way than A2780 p53− cells. Altogether, p53 appears not to be necessary in the cellular response to AT514 exposure although its accumulation is induced by the

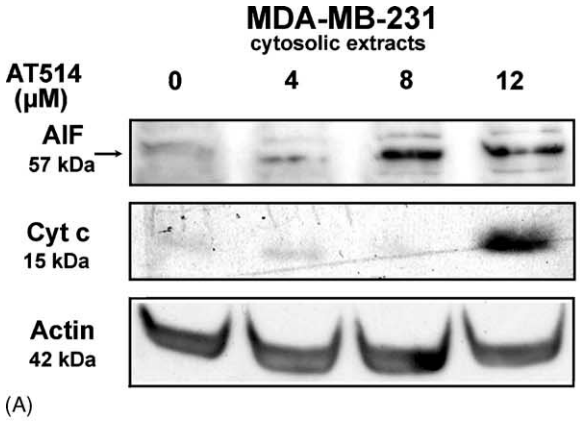

(A)

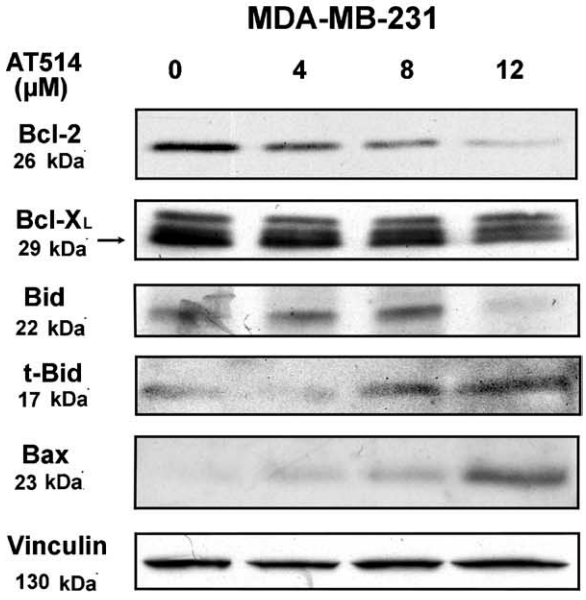

(B)

GENE EXPRESSION MODIFICATIONS BY RT-PCR

gene	μM AT514	Normalized change folds	S.E.M.
bcl-2	0	1	0,48
	4	1,06	0,38
	8	0,92	0,37
	12	0,95	0,47
bax	0	1	0,42
	4	1,05	0,39
	8	0,70	0,31
	12	0,61	0,24
bcl-X_L	0	1	0,58
	4	0,96	0,46
	8	0,79	0,21
	12	0,81	0,39

(C)

Fig. 5 – Involvement of Bcl-2 family members in MDA-MB-231 mitochondrial disruption. Cells were treated with 4, 8, and 12 μM AT514 for 24 h. (A) Cytosolic extracts were isolated in order to analyze the appearance of mitochondrial apoptogenic factors such as AIF and cytochrome c by Western blotting. Actin is shown as a loading control. (B) Total extracts were used to analyze Bcl-2, Bcl-X_L, Bid, t-Bid and Bax protein levels after AT514 treatment. Vinculin is shown as a loading control. (C) Bcl-2, Bax, and Bcl-X_L gene expression changes analyzed by real-time PCR. The values obtained were normalized using mRNA expression of GAPDH.

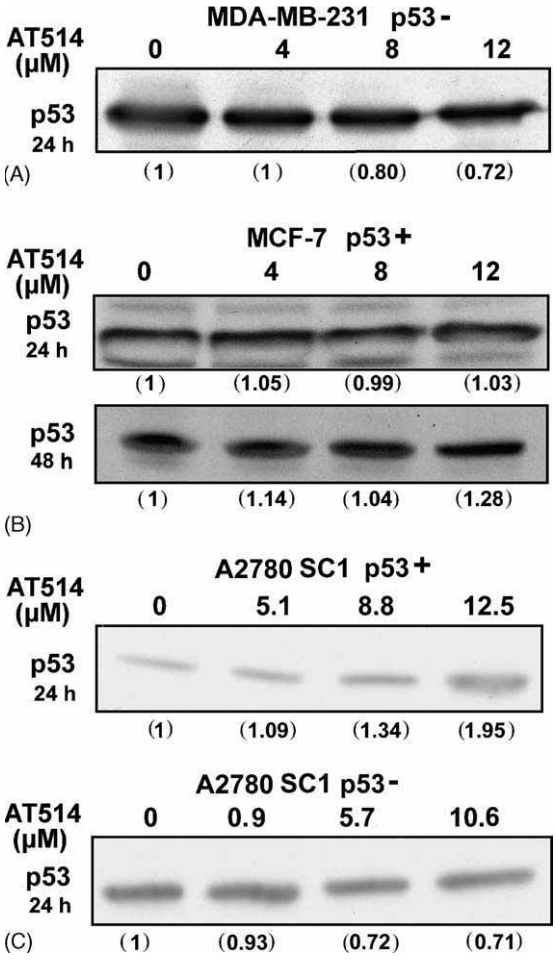

Fig. 6 – Analysis of p53 protein accumulation after AT514 treatment. Cells, p53 mutated (p53−) or p53 wild type (p53+), were incubated with increasing concentrations of AT514 for 24 h or 48 h and p53 protein levels were analyzed by Western blot. Quantification of the bands was performed and normalized change folds respect non-treated cells are shown in brackets. Normalization has been done using vinculin as a loading control.

AT514 cytotoxic effect in those cells with functional p53, but not when AT514 induces cell cycle arrest.

4. Discussion

The induction of apoptosis, or programmed cell death, is thought to be one of the most interesting therapeutic strategies with which to specifically target cancer cells [16]. The limited efficacy of current conventional chemotherapy treatments necessitates the development of new therapeutic agents. The emergence of new anticancer compounds from natural sources with advantageous properties and novel mechanisms of action is continuous, and offers a promising future in the battle against cancer. The cyclodepsipeptides are a broad family of natural products characterized by the presence of at least one ester linkage [1]. Many depsipeptides exhibit a diverse range of biological activities, including antibiotic, antifungal, immunosuppressant or anti-inflammatory and antitumoral effects. Many of the cyclodepsipeptides discovered so far have remarkable in vitro and in vivo anticancer properties against a wide range of tumoral cell lines and some of them are currently undergoing clinical trials in humans [17]. In this study, we have provided the first evidence that the ciclodepsipeptide serratamolide (AT514) induces cell cycle arrest and cell death in various cancer cells. Cell death mediated by AT514 caused caspase activation and induced morphological features typical of apoptosis. This is consistent with the characterization of other depsipeptides, such as FR901228 and IC101, as proapoptotic agents [18–20], a feature shared by almost all currently used chemotherapeutic agents.

Most cytotoxic agents, irrespective of their primary targets, are now thought to kill cells predominantly through the induction of mitochondrial modifications [8,21]. Thus, members of the Bcl-2 family constitute a group of proteins that play important roles in apoptosis regulation [21]. Among the various Bcl-2 homologs identified to date, Bcl-2, Bcl-X_L, and Bax represent the best-characterized members [22]. In this study, we found that AT514 induces downregulation of Bcl-2 and Bcl-X_L and upregulation of Bax in breast cancer cells. Interestingly, real-time PCR analysis showed that AT-514 treatment did not result in changes in Bcl-2, Bcl-X_L, or Bax mRNA levels, suggesting that the effects of the ciclodepsipeptide on this protein family occur at a translational level. Bcl-X_L expression has very recently been proposed to serve as a molecular target for anticancer therapy. Thus, new anticancer agents currently under investigation such as 2,3-DCPE [23] are able to downregulate Bcl-X_L expression, resulting in mitochondria-mediated cell death. Similarly, in the present study we are also able to observe a Bcl-X_L decrease after AT514 treatment, which might be involved in the mitochondrial disruption. However, downregulation of Bcl-X_L is not observed in apoptosis induced by 5-fluouracil or paclitaxel, suggesting that apoptosis itself does not result in downregulation of Bcl-X_L [23]. Another proapoptotic member of the Bcl-2 family is t-Bid. As we have shown here, after treatment with 12 μM AT514 the inactive precursor bid (~22 kDa) almost disappears and the truncated form (t-Bid) is generated. This process may mediate Bax translocation to the mitochondria and cause the release of cytochrome *c* [24]. Similar to our results, t-Bid and the initiator caspase 2, which can activate apoptosis by the intrinsic pathway in response to DNA damage, do actively participate in the apoptotic process induced by other depsipeptides such as FR901228 [25].

AIF, a resident protein of the inter-mitochondrial space, has been implicated as a crucial early effector of apoptosis in a caspase-independent process [26]. We show how AIF was released from mitochondria in a dose-dependent manner starting at 4 μM (IC_{25}) AT514, while cytochrome *c* and caspase activation were not detected until 12 μM (IC_{75}) AT514. Moreover, flow cytometry studies at 4 μM showed no cell cycle arrest (data not shown). These observations suggest that in the presence of low AT514 concentrations AIF released from the mitochondria triggers caspase-independent apoptosis. When we increased the amount of the drug, cytochrome *c* appeared in the cytosol and triggered caspase-dependent apoptosis.

This is corroborated by the caspase activation that was observed at higher doses. The ability to induce cell death both by the caspase-independent and the caspase-dependent apoptotic pathway is a property shared with other proapoptotic drugs such as irufolven, a chemotherapeutic agent currently under clinical trials [27].

In reference to the mechanism of action of the depsipeptides, it has been observed that KF induces cell death preferentially via oncosis in tumor cells. KF-treated cells underwent a series of profound alterations including severe cytoplasmic swelling and vacuolization, dilatation and vesiculization of the endoplasmic reticulum, mitochondrial damage, and plasma membrane rupture, however, the nuclear envelope was preserved and no DNA degradation was detected [28]. Another depsipeptide, FR901228, is a histone deacetylase inhibitor and has been shown to acetylate histones H3 and H4 concomitant with induction of cell death by apoptosis in many solid tumors, T-cell leukemias and multiple myeloma [29]. FR901228 is currently under clinical trials for B-cell chronic lymphocytic leukemia treatment. Increased acetylation of H3 and H4 histones upon treatment with AT514 was not observed (data not shown) indicating that both depsipeptides activate different mechanisms for the induction of apoptosis. In a recent paper, we have been able to demonstrate that AT514 interferes with the Akt/NF-kB survival pathway, inducing Akt dephosphorylation at Ser 473 and decreasing NF-kB activity by dramatically reducing the levels of the p65 NF-kB component in B-cell chronic lymphocytic leukemia [30]. However, the molecular target of AT514 remains to be elucidated.

Differences were observed in the response of the two breast cancer cells, MCF-7 and MDA-MB-231, to AT514 treatment. MCF-7 cells underwent cell cycle arrest in G_0/G_1 while MDA-MB-231 died by apoptosis at the same doses and times. The latter is a cell line that has mutated p53, a protein able to induce cell cycle arrest or apoptosis depending upon the level of DNA damage. This suggested the possibility that accumulation of active p53 could be mediating the cell cycle blockade induced by AT514. However, since no p53 accumulation was observed in MCF-7 cells at the cytostatic conditions, this possibility could be ruled out. Moreover, at cytotoxic conditions, we could observe a p53 increase in both wild-type p53 cells used (MCF-7 and A2780 SC1 p53+). Therefore, cellular responses to AT514 exposure are triggered either in wild-type or mutated p53 cells. This suggests that p53 is not essential for the execution of these processes but p53 is implicated when it has a functional status. This property is a potential therapeutic advantage, as p53 is mutated in the vast majority of human tumors [31]. Another possible explanation for the delayed apoptosis in MCF-7 cells might be due to caspase 3 deficiency caused by a gene mutation [32]. This caspase is the most important effector caspase described, and deficiency in its gene product could confer a slight resistance to the drug. This phenomenon has already been characterized in these cells in response to other proapoptotic factors such as UV light [33]. The induction of apoptosis by AT514 even in the absence of caspase 3 is another promising therapeutic property.

Taken together, these results suggest that relatively low concentrations of AT514 induce cell cycle arrest and apoptosis in cancer cells irrespectively of p53 status raising the possibility of its use as a new anticancer drug.

Acknowledgements

This work was supported by grant 301888 from CIDEM (Generalitat de Catalunya) and Fundació Bosch i Gimpera. The authors would like to thank Dr. Karran (Cancer Research, London, UK) for the generous gift of the A2780 SC1 cell lines and E. Llagostera, W. Castillo-Ávila and Serveis Cientificotècnics (Campus Bellvitge, Universitat de Barcelona) for technical assistance. We also thank Robin Rycroft for linguistic support.

REFERENCES

[1] Ballard CE, Yu H, Wang B. Recent developments in depsipeptide research. Curr Med Chem 2002;9:471–98.
[2] Hochster H, Oratz R, Ettinger D, Borden E. A phase II study of Didemnin B (NSC 325319) in advanced malignant melanoma: an Eastern cooperative oncology group study (PB687). Invest New Drugs 1999;16:259–63.
[3] Brown AP, Morrissey RL, Faircloth GT, Levine BS. Preclinical toxicity studies of Kahalalide F, a new anticancer agent: single and multiple dosing regimens in the rat. Cancer Chemother Pharmacol 2002;50:333–40.
[4] Fecteau KA, Mei J, Wang HC. Differential modulation of signaling pathways and apoptosis of ras-transformed 10T1/2 cells by the depsipeptide FR901228. J Pharmacol Exp Ther 2002;300:890–9.
[5] Green D. Apoptotic pathways: the roads to ruin. Cell 1998;94:695–8.
[6] Cory S, Adams J. The Bcl2 family: regulators of the cellular life-or-death switch. Nat Rev Cancer 2002;2:647–56.
[7] Salvesen G, Dixit V. Caspases: intracellular signaling by proteolysis. Cell 1997;91:443–6.
[8] Kroemer G, Reed J. Mitochondrial control of cell death. Nat Med 2000;6:513–9.
[9] Los M, Burek CJ, Stroh C, Benedyk K, Hug H, Mackiewicz A. Anticancer drugs of tomorrow: apoptotic pathways as targets for drug design. Drug Discov Today 2003;8:67–77.
[10] Fisher D. Apoptosis in cancer therapy: crossing the threshold. Cell 1994;78:539–42.
[11] Matsuyama T, Bhasin A, Harshey R. Mutational analysis of glagellum-independent surface spreading of *Serratia marcescens* 274 on a low-agar medium. J Bacteriol 1995;177:987–91.
[12] Miyazaki Y, Oka S, Hara-Hotta H, Yano I. Stimulation and inhibition of polymorphonuclear leukocytes phagocytosis by lipoamino acids isolated from *Serratia marcescens*. FEMS Immunol Med Microbiol 1993;6:265–72.
[13] Hassal CH, Moschidis MC, Thomas WA. The conformations of serratamolide and related cyclotradepsipeptides in solution. J Chem Soc (B) 1971;1757–61.
[14] Branch P, Masson M, Aquilina G, Bignami M, Karran P. Spontaneous development of drug resistance: mismatch repair and p53 defects in resistance to cisplatin in human tumor cells. Oncogene 2000;28:3138–45.
[15] Mosmann T. Rapid colorimetric assay for cellular growth and survival: application to proliferation and cytotoxicity assays. J Immunol Meth 1983;65:55–63.
[16] Kasibhatla S, Tseng B. Why target apoptosis in cancer treatment? Mol Cancer Ther 2003;2:573–80.

[17] Sarabia F, Chamma S, Ruiz AS, Ortiz LM, Herrera JL. Chemistry and biology of cyclic depsipeptides of medicinal and biological interest. Curr Med Chem 2004;11:1309–32.
[18] Byrd JC, Shinn C, Ravi R, Willis CR, Waselenko JK, Flinn IW, et al. Depsipeptide (FR901228): a novel therapeutic agent with selective, in vitro activity against human B-cell chronic lymphocytic leukemia cells. Blood 1999;94:1401–8.
[19] Klisovic D, Katz S, Effron D, Klisovic MI, Wickham J, Parthun MR, et al. Depsipeptide (FR901228) inhibits proliferation and induces apoptosis in primary and metastatic human uveal melanoma cell lines. Ophthalmol Vis Sci 2003;44:2390–8.
[20] Fujiwara H, Yamakuni T, Ueno M, Ishizuka M, Shinkawa T, Isobe T, et al. IC101 induces apoptosis by Akt dephosphorylation via an inhibition of heat shock protein 90-ATP binding activity accompanied by preventing the interaction with Akt in L1210 cells. J Pharmacol Exp Ther 2004;310:1288–95.
[21] Cory S, Adams JM. The Bcl2 family: regulators of the cellular life-or-death switch. Nat Rev Cancer 2002;2:647–56.
[22] Hou QH, Cymbalyuk SC, Hsu M, Hsu YT. Apoptosis modulatory activities of transiently expressed Bcl-2: roles in cytochrome c release and Bax regulation. Apoptosis 2003;8:617–29.
[23] Wu S, Zhu H, Gu J, Zhang L, Teraishi F, Davis JJ, et al. Induction of apoptosis and down-regulation of Bcl-X_L in cancer cells by a novel small molecule, 2[[3-(2,3-dichlorophenoxy)propyl]amino] ethanol. Cancer Res 2004;64:1110–3.
[24] Korsmeyer SJ, Wei MC, Saito M, Weiler S, Oh KJ, Schlesinger PH. Proapoptotic cascade activates BID, which oligomerizes BAK or BAX into pores that result in the release of cytochrome *c*. Cell Death Differ 2000;7:1166–73.
[25] Peart MJ, Tainton KM, Ruefli AA, Dear AE, Sedelies KA, O'Reilly LA, et al. Novel mechanisms of apoptosis induced by histone deacetylase inhibitors. Cancer Res 2003;63:4460–71.
[26] Cregan SP, Dawson VL, Slack RS. Role of AIF in caspase-dependent and caspase-independent cell death. Oncogene 2004;23:2785–96.
[27] Liang H, Salinas RA, Leal BZ, Kosakowska-Cholody T, Michejda CJ, Waters SJ, et al. Caspase-mediated apoptosis and caspase-independent cell death induced by irofulven in prostate cancer cells. Mol Cancer Ther 2004;3:1385–96.
[28] Suarez Y, Gonzalez L, Cuadrado A, Berciano M, Lafarga M, Muñoz A. Kahalalide F, a new marine-derived compound, induces oncosis in human prostate and breast cancer cells. Mol Cancer Ther 2003;2:863–72.
[29] Aron JL, Parthun MR, Marcucci G, Kitada S, Mone AP, Davis ME, et al. Depsipeptide FR901228 induces histone acetylation and inhibition of histone deacetylase in chronic lymphocytic leukemia cells concurrent with activation of caspase-8-mediated apoptosis and down-regulation of c-FLIP protein. Blood 2003;102:652–8.
[30] Escobar-Díaz E, López-Martín EM, Hernández del Cerro M, Puig-Kroger A, Soto-Cerrato V, Montaner B, et al. AT514, a cyclic depsipeptide from *Serratia marcescens*, induces apoptosis of B-chronic lymphocytic leukemia cells: interference with the Akt/NF-kappaB survival pathway. Leukemia 2005;19(4):572–9.
[31] Lowe SW, Ruley HE, Jacks T, Housman DE. p53-dependent apoptosis modulates the cytotoxicity of anticancer agents. Cell 1993;74:957–67.
[32] Janicke RU, Sprengart ML, Wati MR, Porter AG. Caspase-3 is required for DNA fragmentation and morphological changes associated with apoptosis. J Biol Chem 1998;273:9357–60.
[33] Sasai K, Yajima H, Suzuki F. Suppression of postmitochondrial signaling and delayed response to UV-induced nuclear apoptosis in HeLa cells. Jpn J Cancer Res 2002;93:275–83.

APÉNDICE I: Resultados complementarios del Capítulo 1.1. Ampliación del estudio del efecto *in vitro* sobre la viabilidad celular del agente anticanceroso AT514 en otras células humanas cancerosas.

Además de los estudios realizados del efecto de AT514 sobre la viabilidad de diferentes líneas celulares de cáncer de mama y ovario, también se analizó dicho efecto en otras líneas celulares cancerosas y no cancerosas de diferentes orígenes.

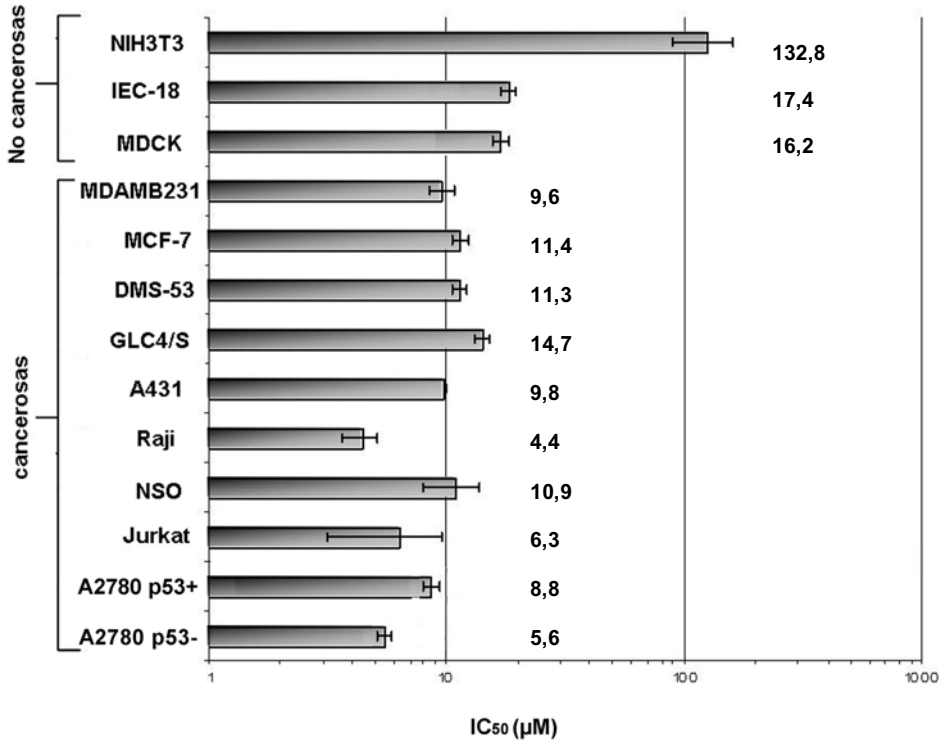

Figura 28. Valores de IC_{50} de diferentes líneas celulares tras el tratamiento con AT514.

El resultado general obtenido tras el análisis de las diferentes líneas celulares se muestra en la figura 28. Los rangos de IC_{50} de las cancerosas van desde 4,4 µM para las células de origen hematopoyético Raji hasta los 14,7 µM que necesita la línea de cáncer de pulmón GLC4/S, siendo ésta la menos sensible al tratamiento con AT514. Por otro lado, los valores de las líneas no cancerosas van de 16,2 µM para las células normales de riñón MDCK, hasta 132,8 para los fibroblastos NIH3T3. El resultado general obtenido tras el análisis de las diferentes líneas celulares permite concluir que las células cancerosas son algo más sensibles a AT514 que las no cancerosas.

Capítulo 1.2. Obtención de modelos de cáncer de mama y estudio de la toxicidad de AT514 *in vivo*.

Una vez comprobada satisfactoriamente la capacidad anticancerosa *in vitro* de AT514, procedimos a desarrollar modelos de cáncer de mama humano y a evaluar la toxicidad de dicha sustancia en ratones, con el fin de poder designar una dosis máxima tolerable y con ella valorar la posible capacidad terapéutica antitumoral y/o antimetastásica de AT514 en tumores humanos.

1.2.1. Obtención de modelos de cáncer de mama

Objetivo

Implantación de líneas tumorales humanas, de forma ectotópica y ortotópica, en ratones atímicos con la consecuente obtención de tumores. Se estudiará su evolución y desarrollo desde su detección, evaluando su tamaño y velocidad de crecimiento para poder diseñar la curva de crecimiento tumoral. Asimismo, valoraremos la vascularización, grado de necrosis del tumor y la posible aparición de metástasis en otros órganos.

Material

Animales: Para la realización de estos estudios se utilizaron ratones atímicos hembra de 4-6 semanas de la cepa Balb/c Nude (Charles River Laboratories España S.A.) que se mantuvieron en cámaras aisladas para evitar su contacto directo con patógenos. Se les proporcionó comida y bebida *ad libitum*, se mantuvieron a una temperatura controlada de 20-22ºC y con ciclos de luz/oscuridad de 12/12h. Fueron estabulados en el animalario de pequeños roedores del Institut de Recerca Oncològica. La experimentación se llevó a cabo en cabinas de flujo laminar vertical, en condiciones específicas libres de patógenos. Todos los procedimientos a los que se sometieron los animales se realizaron de acuerdo con las recomendaciones para el correcto tratamiento y uso de animales de laboratorio, así como los procedimientos de trabajo fueron minuciosamente evaluados por un comité ético especialista en experimentación animal.

Líneas celulares: MDA-MB-231 y MDA-MB-468.

Diseño y metodología

Inducción de tumores mamarios: Las líneas celulares MDA-MB-231 y MDA-MB-468 se mantuvieron en cultivo exponencial *in vitro* sin ningún tipo de antibiótico dos pases antes de la inoculación en los animales. También se comprobó que estaban libres de micoplasmas. Los tumores ectotópicos se indujeron inoculando de forma subcutánea (SC) las células resuspendidas en 200 µl de medio DMEM:HAM. Se procedió elevando la piel de la zona dorsal del animal, se introdujo la aguja y, si ésta se pudo mover hacia los laterales con libertad, se procedió a la introducción de las células. Para la inducción de los tumores ortotópicos se realizaron técnicas quirúrgicas con tal de inocular las células en el órgano del cual procedían, en este caso la mama (IMFP, de intramammary fat pad; almohadilla de grasa mamaria). Previamente se anestesiaron las ratonas por vía intraperitoneal con 0,20-0,25 ml (según sus pesos) de una solución anestésica compuesta por Ketamina (100 mg/kg ratón) y Xilacina (10 mg/kg ratón). Se procedió a desinfectar la región inguinal donde se encontraba la mama con una solución dérmica de povidona yodada (Topionic®) y se realizó una apertura de unos 5 mm para poder visualizar el tejido mamario y poder realizar la punción. Para inocular las células en 200 µl de medio DMEM:HAM dentro de la grasa mamaria se usó una jeringuilla de insulina con aguja de 27G y material de cirugía estéril. La aparición de una burbuja de líquido nos sirvió de control para saber que no se había derramado nada sobre la superficie. Antes y después de inocular las células se limpió con alcohol de 70º la zona del órgano en la que se realizó la punción. Con ello evitamos la diseminación de éstas en otras zonas que no fueran las deseadas, de forma que obtuvimos tumores experimentales bien localizados los cuales podían provocar la posible aparición de metástasis espontáneas. Después de la intervención se suministró el analgésico Buprenorfina (0,05 – 0,1 mg/kg) cada 12 horas. Una vez terminada la intervención para inocular las células, se cerró la incisión utilizando grapas de 9 mm (Becton-Dickinson®) y se volvió a desinfectar el área operada con una solución de povidona yodada (Topionic®), dejando reposar a los animales sobre una gasa estéril y bajo el calor que proporciona una lámpara con bombilla de 100 W a unos 20 cm hasta que se despertaron de la anestesia.

Seguimiento del crecimiento del tumor: Una vez el tumor primario fue externamente palpable, se midió su tamaño cada 2-3 días con un pie de rey para seguir su evolución. Se registró el diámetro longitudinal (l) y el transversal (t) para así calcular el volumen total del tumor mediante la fórmula: $V = (l \times t^2)/2$. Al alcanzar un volumen de 100-500 mm^3, alrededor de 1 x 1 cm, se extirparon (exéresis). Para ello se volvieron a anestesiar los animales y después de desinfectar la zona del tumor con povidona yodada (Topionic®) se

realizó una incisión para extraerlo. Antes de suturar con grapas la piel del animal se realizó una pequeña presión con un hirsuto empapado en alcohol de 70º para evitar el sangrado. Finalmente se mantuvieron bajo la fuente de calor (lámpara con bombilla de 100 W a unos 20 cm) hasta su completa recuperación. Los tumores se lavaron con suero fisiológico y siguieron diferentes protocolos según la finalidad que tuvieran. Con otros se establecieron cultivos primarios con el fin de obtener líneas celulares más tumorigénicas que pudieran generar tumores en ratones atímicos de manera más rápida y eficaz.

Procesamiento de muestras para anatomía patológica:

Con la mayoría de los tumores se realizó el procesamiento del tejido para analizar la anatomía patológica del mismo y evaluar su morfología así como el grado de angiogénesis y necrosis de éste. El protocolo que se siguió fue el siguiente:

1. Fijación: Inmersión en una solución de paraformaldehido al 10 % durante 16-24 h.
2. Aclarar con agua destilada.
3. Colocar dentro de unas cajitas de plástico individuales llamadas cassettes y etiquetar para poder identificar la muestra una vez dentro del procesador de tejidos.
4. Deshidratación: 5 h en alcohol 70º, 12 h en alcohol 96º, 3 h en alcohol 100º.
5. 1 h 30 min en xileno.
6. Inclusión en parafina: Sumergir toda la noche en parafina, 3 h en otro baño de parafina limpia.
7. Hacer los bloques de parafina con la ayuda de moldes metálicos y dejar enfriar.
8. Realizar cortes de 5 μm de grosor con el micrótomo y recogerlos en portaobjetos.
9. Desparafinar sumergiendo los cortes en dos baños de xileno consecutivamente durante 10 min cada uno.
10. Rehidratación: 3 min en alcohol 100º, 3 min en alcohol 96º, 3 min en alcohol 70º, aclarar con agua destilada.
11. Tinción hematoxilina-eosina: 2 min hematoxilina, aclarar con agua del grifo, 4 s alcohol clorhídrico (1%), aclarar varias veces con agua del grifo, 4 min eosina, aclarar con agua destilada.
12. Deshidratación: 3 min en alcohol 70º, 3 min en alcohol 96º, 3 min en alcohol 100º.
13. Cubrir el corte 1 min con xileno y 1 min con xileno:eucaliptol (1:1).

14. Montaje: Poner una gota de la resina sintética DPX sobre la preparación, colocar el cubreobjetos y dejar secar.

Establecimiento de un cultivo primario:

Tras la obtención del tumor en condiciones estériles, se procede a la disgregación de las células del mismo. Para ello se corta con la ayuda de un bisturí en trocitos lo más pequeños posibles y se colocan con tripsina en un baño a 37º y agitación durante 1 h. Posteriormente se intentan acabar de disgregar con una micropipeta y se centrifuga a 1.500 rpm (de revoluciones por minuto) durante 5 min. Se resuspende en medio de cultivo (DMEM:HAM, 10% suero fetal, 2 mM L-glutamina, 100 U/ml penicilina, 100 µg/ml estreptomicina (GIBCO BRL, Paisley, UK) y se colocan en placas de Petri dentro de un incubador con 5 % CO_2 a 37º.

Resultados

Inducción de tumores mamarios: Primero se realizaron una tanda de experimentos donde se inoculó la línea celular MDA-MB-231, la cual llevaba un tiempo siendo cultivada *in vitro* en el laboratorio. Los experimentos fueron los siguientes:

- E42/03A. 6 animales inoculados para crear tumor ectotópico: 2 ratones con 2 x 10^6, 2 con 4 x 10^6 y 2 con 12 x 10^6 células MDA-MB-231.
  Inicio de experimento: 18/12/03.
  Extirpación del tumor: -
  Sacrificio animales: 16/4/04.

- E42/03B. 6 animales inoculados para crear tumor ortotópico: 2 ratones con 2 x 10^6, 2 con 4 x 10^6 y 2 con 10 x 10^6 células MDA-MB-231.
  Inicio de experimento: 18/12/03.
  Extirpación del tumor: -
  Sacrificio animales: 16/4/04.

- E43/03A. 3 animales inoculados para crear tumor ortotópico con 3 x 10^6 células y 2 ectotópicos con 12 x 10^6 células MDA-MB-231.
  Inicio de experimento: 12/12/03.
  Extirpación del tumor: -
  Sacrificio animales: 16/4/04.

Los resultados obtenidos no fueron concluyentes (Tabla 10), ya que tan sólo se obtuvo un tumor y el resto de animales evolucionó reabsorbiendo el inóculo y aumentando progresivamente de peso.

EXPERIMENTO	**E42/03A**		**E42/03B**		**E43/03A**	
	Inóculo	**Tumor**	**Inóculo**	**Tumor**	**Inóculo**	**Tumor**
Individuo 1	2 x 10^6 SC	ND	2 x 10^6 IMFP	ND	3 x 10^6 IMFP	ND
Individuo 2	2 x 10^6 SC	ND	2 x 10^6 IMFP	ND	3 x 10^6 IMFP	ND
Individuo 3	4 x 10^6 SC	ND	4 x 10^6 IMFP	ND	3 x 10^6 IMFP	ND
Individuo 4	4 x 10^6 SC	ND	4 x 10^6 IMFP	ND	12 x 10^6 SC	ND/†
Individuo 5	12 x 10^6 SC	E	10 x 10^6 IMFP	ND	12 x 10^6 SC	ND
Individuo 6	12 x 10^6 SC	ND	10 x 10^6 IMFP	ND		

Tabla 10. Resultados inducción de tumores I. SC: subcutáneo; IMFP: mamario; E: exéresis; ND: No detectable; †: sacrificio.

La falta de éxito y reproducibilidad en la inducción de tumores nos hizo pensar que la línea celular podía haber sufrido modificaciones durante su cultivo *in vitro* desde su adquisición del banco de células, perdiendo con ello su capacidad tumorigénica. Por lo tanto procedimos a la adquisición de una nueva muestra de MDA-MB-231 de la ECACC junto con otra muestra de una línea de cáncer de mama que se ha descrito como muy tumorigénica, la MDA-MB-468. Se realizó una tanda de experimentos con cada una de ellas.

- E14/04. 5 animales inoculados subcutáneamente con 10 x 10^6 células MDA-MB-231.

  Inicio de experimento: 21/6/04.

  Extirpación del tumor: 9/8/04.

  Sacrificio animales: 25/11/04.

- E14/03. 5 animales inoculados subcutáneamente con 10 x 10^6 células MDA-MB-468.

  Inicio de experimento: 20/7/04.

  Extirpación del tumor: 9/8/04.

  Sacrificio animales: 25/11/04.

Los resultados obtenidos se detallan a continuación (Tabla 11) observando un 100 % de éxito en la aparición de tumores tras la inoculación tanto de la nueva línea MDA-MB-231 como de MDA-MB-468.

EXPERIMENTO	**E14/04** **10 x 10^6 SC MDA-231** **Tumor (l x t (cm))**	**E14/03** **10 x 10^6 SC MDA-468** **Tumor (l x t (cm))**
Individuo 1	E, 1.3 x 0.95	E, 1.1 x 0.7
Individuo 2	E, 1.3 x 0.8	E, 0.9 x 0.6
Individuo 3	E, 1 x 0.6	E, 0.8 x 0.7
Individuo 4	E, 0.5 x 0.4	E, 0.9 x 0.6
Individuo 5	E, 0.85 x 0.55	E, 0.8 x 0.5

Tabla 11. Resultados inducción de tumores II. SC: subcutáneo; l: largo; t: transversal; E: exéresis.

Los tumores SC que aparecieron en los ratones tenían una apariencia externa saludable, sin yagas ni zonas necrosadas como se puede observar en la figura 29.

Figura 29. Ratón con tumor ectotópico de células MDA-MB-231.

La evolución de los pesos de los ratones durante los dos estudios fue diferente. Mientras que los ratones inoculados con las células MDA-MB-231 mostraron una clara ganancia de peso (Gráfica 1), los inoculados con MDA-MB-468 tuvieron una ganancia de peso muy ligera (Gráfica 2), aunque el estado general de ambos grupos de ratones fue igual de bueno.

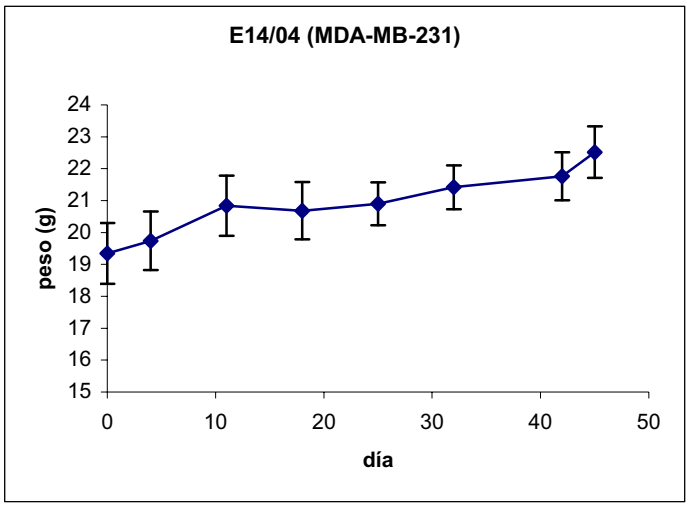

Gráfica 1. Control de peso ratones experimento E14/04 (media ± SEM de 5 ratones inoculados).

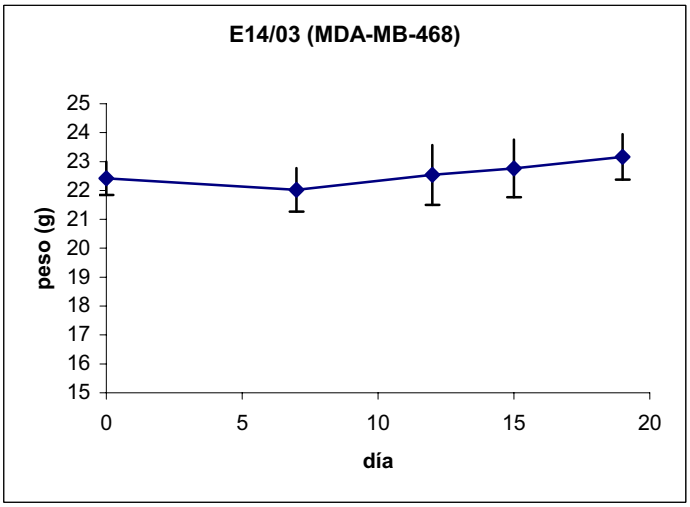

Gráfica 2. Control de peso ratones experimento E14/03 (media ± SEM de 5 ratones inoculados).

Respecto al crecimiento de los tumores, estos lo hicieron de forma exponencial en un corto período de tiempo tras un período de latencia más o menos largo. En el caso de MDA-MB-231 el período durante el que el tumor no fue detectable duró 25 días aproximadamente, mientras que en el caso de MDA-MB-468 éste fue de 15 días aproximadamente (Gráficas 3 y 4). Durante este período se reabsorbió el inóculo y por ello apreciamos una bajada en el volumen del tumor. Tras más de 3 meses después de la

exéresis de los tumores, tan sólo hubo que sacrificar un ratón por síntomas de caquexia al que se le realizó necropsia sin encontrar metástasis en ningún órgano vital.

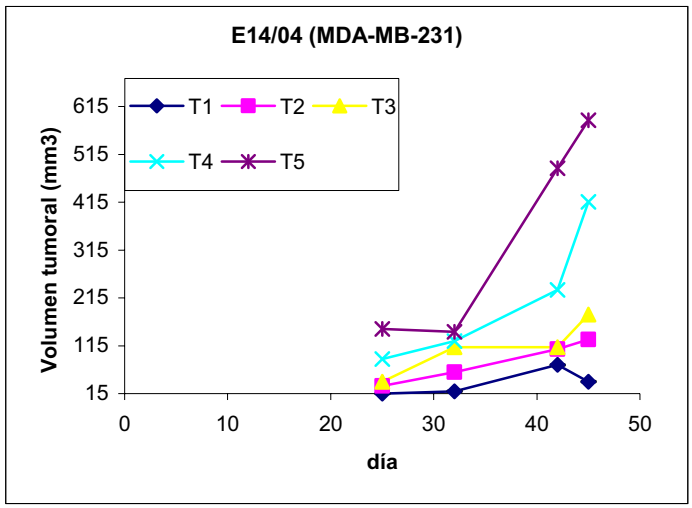

Gráfica 3. Control volumen tumoral experimento E14/04. T simboliza la evolución del tumor de cada uno de los ratones 1-5.

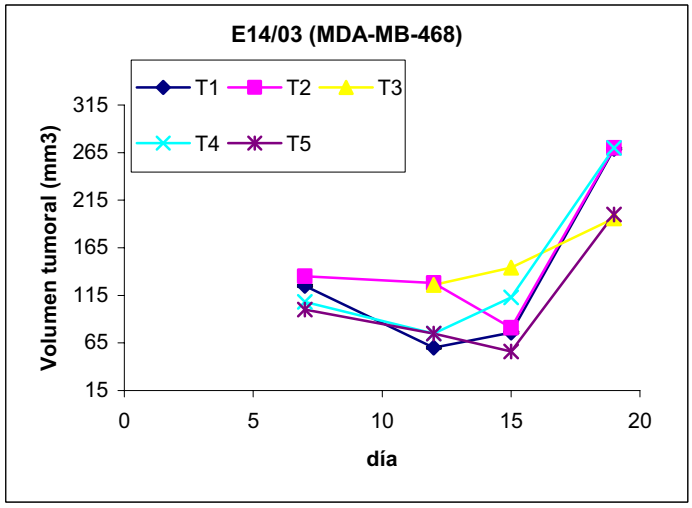

Gráfica 4. Control volumen tumoral experimento E14/03. T simboliza la evolución del tumor de cada uno de los ratones 1-5.

Estudio anatomo-patológico de los tumores

La morfología de los tumores fue estudiada por microscopía óptica tras su procesamiento y realización de la tinción histológica hematoxilina-eosina (Figura 30).

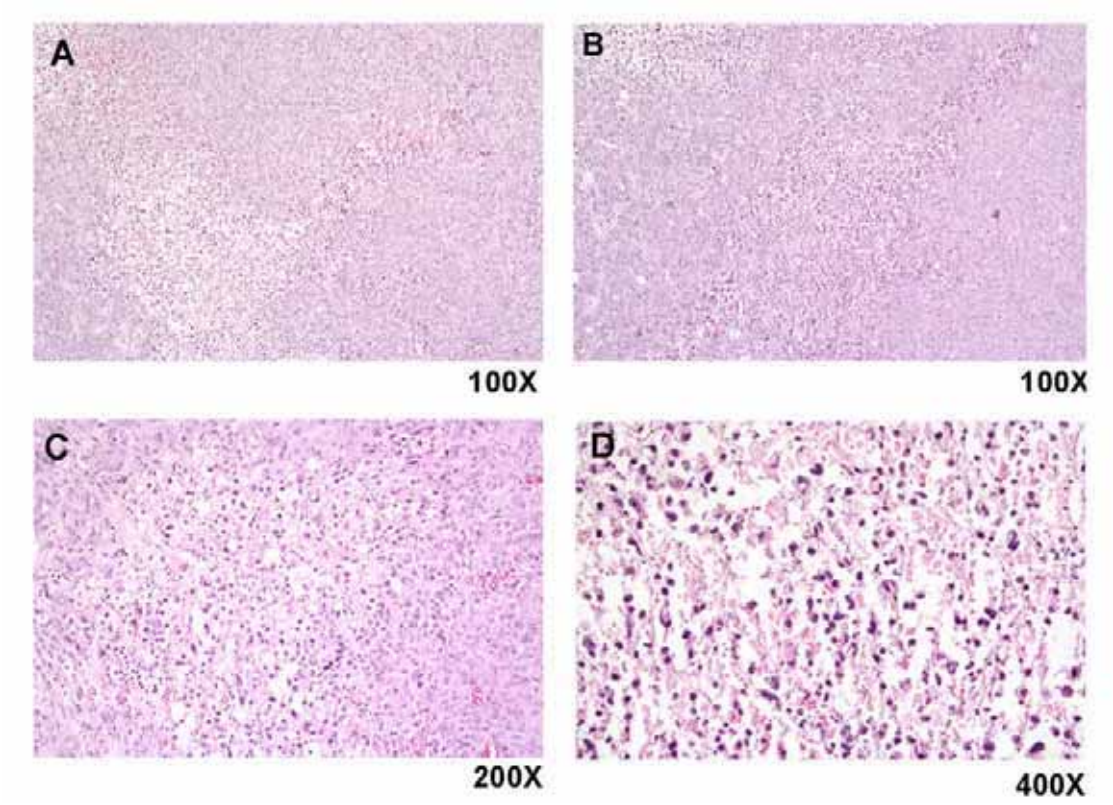

Figura 30. Cortes de tumores tras la tinción hematoxilina-eosina.

En las fotografías A y B podemos observar cortes de dos tumores ectotópicos diferentes, uno formado tras el inóculo de células MDA-MB-231 (Figura 30, A) y el otro formado por células MDA-MB-468 (Figura 30, B). Ambos muestran un cierto grado de heterogeneidad, mostrando zonas más oscuras donde las células se encuentran más apretadas y zonas más claras con las células más separadas. A mayor aumento del tumor generado por las células MDA-MB-231, podemos observar con más detalle que hay zonas donde las células se encuentran separadas unas de otras y tienen la cromatina más condensada, siendo las áreas de mayor actividad proliferativa (Figura 30, C). No se han identificado zonas necróticas y, por el contrario, sí que se ha visto un elevado grado de irrigación del tumor (D).

Establecimiento de cultivos primarios

Se procedió a la obtención de cultivos primarios obtenidos de un par de tumores generados por las células MDA-MB-231. Se mantuvieron en cultivo *in vitro* hasta obtener la cantidad adecuada de células para su almacenamiento mediante crioconservación. Estas células podrán ser utilizadas en futuros ensayos de obtención de tumores de mama *in vivo*.

Conclusiones

Podemos concluir que la línea de cáncer de mama MDA-MB-231 induce tumores ectotópicos en ratones atímicos tras un inóculo inicial de 10 x 10^6. Su curva de crecimiento abarca un período de latencia de unos 25 días y otros 25 hasta llegar a un tamaño aproximado de 1 x 1 cm. La línea celular MDA-MB-468 es algo más tumorigénica que la anterior ya que, partiendo del mismo inóculo, induce tumores que llegan al tamaño antes mencionado en un total de 19 días. Ambas líneas celulares no provocan metástasis tras un período de más de 3 meses después de la exéresis.

1.2.2. Evaluación de la toxicidad de AT514 *in vivo*

Objetivo

Determinación de la dosis máxima tolerable *in vivo* de AT514 en ratones sanos, no portadores de tumor, sin que manifiesten ningún síntoma de malestar ni deterioro en su salud. Los resultados obtenidos con este procedimiento permitirán que se diseñe un nuevo ensayo para evaluar la capacidad antitumoral de este fármaco en animales a los que previamente se les ha inducido un tumor.

Material

Animales: Para la realización de estos estudios se utilizaron ratones hembra de la cepa Balb/c, ya que son la cepa parental a partir de la que se obtienen los ratones atímicos Balb/c nude, utilizados para la obtención de tumores y por ello son el modelo más cercano para la evaluación de la toxicidad del fármaco en dichos ratones. La elección del sexo está condicionada por el modelo experimental (mama) y sólo se inocularan hembras.

Droga: AT514 fue sintetizada químicamente. Tiene una estructura química de ciclodepsipéptido y es poco soluble en soluciones acuosas, por ello el diluyente utilizado fue DMSO (de dimetil sulfóxido).

Diseño y metodología

Al no existir estudios previos de toxicidad en ratones con AT514 se analizaron estudios que se hubieran realizado con compuestos similares. El de mayor afinidad con nuestra molécula es uno realizado en ratas con otro depsipéptido llamado Kahalalido F (Brown AP, et al., 2002). Por lo tanto, se propuso usar como referencia la máxima dosis tolerada utilizada en este estudio, la cual fue de 300 μg/kg en una dosis única. Al igual que los autores del estudio con Kahalalido F, la pauta de administración elegida fue la dosificación múltiple, ya que no observaron efectos tóxicos administrando dosis de 80 μg/kg por vía intravenosa durante 5 días consecutivos, aún cuando este tratamiento superaba la máxima dosis tolerada en el caso de administración única. Por lo tanto, se planteó un primer experimento (E3/04) en el que se administró 80 μg/kg durante 5 días seguidos, 5 días alternos o bien 10 días alternos, con sus respectivos grupos control a los que les fue inoculado el diluyente del fármaco en la misma pauta de administración y un grupo control negativo al que le administramos suero fisiológico. El método de administración usado fue la vía intraperitoneal, ya que es una vía de administración menos estresante para el ratón y presenta mayor facilidad de aplicación y menor riesgo para el operador. Se realizó un segundo experimento (E9/04) en el que se aumentó la dosis utilizada. Las dosis que se usaron fueron 2 y 10 mg/kg durante 5 días seguidos o alternos, respectivamente. El sacrificio del animal se realizó mediante atmósfera saturada de CO_2 y se procedió a realizar la necropsia.

Resultados

Los resultados de ambos experimentos vienen detallados en la tabla 12. Las diferentes pautas de administración así como las diversas dosis de droga utilizadas no provocaron pérdida de peso ni toxicidad en órganos vitales, llegando a inyectar una dosis final de 50 mg/kg, más de 100 veces superior a la dosis de Kahalalido F tolerada por las ratas. Los ensayos no se pudieron continuar al no haber cantidad suficiente de droga y no tener los recursos económicos para sintetizar más cantidad y con ello seguir escalando la dosis.

Experimento (Fecha inicio)	Grupo	Nº ratones	Tratamiento	Sacrificio	Pesos medios jaula (g) (inicio-final)	Necropsias
E3/04 (26/2/04)	A	5	80 µg/kg AT514, 5 días seguidos	19/3/04	19.9-21.34	normal
	B	5	80 µg/kg AT514, 5 días alternos	19/3/04	19.8-21.26	normal
	C	5	80 µg/kg AT514, 10 días alternos	19/3/04	19.7-21.14	normal
	D	5	DMSO, 5 días seguidos	19/3/04	18.6-20.2	normal
	E	2	DMSO, 5 días alternos	19/3/04	17.5-19.05	normal
	F	2	DMSO, 10 días alternos	19/3/04	17.85-20.35	normal
	G	3	Suero fisiológico, 10 días alternos	19/3/04	19.4-21.16	normal
E9/04 (16/4/04)	A	3	Suero fisiológico, 10 días seguidos	7/5/04	19.9-23.5	normal
	B	3	DMSO, 5 días alternos	28/6/04	20.73-21.4	normal
	C	3	DMSO, 5 días seguidos	7/5/04	20.1-21.4	normal
	D	5	10 mg/kg AT514, 5 días alternos	28/6/04	19.88-21.44	normal
	E	5	2 mg/kg AT514, 5 días seguidos	7/5/04	19.92-20.64	normal

Tabla 12. Cuadro resumen de los procedimientos y resultados obtenidos en estudios de toxicidad con AT514.

Al ver la baja toxicidad de AT514, hicimos estudios de interacción con la albúmina, proteína mayoritaria de la sangre, para ver si podíamos dar explicación a dicho fenómeno. En la gráfica 5 vemos que tan solo un 1% de una solución de albúmina a la concentración que encontramos en sangre (0.6 g/ml) es suficiente para anular casi por completo el efecto citotóxico de la droga (pasamos de más de un 50% a un 10% de muerte) y se mantiene conforme aumentamos la cantidad de albúmina.

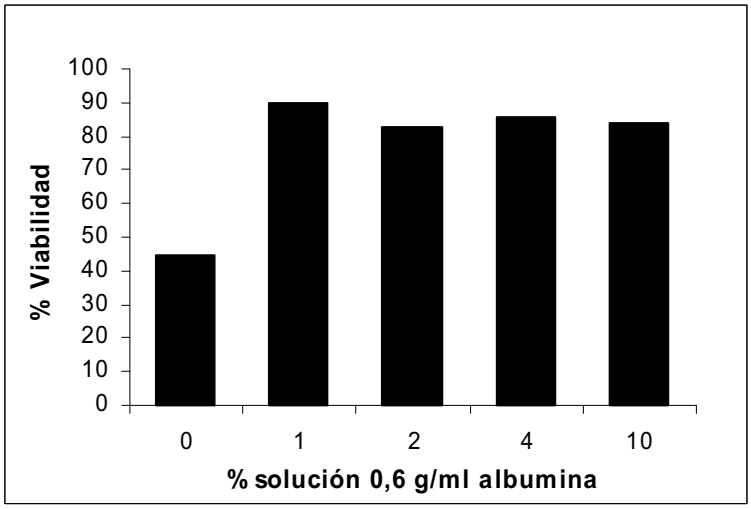

Gráfica 5. Viabilidad tras la exposición a la IC_{50} de AT514 y diferentes concentraciones de albúmina.

Conclusiones

Un dosis total de 50 mg/kg de AT514 administrada durante 5 días alternos en ratones Balb/c hembras no causó toxicidad alguna, impidiéndonos determinar la máxima dosis tolerada al no poder realizar más estudios por no disponer de cantidades tan elevadas del fármaco en evaluación. Por ello se tuvo que abortar el procedimiento previsto para evaluar la capacidad antitumoral de este fármaco en animales a los que previamente se les hubiera inducido un tumor de mama. La baja toxicidad de AT514 podría ser debida a su interacción con la albúmina sanguínea.

Capítulo 1.3. Caracterización de la apoptosis producida por AT514 e identificación de sus dianas moleculares en células de leucemia.

("Escobar-Díaz E, López-Martín EM, Hernández del Cerro M, Puig-Kroger A, Soto-Cerrato V, Montaner B, Giralt E, García-Marco JA, Pérez-Tomás R, García-Pardo A. AT514, a cyclic depsipeptide from *Serratia marcescens*, induces apoptosis of B-chronic lymphocytic leukemia cells: interference with the Akt/NF-kappaB survival pathway. Leukemia 2005;19(4):572-9").

Con el propósito de evaluar AT514 en un modelo *ex vivo* y profundizar más en su mecanismo de acción se realizaron estudios en células B de leucemia linfocítica crónica (B-CLL). El éxito del tratamiento clínico de la B-CLL está limitado por la resistencia que se crea a la droga y la baja selectividad frente a las células cancerosas de la mayoría de los fármacos en uso. En este estudio evaluamos el efecto del ciclodepsipéptido AT514, obtenido de *Serratia marcescens*, en la viabilidad de células de B-CLL. AT514 indujo apoptosis en las células B de los 21 pacientes estudiados, como lo confirma el marcaje de anexina V y la condensación nuclear, con una IC_{50} media de 13 μM. AT514 fue eficaz incluso en los pacientes resistentes a fludarabina, a la vez que no tenía efecto en los linfocitos sanos de estos pacientes. Además, AT514 activó de forma preferencial la vía apoptótica intrínseca, evidenciado por pérdida en el potencial de membrana, salida de citocromo c al citoplasma y activación de las caspasas-9 y -3, pero no de caspasa-8. Es importante remarcar que AT514 interfirió con las señales de supervivencia provocadas por las quinasas fosfatidilinositol-3 y la proteína quinasa C, induciendo desfosforilación de AKT en la serina 473. AT514 también disminuyó la actividad de NF-κB mediante la reducción en la expresión de la subunidad p65. Esto fue confirmado por ensayos funcionales en los que se usó células Raji transfectadas con un vector luciferasa que expresaba NF-κB y con experimentos en linfocitos de ratones transgénicos. Todos estos resultados muestran que AT514 induce apoptosis en células de B-CLL y sugieren que podría ser de utilidad en el tratamiento clínico de esta enfermedad.

(Estudio realizado en colaboración con el grupo de la Dra. A. García Pardo en el que he contribuido de forma parcial).

Leukemia (2005) 19, 572–579

www.nature.com/leu

AT514, a cyclic depsipeptide from *Serratia marcescens*, induces apoptosis of B-chronic lymphocytic leukemia cells: interference with the Akt/NF-κB survival pathway

E Escobar-Díaz[1], EM López-Martín[1], M Hernández del Cerro[1], A Puig-Kroger[1], V Soto-Cerrato[2], B Montaner[2], E Giralt[3], JA García-Marco[4], R Pérez-Tomás[2] and A Garcia-Pardo[1]

[1]*Departamento de Inmunología, Centro de Investigaciones Biológicas, CSIC, Madrid, Spain;* [2]*Departament de Biologia Cel.lular i Anatomia Patològica, Facultat de Medicina, Universitat de Barcelona, Barcelona, Spain;* [3]*Departament de Química Orgànica, IRBB-PCB Universitat de Barcelona, Barcelona; and* [4]*Servicio de Hematología, Hospital Universitario Puerta de Hierro, Madrid*

Clinical treatment of B-cell chronic lymphocytic leukemia (B-CLL) is limited by the progressive drug resistance and nonselectivity of most drugs towards malignant cells. Depsipeptides are present in certain bacteria and display potent antitumor activity. We have studied the effect of the novel cyclodepsipeptide AT514 (serratamolide) from *Serratia marcescens* on B-CLL cell viability. AT514 induced apoptosis of B-CLL cells from the 21 patients studied, as confirmed by Annexin-V binding and nuclei condensation, with an average IC_{50} of 13 μM. AT514 was effective in those B-CLL cases resistant to fludarabine, but had no effect on normal PBL. AT514 preferentially activated the intrinsic apoptotic pathway, as evidenced by loss of mitochondrial membrane potential, release of cytochrome *c* and activation of caspase-9 and -3, but not of caspase-8. Importantly, AT514 interfered with phosphatidylinositol-3 kinase and protein kinase C survival signals since it increased the apoptotic effect of LY294002 and Bisl inhibitors, and induced Akt dephosphorylation at Ser 473. AT514 also decreased NF-κB activity by dramatically reducing the levels of p65 in B-CLL. This was confirmed on functional assays using NF-κB-luc-transfected Raji cells and transgenic mice. Our results establish that AT514 induces apoptosis of primary B-CLL cells and could be useful for clinical treatment of this malignancy.
Leukemia (2005) **19,** 572–579. doi:10.1038/sj.leu.2403679
Published online 3 March 2005
Keywords: B-CLL; apoptosis; depsipeptide; caspase activation; Akt/NF-κB pathway

Introduction

B-cell chronic lymphocytic leukemia (B-CLL) is characterized by the progressive accumulation of monoclonal $CD5^+$ B lymphocytes arrested in the G_0/G_1 phase of the cell cycle.[1,2] Malignant cell accumulation is mainly due to inhibition of apoptosis rather than to increased proliferation.[3] Indeed, protein kinases involved in survival pathways, such as phosphatidylinositol-3 kinase (PI3-K), protein kinase C (PKC) and Akt/protein kinase B, are constitutively activated in B-CLL.[4–6] Likewise, the activity of the NF-κB family of transcription factors is also constitutively high in B-CLL.[6,7] Consequently, the expression of many genes, including those that regulate apoptosis such as the Bcl-2 family, is altered in this malignancy[3,8] and is modulated *in vitro* during spontaneous and drug-induced apoptosis.[9,10] Chemotherapeutic drugs, such as fludarabine, chlorambucil, prednisone, and certain monoclonal antibodies directed to specific cell surface proteins, also induce B-CLL apoptosis *in vivo*, although complete remission is difficult to attain and all patients eventually relapse.[11] It is therefore important to search for new agents which may be useful as novel therapies for B-CLL, alone or in combination with already known drugs.

Depsipeptides are naturally present in certain bacteria strains and have been shown to display antitumor activity.[12] The depsipeptide FR901228, for example, is a histone deacetylase inhibitor that induces cell death in many solid tumors, T cell leukemias and multiple myeloma.[13] FR901228 also induces apoptosis of B-CLL cells and is currently under clinical trials for treatment of this malignancy.[14,15] Depsipeptides may therefore be potent therapeutic agents for B-CLL.

During the search for new potential anticancer agents, we isolated the compound AT514 from cultures of *Serratia marcescens* and identified it as the water-insoluble cyclic depsipeptide serratamolide.[16] We have investigated the activity of this compound and recently found that AT514 inhibits cell growth and induces apoptosis of several cell lines derived from breast, lung and colon human tumors, as well as from T-cell leukemia or Burkitt lymphoma (Soto-Cerrato *et al.*, submitted for publication). In the present report, we have studied the effect of AT514 on primary B-CLL cells. We show that AT514 induces apoptosis of these cells by affecting the Akt survival pathway and this involves reduction in NF-κB activity, modulation in expression of Bcl-2 family members and caspase activation.

Materials and methods

Patients, B-CLL cell purification and normal peripheral blood lymphocytes (PBL)

A total of 21 patients with B-CLL diagnosis according to established clinical and laboratory criteria were studied; 19 of them had not received treatment at the time of this study. $CD5^+$ B-lymphocytes were purified from the peripheral blood of these patients after informed consent, by Ficoll–Hypaque (Nycomed, Oslo, Norway) centrifugation. PBL from healthy donors were purified from buffy coats by Ficoll–Hypaque centrifugation, passage through anti-CD14-conjugated microbeads and MACS separation columns (Miltenyi Biotec, Bergisch Gladbach, Germany) to remove monocytes.

Analysis of mitochondrial membrane potential ($\Delta\psi_m$) and cytochrome c *release*

For $\Delta\psi_m$ measurements, B-CLL cells were incubated for 24 h with or without 20 μM AT514 and treated for 20 min with 20 nM $DiOC_6$ (Cabiochem) at room temperature in the dark. Cells were washed, resuspended in PBS and analyzed by flow cytometry. For analysis of cytochrome *c* release into the cytosol, 30×10^6 cells were incubated for 24 h with or without 20 μM AT514. Cells were washed once in cold PBS and gently lysed in 200 μl

Correspondence: Dr A Garcia-Pardo, Centro de Investigaciones Biológicas, CSIC, Ramiro de Maeztu 9, 28040 Madrid, Spain;
Fax: 34 91 536 0432; E-mail: agarciapardo@cib.csic.es
Received 16 June 2004; accepted 10 January 2005; Published online 3 March 2005

ice-cold lysis buffer (25 mM Tris pH 6.8, 80 mM KCl, 250 mM sucrose, 1 mM EDTA, 1 mM DTT, 0.1% digitonin, 10 μg/ml leupeptin, 1 μg/ml aprotinin, 1 μg/ml pepstatin, 0.1 mM phenylmethylsulfonyl fluoride). After centrifugation at 12 000*g*, 4°C, 5 min, the cytosolic fraction was recovered in the supernatant and its protein content determined by the BCA assay (Pierce, Rockford, IL, USA). Equal amounts of protein were analyzed on 15% polyacrylamide SDS-PAGE and by Western blotting.

Analysis of NF-κB activity in transgenic mice and transfected Raji cells

Transgenic mice containing the NF-κB luciferase reporter gene were obtained from Dr Mercedes Rincón (University of Vermont, Burlington, USA).[17] Lymphocytes isolated from the spleen of these mice or Raji cells transfected with the NF-κB-luc or D3005 plasmids were cultured for 24 h in the absence or presence of 20 μM AT514. Incubation with anti-CD40 mAb was for 6 h. 10×10^6 cells for each condition were lysed in 40 μl passive lysis buffer (Promega Co., Madison, WI, USA) for 20 min at room temperature. After centrifugation, 20 μl of each supernatant was added to 50 μl luciferase substrate (Promega) and luciferase activity was determined on a TD-20/20 luminometer (Turner Designs, Sunnyvale, CA, USA) and normalized with respect to the total amount of protein in each supernatant and transfection efficiency, if applicable.

Results

AT514 induces apoptosis of B-CLL cells

To determine the effect of AT514 on B-CLL cell viability, cells from the 21 patients studied were incubated with various concentrations of AT514 for 24 h and their viability was measured by the MTT assay. Table 1 (Supplementary Information) lists the results obtained for each individual patient and Figure 1a represents the mean viability for the 21 cases. As can be observed, control cells, which received no drug, were highly viable (86% average) after 24 h. However, AT514 clearly induced B-CLL cell death in a dose-dependent manner, with an IC_{50} of 13 μM (Figure 1a). For comparison, we also treated the 21 cell samples with fludarabine, a drug known to induce apoptosis of B-CLL cells *in vitro* and commonly used for clinical treatment of these patients.[11] While most samples were sensitive to fludarabine after 48 h (not shown), patients 4, 10, 11, 12 and 18 were resistant to this drug (5–15% cell death, not shown), but were clearly sensitive to AT514 (Supplementary Table 1). Therefore, in these cases, AT514 appeared to be a more efficient agent in inducing B-CLL cell death. We also measured the effect of AT514 on normal PBL. As shown in Figure 1b, AT514 had a very limited effect on these cells decreasing their viability only to 75% after 24 h of treatment.

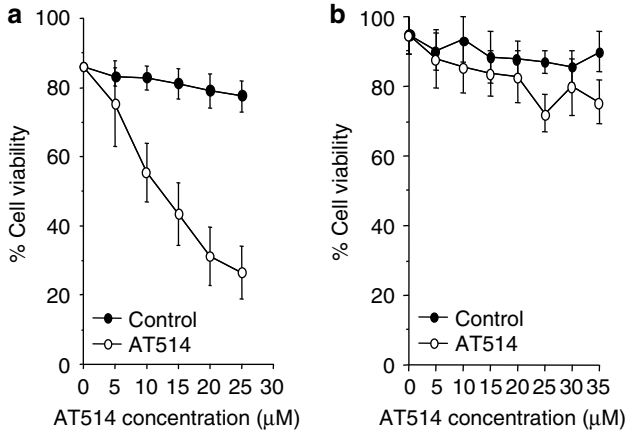

Figure 1 (a) Effect of AT514 on B-CLL cell viability. B-CLL cells were incubated in 96-well plates (2×10^5 cells/100 μl) with or without the indicated concentrations of AT514. After 24 h, cell viability was determined by the MTT method. All determinations were carried out in triplicate and values represent the average of the 21 cases studied. (b) PBL from four different healthy individuals were incubated as above and the viability was measured after 24 h. Determinations were carried out in triplicate and values are the average of the four cases studied.

To confirm that the cell death induced by AT514 was due to apoptosis, we first measured by flow cytometry the exposure of membrane phosphatidylserine using FITC-labelled Annexin V, and of cellular DNA using propidium iodide. As shown in Figure 2a for patient 4, AT514 had very little effect after 6 h of exposure as only 4.9% of cells were early apoptotic (Annexin-V+, PI−). However, after 15 h of AT514 treatment, the percentage of early and late (Annexin-V+, PI+) apoptotic cells increased (Figure 2a). After 24 h of exposure to AT514, 66.7% of cells were late apoptotic (Figure 2a). At this time, 4.2% of control cells were early apoptotic and 22.9% late apoptotic (Figure 2a). We also studied whether AT514 induced nuclei condensation and/or fragmentation. B-CLL cells were incubated with or without 20 μM AT514 for 24 h and stained for actin with TRITC-phalloidin (not shown) and with Hoechst to visualize the nucleus. As shown in Figure 2b, control cells contained an intact and uniformly stained nucleus, while cells treated with AT514 had condensed nuclei, characteristic of apoptotic cells. These results therefore indicated that AT514 induced apoptosis of B-CLL cells.

AT514 disrupts the mitochondrial membrane potential, induces release of cytochrome c *and activates caspase-9 and -3*

To determine the role of mitochondria in AT514-induced apoptosis, we first studied whether AT514 affected the mitochondrial membrane potential. B-CLL cells from patients 4 and 13 were incubated for 24 h in the absence or presence of 20 μM AT514, treated with $DiOC_6$ and analyzed by flow cytometry. As shown in Figure 3a, AT514 induced a loss of the mitochondrial membrane potential, increasing the number of $DiOC_6$-negative, apoptotic cells in both cases. We then analyzed by Western blotting the release of cytochrome *c* to the cytosolic fraction after treatment of B-CLL cells with AT514. As shown in Figure 3b for patients 4 and 13, cytochrome *c* was clearly increased in this fraction compared to the control. To determine if this resulted in activation of the initiator caspase 9, B-CLL cells were cultured for 24 h with or without 20 μM AT514, lysed and analyzed by Western blotting. As shown in Figure 3c for five different patients, AT514 effectively induced cleavage of 46 kDa procaspase-9 to the active form of 35 kDa. Likewise, PARP, a substrate of the effector caspase-3, was processed in these lysates and in lysates from cases 6, 9 and 16 (data not shown), from the native 116 kDa form to the 85 kDa product, indicating that caspase-3 had been activated by caspase-9.[18] Indeed, immunoblotting analyses confirmed the processing of caspase-3 from the native 32 kDa form to the 17 kDa active

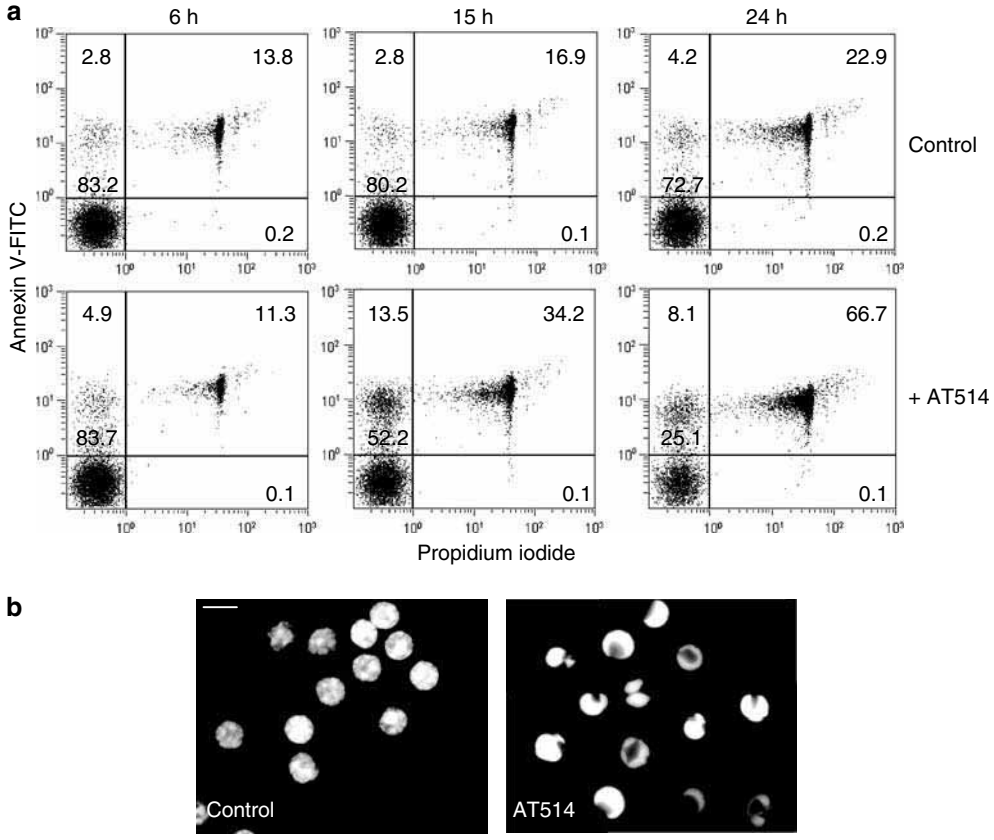

Figure 2 AT514 induces apoptosis in B-CLL cells. (a) B-CLL cells from patient 4 were treated with or without 20 μM AT514 for the indicated times, washed and incubated with Annexin V-FITC and propidium iodide and analyzed by flow cytometry. Numbers represent the percentage of cells in each compartment. (b) Cells from patient 4 were treated with 20 μM AT514 for 24 h, placed in poly-D-lysine-coated coverslips and stained with Hoechst. Bar, 10 μm.

subunit (shown in Figure 3c for patients 4, 13 and 20). To further characterize the apoptotic pathway involved, we analyzed the possible activation of caspase-8, another initiator caspase which can also activate caspase-3. As shown in Figure 3d for patients 4, 13 and 20, no significant decrease in procaspase-8 levels was observed. Consequently, cleavage of the caspase-8 substrate Bid was not observed (Figure 3d). Altogether, these results suggested that AT514 primarily activated the intrinsic apoptotic pathway in B-CLL.

AT514 decreases the Bcl2/Bax ratio in B-CLL cells

To establish whether AT514 regulated the Bcl-2/Bax ratio, we measured the levels of both proteins in lysates of B-CLL cells from seven different patients, treated with or without 20 μM AT514 for 24 h. We found that AT514 consistently increased the levels of Bax (proapoptotic) and generally decreased the levels of Bcl-2 (antiapoptotic) (Supplementary Figure 1). Consequently, the Bcl-2/Bax ratio was greatly reduced in samples treated with AT514 compared to controls for the seven patients studied (Table 2, Supplementary Information).

AT514 affects the PI3-K/Akt survival pathway

Previous studies have shown that PI3-K and PKC are constitutively activated in B-CLL cells and contribute to the survival of these cells.[4–6] To determine whether AT514 was affecting this pathway, we first studied if AT514 enhanced the reported apoptotic effect of LY294002 and BisI, inhibitors of PI3-K and PKC, respectively.[4,5] To this end, we used suboptimal concentrations of AT514 (10 μM) and of both inhibitors (20 and 5 μM, respectively). Cells were incubated with inhibitors for 1 h prior to adding AT514. Figure 4a shows representative results for two patients out of the four studied with identical results. When used individually, AT514, LY294002 and BisI produced partial B-CLL apoptosis. However, when AT514 was combined with either inhibitor, apoptosis increased in all four cases, and the combination of AT514 with both LY294002 and BisI further reduced cell viability to 10–15% (shown in Figure 4a for patients 13 and 18), suggesting that AT514 was cooperating with both kinase inhibitors. Incubation with the ERK inhibitor U0126 (5 μM) had no effect on B-CLL viability, in agreement with previous reports[4,5] and the combination of U0126 with AT514 did not modify this effect (Figure 4a).

We next examined if AT514 affected the phosphorylation of Akt, the key effector of PI3-K-dependent survival signaling. As shown in Figure 4b for patients 13 and 18, Akt was phosphorylated in control cells after 24 h of culture. However, treatment with AT514 clearly inhibited Akt phosphorylation in a dose-dependent manner. As a control, incubation with LY294002 also inhibited Akt phosphorylation in both cases (Figure 4b), confirming that Akt activation was PI3-K dependent. These results suggested that AT514 was inhibiting the PI3-K/Akt survival pathway in B-CLL cells.

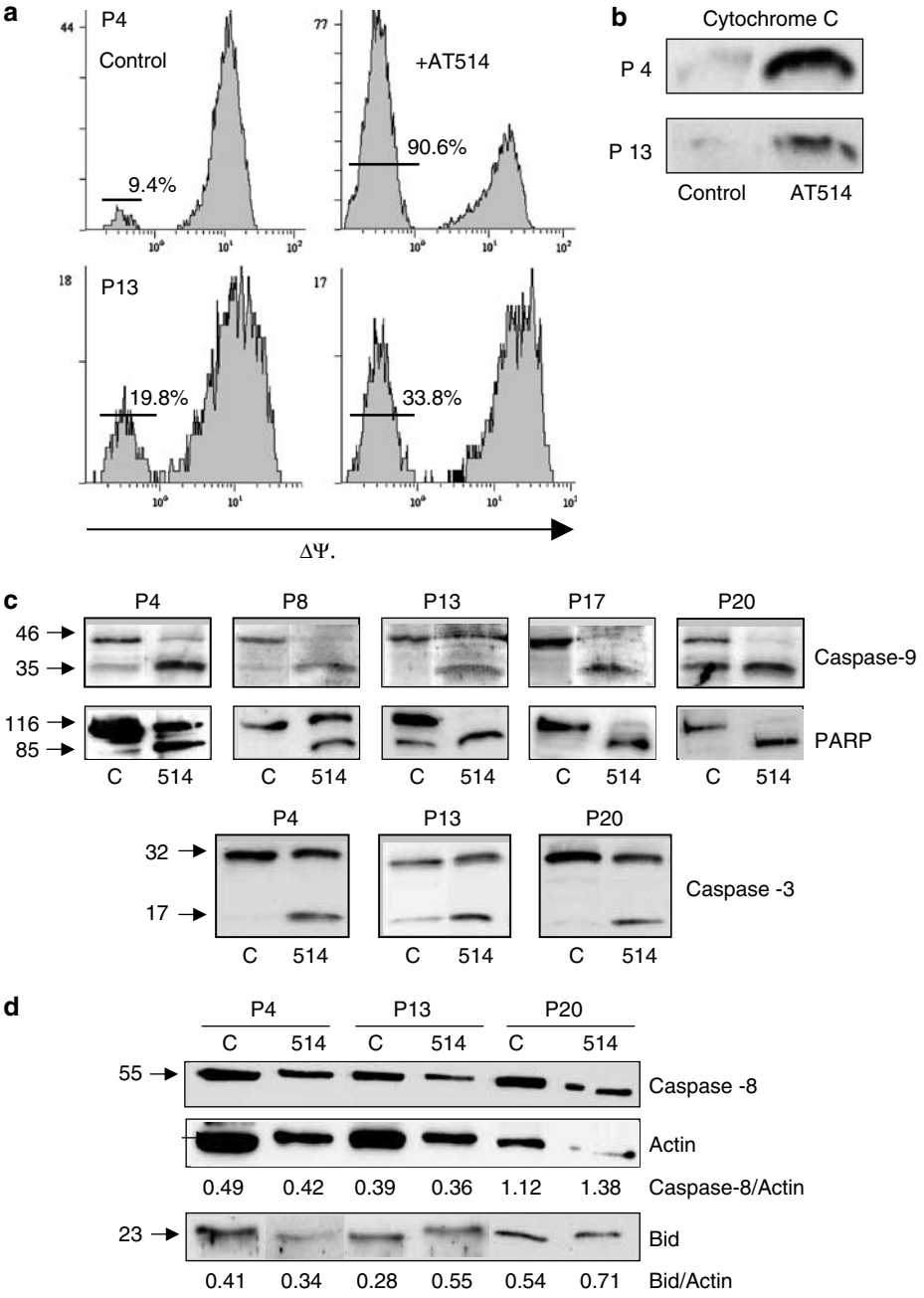

Figure 3 AT514 primarily activates the mitochondrial apoptotic pathway in B-CLL. (a) Flow cytometric analysis of the loss of mitochondrial membrane potential ($\Delta\psi_m$) after incubation of B-CLL cells with 20 μM AT514 for 24 h. (b) 30×10^6 B-CLL cells were treated or not with 20 μM AT514 and lysed. Protein (100 μg) from the cytosolic fractions was analyzed by Western blotting using an anti-cytochrome *c* Ab. (c) AT514 induces activation of caspase-9 and -3 and PARP cleavage. B-CLL cells from the indicated patients were incubated with or without (C, control) 20 μM AT514 for 24 h. Cells were then lysed and analyzed by Western blotting with specific antibodies. Conversion from the proactive forms of caspase-9 (46 kDa) and caspase-3 (32 kDa) to the active enzymes of 35 and 17 kDa, respectively, as well as the cleaved product (85 kDa) of PARP is indicated. (d) Lysates were also analyzed for caspase-8 activation and Bid cleavage using specific antibodies. Quantitation of protein bands was performed by the ECL method and values were corrected using actin as an internal control. Reduction in the levels of pro-caspase-8 (55 kDa) and Bid (23 kDa) was not observed.

AT514 decreases NF-κB activity

Akt suppression of apoptosis has been shown to involve the NF-κB transcription factor.[19,20] Consequently, NF-κB activity is constitutively high in B-CLL cells.[6,7] To determine if NF-κB was affected by AT514, we first analyzed by Western blotting the levels of NF-κB in the nuclear and cytosolic fractions of lysates of B-CLL cells treated with AT514. Figure 5a shows that in control cells NF-κB was present in both fractions, indicating a certain basal activity (NF-κB in the nucleus), as reported.[6,7] Treatment with AT514 dramatically reduced the levels of NF-κB in both fractions (Figure 5a), suggesting that AT514 was blocking the biosynthesis and/or transcription of NF-κB. To establish that this resulted in a reduced NF-κB activity, we took advantage of

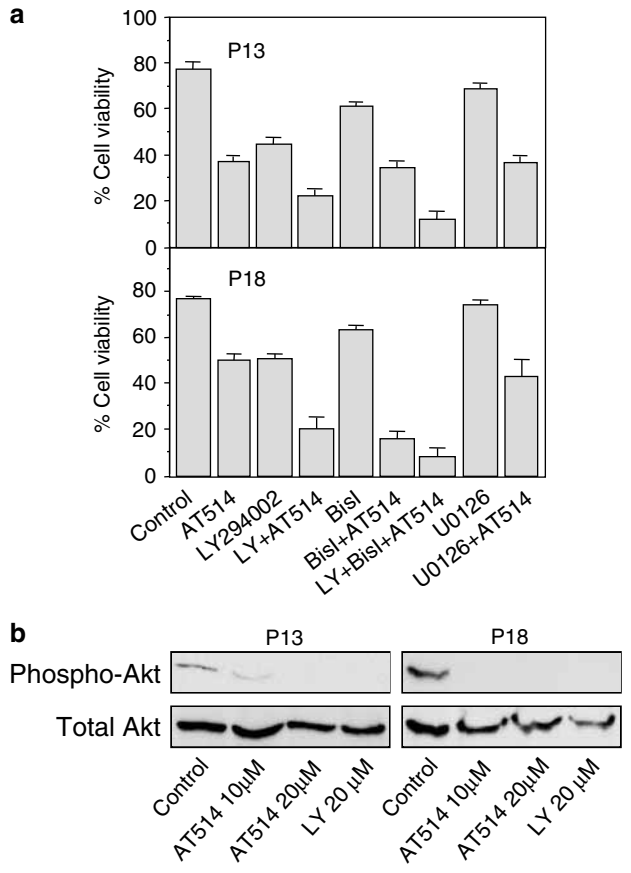

Figure 4 AT514 interferes with the PI3K/Akt survival pathway. (a) B-CLL cells from two representative patients were incubated for 1 h in the presence or absence of 20 μM LY294002, 5 μM BisI, or 5 μM U0126, prior to the addition of 10 μM AT514. After 24 h, cell viability was analyzed by flow cytometry using Annexin V and propidium iodide. Values represent the average of duplicate determinations. (b) B-CLL cells ($10–20 \times 10^6$) were incubated with or without 10 and 20 μM AT514 or 20 μM LY294002 for 24 h and lysed. Akt phosphorylation was analyzed by Western blotting using specific antibodies against total Akt or the phosphorylated form (Ser 473) of this kinase.

the NF-κB-luc reporter plasmid.[21] Owing to the difficulty of transfecting primary B-CLL cells, we used the B lymphoma cell line Raji for these experiments. AT514 effectively induced apoptosis of Raji cells in a dose-dependent manner (Figure 5b). These cells were transfected with NF-κB-luc or the control D3005 plasmid, incubated with or without 20 μM AT514 for 24 h, lysed and their activity was analyzed on a luminometer. Figure 5c shows that AT514 clearly reduced the luciferase activity displayed by untreated cells. This activity was also reduced to similar levels by LY294002, confirming that the NF-κB activity was regulated by PI3-K. NF-κB activity was effectively enhanced by an anti-CD40 mAb (Figure 5c), in agreement with a previous report.[7] Control cells transfected with D3005 had very low luciferase activity and this was not affected by treatment with AT514, LY29002 or anti-CD40 mAb (Figure 5c).

To further confirm that AT514 was inhibiting NF-κB activity, we purified lymphocytes from the spleen of transgenic mice containing the NF-κB luciferase reporter gene.[17] As shown in Figure 5d, these lymphocytes were partially sensitive to AT514, which decreased their viability to 55% after 24 h. Incubation of spleen lymphocytes from three different mice with AT514 clearly reduced the luciferase activity exhibited by untreated cells (Figure 5e). The control LY294002 produced a similar effect. These three sets of results clearly indicate that NF-κB plays an important role in the apoptotic mechanism induced by AT514.

Discussion

In this report, we show that the novel cyclodepsipeptide AT514 (serratamolide), naturally occurring in *S. marcescens*, is an efficient inducer of apoptosis in B-CLL cells. The present results expand our previous studies on established cancer cell lines (Soto-Cerrato *et al*., submitted) and represent the first evidence that AT514 induces apoptosis in human primary cancer cells.

The viability of B-CLL cells from the 21 patients studied here clearly diminished when exposed to AT514. Our results show that this was due to induction of apoptosis since cell death was accompanied by Annexin-V uptake, nuclei condensation, mitochondrial damage and caspase activation. Interestingly, AT514 had very little effect on normal PBL and was effective in the B-CLL cases that showed resistance to fludarabine, a drug commonly used in the treatment of these patients. This suggests that AT514 may be a very useful therapeutic agent for patients who are totally or partially resistant to fludarabine. Other differences between the mode of action of the two drugs include the p53 pathway. It is well established that fludarabine induces p53 expression[22] and we have shown that interfering with this expression by crosslinking $\alpha4\beta1$ integrin induces cell survival.[23] In results not shown, we did not observe induction of p53 in the present study, thus ruling out a role for this protein in the AT514 apoptotic pathway.

Both the intrinsic and extrinsic apoptotic pathways have been shown to operate in B-CLL. Thus, while some cytotoxic drugs (chlorambucil, fludarabine, rolipram) and γ-radiation activate caspase-8 and subsequent effector caspases,[24,25] induction of apoptosis by anti-CD22 inmunotoxins mainly involved the caspase-9 pathway.[26] Concomitant activation of both initiator caspases was also observed when apoptosis was induced by acadesine[27] or the histone deacetylase inhibitor MS-275.[28] Our present results indicate that AT514 preferentially activates the intrinsic, mitochondria-mediated, apoptotic pathway in B-CLL, since cytochrome *c* release and activation of caspase-9, but not of caspase-8, was clearly evident. This could be an important mechanistic difference with respect to the previously described effect of depsipeptide FR901228, which activates the extrinsic, caspase-8 mediated, apoptotic pathway in B-CLL.[15] Another major difference between depsipeptides FR901228 and AT514 is that FR901228 is a histone deacetylase inhibitor and was shown to acetylate histones H3 and H4 concomitant with induction of apoptosis.[15] In the present report, we did not observe increased acetylation of H3 and H4 histones upon B-CLL treatment with AT514 (results not shown), indicating that both depsipeptides activate different mechanisms for induction of apoptosis.

Several reports have recently shown that protein kinases such as PI3-K/Akt and PKC as well as the transcription factor NF-κB are constitutively activated in B-CLL and contribute to the defective apoptosis of these cells.[4–6,29] Our present results clearly show that AT514 interfered with this survival pathway, since it significantly increased the apoptotic effect of specific inhibitors for PI3-K and PKC. Moreover, we show that B-CLL cells had constitutively phosphorylated Akt, in agreement with a previous study,[6] and AT514 induced Akt dephosphorylation at

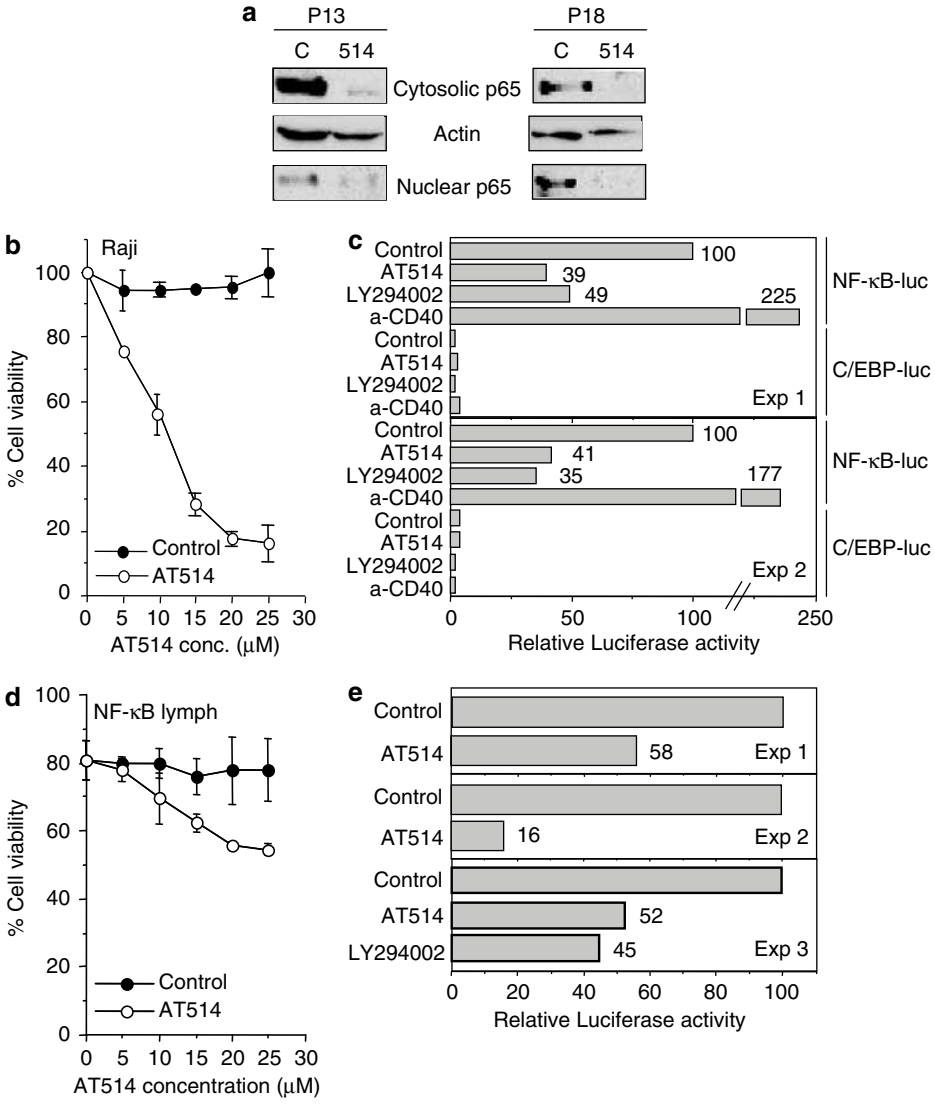

Figure 5 AT514 inhibits NF-κB activity. (a) B-CLL cells ($10–20 \times 10^6$) from two representative patients were incubated for 24 h with or without AT514; nuclear and cytosolic extracts were prepared and equal amounts of total protein were analyzed by Western blotting using an anti-p65 antibody. Actin was used as a loading control. (b) Raji cells were incubated with the indicated concentrations of AT514 and their viability determined after 24 h by the MTT method. (c) NF-κB-luc- or C/EBP-luc-transfected Raji cells were incubated with AT514 for 24 h, lysed and the luciferase activity determined on a luminometer. The effect of LY294002 and an anti-CD40 mAb is also indicated. The results from two independent experiments are shown. Values were corrected for transfection efficiency and total protein content on each lysate. (d) Spleen lymphocytes from NF-κB transgenic mice were incubated with the indicated concentrations of AT514 and their viability determined after 24 h by the MTT method. (e) Luciferase activity of these lymphocytes after treatment with AT514 for 24 h. Three different mice were studied (exps 1, 2 and 3) and values are normalized according to the total protein content on each lysate.

Ser 473. Constitutively activated Akt in B-CLL was not observed in another report[5] and this discrepancy remains to be explained. Akt controls cell survival by inducing phosphorylation and inactivation of proteins involved in apoptosis,[30] but also by activating NF-κB and thus the expression of survival genes.[20] In agreement with this pathway, we show in the present study that AT514 dramatically reduced the total levels of the p65 NF-κB component, thus directly affecting the activity of this transcription factor in B-CLL. We used two independent functional approaches, consisting of NF-κB-luc-transfected Raji cells and NF-κB-luc transgenic mice, to confirm that AT514 inhibited NF-κB activity. Our results clearly demonstrate that AT514 treatment induced a reduction in the activity of NF-κB in both cases.

The present findings provide a mechanism for AT514 induction of apoptosis in B-CLL cells, primarily involving the mitochondria-mediated apoptotic pathway and interference with Akt/NF-κB survival signals. To our knowledge, this is the first evidence showing a direct inhibition of Akt and NF-κB activation by a depsipeptide in B-CLL. A previous report[31] has shown that FR901228 (another depsipeptide known to induce apoptosis in B-CLL) diminished Akt activity of *ras*-transformed 10T1/2 cells, by reducing the total levels of this kinase. As we show in our study, AT514 inhibited Akt phosphorylation in B-CLL without affecting total Akt levels.

NF-κB controls the expression of several genes involved in apoptosis, including members of the Bcl-2 protein family.[32] Accordingly, we have found a highly consistent downregulation

of the antiapoptotic protein Bcl-2 concomitant with induction of apoptosis by AT514. In contrast, the levels of the proapoptotic protein Bax were dramatically increased by AT514 treatment. Although Bax is not under NF-κB control, it plays an important role in B-CLL apoptosis by determining the Bcl-2/Bax ratio, an important survival marker on these cells,[2,3] and we show in this report that AT514 consistently decreased this ratio. Bax may also be playing a crucial role in the mitochondrial-mediated apoptotic pathway initiated by AT514. It was recently shown that induction of B-CLL apoptosis by proteasome inhibitors produces a conformational change and mitochondrial translocation of Bax, which does not require caspase activation.[33] Although the initial stimulus that leads to these events is not known yet, it is interesting that PI3-K and Akt activities prevent Bax conformational change and translocation to mitochondria.[34,35] It is tempting to speculate that inhibition of PI3-K/Akt by AT514 initiates Bax-mediated mitochondria perturbation and subsequent caspase-9 and caspase-3 activation and apoptosis.

In conclusion, we show in this study that cyclodepsipeptide AT514 is a novel apoptotic agent for primary B-CLL cells, which directly blocks the PI3-K/Akt/NF-κB survival pathway and activates the mitochondria-mediated apoptotic cascade. It is noteworthy that several current cancer therapies are aimed at the inhibition of this survival pathway.[36] AT514 may therefore constitute an efficient drug for the clinical treatment of B-CLL, alone or in combination with conventional protocols.

Acknowledgements

We thank the B-CLL patients who donated blood samples for this research and Dr Maria José Terol (Hospital Clínico, Valencia, Spain) for providing some of these samples. Drs Angel Corbí and José L Rodríguez-Fernández for valuable help and advice with the NF-κB studies and for reviewing the manuscript, and Dr Pedro Lastres for help with the flow cytometry analyses. This work was supported by grants 08.3/0030.1/2003 from the Comunidad Autónoma de Madrid, SAF2003-00824 from the Ministerio de Ciencia y Tecnología (MCyT), and 01/1183 from Fondo de Investigación Sanitaria (to AGP); and CIDEM Grant 301888 (Generalitat de Catalunya)/Fundació Bosch i Gimpera, to RPT). E Escobar and E López-Martín were supported by fellowships from MCyT.

Supplementary Information

Supplementary Information accompanies the paper on the Leukemia website (http://www.nature.com/leu).

References

1 Kroft SH, Finn WG, Peterson LC. The pathology of the chronic lymphoid leukaemias. *Blood Rev* 1995; **9**: 234–250.
2 Bannerji R, Byrd JC. Update on the biology of chronic lymphocytic leukemia. *Curr Opin Oncol* 1998; **12**: 22–29.
3 Jewell AP. Role of apoptosis in the pathogenesis of B-cell chronic lymphocytic leukaemia. *Br J Biomed Sci* 2002; **59**: 235–238.
4 Barragán M, Bellosillo B, Campas C, Colomer D, Pons G, Gil J. Involvement of protein kinase C and phosphatidyl-inositol 3-kinase pathways in the survival of chronic lymphocytic leukemia cells. *Blood* 2002; **99**: 2969–2976.
5 Ringshausen I, Schneller F, Bogner C, Hipp S, Duyster J, Peschel C *et al*. Constitutively activated phosphatidyl-inositol 3-kinase (PI3-K) is involved in the effect of apoptosis in B-CLL: association with protein kinase Cδ. *Blood* 2002; **100**: 3741–3748.
6 Cuní S, Pérez-Aciego P, Pérez-Chacón G, Vargas JA, Sánchez A, Martín-Saavedra FM *et al*. A sustained activation of PI3K/NF-κB pathway is critical for the survival of chronic lymphocytic leukemia B cells. *Leukemia* 2004; **18**: 1391–1400.
7 Furman RR, Asgary Z, Mascarenhas JO, Liou HC, Schattner EJ. Modulation of NF-κB activity and apoptosis in chronic lymphocytic leukemia B cells. *J Immunol* 2000; **164**: 2200–2206.
8 Hanada M, Delia D, Aiello A, Stadtmauer E, Reed JC. Bcl-2 gene hypomethylation and high-level expression in B-cell chronic lymphocytic leukemia. *Blood* 1993; **82**: 1820–1828.
9 Pepper C, Hoy T, Bentley DP. Bcl-2/Bax ratios in chronic lymphocytic leukaemia and their correlation with *in vitro* and clinical drug resistance. *Br J Cancer* 1997; **76**: 935–938.
10 Thomas A, El Rouby S, Reed JC, Krajewsky S, Silber R, Potmesil M *et al*. Drug-induced apoptosis in B-cell chronic lymphocytic leukemia: relationship between p53 mutations and bcl-2/bax proteins in drug resistance. *Oncogene* 1996; **12**: 1055–1062.
11 Schriever F, Huhn D. New directions in the diagnosis and treatment of chronic lymphocytic leukaemia. *Drugs* 2003; **63**: 953–969.
12 Ballard CE, Yu H, Wang B. Recent developments in depsipeptide research. *Curr Med Chem* 2002; **9**: 471–498.
13 Khan SB, Maududi T, Barton K, Ayers J, Alkan S. Analysis of histone deacetylase inhibitor, depsipeptide (FR901228), effect on multiple myeloma. *Br J Haematol* 2004; **125**: 156–161.
14 Byrd JC, Shinn C, Ravi R, Willis CR, Waselenko JK, Flinn IW *et al*. Depsipeptide (FR901228): a novel therapeutic agent with selective, *in vitro* activity against human B-cell chronic lymphocytic leukemia cells. *Blood* 1999; **94**: 1401–1408.
15 Aron JL, Parthun MR, Marcucci G, Kitada S, Mone AP, Davis ME *et al*. Depsipeptide FR901228 induces histone acetylation and inhibition of histone deacetylase in chronic lymphocytic leukemia cells concurrent with activation of caspase 8-mediated apoptosis and down-regulation of c-FLIP protein. *Blood* 2003; **102**: 652–658.
16 Bar-Ness R, Avrahamy N, Matsuyama T, Rosenberg M. Increased cell surface hydrophobicity of a *Serratia marcescens* NS 38 mutant lacking wetting activity. *J Bacteriol* 1988; **170**: 4361–4364.
17 Millet I, Phillips RJ, Sherwin RS, Ghosh S, Voll RE, Flavell RA *et al*. Inhibition of NF-κB activity and enhancement of apoptosis by the neuropeptide calcitonin gene-related peptide. *J Biol Chem* 2000; **275**: 15114–15121.
18 Cohen GM. Caspases: the executioners of apoptosis. *Biochem J* 1997; **326**: 1–16.
19 Kane LP, Shapiro VS, Stokoe D, Weiss A. Induction of NF-κB by the Akt/PKB kinase. *Curr Biol* 1999; **9**: 601–604.
20 Madrid LV, Wang CY, Gurrtidge DC, Schottelius AJ, Baldwin Jr S, Mayo MW. Akt suppresses apoptosis by stimulating the transactivation potential of the RelA/p65 subunit of NF-κB. *Mol Cell Biol* 2000; **20**: 1626–1638.
21 Yano O, Kanellopoulos J, Kieran M, Le Bail O, Israel A, Kourilsky P. Purification of KBF1, a common factor binding to both H-2 and beta 2-microglobulin enhancers. *EMBO J* 1987; **6**: 3317–3324.
22 Bellosillo B, Villamor N, Colomer D, Pons G, Montserrat E, Gil J. *In vitro* evaluation of fludarabine in combination with cyclophosphamide and/or mitoxantrone in B-cell chronic lymphocytic leukemia. *Blood* 1999; **94**: 2836–2843.
23 De la Fuente MT, Casanova B, Cantero E, Hernández del Cerro M, García-Marco J, Silva A *et al*. Involvement of p53 in α4β1 integrin-mediated resistance of B-CLL cells to fludarabine. *Biochem Biophys Res Comm* 2003; **311**: 708–712.
24 Jones DT, Ganeshaguru K, Virchis AE, Folarin NI, Lowdell MW, Mehta AB *et al*. Caspase 8 activation independent of Fas (CD95/APO-1) signaling may mediate killing of B-chronic lymphocytic leukemia cells by cytotoxic drugs or γ radiation. *Blood* 2001; **98**: 2800–2807.
25 Moon EY, Adam L. PDE4 inhibitors activate a mitochondrial apoptotic pathway in chronic lymphocytic leukemia cells that is regulated by protein phosphatase 2A. *Blood* 2003; **101**: 4122–4130.
26 Decker T, Oelsner M, Kreitman RJ, Salvatore G, Wang Q-C, Pastan I *et al*. Induction of caspase-dependent programmed cell death in B-cell chronic lymphocytic leukemia by anti-CD22 immunotoxins. *Blood* 2004; **103**: 2718–2726.

27 Campas C, López JM, Santidrián AF, Barragán M, Bellosillo B, Colomer D *et al*. Acadesine activates AMPK and induces apoptosis in B-cell chronic lymphocytic leukemia cells but not in T lymphocytes. *Blood* 2003; **101**: 3674–3680.
28 Lucas DM, Davis ME, Parthun MR, Mone AP, Kitada S, Cunningham KD *et al*. The histone deacetylase inhibitor MS-275 induces caspase-dependent apoptosis in B-cell chronic lymphocytic leukemia cells. *Leukemia* 2004; **18**: 1207–1214.
29 Jones DT, Ganeshaguru K, Anderson RJ, Jackson TR, Bruckdorfer KR, Low SY *et al*. Albumin activates the Akt signaling pathway and protects B-chronic lymphocytic leukemia cells from chlorambucil-and radiation-induced apoptosis. *Blood* 2003; **101**: 3174–3180.
30 Kandel ES, Hay N. The regulation and activities of the multifunctional serine/threonine kinase Akt/PKB. *Exp Cell Res* 1999; **253**: 210–229.
31 Fecteau KA, Mei J, Wang H-CR. Differential modulation of signalling pathways and apoptosis of ras-transformed 10T1/2 cells by the depsipeptide FR901228. *J Pharmacol Exp Ther* 2002; **300**: 890–899.
32 Burstein E, Duckett CS. Dying for NF-κB? Control of cell death by transcriptional regulation of the apoptotic machinery. *Curr Opin Cell Biol* 2003; **15**: 732–737.
33 Dewson G, Snowden RT, Almond JB, Dyer MJS, Cohen GM. Conformational change and mitochondrial translocation of Bax accompany proteasome inhibitor-induced apoptosis of chronic lymphocytic leukemic cells. *Oncogene* 2003; **22**: 2643–2654.
34 Yamaguchi H, Wang HG. The protein kinase PKB/Akt regulates cell survival and apoptosis by inhibiting Bax conformational change. *Oncogene* 2001; **20**: 7779–7786.
35 Tsuruta F, Masuyama N, Gotoh Y. The phosphatidylinositol 3-kinase (PI3-K)-Akt pathway suppresses Bax translocation to mitochondria. *J Biol Chem* 2002; **277**: 14040–14047.
36 Senderowicz AM. Targeting cell cycle and apoptosis for the treatment of human malignancies. *Curr Opin Cell Biol* 2004; **16**: 670–678.

2. CARACTERIZACIÓN DEL EFECTO ANTICANCEROSO DEL TRIPIRROL PRODIGIOSINA EN CÁNCER DE MAMA

Capítulo 2.1. Estudio de la ruta apoptótica inducida por el agente anticanceroso prodigiosina y evaluación de su eficacia en células de cáncer de mama con resistencia a múltiples fármacos quimioterapéuticos.

("Soto-Cerrato V, Llagostera E, Montaner B, Scheffer GL, Pérez-Tomás R. Mitochondria-mediated apoptosis operating irrespective of multidrug resistance in breast cancer cells by the anticancer agent prodigiosin. Biochem Pharmacol 2004;68(7):1345-52").

El cáncer de mama representa un tercio de todos los cánceres diagnosticados en mujeres y es la segunda causa de muerte por dicha enfermedad en las sociedades occidentales. Es por ello que son necesarias mejores terapias, especialmente para tumores que no responden a terapia hormonal y metastásicos. Además, la resistencia a múltiples fármacos es un fenómeno muy común durante la quimioterapia, haciendo falta tratamientos más agresivos para los tumores que lo desarrollan ya que su pronóstico empeora. Prodigiosina (2-metil-3-pentil-6-metoxiprodigioseno) es un es un metabolito secundario producido por la bacteria *Serratia marcescens* del cual se han descrito propiedades pro-apoptóticas en líneas celulares cancerosas hematopoyéticas y gastrointestinales, sin una marcada toxicidad en células no malignas. El objetivo principal de este trabajo fue el de ampliar nuestro conocimiento acerca de los mecanismos de inducción de apoptosis por prodigiosina en el modelo de células de cáncer de mama. Esta droga mostró un potente efecto citotóxico tanto en células de cáncer de mama con receptores de estrógenos (MCF-7) como en células que no los expresaban (MDA-MB-231). La salida de citocromo c de la mitocondria al citoplasma, la activación de las caspasas-9, -8 y -7 y la rotura de la proteína poli (ADP-ribosa) polimerasa caracterizaron el evento apoptótico. Además, la inhibición de las caspasas reveló que la vía de actuación de la prodigiosina era a través de la ruta mitocondrial. Por último, en una línea celular derivada de MCF-7, resistente a múltiples drogas gracias a la sobreexpresión de la proteína ABCG2, se observó como la actividad citotóxica de prodigiosina se veía ligeramente reducida. Sin embargo, al analizar por citometría de flujo la acumulación y el flujo (entrada/salida) de prodigiosina en estas células, observamos como esta droga no era un sustrato de la proteína que confiere la resistencia. Estos resultados sugieren que prodigiosina es un potente agente proapoptótico que podría ser utilizado para el tratamiento de cáncer de mama incluso en presencia de proteínas de resistencia a múltiples fármacos.

Available online at www.sciencedirect.com
SCIENCE DIRECT
Biochemical Pharmacology 68 (2004) 1345–1352
Biochemical Pharmacology
www.elsevier.com/locate/biochempharm

Mitochondria-mediated apoptosis operating irrespective of multidrug resistance in breast cancer cells by the anticancer agent prodigiosin

Vanessa Soto-Cerrato[a], Esther Llagostera[a], Beatriz Montaner[a], George L. Scheffer[b], Ricardo Perez-Tomas[a,*]

[a]*Departament de Biologia Cel·lular i Anatomia Patològica, Cancer Cell Biology Research Group, Universitat de Barcelona, Barcelona, Spain*
[b]*Department of Pathology, VUmc, Amsterdam, The Netherlands*

Received 24 February 2004; accepted 26 May 2004

Abstract

Prodigiosin (PG) is a red pigment produced by *Serratia marcescens* with pro-apoptotic activity in haematopoietic and gastrointestinal cancer cell lines, but no marked toxicity in non-malignant cells. Breast cancer is the most frequent malignancy among women in the European Union and better therapies are needed, especially for metastatic tumors. Moreover, multidrug resistance is a common phenomenon that appears during chemotherapy, necessitating more aggressive treatment as prognosis worsens. In this work, we extend our experiments on PG-induced apoptosis to breast cancer cells. PG was potently cytotoxic in both estrogen receptor positive (MCF-7) and negative (MDA-MB-231) breast cancer cell lines. Cytochrome *c* release, activation of caspases-9, -8 and -7 and cleavage of poly (ADP-ribose) polymerase protein typified the apoptotic event and caspase inhibition revealed that PG acts via the mitochondrial pathway. In a multidrug-resistant subline of MCF-7 cells that over-expresses the breast cancer resistance protein, the cytotoxic activity of PG was slightly reduced. However, flow-cytometry analysis of PG accumulation and efflux in MCF-7 sublines showed that PG is not a substrate for this resistance protein. These results suggest that PG is an interesting and potent new pro-apoptotic agent for the treatment of breast cancer even when multidrug resistance transporter molecules are present.

Keywords: Prodigiosin; Breast cancer; Estrogen receptor positive/negative; Mitochondria-mediated apoptosis; Caspases; Multidrug resistance

1. Introduction

Breast carcinoma represents the third of all cancers diagnosed in women and is the second leading cause of cancer death in Western European and North American women (American Cancer Society). Cytotoxic chemotherapy plays an important role in the management of patients with hormone-insensitive or metastatic breast carcinoma, although most of them ultimately develop recurrences. Therefore, there is a need for novel cytotoxic agents and treatment strategies in patients with advanced breast carcinoma that is refractory to conventional chemotherapy [1].

Apoptosis is a physiologically programmed mechanism of cell death involved in cellular stress response, such as genotoxic agents exposure [2]. One of the major proteins involved in this process is the tumor suppressor protein p53, which mediates either cell cycle arrest or apoptosis [3]. Two major pathways mediating drug-induced apoptosis have been characterized; one requires the activation of cell surface receptors, whilst the other directly targets mitochondria [4]. Both apoptotic signals seem to be integrated at the mitochondrial level and are typically accompanied by the activation of aspartate-specific proteases called caspases [5]. Whilst the former induces caspase-8 activation, the mitochondrial pathway leads to the release of apoptogenic factors such as cytochrome *c* (cyt-*c*), which binds Apaf-1 and procaspase-9, inducing caspase-9 activation in the cytoplasm [6]. Both pathways then activate the effector caspases-3 and -7, which cleave a number of

Abbreviations: ABC, ATP binding cassette; BCRP, breast cancer resistance protein (ABCG2/MXR); ER+/−, estrogen receptor positive/negative; MDR, multidrug resistance; MRP-1, multidrug resistance protein 1 (ABCC1); MTT, methyl-thiazole-tetrazolium; PARP, poly (ADP-ribose) polymerase protein; PG, prodigiosin; P-gp, P-glycoprotein (MDR1/ABCB1); Z-VAD.fmk, Z-Val-Ala-dl-Asp (OMe)-fluoromethylketone

* Corresponding author. Tel.: +34 93 402 42 88; fax: +34 93 402 90 82.
E-mail address: rperez@ub.edu (R. Perez-Tomas).

0006-2952/$ – see front matter © 2004 Elsevier Inc. All rights reserved.
doi:10.1016/j.bcp.2004.05.056

substrate proteins, including the poly (ADP-ribose) polymerase protein (PARP).

Apoptosis-inducing compounds are candidate antitumor agents. In this view, prodigiosin (PG), a red bacterial pigment with a pyrrolylpyrromethene skeleton, has a number of concentration-dependent effects as an immunosuppressive agent [7,8] and has significant anti-neoplastic activity against a variety of human cancer cells, including haematopoietic and gastrointestinal cells, with no marked toxicity in non-malignant cell lines [9–12]. Furthermore, the apoptotic drug PG triggers the reorganization of actin cytoskeleton promoting the breakdown of actin microfilaments [10], down-regulates the expression of cyclin E-cdk2 and p27, the induction of the cyclin A-cdk2 and cyclin E-cdk2 kinase activity and the phosphorylation of retinoblastoma [13].

Individual tumor cells, after drug treatment exposure, may develop resistance to a broad range of structurally unrelated drugs giving rise to a phenomenon that is known as multidrug resistance (MDR) [14], a significant limiting factor in chemotherapy effectiveness. The ATP binding cassette (ABC), superfamily of membrane transporters, is associated with MDR to anticancer drugs. These ABC proteins act as efflux pumps that cause a decrease in intracellular concentrations of cytotoxic drugs [15]. P-glycoprotein (P-gp/MDR1/ABCB1) [16], multidrug resistance protein 1 (MRP1/ABCC1) [17] and the mitoxantrone resistance protein (MXR/BCRP/ABCG2) [18] are ABC transporters, which participate in the multidrug resistance of tumors.

In the present study, we have examined the effectiveness of PG on ER+ (MCF-7) and ER− (MDA-MB-231) human breast cancer cells and its mechanism of action. In addition, we tested the sensitivity of the BCRP over-expressing MCF-7 MR cells to PG treatment. FACS analysis of uptake and efflux of PG in MCF-7 sublines was used to determine whether PG is a substrate for BCRP or instead acts independently of the presence of such transporter molecules.

2. Materials and methods

2.1. PG purification

2-Methyl-3-pentyl-6-methoxyprodigiosene (PG) was purified from *Serratia marcescens* 2170, as previously described [9]. It was then solubilized and its concentration determined by UV–vis in 95% EtOH–HCl ($\in_{535}$ = 112000/M cm).

2.2. Cell culture conditions

MCF-7 and the mitoxantrone resistant subline MCF-7 MR are human ER+ breast cancer cell lines. MDA-MB-231 is an ER− breast cancer cell line that was purchased from the American type culture collection (ATCC). Cells were cultured in DMEM:F-12 (1:1) (Biological Industries) supplemented with 10% heat-inactivated fetal bovine serum (Gibco BRL), 2 mM l-glutamine, 100 u/mL penicillin, 100 μg/mL streptomycin, 50 μg/mL gentamycin and 10 μg/mL insulin at 37°C in a 5% CO_2 atmosphere.

2.3. Cell viability assay

The viability of cultured cells was determined by assaying the reduction of MTT (Sigma Chemical Co.) to formazan [19]. Briefly, 2×10^4 cells were seeded in 96-well microtiter cell culture plates. After 24 h, they were incubated in the absence (control cells) or presence of 0.25–2.75 μM PG in a final volume of 100 μL, for 4, 8, 16 or 24 h. Then, 10 mM MTT (diluted in PBS) was added to each well for an additional 2 h at 37°C. The blue formazan precipitate was dissolved in 100 μL of isopropanol:1N HCl (24:1) and the absorbance was measured at 550 nm in a multiwell plate reader. Cell viability was expressed as a percentage of control. IC_{50} was determined as the concentration of drug that produced a 50% reduction of absorbance at 550 nm.

2.4. Western blot analysis

Cells (5×10^5 cells/mL) were exposed to 0.2, 0.6 and 1 μM PG for 16 h. They were then washed in PBS and a lysis buffer was added (85 mM Tris, pH 6.8, 2% SDS, 1 μg/mL aprotinin, 1 μg/mL leupeptin and 0.1 mM phenylmethanesulfonyl fluoride). Later, 80 μg of protein extracts was separated by SDS–PAGE on a 12 or 15% polyacrylamide gel and transferred to immobilon-P membranes (Millipore). Blots were blocked in 5% dry milk diluted in TBS-T (50 mM Tris–HCl, pH 7.5, 150 mM NaCl, 0.1% Tween-20) for 1 h and then incubated overnight with polyclonal antibodies against cleaved caspase-7 or -9 (Cell Signalling Technology, New England Biolabs, ref. 9491 or 9501S, respectively), anti-PARP or anti-Bax (Santa Cruz Biotechnologies, ref. sc-7150 or sc-526-G) and with the monoclonal antibodies, anti-caspase-8, anti-cytochrome *c* or anti-p21 (Pharmingen, BD biosciences, ref. 559932, 556433, 65951A) or anti-p53 (Neomarkers, ref. MS-186-P1), according to the manufacturer's instructions. Antibody binding was detected with goat anti-rabbit or goat anti-mouse IgG secondary antibodies conjugated to HRP (Biorad) and the ECL detection kit (Amersham).

2.5. Measurement of cytochrome c release

Release of cytochrome *c* from mitochondria to cytosol was measured by Western blot (method described above) with some modifications. Cells (5×10^5 cells/mL) were exposed to 1 μM PG over different time periods, from 15 min to 24 h. Later, they were washed with ice-cold PBS and gently lysed for 30 s in 80 μL ice-cold lysis buffer

(250 mM sucrose, 1 mM EDTA, 0.05% digitonin, 25 mM Tris, pH 6.8, 1 mM dithiothreitol, 1 μg/mL leupeptin, 1 μg/mL pepstatin, 1 μg/mL aprotinin and 100 μM phenylmethanesulfonyl fluoride). Lysates were centrifuged at 12,000 × *g* at 4°C for 3 min to obtain the supernatants (cytosolic extracts free of mitochondria) and the pellets (fractions that contain mitochondria). Supernatants (40 μg) were then electrophoresed on a 15% polyacrylamide gel and analyzed by Western blot using the monoclonal anti-cytochrome *c* antibody (Pharmingen). In experiments with the caspase inhibitor Z-Vad.fmk (Z-Val-Ala-dl-Asp (OMe)-fluoromethylketone) (Bachem), it was added at 100 μM 1 h before PG treatment [20].

2.6. FACS analysis

Approximately 1 × 10^6 MCF-7 or MCF-7 MR cells were loaded with fluorescent drug in a volume of 500 μL for 1 h at 37°C. The final concentration of mitoxantrone was 19 μM, whilst PG was used at a final concentration of 0.48 μM. After loading, cells were spun down, split into two batches and re-suspended in 2 mL of fresh, ice-cold medium without drug. Half of the cells were kept on ice (time zero of efflux) and in the other half, efflux of the drug was allowed at 37°C for 60 min. The efflux was stopped by placing the cells on ice. Experiments were also performed in the presence of 100 nM Ko143, a known BCRP blocker [21], both during the loading and efflux phase. Cells without drug treatment were used as time zero for loading and auto-fluorescence levels. Fluorescence levels were determined with a FACS-Star flow cytometer (Becton–Dickinson) and measured at the appropriate wavelength for PG (excitation 488 nm / emission 575 nm) or mitoxantrone (excitation 635 nm / emission 670 nm). A total of 5000 cells were measured per sample.

2.7. Statistical analysis

Data are shown as mean ± S.E.M. of three independent experiments performed in triplicate. They were analyzed by ANOVA and Student's *t*-test. A *P* value of less than 0.05 was considered significant. IC_{50} values were calculated by non-linear regression analysis of the data.

3. Results

3.1. Cytotoxicity of prodigiosin in breast cancer cell lines

To determine whether PG induced a decrease in the cell viability of human breast cancer cells, the estrogen sensitive MCF-7, its mitoxantrone resistant MCF-7 MR subline and the estrogen independent MDA-MB-231 cell lines were treated with PG in a time- and dose-dependent manner (Fig. 1). The effect of the pigment on viability was measured by metabolism of the tetrazolium salt in a cell titer proliferation assay. PG caused a dose-dependent decrease in viability in every cell line examined. Differences between MCF-7 and MCF-7 MR cells were observed, MCF-7 being more sensitive to PG than MCF-7 MR. The IC_{50} values at 24 h for MCF-7 MR (2.21 μM ± 0.6) were twice as high as for MCF-7 cells (1.10 μM ± 0.04). In contrast, MDA-MB-231 cells exhibited a similar cytotoxic response to PG as MCF-7 cells, showing an IC_{50} value of 1.14 μM ± 0.12 at 24 h.

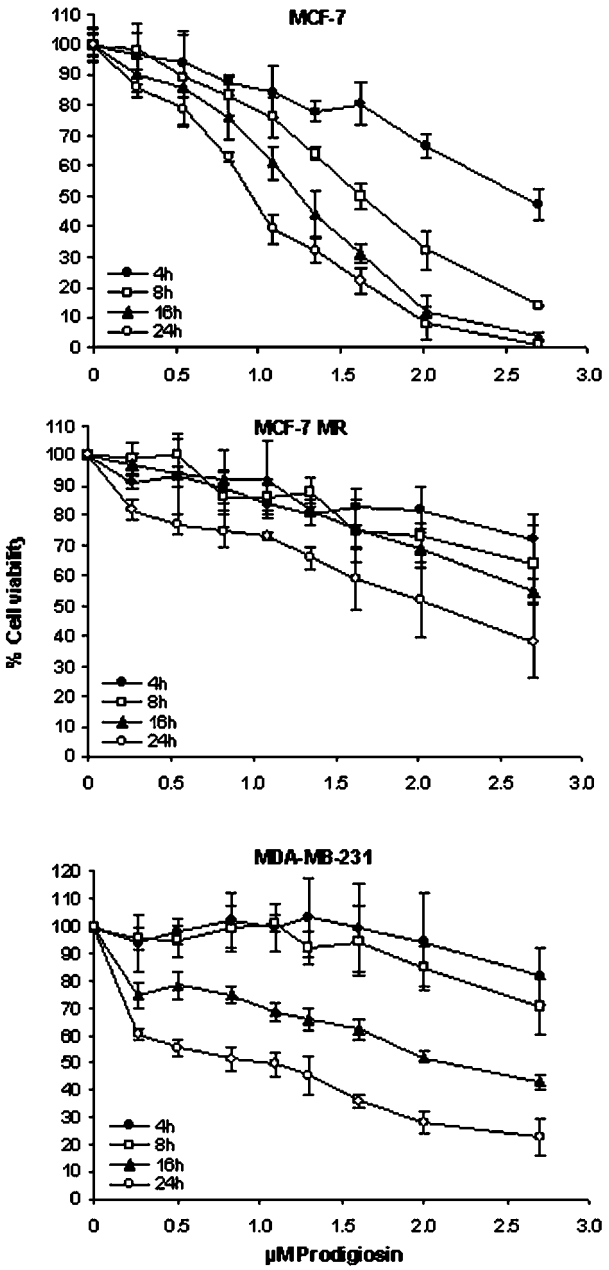

Fig. 1. Cell viability in PG-treated cells. MCF-7, MCF-7 MR and MDA-MB-231 cells (4 × 10^4) were treated with a range of concentrations (0–2.7 μM) of PG over different time periods and their viability was determined by MTT assay. The percentage of viable cells was calculated as a ratio of A_{550} between treated and control cells. Values are shown as mean ± S.E.M. of three independent experiments performed in triplicate.

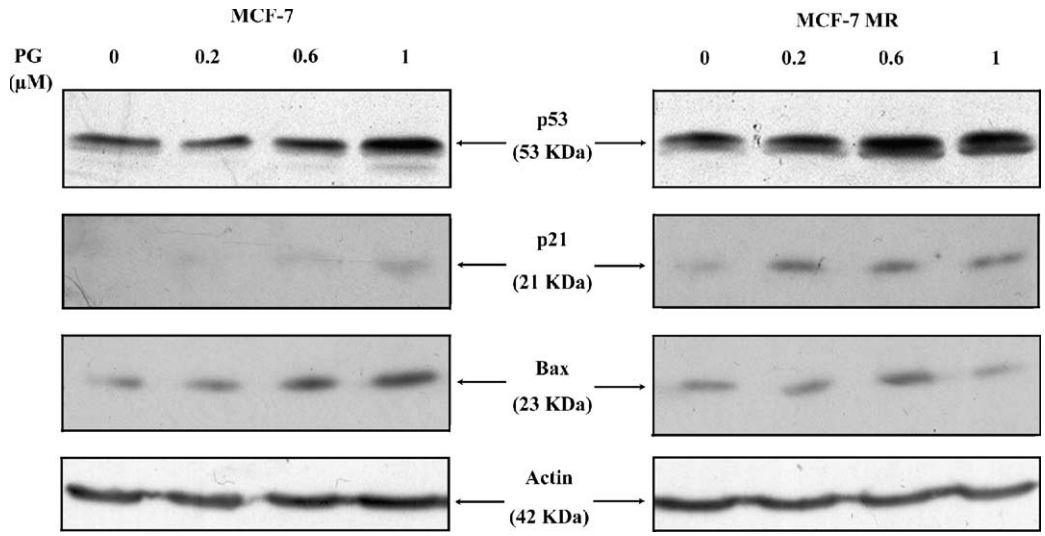

Fig. 2. Effect of PG on p53 and its downstream effectors p21 and Bax. MCF-7 and MCF-7 MR cells treated with PG concentrations ranging from 0.2 to 1 μM for 16 h and incubated with the appropriate antibodies. Results shown are typical examples of data from multiple experiments.

3.2. PG-induced apoptosis in human breast cancer cells

To understand the cell death mechanism induced by PG, MCF-7 and its subline, MCF-7 MR were used to determine whether differences in their sensitivity to PG were related to differences in the molecular process triggered by this cytotoxic agent.

3.2.1. Changes in p53, p21 and Bax protein levels

The p53 has been found to be importantly involved in apoptosis induced by a broad range of agents. We examined, by Western blot analysis, whether PG has any effect on this protein and on p21 and Bax, as it is known that p53 may induce their transcription upon stress signal. As observed in Fig. 2, p53 accumulation was detected in both cell lines upon PG treatment, it being higher in MCF-7 MR. The levels of the downstream effector protein p21 were considerably different between both cell lines starting to increase from as early as 0.2 μM in MCF-7 MR while it was almost undetectable in MCF-7. Conversely, the proapoptotic protein Bax was induced in a clear-way in MCF-7 cells suggesting that different cell effects might have been induced by PG in each cell lines.

3.2.2. Cytochrome c release

During apoptosis, cytochrome *c* is released from mitochondria into the cytosol where it helps in activating caspases. We, therefore, investigated cytochrome *c* release kinetics in response to PG exposure in MCF-7 and MCF-7 MR cells by Western blotting. Fig. 3 shows the time-dependent release of cytochrome *c* into the cytosol upon exposure to PG (1 μM) in both cell lines. Moderately increased levels of cytochrome *c* in the cytosol were detectable in MCF-7 as early as 30 min after PG treatment and a marked increase was observed at 12 h. In cytosolic fractions from MCF-7 MR, cytochrome *c* levels increased as a function of time.

3.2.3. Induction of caspases-9, -8 and -7 activation and PARP cleavage

In both cell lines, PG induced the activation of the main proteases that executes apoptosis such as the initiator caspases-9 and -8 and also the effector caspase-7, as well as cleavage of the caspase substrate called PARP. PG induced processing of caspase-9 and -8, as shown by the appearance of their active form of 37 and 23 kDa, respectively (Fig. 4(A)). In the absence of detectable caspase-3, due to a gene deletion in the MCF-7 and MCF-7 MR

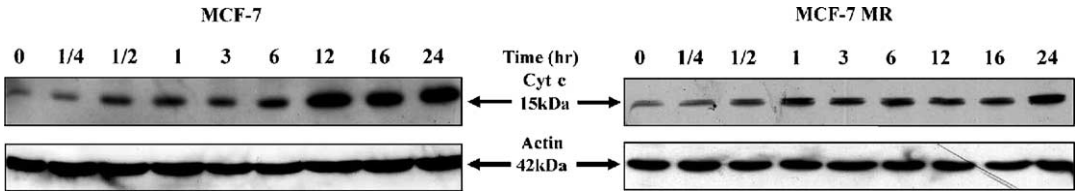

Fig. 3. Time-course of cytochrome c release from mitochondria to the cytosol in response to PG treatment. Cytosolic extracts (40 μg of protein) from MCF-7 and MCF-7 MR cells treated with 1 μM PG for the indicated times were resolved by SDS-PAGE and probed for cytochrome c. Results shown are typical examples of data from multiple experiments.

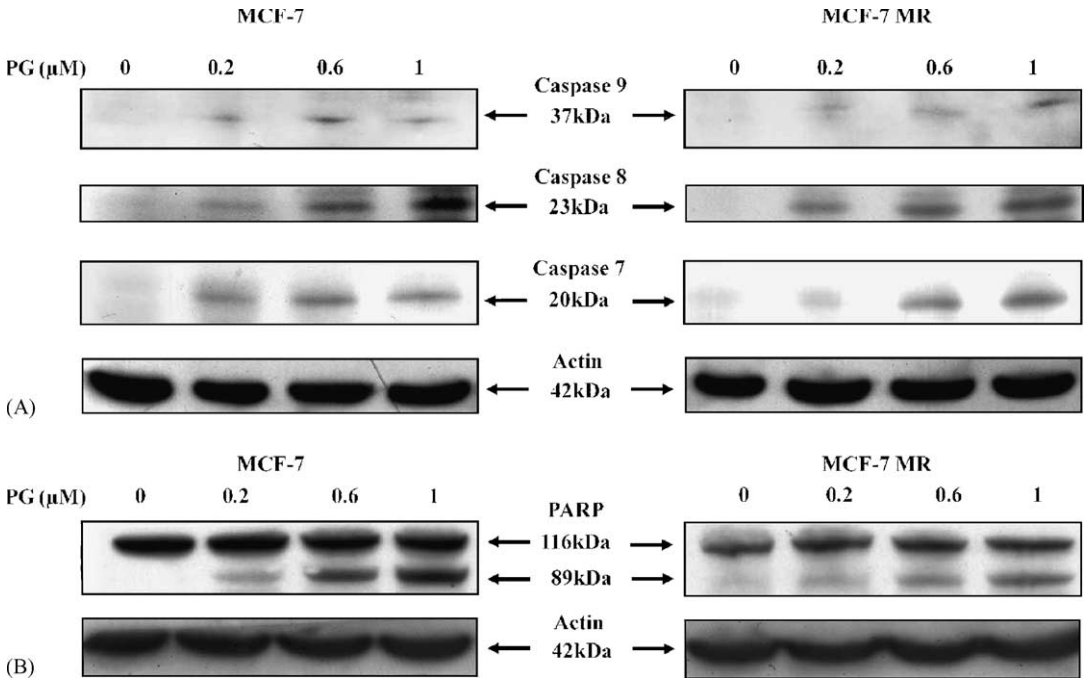

Fig. 4. Western blot analysis of PG-induced apoptosis through caspase activation and PARP cleavage. (A) Cleavage products of procaspase-9, -8 and -7; and (B) PARP cleavage in MCF-7 and MCF-7 MR. Cells were treated with the indicated PG concentrations for 16 h. Results shown are typical examples of data from multiple experiments.

genomes, we analyzed caspase-7 processing as a possible substitute. PG also induced processing of caspase-7, as shown by the appearance of its active form (20 kDa) (Fig. 4(A)). Furthermore, we compared cleavage of PARP, a DNA repair protein, in both PG-treated cell lines as a downstream signalling event indicative of apoptosis. All cells were treated with different doses of PG (0–1 μM) and cell extracts subjected to immunoblot analysis using an anti-PARP antibody that recognizes both the 116 kDa parent PARP and the 89 kDa cleavage product. As shown in Fig. 4(B), dose-dependant PARP cleavage was observed in both cell lines in response to PG treatment.

Finally, morphological changes associated with apoptosis were analyzed using Hoechst 33342 staining. The nuclei of both cell lines gave strong blue fluorescence and were condensed after PG treatment, although apoptotic bodies were not observed due to the atypical apoptosis that these cells undergo (data not shown) [22].

3.2.4. Triggering of mitochondrial apoptotic pathway

To further analyze the apoptotic pathway triggered by PG, we studied whether cytochrome *c* release was dependent or independent of caspase activity. MCF-7 cells were treated with PG in the presence or absence of the caspase inhibitor Z-VAD.fmk. We observed that cytochrome *c* was released from mitochondria even when caspases were not activated. As shown in Fig. 5, although caspase-9 was not active and the caspase substrate PARP was not cleaved in the presence of Z-VAD.fmk, cytochrome *c* was nevertheless released. This indicates that cytochrome *c* release precedes caspase activation, thus suggesting that PG-mediated apoptosis occurs using primarily mitochondria to transduce its death-inducing message.

3.3. No PG transportation by BCRP

FACS analysis of the uptake and efflux of auto-fluorescent PG was performed to determine whether this agent could be a substrate for the MDR transporter BCRP. The cells used in these experiments were the parental MCF-7 cells (very low levels of BCRP) and the MCF-7 MR cells

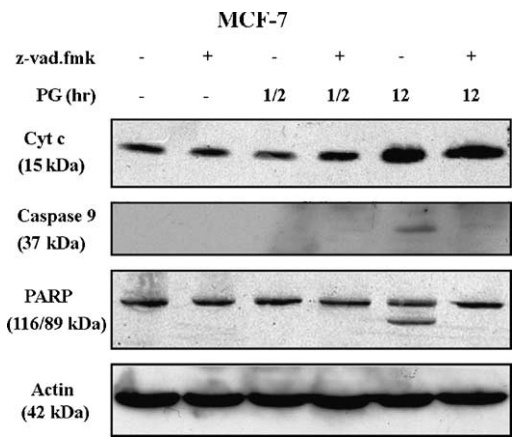

Fig. 5. Effect of PG on cytochrome c release, caspase-9 activation and PARP cleavage. MCF-7 cells were pre-treated with or without 100 μM Z-VAD.fmk 1 h before 1 μM PG treatment. Cytochrome c release and caspase-9 activation were analyzed in the cytosolic fraction, whilst PARP cleavage was observed in the nuclear containing extract. Results shown are typical examples of Western blot data from multiple experiments.

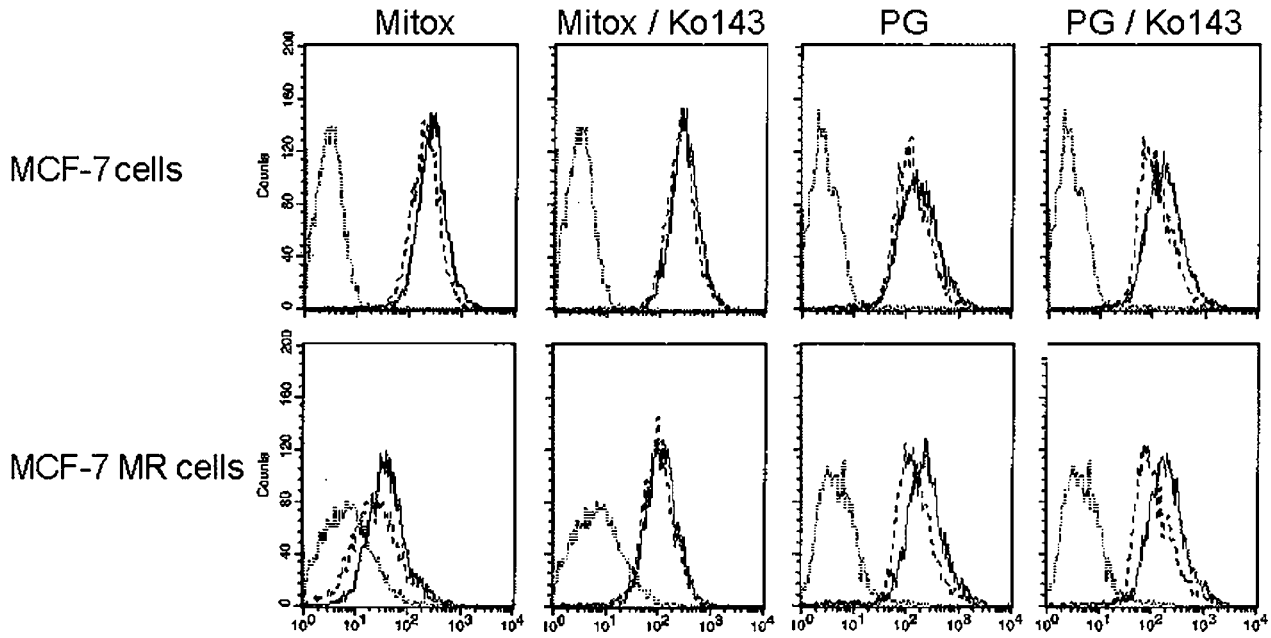

Fig. 6. FACS analysis of uptake and efflux of mitoxantrone and PG in a panel of MCF-7 cells. Upper panel: MCF-7 parent cells; no drug (auto fluorescence; dotted line) accumulation at time zero of efflux (sold line) and fluorescence levels after 60 min of efflux (dashed line) in the presence or absence of Ko143 with the appropriate drug. Lower panel: as above, but for MCF-7 MR (BCRP over-expressing cells).

(high levels of BCRP). As a positive control for BCRP activity, the drug mitoxantrone was used as a substrate. Furthermore, accumulation and efflux experiments were also performed in the presence of Ko143, a specific blocker of BCRP.

As expected, the MCF-7 parent cells accumulated high levels of both mitoxantrone and PG after the loading period and showed almost no active efflux after 60 min in fresh medium. The very low level of mitoxantrone efflux was inhibited when Ko143 was added during the efflux period (Fig. 6, upper panel). MCF-7 MR cells showed high levels of functionally active BCRP, as they accumulated much less of the typical BCRP–substrate mitoxantrone than the parental cells. After 60 min of efflux, the levels decreased even further. The accumulation of the drug could be significantly enhanced, almost to the levels of the parental cells, when the experiment was performed in the presence of Ko143. Under these conditions, no efflux of mitoxantrone was observed after 60 min, again confirming mitoxantrone as a typical substrate for the BCRP transporter. In contrast, PG accumulated to high levels in these MCF-7 MR cells, as high as observed in the parental cells. Some decrease in fluorescence levels after 60 min of efflux was noted, but the accumulation and efflux levels were not affected by the presence of Ko143 during the loading and/or efflux period (Fig. 6, lower panel).

These results indicate that PG is not a substrate for BCRP and it is unlikely that the effectiveness of this antineoplastic agent will be affected by the presence of the MDR transporter in tumor cells.

4. Discussion

Prodigiosins is a family of naturally occurring polypyrrole red pigments produced by a restricted group of microorganisms including some *Streptomyces* and *Serratia* strains. Some members of this family, including PG, have shown immunosuppressive [7,23,24] and apoptotic activities [9–12,25,26]. In the present study, we have extended our experiments on PG-induced apoptosis to breast cancer cells. Our results indicate that PG is an effective inducer of apoptosis in ER+ and ER− human breast cancer cells. The p53 accumulation, cytochrome *c* release, caspase activation, cleavage of PARP and distinctive morphological changes in the nucleus typified the apoptotic process. In addition, experiments with the caspase inhibitor Z-VAD.fmk elucidated the specific molecular pathway via mitochondria, triggered by PG. Finally, FACS analysis of PG accumulation and efflux in MCF-7 sublines showed that PG is not a substrate for the MDR transporter BCRP.

PG caused dose- and time-dependent cytotoxicity (reduction of cell number below the initial plating density) in MCF-7, MCF-7 MR and MDA-MB-231 cells. Cycloprodigiosin hydrochloride (*c*PrG·HCl) also has similar cytotoxic properties in many cancer cell lines, especially in breast cancer cells [25]. However, our cytotoxic assays were performed over shorter periods due to the more potent effect of PG observed in different cell lines [9,10,12]. The different effect could be a consequence of the C-6 methoxy substituent in PG since its substitution by a larger alkoxy substituent progressively reduced the activity of this compound [27].

Other novel anticancer agents for breast cancer have been reported. Among them, the marine compounds neoamphimedine and dehydrothyrsiferol [28,29] have been shown to have anti-neoplastic activities in both MCF-7 (IC_{50} = 1.8 μM at 72 h) and in MDA-MB-231 (IC_{50} = 14.8 μg/ml ± 1.2 at 48 h), respectively. Both of them are less effective than PG as shown by the lower PG IC_{50} values even at shorter times. Furthermore, paclitaxel, a drug currently used in breast cancer treatment, also showed a higher IC_{50} value for MDA-MB-231 cells in vitro (25 ± 1 μM at 24 h) [30]. Taken together, these results are very promising, especially for the estrogen-independent MDA-MB-231 cells as this kind of cancer is associated with a poorer prognosis and shorter survival.

Upon stress signals, p53 accumulation may induce two different sets of genes acting on growth control, undergoing cell cycle arrest due to an increase in p21 levels or on apoptosis and up-regulating the proapoptotic Bcl-2 family member Bax [3]. In MCF-7 cells, we have observed an increase in p53 levels as well as its DNA-binding activity followed by protein Bax expression leading to apoptosis as occurs with other drugs [31,32]. On the other hand, MCF-7 MR response to PG seems to be different at the doses examined since p53 is increasing p21 levels suggesting that these cells might try to undergo cell cycle arrest but finally the apoptotic process is driven. This could explain why the MCF-7 MR IC_{50} is slightly higher than that from its parental cell line. However, we have previous observations indicating that PG is able to induce apoptosis in a p53-independent manner [9,12] The ability of PG to induce apoptosis without the involvement of p53 may prove useful in therapy because p53 mutation is also associated with multidrug resistance in breast cancer [33].

The subcellular fractionation experiments revealed that PG induced mitochondrial cytochrome *c* release to the cytosol, indicating that outer mitochondrial membrane permeabilization is an early event in PG-induced apoptosis. It has been reported that this organelle has a central role in the apoptosis induced by many anticancer drugs, such as vitamin E isoforms in breast cancer cells [34]. Next, the activation of caspases-9, -8 and caspase-7 (as a caspase-3 alternative), as well as PARP cleavage, as a substrate for caspases, was also observed in PG-treated MCF-7 and MCF-7 MR cells. The lack of inhibition of cytochrome *c* release to the cytosol in the presence of the caspase inhibitor Z-VAD.fmk indicated that PG-induced apoptosis occurs via the mitochondrial pathway. Furthermore, in agreement with the previous data [22], we confirmed that MCF-7 cells do not express caspase-3 (data not shown). PG, even in the absence of caspase-3, induced a potent apoptosis in MCF-7 cells. Interestingly, the apoptotic process induced by doxorubicin and etoposide (currently used in breast cancer treatment), as well as cisplatin, an active chemotherapeutic agent used in clinical oncology, were all strongly enhanced by restoring caspase-3 in MCF-7 cells [35,36]. It remains to be seen whether a similar enhancement of PG cytotoxicity could appear in the presence of functional effector caspase-3.

The anthracyclines (doxorubicin, epirubicin) and taxanes (paclitaxel, docetaxel) are considered the most active agents for patients with advanced breast cancer [1]. However, some tumors do not respond and others eventually acquire resistance to several unrelated drugs. Some members of the ABC superfamily of transporter proteins can contribute to multidrug resistance in cancer chemotherapy. P-gp, MRP1 and the half-transporter BCRP are particularly implicated in this respect [37]. Over-expression of MDR1 P-gp confers resistance to vinblastine, vincristine, doxorubicin, daunorubicin, etoposide, teniposide, paclitaxel, docetaxel and many other drugs, whereas BCRP has relatively high affinity for mitoxantrone, topotecan and prazosin [15]. The MDR breast cancer cell line employed in this study was MCF-7 MR, a mitoxantrone-resistant cell line with a non-P-gp, non-MRP1 phenotype and elevated levels of BCRP mRNA [38–40]. These cells displayed a very high degree of resistance to mitoxantrone (1208-folds) [39], which is an inconvenience in cancer treatment, whilst the resistance showed to PG is very low (only 2-folds). In agreement with this low level of resistance to PG in this cell line, FACS analysis of accumulation and efflux of PG showed that this pro-apoptotic agent is not a substrate for the BCRP transporter. Furthermore, similar FACS experiments in the MDR1 P-gp over-expressing MCF-7 Dox40 cell line indicated that PG is also a rather poor substrate for this MDR transporter (data not shown). Moreover, PG has been shown to operate independently of the presence of the MRP-1 protein in a study performed in doxorubicin resistant small lung cancer cells that over-express MRP-1 [41].

In conclusion, the data reported here indicate that PG is a novel pro-apoptotic agent with potential as an anticancer agent, which may be effective irrespective of the presence of MDR transporter molecules.

Acknowledgements

The work presented in this paper was supported by a grant from the Ministry of Science and Technology and the European Union (SAF2001-3545), and by a ‘‘Marató de TV3’’ grant (Ref. no. 001510).

References

[1] Esteva FJ, Valero V, Pusztai L, Boehnke-Michaud L, Buzdar AU, Hortobagyi GN. Chemotherapy of metastatic breast cancer: what to expect in 2001 and beyond. Oncologist 2001;6:133–46.
[2] Kerr JFR, Wyllie AH, Currie AR. Apoptosis: a basic biological phenomenon with wide-ranging implications in tissue kinetics. Br J Cancer 1972;26:239–57.
[3] Slee EA, O’Connor DJ, Lu X. To die or not to die: how does p53 decide? Oncogene 2004;23 (16):2809–18.

[4] Green DR. Apoptotic pathways: the roads to ruin. Cell 1998;94:695–8.
[5] Salvesen GS, Dixit VM. Caspases: intracellular signalling by proteolysis. Cell 1997;91:443–6.
[6] Li P, Nijhawan D, Budihardjo I, Srinivasula SM, Ahmad M, Alnemri ES, et al. Cytochrome c and dATP-dependent formation of Apaf-1/caspase-9 complex initiates an apoptotic protease cascade. Cell 1997;91:479–89.
[7] Han SB, Kim HM, Kim YH, Lee CW, Jang ES, Son KH, et al. T-cell specific immunosuppression by prodigiosin isolated from *Serratia marcescens*. Int J Immunopharmacol 1998;20:1–13.
[8] Han SB, Park SH, Jeon YJ, Kim YK, Kim HM, Yang KH. Prodigiosin blocks T-cell activation by inhibiting interleukin-2R alpha expression and delays progression of autoimmune diabetes and collagen-induced arthritis. J Pharmacol Exp Ther 2001;299:415–25.
[9] Montaner B, Navarro S, Pique M, Vilaseca M, Martinell M, Giralt E, et al. Prodigiosin from the supernatant of *Serratia marcescens* induces apoptosis in haematopoietic cancer cell lines. Br J Pharmacol 2000;131:585–93.
[10] Diaz-Ruiz C, Montaner B, Perez-Tomas R. Prodigiosin induces cell death and morphological changes indicative of apoptosis in gastric cancer cell line HGT-1. Histol Histopathol 2001;16:415–21.
[11] Ramoneda BM, Perez-Tomas R. Activation of protein kinase C for protection of cells against apoptosis induced by the immunosuppressor prodigiosin. Biochem Pharmacol 2002;63:463–9.
[12] Campas C, Dalmau M, Montaner B, Barragan M, Bellosillo B, Colomer D, et al. Prodigiosin induces apoptosis of B- and T-cells from B-cell chronic lymphocytic leukemia. Leukemia 2003;17:746–50.
[13] Perez-Tomas R, Montaner B. Effects of the proapoptotic drug prodigiosin on cell cycle-related proteins in Jurkat T-cells. Histol Histopathol 2003;18:379–85.
[14] Gerlach JH, Kartner N, Bell DR, Ling V. Multidrug resistance. Cancer Surveys 1986;5:25–46.
[15] Litman T, Druley TE, Stein WD, Bates SE. From MDR to MXR: new understanding of multidrug resistance systems, their properties and clinical significance. Cell Mol Life Sci 2001;58:931–59.
[16] Juliano RL, Ling V. A surface glycoprotein modulating drug permeability in Chinese hamster ovary cells mutant. Biochim Biophys Acta 1976;455 (1):152–62.
[17] Cole SPC, Bhardwaj G, Gerlach JH, Mackie JE, Grant CE, Almquist KC, et al. Overexpression of a transporter gene in a multidrug-resistant human lung cancer cell line. Science 1992;258:1650–4.
[18] Doyle LA, Yang W, Abruzzo LV, Krogmann T, Gao Y, Rishi AK, et al. A multidrug resistance transporter from human MCF-7 breast cancer cells. Proc Natl Acad Sci USA 1998;95:15665–70.
[19] Mosmann T. Rapid colorimetric assay for cellular growth and survival: application to proliferation and cytotoxicity assays. J Immunol Methods 1983;65:55–63.
[20] Pique M, Barragan M, Dalmau M, Bellosillo B, Pons G, Gil J. Aspirin induces apoptosis through mitochondrial cytochrome *c* release. FEBS Lett 2000;480:193–6.
[21] Allen JD, van Loevezijn A, Lakhai JM, van der Valk MA, van Tellingen O, Reid G, et al. Potent and specific inhibition of the breast cancer resistance protein multidrug transporter in vitro and in mouse intestine by a novel analogue of fumitremorgin C. C Mol Cancer Ther 2002;1:417–25.
[22] Janicke RU, Sprengart ML, Wati MR, Porter AG. Caspase-3 is required for DNA fragmentation and morphological changes associated with apoptosis. J Biol Chem 1998;273:9357–60.
[23] Songia S, Mortellaro A, Taverna S, Fornasiero C, Scheiber EA, Erba E, et al. Characterization of the new immunosuppressive drug undecylprodigiosin in human lymphocytes. J Immunol 1997;158:3987–95.
[24] Kawauchi K, Shibutani K, Yagisawa H, Kamata H, Nakatsuji S, Anzai H, et al. A possible immunosuppressant, cycloprodigiosin hydrochloride, obtained from *Pseudoalteromonas denitrificans*. Biochem Bioph Res Co 1997;237:543–7.
[25] Yamamoto D, Kiyozuka Y, Uemura Y, Yamamoto C, Takemoto H, Hirata H, et al. Cycloprodigiosin hydrochloride, a H^+/Cl^- symporter, induces apoptosis in human breast cancer cell lines. J Cancer Res Clin Oncol 2000;126:191–7.
[26] Yamamoto D, Uemura Y, Tanaka K, Nakai K, Yamamoto C, Takemoto H, et al. Cycloprodigiosin hydrochloride, H^+/Cl^- symporter, induces apoptosis and differentiation in HL-60 cells. Int J Cancer 2000;88:121–8.
[27] D'Alessio R, Bargiotti A, Carlini O, Colotta F, Ferrari M, Gnocchi P, et al. Synthesis and immunosuppressive activity of novel prodigiosin derivatives. J Med Chem 2000;43:2557–65.
[28] Marshall KM, Matsumoto SS, Holden JA, Concepcion GP, Tasdemir D, Ireland CM, et al. The anti-neoplastic and novel topoisomerase II-mediated cytotoxicity of neoamphimedine, a marine pyridoacridine. Biochem Pharmacol 2003;66 (3):447–58.
[29] Pec MK, Aguirre A, Moser-Thier K, Fernandez JJ, Souto ML, Dorta J, et al. Induction of apoptosis in estrogen dependent and independent breast cancer cells by the marine terpenoid dehydrothyrsiferol. Biochem Pharmacol 2003;65:1451–61.
[30] Menendez JA, Barbacid MM, Montero S, Sevilla E, Escrich E, Solanas M, et al. Effects of gamma-linolenic acid and oleic acid on paclitaxel cytotoxicity in human breast cancer cells. Eur J Cancer 2001;37:402–13.
[31] Lowe SW, Ruley HE, Jacks T, Housman DE. p53-Dependent apoptosis modulates the cytotoxicity of anticancer agents. Cell 1993;74:957–67.
[32] Choudhuri T, Pal S, Agwarwal ML, Das T, Sa G. Curcumin induces apoptosis in human breast cancer cells through p53-dependent Bax induction. FEBS Letters 2002;512:334–40.
[33] Berns EM, Foekens JA, Vossen R, Look MP, Devilee P, Henzen-Logmans SC, et al. Complete sequencing of TP53 predicts poor response to systemic therapy of advanced breast cancer. Cancer Res 2000;60:2155–62.
[34] Takahashi K, Loo G. Disruption of mitochondria during tocotrienol-induced apoptosis in MDA-MB-231 human breast cancer cells. Biochem Pharmacol 2004;67:315–24.
[35] Yang XH, Sladek TL, Liu X, Butler BR, Froelich CJ, Thor AD. Reconstitution of caspase-3 sensitizes MCF-7 breast cancer cells to doxorubicin- and etoposide-induced apoptosis. Cancer Res 2001;61:348–54.
[36] Blanc C, Deveraux QL, Krajewski S, Janicke RU, Porter AG, Reed JC, et al. Caspase-3 is essential for procaspase-9 processing and cisplatin-induced apoptosis of MCF-7 breast cancer cells. Cancer Res 2000;60:4386–90.
[37] Borst P, Elferink RO. Mammalian ABC transporters in health and disease. Ann Rev Biochem 2002;71:537–92.
[38] Miyake K, Mickley L, Litman T, Zhan Z, Robey R, Cristensen B, et al. Molecular cloning of cDNAs which are highly overexpressed in mitoxantrone-resistant cells: demonstration of homology to ABC transport genes. Cancer Res 1999;59:8–13.
[39] Taylor CW, Dalton WS, Parrish PR, Gleason MC, Bellamy WT, Thompson FH, et al. Different mechanism of decreased drug accumulation in doxorubicin and mitoxantrone resistant variants of the MCF-7 human breast cancer cell line. Br J Cancer 1991;63:923–9.
[40] Scheffer GL, Maliepaard M, Pijnenborg AC, van Gastelen MA, de Jong MC, Schroeijers AB, et al. Breast cancer resistance protein is localized at the plasma membrane in mitoxantrone- and topotecan-resistant cell lines. Cancer Res 2000;60:2589–93.
[41] Llagostera E, Soto-Cerrato V, Montaner B, Perez-Tomas R. Prodigiosin triggers apoptosis in breast and lung cancer cell lines. In: Marc Diederich, editor. Proceedings of the apoptosis 2003, from signalling pathways to therapeutic tools meeting. Kirchberg, Luxemborg, 26 January–1 February 2003; 2003; 88.

Capítulo 2.2. Identificación de dianas moleculares de prodigiosina mediante el análisis de la expresión génica. Estudio de la inducción del gen proapoptótico NAG-1 en células humanas de cáncer de mama.

("Soto-Cerrato V, Viñals F, Lambert JR, Kelly JA, Pérez-Tomás R. Prodigiosin induces the proapoptotic gene NAG-1 via glycogen synthase kinase-3 beta activity in human breast cancer cells. Mol Cancer Ther 2007;6(1):362-9").

Una vez caracterizado el efecto proapoptótico que induce prodigiosina en células de cáncer de mama MCF-7, quisimos profundizar en los mecanismos moleculares responsables de desencadenar dicho proceso celular. Con esta finalidad, analizamos los cambios en la expresión génica de estas células, tras el tratamiento con prodigiosina durante 24 h, mediante experimentos con matrices de cDNA de genes relacionados con cáncer. La mayoría de los genes significativamente modificados estaban relacionados con apoptosis, ciclo celular, adhesión celular o regulación de la transcripción. El impresionante aumento en la expresión del gen proapoptótico NAG-1 nos hizo pensar en él como un candidato interesante, el cual podía estar implicado en el mecanismo de inducción de citotoxicidad en MCF-7. Los resultados mostraron que prodigiosina inducía la acumulación del gen supresor de tumores p53 pero que la inducción de NAG-1 era independiente de éste. Además, prodigiosina causó desfosforilación de AKT y activación de GSK-3β, efectos que se correlacionaban con la expresión de NAG-1. La apoptosis inducida por prodigiosina se bloqueaba al inhibir GSK-3β. Esto debía ser causado, al menos en parte, por el bloqueo de la sobreexpresión inducida por GSK-3β, de los receptores de muerte DR-4 y DR-5. Todo ello nos sugiere que la activación de GSK-3β tras el tratamiento con prodigiosina es un acontecimiento clave en la regulación de las rutas moleculares que activan la apoptosis inducida por este agente anticanceroso.

Prodigiosin induces the proapoptotic gene *NAG-1* via glycogen synthase kinase-3β activity in human breast cancer cells

Vanessa Soto-Cerrato,[1] Francesc Viñals,[2] James R. Lambert,[3] Julie A. Kelly,[3] and Ricardo Pérez-Tomás[1]

[1]Department of Pathology and Experimental Therapeutics, Cancer Cell Biology Research Group and [2]Departament de Ciències Fisiològiques II, Campus de Bellvitge, Universitat de Barcelona, Barcelona, Spain; and [3]Department of Pathology, University of Colorado Denver and Health Science Center, Aurora, Colorado

Abstract

Prodigiosin (2-methyl-3-pentyl-6-methoxyprodigiosene) is a bacterial metabolite that has anticancer and antimetastatic properties. However, the molecular mechanisms responsible for these abilities are not fully understood. Gene expression profiling of the human breast cancer cell line MCF-7 treated with prodigiosin was analyzed by cDNA array technology. The majority of the significantly modified genes were related to apoptosis, cell cycle, cellular adhesion, or transcription regulation. The dramatic increase of the *nonsteroidal anti-inflammatory drug-activated gene 1* (*NAG-1*) made this gene an interesting candidate regarding the possible mechanism by which prodigiosin induces cytotoxicity in MCF-7 cells. Our results show that prodigiosin triggers accumulation of the DNA-damage response tumor-suppressor protein p53 but that NAG-1 induction was independent of p53 accumulation. Moreover, prodigiosin caused AKT dephosphorylation and glycogen synthase kinase-3β (GSK-3β) activation, which correlated with NAG-1 expression. Prodigiosin-induced apoptosis was recovered by inhibiting GSK-3β, which might be due, at least in part, to the blockade of the GSK-3β–dependent up-regulation of death receptors 4 and 5 expression. These findings suggest that prodigiosin-mediated GSK-3β activation is a key event in regulating the molecular pathways that trigger the apoptosis induced by this anticancer agent. [Mol Cancer Ther 2007;6(1):362–9]

Received 5/9/06; revised 10/13/06; accepted 11/27/06.

Grant support: Ministerio de Ciencia y Tecnología and European Union grant SAF2001-3545 (R. Pérez-Tomás) and American Cancer Society Research Scholar award RSG-04-170-01-CNE (J.R. Lambert).

The costs of publication of this article were defrayed in part by the payment of page charges. This article must therefore be hereby marked *advertisement* in accordance with 18 U.S.C. Section 1734 solely to indicate this fact.

Requests for reprints: Ricardo Pérez-Tomás, Department of Pathology and Experimental Therapeutics, Cancer Cell Biology Research Group, Universitat de Barcelona, Pavelló Central, 5a planta, LR 5101 C/Feixa Llarga s/n, E 08907 L'Hospitalet, Barcelona, Spain.
Phone: 34-934024288; Fax: 34-934029082. E-mail: rperez@ub.edu

doi:10.1158/1535-7163.MCT-06-0266

Introduction

Cancer is a major public health problem in most developed countries. In particular, breast cancer is the most commonly diagnosed cancer among women and the second greatest cause of cancer deaths in women in most Western societies (1). Adjuvant chemotherapy has been proven to decrease the risk of relapse and cancer-related mortality in women with early-stage breast cancer. Moreover, chemotherapy is the treatment of choice for patients with hormone-insensitive and metastatic breast carcinomas (2). Unfortunately, most patients eventually develop recurrences due to the appearance of resistance to drugs after its reiterated administration. Thus, there is a need for new chemotherapeutic agents with novel and well-defined mechanisms of action.

The antimalarial, immunosuppressive, and procytotoxic bacterial metabolite prodigiosin (3) has recently been described as a novel anticancer and antimetastatic agent (4, 5). Prodigiosin promotes apoptosis in a wide variety of human cancer cell lines, including hematopoietic, gastrointestinal, and breast and lung cancer cells, with no marked toxicity in nonmalignant cells (4, 6–10). Prodigiosin triggers mitochondria-mediated apoptosis irrespective of multidrug resistance phenotype (9), and this apoptosis can be induced in p53-deficient cells (4). These features suggest an advantage to prodigiosin as an anticancer agent because they are very common phenomena that limit chemotherapy effectiveness. The molecular mechanism of prodigiosin cytotoxicity seems to be complex as it alters several biological processes of potential importance to cell viability. For example, prodigiosin has been shown to modulate intracellular pH through lysosomal alkalinization (11, 12), inhibit cell proliferation via G_1-S transition arrest (13), and interact with DNA inducing single- and double-strand breaks and topoisomerase I and II inhibition (14, 15).

Although the anticancer and proapoptotic activities of prodigiosin have been intensively studied, the molecular targets responsible for these properties have not yet been elucidated. To this end, we did gene expression profiling of MCF-7 breast cancer cells after treatment with prodigiosin. The most highly induced gene identified was *nonsteroidal anti-inflammatory drug-activated gene 1/growth differentiation factor 15* (*NAG-1*). NAG-1 is a secreted protein with homology to members of the transforming growth factor-β superfamily. Forced expression of NAG-1 in a variety of cell types has been related to cell cycle arrest and apoptosis (16–18). Many antitumorigenic compounds, including cyclooxygenase inhibitors (19), 2-(4-amino-3-methylphenyl)-5-fluorobenzothiazole (20), retinoids (21), genistein (22), resveratrol (23), and vitamin D (24) have been shown to up-regulate NAG-1 expression. Several

mechanisms of NAG-1 induction have been described. NAG-1 expression can be induced in a p53-dependent (22–25) or p53-independent (26) manner. Other proteins that have been linked to NAG-1 expression are the early growth response gene-1 (27, 28), protein kinase C through nuclear factor-κB binding to NAG-1 promoter (29), and glycogen synthase kinase-3β (GSK-3β) through the phosphatidylinositol 3-kinase (PI3K)/AKT/GSK-3β pathway (30).

In the present study, we examine the molecular mechanism of prodigiosin-mediated induction of NAG-1 in MCF-7 cells and provide new insight into the molecular mechanism by which prodigiosin induces apoptosis in breast cancer cells.

Materials and Methods

Purification of Prodigiosin

Prodigiosin (2-methyl-3-pentyl-6-methoxyprodigiosene; Fig. 1) was extracted by shaking the *Serratia marcescens* 2170 cells with a mixture of methanol/1 N HCl (24:1). After centrifugation (68,006 × *g* for 15 min), the solvent of the supernatant was evaporated under vacuum. Atmospheric pressure liquid chromatography of the extract was done on silica gel with chloroform and methanol as solvents. The eluted pigmented fractions were pooled and the chloroform/methanol extract was vacuum evaporated, redissolved in H_2O, and lyophilized. The isolated pigment was redissolved in methanol and analyzed by electrospray ionization mass spectrometry using a VG-Quattro triple quadrupole mass spectrometer (Micromass, VG-Biotech, Manchester, United Kingdom). The isolated pigment was repurified by subsequent semipreparative high-performance liquid chromatography carried out on a Shimadzu instrument (Shimadzu, Kyoto, Japan). A Nucleosil C18 reversed-phase column (25,064 mm, 10 mm) was used with a 0 ± 100% linear gradient in 30 min [A, 0.01 mol/L ammonium acetate (pH 7); B, 100% acetonitrile]. The elution was monitored by both using diode-array UV detector (SPD-M10AVP Shimadzu) and electrospray ionization mass spectrometry. After repeated injections, the pooled fractions containing the major peak were vacuum evaporated, redissolved in H_2O, lyophilized, and characterized by electrospray ionization mass spectrometry and ^1H nuclear magnetic resonance. Electrospray ionization, *m/z* 324.4 (M+H)+, [$C_{20}H_{25}N_3O$ requires 323.4381 (molecular weight average)]. ^1H nuclear magnetic resonance (CD3OD, 500 MHz, ppm); 10.71 (m, NH), 8.54 (m, NH), 7.08 (s, 1H), 6.95 (s, 1H), 6.88 (m, 1H), 6.83 (m, 1H), 6.30 (m, 1H), 6.25 (s, 1H), 3.96 (s, 3H), 2.43 (t, 2H), 1.58 (s, 3H), 1.2 ± 1.4 (m, 6H), 0.91 (t, 3H). Stock solutions, with purity >95%, were prepared in methanol, and concentrations were determined by UV-Vis in 95% ethanol-HCl (ϵ_{535} = 11,2000/M cm).

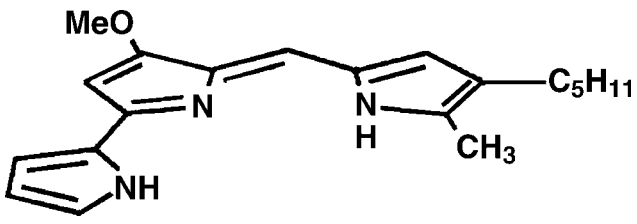

Figure 1. Side-on view of 2-methyl-3-pentyl-6-methoxyprodigiosene (prodigiosin) showing the planar arrangement of the three pyrrole rings.

Drugs

AR-A014418 was purchased from Calbiochem (EMD Biosciences, Darmstadt, Germany).

Cell Lines and Culture Conditions

Human breast cancer cell lines MCF-7 and MDA-MB-231 were purchased from American Type Culture Collection (Manassas, VA) and cultured in DMEM:Ham's F-12 (1:1; Biological Industries, Beit Haemek, Israel) supplemented with 10% heat-inactivated fetal bovine serum (FBS; Life Technologies, Carlsbad, CA), 100 units/mL penicillin, 100 μg/mL streptomycin, and 2 mmol/L L-glutamine. Cells were grown at 37°C in a 5% CO_2 atmosphere.

cDNA Array Analysis

MCF-7 cells were left untreated or treated with 0.5 μmol/L prodigiosin for 24 h. Atlas Pure Total RNA Labeling kit (Clontech, BD Biosciences, Palo Alto, CA) was used for total RNA isolation, polyadenylated RNA enrichment, and probe synthesis according to the manufacturer's instructions. Gene expression profiles were determined by hybridization to cDNA arrays (Atlas Human Cancer Array 1.2 from Clontech, BD Biosciences) and analyzed using AtlasImage 2.7 software. Three replicate arrays for each condition were averaged, and the composite arrays created were compared. Global normalization using the sum method, which adds the values of signal over background for all genes on the arrays to calculate the normalization coefficient, was used. The ratio corresponds to the expression of each gene relative to the untreated control cells (treated array gene adjusted intensity/control array gene adjusted intensity). A value of >2 or <0.5 is displayed in the ratio column when numerical values cannot be calculated because the gene signal on one array is at background level and is thus considered 0.

Quantitative Real-time Reverse Transcription-PCR

MCF-7 cells were treated with 0.5 μmol/L prodigiosin for 24 h. The inhibitor AR-A014418 (50 μmol/L) was added 30 min before prodigiosin treatment. Total RNA extraction was done using TRIzol reagent (Invitrogen Life Technologies), and cDNA synthesis was done using random hexamers and MuLV reverse transcriptase according to the manufacturer's instructions (Applied Biosystems, Warrington, United Kingdom). Each cDNA sample was analyzed for the expression of several genes using the fluorescent TaqMan 5′ nuclease assay. Oligonucleotide primers *nag-1* (*gdf-15*), *dr-4* (*tnfrsf10a*), *dr-5* (*tnfrsf10b*), *β-actin* (*actb*), and probes were purchased as Assay-on-Demand Gene Expression Products (Applied Biosystems). PCR assays were done using the ABI PRISM 7700 Sequence Detection System (Applied Biosystems). Gene expression levels were normalized to β-actin, and relative mRNA expression was presented in relation to the control. Data were analyzed using Sequence Detector Software (version

1.9, Applied Biosystems) and are presented as mean ± SD of three independent experiments. For statistical analysis among treatment groups, ANOVA and least significant difference tests were done with the Statgraphics plus 5.1 statistical software.

Western Blot Analysis

MCF-7 cells were treated with several concentrations of prodigiosin for different times depending on the experiment. AR-A014418, when used, was added 30 min before prodigiosin treatment. Supernatants were collected, and cells were washed with PBS before addition of lysis buffer [85 mmol/L Tris-HCl (pH 6.8), 2% SDS, 1 μg/mL aprotinin, 1 μg/mL leupeptin, and 0.1 mmol/L phenylmethylsulfonyl fluoride]. Protein concentration was determined with BCA protein assay (Pierce, Rockford, IL) using bovine serum albumin as standard. Fifty micrograms of protein extracts were separated by 12% SDS-PAGE and transferred to Immobilon-P membranes (Millipore, Bedford, MA). Blots were developed with primary antibodies according to the manufacturer's instructions. Antibodies were obtained from the following sources: anti–NAG-1/PTGF-β and anti–POLY(ADP)RIBOSE POLYMERASE were from Santa Cruz Biotechnology (Santa Cruz, CA); anti–CASPASE-8 was from PharMingen (BD Biosciences); anti-P53 was from Neomarkers (Fremont, CA); phosphorylated AKT (Ser^{473}) was from Cell Signaling Technology (Beverly, MA); and anti–β-ACTIN and anti-VINCULIN were from Sigma Chemical Co. (St. Louis, MO). Antibody binding was detected with the appropriate secondary antibodies conjugated to horseradish peroxidase, and signals were detected using the enhanced chemiluminescence detection kit (Amersham, Buckinghamshire, United Kingdom). Vinculin was used as gel loading controls. Results shown are representative data obtained from three independent experiments.

Dominant Negative p53 Retrovirus Production and Infection of MCF-7 Cells

An amphotropic packaging cell line (Phoenix cells, a gift from Dr. Garry Nolan, Stanford University, Stanford, CA) was used to prepare dominant negative p53 retrovirus capable of infecting human MCF-7 cells. Eighteen hours before transfection, Phoenix cells were plated at 1×10^6 per 6-cm dish in 3 mL DMEM + 10% FBS. The cells were transfected with 10 μg pMSCV-IRES-GFP-p53dd or empty vector (gifts from Dr. James DeGregori, University of Colorado Health Sciences Center, Aurora, CO) using FuGENE 6 reagent (2 μL of FuGENE 6 per microgram of DNA). Twenty-four hours posttransfection, the medium on transfected Phoenix cells was changed to 3 mL fresh DMEM + 10% FBS. On this day, MCF-7 cells were plated at 2×10^5 per 6-cm dish in 3 mL DMEM + 10% FBS for viral infection. Forty-eight hours posttransfection, 3 mL of medium from transfected Phoenix cells were collected and filtered through a 0.45-μm filter to remove cellular debris. One milliliter of medium was removed and discarded from MCF-7 cells plated 24 h earlier. Three microliters of polybrene (5 mg/mL) were added to the remaining 2 mL medium on MCF-7 cells, and the plate was gently rocked to ensure mixing. Filtered viral medium (1 mL) was added dropwise to MCF-7 cells. Cells were allowed to incubate at 37°C for 24 h. Twenty-four hours postinfection, the medium on MCF-7 cells was refreshed with 3 mL DMEM + 10% FBS. Infected MCF-7 cells were fed and passaged as needed in DMEM + 10% FBS. pMSCV-IRES-GFP-p53dd contains the green fluorescent protein gene, which facilitated the identification of virally infected cells by flow cytometry. A pool of green fluorescent cells was recovered from infection with both empty viral vector and p53 dominant negative.

Cell Viability Assay

MCF-7 cell viability was determined using the 3-(4,5-dimethylthiazol-2-yl)-2,5-diphenyltetrazolium bromide (MTT) assay (31). Cells were plated in triplicate wells (2.5×10^4 per well) in 100 μL of growth medium in 96-well plates and incubated for 24 h. Then, cells were pretreated for 30 min with 50 μmol/L AR-A014418 before treatment with 1.4 μmol/L prodigiosin. After 24-h incubation, 10 μmol/L MTT (Sigma Chemical) was added to each well for an additional 4 h. The formazan precipitate was dissolved in 100 μL of isopropanol/1 N HCl (24:1), and absorbance at 570 nm was measured on a multiwell plate reader. Cell viability was expressed as a percentage of control and data are shown as the mean value ± SD of three independent experiments. Statistical analysis (ANOVA and least significant difference tests) was carried out with the Statgraphics plus 5.1. statistical software.

Results

Gene Expression Profiling Identifies *NAG-1* as a Prodigiosin Target Gene in MCF-7 Cells

To elucidate which genes are potentially involved in the cytotoxic cellular response of the anticancer agent prodigiosin (Fig. 1) in MCF-7 cells, changes in the expression profile of 1,176 genes on the Atlas Human Cancer Array 1.2 (BD Biosciences Clontech) were analyzed. MCF-7 cells were treated with 0.5 μmol/L prodigiosin for 24 h. This concentration of prodigiosin was used because it represents the IC_{25} (drug concentration that caused a cell viability decrease of 25% in cell viability) previously reported (9). Genes whose expression was up-regulated >2-fold or down-regulated >0.5-fold were considered to be significantly modulated by prodigiosin treatment (Table 1). Among the 20 up-regulated and 17 down-regulated genes, most of them were related to apoptosis, cell cycle, cellular adhesion, or transcriptional regulation. One particular gene, *NAG-1*, was the most highly induced after prodigiosin treatment. This gene, encoding a protein implicated in cell cycle blockage and apoptosis, was chosen for further study. Quantitative real-time reverse transcription-PCR and immunoblotting assays were done to confirm up-regulation of NAG-1 by prodigiosin treatment of MCF-7 cells. Total RNA and protein were prepared from MCF-7 cells treated with 0.5 μmol/L prodigiosin for 1, 8, and 24 h. NAG-1 mRNA levels

increased significantly in a time-dependent manner (79-fold increase at 24 h; Fig. 2A). A concomitant increase in NAG-1 protein was also observed starting at 4 h of prodigiosin treatment (Fig. 2B).

Prodigiosin-Mediated Induction of *NAG-1* Is p53 Independent

NAG-1 is a p53 target gene (17). However, the induction of NAG-1 by various compounds has been shown to be both p53 dependent and p53 independent. For example, resveratrol increases the cellular level of p53 in human colorectal cancer cells, thus promoting NAG-1 expression (23). We therefore examined p53 levels in MCF-7 and MDA-MB-231 breast cancer cells after prodigiosin treatment. MCF-7 cells were treated with 0.5 μmol/L prodigiosin for various times and p53 levels were determined by immunoblot analysis. Although a decrease in p53 levels at 4 and 8 h of treatment was observed, at 16 and 24 h of treatment, p53 protein levels increased, which correlated with increased NAG-1 protein levels (Fig. 3A). Moreover, when MCF-7 cells were treated with higher doses of prodigiosin corresponding to IC_{25}, IC_{50}, and IC_{75} values for 24 h, a parallel increase in p53 and NAG-1 protein levels was observed (Fig. 3B). However, p53 accumulation is not necessary for NAG-1 expression induced by prodigiosin because cells harboring mutant p53 (MDA-MB-231) treated with prodigiosin (doses corresponding to IC_{25}, IC_{50}, and IC_{75} values at 24 h for these cells) also express NAG-1 despite the lack of functional p53 (Fig. 2B). To further investigate the p53 independence of prodigiosin-mediated induction of NAG-1, we expressed a dominant negative

Table 1. Differentially expressed genes in MCF-7 cells after prodigiosin treatment

Gene name	Genbank no.	SwissProt no.	Ratio	Classification
Up-regulated genes				
Interferon induced transmembrane protein 1 (9-27) (IFITM1)	J04164	P13164	2.06	Cell cycle
Cyclin-dependent kinase inhibitor 1 (CDKN1A/p21)	U09579	P38936	>2	Cell cycle
Fms-related tyrosine kinase 1 (FLT1)	X51602	P17948	>2	Cell cycle
Junction plakoglobin (JUP)	M23410	P14923	>2	Cell adhesion
Ubiquitin-conjugating enzyme E2 17-kDa (UBE2A)	M74524	P49459	>2	Protein turnover
Purine-rich ssDNA-binding protein α (PURA)	M96684	Q00577	>2	Transcription regulator and DNA replication
Zinc finger protein 36 (ZFP36L1)	X79067	Q07352	>2	Transcription regulator
Integrin β_4 (ITGB4)	X53587	P16144	>2	Cell adhesion
HLA-G histocompatibility antigen, class I, G (HLA-G)	M32800	Q30182	>2	Cellular defense response
Procollagen (type III) N-endopeptidase (PCOLN3)	U58048	Q15779	>2	Cell cycle
Teratocarcinoma-derived growth factor 3 (TDGF3)	M96956	P13385	>2	Cell differentiation
Interleukin-1, β (IL1B)	K02770	P01584	>2	Cell cycle and apoptosis
Cell division cycle 34 (CDC34)	L22005	P49427	>2	Protein turnover and cell cycle
Nonsteroidal anti-inflammatory drug-activated gene 1/growth differentiation factor 15 (NAG-1/GDF15)	AF019770	Q99988	11.72	Cytokine activity, cell cycle and apoptosis
RAN binding protein 2 (RANBP2)	L41840	P49792	>2	Trafficking/targeting protein
Keratin 7 (KRT7)	X03212	P08729	>2	Cytoskeleton protein
IFN-stimulated exonuclease gene 20 kDa (ISG20)	U88964	O00586	>2	Cell cycle
Proteasome activator subunit 1 (PSME1)	L07633	Q06323	>2	Protein turnover
Eukaryotic translation elongation factor 1α1 (EEF1A1)	M27364	Q14222	2.22	Translation elongation
Insulin-induced gene 1 (INSIG1)	U96876	O15503	>2	Metabolism
Down-regulated genes				
Deleted in colorectal carcinoma (DCC)	X76132	P43146	<0.5	Cell cycle and apoptosis
v-myc myelocytomatosis viral oncogene homologue (MYC/c-myc)	V00568	P01106	0.36	Cell cycle
Notch homologue 4 (NOTCH4)	U95299	O00306	<0.5	Cell differentiation
v-abl Abelson murine leukemia viral oncogene homologue 2 (ABL2)	M35296	P42684	<0.5	Oncogenes
Prostaglandin E synthase (PTGES)	AF010316	O14684	<0.5	Metabolism
Prohibitin 2 (PHB2)	U72511	Q99623	<0.5	Transcription regulator
Guanylate kinase 1 (GUK1)	L76200	Q16774	<0.5	Metabolism
Rho GDP dissociation inhibitor (GDI) α (ARHGDIA)	X69550	P52565	0.44	Cell motility and apoptosis
TNF receptor-associated protein 1 (TRAP1)	U12595	Q12931	0.43	Apoptosis-associated proteins
Retinoic acid receptor, γ (RARG)	M24857	P13631	<0.5	Transcription regulator
Macrophage migration inhibitory factor (MIF)	M25639	P14174	0.47	Apoptosis-associated proteins
TIMP metallopeptidase inhibitor 1 (TIMP1)	X03124	P01033	<0.5	Cell cycle
Vitronectin (VTN)	X03168	P04004	<0.5	Cell adhesion
Keratin 8 (KRT8)	M34225	P05787	0.17	Cytoskeleton protein
Hemoglobin, α1 (HBA1)	V00491	P01922	<0.5	Trafficking/targeting proteins
Keratin 18 (KRT18)	M26326	P05783	<0.5	Cytoskeleton protein
Nonmetastatic cells 4, protein expressed in (NME4)	Y07604	O00746	<0.5	Metabolism

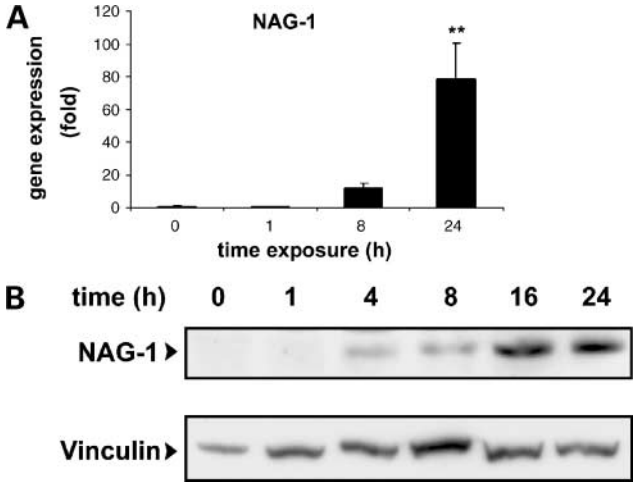

Figure 2. Effect of prodigiosin treatment on NAG-1 expression in MCF-7 cells. **A,** MCF-7 cells were treated for 1, 8, and 24 h with 0.5 μmol/L prodigiosin, and fold changes of gene expression with respect to control cells were determined by quantitative real-time reverse transcription-PCR. *Columns,* mean of triplicate experiments, normalized by using actin mRNA expression; *bars,* SD. *, $P < 0.05$; **, $P < 0.01$, statistical significance among groups. **B,** time course analysis of protein levels in 0.5 μmol/L prodigiosin-treated MCF-7 cells subjected to immunoblotting with NAG-1 antibody. Vinculin is shown as a loading control, and representative blots of independent experiments are shown.

p53 (pMSCV-IRES-GFP-p53dd) in MCF-7 cells and analyzed NAG-1 protein levels. MCF-7 cells were infected with a retrovirus expressing a dominant negative form of p53. Western analysis for NAG-1 and p53 was done on a pool of virally infected cells. We compared protein levels in MCF-7 cells infected with the dominant negative–expressing retrovirus and MCF-7 cells infected with empty virus as a control. As shown in Fig. 3C, expression of dominant negative p53 in MCF-7 cells had no effect on NAG-1 expression. The blot was stripped and reprobed for an indicator of the efficiency of dominant negative p53 function: stabilization of p53. Infection of cells with pMSCV-IRES-GFP-p53dd results in stabilization of p53, indicating strong dominant negative p53 function in these cells. Taken together, although prodigiosin treatment of MCF-7 cells increases p53 protein levels, prodigiosin-mediated NAG-1 induction in breast cancer cells is p53 independent.

Prodigiosin-Mediated Induction of NAG-1 in MCF-7 Cells Is Dependent on GSK-3β Activity

The GSK-3β kinase has been implicated in *NAG-1* gene expression (30). To determine whether GSK-3β contributes to prodigiosin-mediated induction of NAG-1 in MCF-7 cells, experiments using a specific inhibitor of GSK-3β, AR-A014418, were done. MCF-7 cells were preincubated with 50 μmol/L AR-A014418 before treatment with 0.5 μmol/L prodigiosin. Prodigiosin-mediated induction of NAG-1 mRNA and protein was completely blocked after AR-A014418 treatment (Fig. 4). We also observed that prodigiosin caused dephosphorylation of AKT, a negative GSK-3β regulator. This could provoke GSK-3β activation, which may explain NAG-1 accumulation after prodigiosin treatment (Fig. 4B). To investigate whether GSK-3β activity was involved in the apoptotic phenotype induced by prodigiosin, cell viability experiments were done in the presence of AR-A014418. We observed that prodigiosin-mediated MCF-7 cell death was blocked by cotreatment with prodigiosin and AR-A014418 (Fig. 4C).

GSK-3β, through Regulation of Death Receptors 4 and 5 Expression, Is Implicated in Prodigiosin-Induced Apoptosis

It was previously shown that forced expression of NAG-1 significantly induced death receptor-4 (DR-4) and DR-5 induction in gastric cancer cells treated with the proapoptotic drug sulindac sulfide (32). Therefore, we analyzed gene expression of DR-4 and DR-5 in relation to GSK-3β activity in MCF-7 cells treated with prodigiosin (Fig. 5A). We observed a significant increase in DR-4 and DR-5

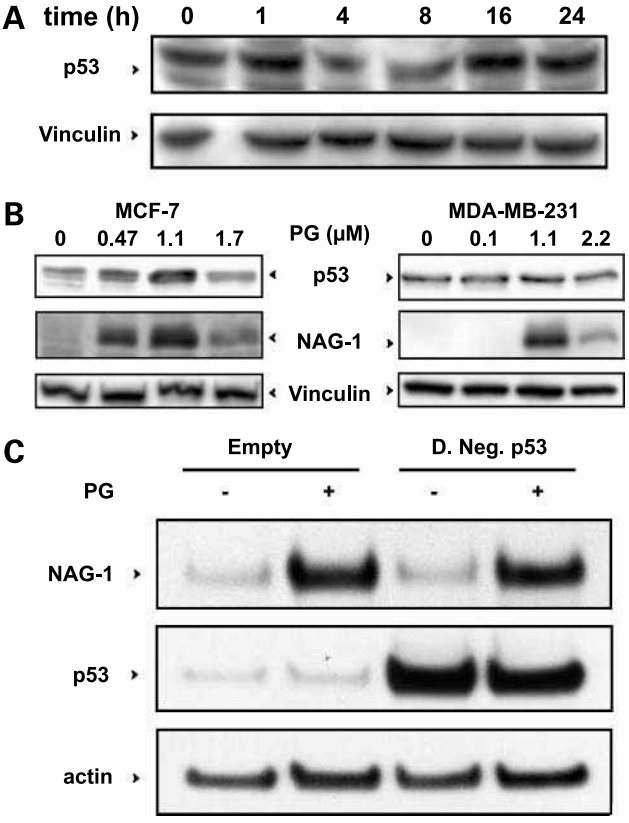

Figure 3. Analysis of p53 protein accumulation after prodigiosin exposure. **A,** cells were treated with 0.5 μmol/L prodigiosin for different times and cell lysates were subjected to Western blotting with p53 antibody. **B,** MCF-7 and MDA-MB-231 cells were incubated with different prodigiosin doses corresponding to their respective IC_{25}, IC_{50}, and IC_{75} values at 24 h and then subjected to immunoblotting for p53 and NAG-1 detection. Vinculin is shown as a loading control. **C,** MCF-7 cells were infected with a retrovirus expressing a dominant negative p53 (*D.Neg.p53*). A pool of infected cells was analyzed for NAG-1 protein levels after prodigiosin (*PG*) treatment (0.5 μmol/L). The same blot was stripped and developed with antibodies against NAG-1, p53, and β-actin as a loading control.

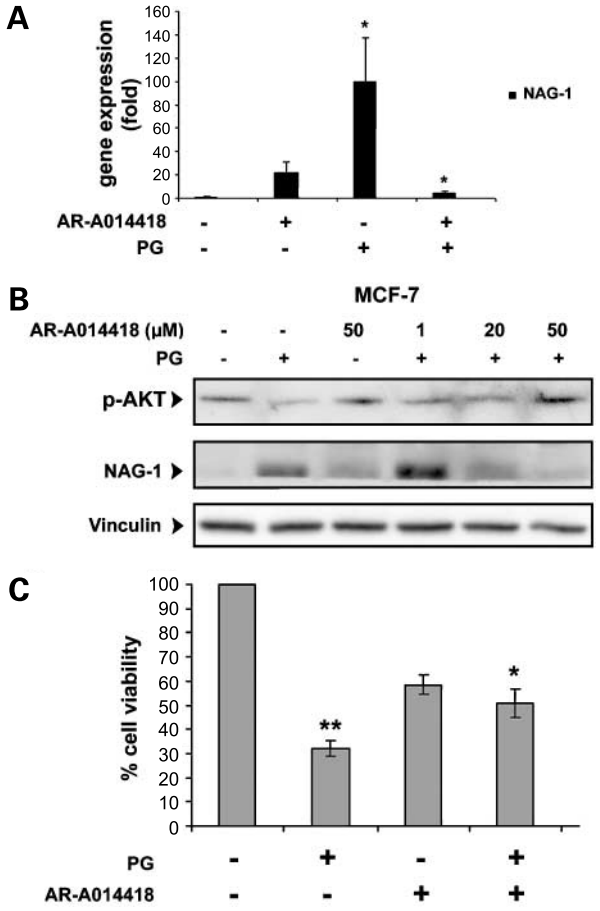

Figure 4. NAG-1 and cell viability regulation by GSK-3β. **A,** MCF-7 cells were exposed to 0.5 μmol/L prodigiosin for 24 h in the absence or presence of 50 μmol/L AR-A014418, and changes in gene expression (fold changes with respect to control cells) were evaluated by quantitative real-time reverse transcription-PCR. *Columns,* means of three independent experiments; *bars,* SD. *, $P < 0.05$, significant induction by prodigiosin or inhibition when combined with AR-A014418. **B,** after treating cells with 0.5 μmol/L prodigiosin for 24 h with or without 1, 20, or 50 μmol/L AR-A014418, cell lysates were collected for Western blot analysis using phosphorylated AKT (*p-AKT*), NAG-1, and vinculin antibodies. The latter is shown as a gel loading control, and representative blots of independent experiments are shown. **C,** cells were incubated with 1.4 μmol/L prodigiosin for 24 h alone or in the presence of 50 μmol/L AR-A014418, and cell viability was measured by the MTT assay. *Columns,* mean percentage of nontreated cells from triplicate experiments; *bars,* SD. *, $P < 0.05$; **, $P < 0.01$, statistical significance.

mRNA (5- and 13-fold, respectively) after 24 h of prodigiosin treatment. Importantly, this induction was inhibited in the presence of 50 μmol/L AR-A014418 (2- and 3-fold for DR-4 and DR-5, respectively), suggesting a critical role of GSK-3β in prodigiosin-mediated induction of DR-4 and DR-5. Finally, to evaluate whether death receptors are activated by prodigiosin treatment, the expression of their substrate, caspase-8, was analyzed (Fig. 5B). Caspase-8 was detected after 8 h of prodigiosin treatment, coinciding with cleaved poly(ADP)ribose polymerase, a caspase substrate indicative of apoptosis. These results show that apoptosis via the death receptor extrinsic pathway is active in these cells. Together, these results suggest that prodigiosin-induced apoptosis is mediated by GSK-3β and that caspase-8 activation through DR-4 and DR-5 might explain, at least in part, this phenomenon.

Discussion

The aim of this study was to identify genes that undergo a change in expression in response to prodigiosin treatment to determine its mechanism of action. This information is used to aid the progress of this treatment to the clinic. The majority of the significantly modified genes in response to prodigiosin treatment, revealed by cDNA array technology, were related to apoptosis, cell cycle, cell adhesion, or transcriptional regulation. We focused our study on the most highly modified gene, *NAG-1*. Our results support that prodigiosin treatment induces accumulation of the DNA-damage response protein p53 but that prodigiosin-mediated NAG-1 expression is p53 independent. Inactivation of the prosurvival pathway PI3K/AKT in MCF-7 cells was observed after prodigiosin treatment. Finally, NAG-1 and DR-4 and DR-5 expressions were abrogated by GSK-3β inactivation, as well as prodigiosin-induced apoptosis, suggesting that this kinase might be a key regulator of the prodigiosin cytotoxic effect.

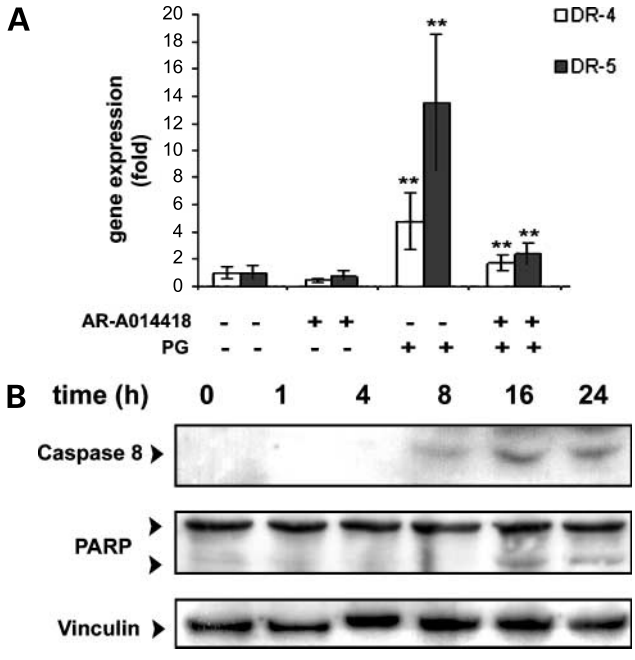

Figure 5. Analysis of apoptosis-related proteins after prodigiosin treatment. **A,** mRNA of MCF-7 cells, nontreated or treated with 50 μmol/L AR-A014418 before 24-h treatment with 0.5 μmol/L prodigiosin, was extracted. DR-4 and DR-5 levels were quantified by quantitative real-time reverse transcription-PCR. *Columns,* mean of triplicate experiments; *bars,* SD. *, $P < 0.05$; **, $P < 0.01$, statistical significance. **B,** cells were exposed to 0.5 μmol/L prodigiosin and a time course analysis of caspase-8, poly(ADP)ribose polymerase (*PARP*), and vinculin proteins was done by immunoblotting. Vinculin is shown as a gel loading control, and representative blots of independent experiments are shown.

Many chemotherapeutic agents currently used in the clinic induce accumulation of the tumor-suppressor protein p53, a key protein signaling growth arrest and apoptosis in response to DNA damage (33). In this regard, prodigiosin was previously described to intercalate to the DNA provoking topoisomerase I and II inhibition and, consequently, DNA cleavage (15). Moreover, accumulation of functional p53 protein and gene expression of the transforming growth factor-β family member NAG-1 after prodigiosin treatment were observed. NAG-1 can be induced in response to both p53-dependent and p53-independent apoptotic signaling events caused by DNA damage (18). Thus, one of the mechanisms of action of prodigiosin seems to be to cause DNA damage, which, in turn, triggers p53 accumulation. However, the ability of prodigiosin to induce apoptosis in cells with deficient p53 (4) indicates that p53 signaling after prodigiosin treatment is not essential for prodigiosin-induced cell death. This may confer prodigiosin an advantage in front of other chemotherapeutic agents that need functional p53 to provoke its cytotoxic effect because this protein is frequently mutated in most human cancers, which is related to poor prognosis (34).

Similar to prodigiosin, many cytotoxic agents have been reported to induce NAG-1 overexpression (19–23), but the exact mechanism by which NAG-1 triggers apoptosis is still poorly understood. NAG-1 induces morphologic changes followed by reduced cell adhesion and cell detachment in prostate cancer cells before undergoing apoptosis (16). Cell anchorage is not merely a structural feature of the cell but mediates pivotal survival signals into the cytoplasm; therefore, disturbance of cell anchorage frequently leads to the initiation of cell death by apoptosis, a process called anoikis (35). Cells treated with prodigiosin undergo progressive morphologic changes, cell detachment, and reorganization of actin microfilaments (7). In addition, the antimetastatic effect of prodigiosin is due to the inhibition of tumor invasion, which include the inhibition of cell adhesion and motility in a RhoA-dependent manner and suppression of matrix metalloproteinase-2 ability (5). Likewise, many of the genes regulated by prodigiosin, shown by the cDNA array experiments, are related to cellular adhesion, motility, or cytoskeleton structure. Taken together, these data suggest that one of the roles for NAG-1 in prodigiosin-induced apoptosis might be through morphologic changes leading to cell detachment, which then leads to prodigiosin-induced cell death.

The PI3K/AKT/GSK-3β signaling pathway has been shown to regulate NAG-1 expression in human colorectal carcinoma cells (30). The serine/threonine kinase AKT plays a key role in protecting cells from apoptosis through the phosphorylation of diverse downstream targets (36). Indeed, the blockade of this pathway sensitizes cells to various apoptotic stimuli, such as the response to the DNA-damaging agent doxorubicin in cancer cells in which the PI3K/AKT pathway is constitutively activated (37). GSK-3β is a negatively regulated AKT target whose overexpression has been shown to induce apoptosis whereas dominant-negative GSK-3β prevented apoptosis after inhibition of PI3K in prostate cancer cells (38). The AKT dephosphorylation caused by prodigiosin treatment allows GSK-3β activation leading to NAG-1 expression. This seems to be one of the molecular signaling events responsible for the apoptosis induced by prodigiosin. This was corroborated because GSK-3β pharmacologic inactivation recovered cell viability, suggesting a crucial role for GSK-3β in prodigiosin-induced apoptosis. Moreover, prodigiosin treatment induced expression of DR-4 and DR-5, which was reduced when GSK-3β was inhibited. These membrane receptors activate the initiator caspase-8, leading to apoptosis signaling through the extrinsic pathway (39). However, DR induction of GSK-3β via NAG-1 remains to be elucidated. NAG-1 cDNA transfection into gastric cancer cells significantly induced apoptosis and DR-4 and DR-5 expressions (33), suggesting a novel NAG-1 signaling pathway that may regulate DR expression.

In summary, the molecular mechanisms of the antitumorigenic potential of prodigiosin is effected by multiple events, giving rise to apoptosis. GSK-3β activation through inhibition of the PI3K/AKT pathway seems to be the most crucial event leading to prodigiosin apoptotic effect. GSK-3β–dependent expression of DR-4 and DR-5 may be through NAG-1 could explain, at least in part, prodigiosin-induced cell death. Furthermore, secretion of NAG-1 provides a route through which molecular signals caused by a cytotoxic agent can be communicated to the neighboring cells, and, thus, amplifying the effect of the cytotoxic agent. Altogether, these results point to prodigiosin as an attractive candidate for chemotherapy, especially in tumors with mutated p53 and activated PI3K/AKT/GSK3β pathway.

Acknowledgments

We thank Esther Castaño and Benjamín Torrejón from Serveis Cientifico-tècnics (Campus de Bellvitge, Universitat de Barcelona) for technical assistance.

References

1. Jemal A, Siegel R, Ward E, et al. Cancer statistics, 2006. CA Cancer J Clin 2006;56:106 – 30.

2. Esteva FJ, Valero V, Pusztai L, Boehnke-Michaud L, Buzdar AU, Hortobagvi GN. Chemotherapy of metastatic breast cancer: what to expect in 2001 and beyond. Oncologist 2001;6:133 – 46.

3. Perez-Tomas R, Montaner B, Llagostera E, Soto-Cerrato V. The prodigiosins, proapoptotic drugs with anticancer properties. Biochem Pharmacol 2003;66:1447 – 52.

4. Montaner B, Navarro S, Pique M, et al. Prodigiosin from the supernatant of *Serratia marcescens* induces apoptosis in haematopoietic cancer cell lines. Br J Pharmacol 2000;131:585 – 93.

5. Zang J, Shen Y, Liu J, Wei D. Antimetastatic effect of prodigiosin through inhibition of tumor invasion. Biochem Pharmacol 2005;69: 407 – 14.

6. Campas C, Dalmau M, Montaner B, et al. Prodigiosin induces apoptosis of B and T cells from B-cell chronic lymphocytic leukemia. Leukemia 2003; 17:746 – 50.

7. Diaz-Ruiz C, Montaner B, Perez-Tomas R. Prodigiosin induces cell death and morphological changes indicative of apoptosis in gastric cancer cell line HGT-1. Histol Histopathol 2001;16:415 – 21.

8. Montaner B, Perez-Tomas R. Prodigiosin-induced apoptosis in human colon cancer cells. Life Sci 2001;68:2025 – 36.

9. Soto-Cerrato V, Llagostera E, Montaner B, Perez-Tomas R. Mitochondria-mediated apoptosis operating irrespective of multidrug resistance in breast cancer cells by the anticancer agent prodigiosin. Biochem Pharmacol 2004;68:1345 – 52.

10. Llagostera E, Soto-Cerrato V, Joshi R, Montaner B, Gimenez-Bonafe P, Perez-Tomas R. High cytotoxic sensitivity of the human small cell lung doxorubicin-resistant carcinoma (GLC4/ADR) cell line to prodigiosin through apoptosis activation. Anticancer Drugs 2005;16:393 – 9.

11. Ohkuma S, Sato T, Okamoto M, et al. Prodigiosins uncouple lysosomal vacuolar-type ATPase through promotion of H^+/Cl^- symport. Biochem J 1998;334:731 – 41.

12. Castillo-Avila W, Abal M, Robine S, Perez-Tomas R. Non-apoptotic concentrations of prodigiosin (H^+/Cl^- symporter) inhibit the acidification of lysosomes and induce cell cycle blockage in colon cancer cells. Life Sci 2005;78:121 – 7.

13. Perez-Tomas R, Montaner B. Effects of the proapoptotic drug prodigiosin on cell cycle-related proteins in Jurkat T cells. Histol Histopathol 2003;18:379 – 85.

14. Melvin MS, Wooton KE, Rich CC, Saluta GR, et al. Copper-nuclease efficiency correlates with cytotoxicity for the 4-methoxypyrrolic natural products. J Inorg Biochem 2001;87:129 – 35.

15. Montaner B, Castillo-Avila W, Martinell M, et al. DNA interaction and dual topoisomerase I and II inhibition properties of the anti-tumor drug prodigiosin. Toxicol Sci 2005;85:870 – 9.

16. Liu T, Bauskin AR, Zaunders J, et al. Macrophage inhibitory cytokine 1 reduces cell adhesion and induces apoptosis in prostate cancer cells. Cancer Res 2003;63:5034 – 40.

17. Tan M, Wang Y, Guan K, Sun Y. PTGF-β, a type β transforming growth factor (TGF-β) superfamily member, is a p53 target gene that inhibits tumor cell growth via TGF-β signalling pathway. Proc Natl Acad Sci U S A 2000;97:109 – 14.

18. Li PX, Wong J, Ayed A, et al. Placental transforming growth factor-β is a downstream mediator of the growth arrest and apoptotic response of tumor cells to DNA damage and p53 overexpression. J Biol Chem 2000; 275:20127 – 35.

19. Baek SJ, Kim KS, Nixon JB, Wilson LC, Eling TE. Cyclooxygenase inhibitors regulate the expression of a TGF-β superfamily member that has proapoptotic and antitumorigenic activities. Mol Pharmacol 2001;59: 901 – 8.

20. Monks A, Harris E, Hose C, Connelly J, Sausville EA. Genotoxic profiling of MCF-7 breast cancer cell line elucidates gene expression modifications underlying toxicity of the anticancer drug 2-(4-amino-3-methylphenyl)-5-fluorobenzothiazole. Mol Pharmacol 2003;63:766 – 72.

21. Newman D, Sakaue M, Koo JS, et al. Differential regulation of nonsteroidal anti-inflammatory drug-activated gene in normal human tracheobronchial epithelial and lung carcinoma cells by retinoids. Mol Pharmacol 2003;63:557 – 64.

22. Wilson LC, Baek SJ, Call A, Eling TE. Nonsteroidal anti-inflammatory drug-activated gene (NAG-1) is induced by genistein through the expression of p53 in colorectal cancer cells. Int J Cancer 2003;105: 747 – 53.

23. Baek SJ, Wilson LC, Eling TE. Resveratrol enhances the expression of non-steroidal anti-inflammatory drug-activated gene (NAG-1) by increasing the expression of p53. Carcinogenesis 2002;23:425 – 34.

24. Lambert JR, Kelly JA, Shim M, et al. Prostate derived factor in human prostate cancer cells: gene induction by vitamin D via a p53-dependent mechanism and inhibition of prostate cancer cell growth. J Cell Physiol 2006;208:566 – 74.

25. Bottone FG, Jr., Baek SJ, Nixon JB, Eling TE. Diallyl disulfide (DADS) induces the antitumorigenic NSAID-activated gene (NAG-1) by a p53-dependent mechanism in human colorectal HCT 116 cells. J Nutr 2002; 132:773 – 8.

26. Lee SH, Kim JS, Yamaguchi K, Eling TE, Baek SJ. Indole-3-carbinol and 3,3′-diindolylmethane induce expression of NAG-1 in a p53-independent manner. Biochem Biophys Res Commun 2005;328:63 – 9.

27. Baek SJ, Kim JS, Moore SM, Lee SH, Martinez J, Eling TE. Cyclooxygenase inhibitors induce the expression of the tumor suppressor gene EGR-1, which results in the up-regulation of NAG-1, an antitumorigenic protein. Mol Pharmacol 2005;67:356 – 64.

28. Chintharlapalli S, Papineni S, Baek SJ, Liu S, Safe S. 1,1-Bis(3′-indolyl)-1-(p-substituted phenyl) methanes are peroxisome proliferator-activated receptor γ agonists but decrease HCT-116 colon cancer cell survival through receptor-independent activation of early growth response-1 and nonsteroidal anti-inflammatory drug-activated gene-1. Mol Pharmacol 2005;68:1782 – 92.

29. Shim M, Eling TE. Protein kinase C-dependent regulation of NAG-1/placental bone morphogenic protein/MIC-1 expression in LNCaP prostate carcinoma cells. J Biol Chem 2005;280:18636 – 42.

30. Yamaguchi K, Lee SH, Eling TE, Baek SJ. Identification of nonsteroidal anti-inflammatory drug-activated gene (NAG-1) as a novel downstream target of phosphatidylinositol 3-kinase/AKT/GSK-3β pathway. J Biol Chem 2004;279:49617 – 23.

31. Mosmann T. Rapid colorimetric assay for cellular growth and survival: application to proliferation and cytotoxicity assays. J Immunol Methods 1983;65:55 – 63.

32. Jang TJ, Kang HJ, Kim JR, Yang CH. Non-steroidal anti-inflammatory drug activated gene (NAG-1) expression is closely related to death receptor-4 and -5 induction, which may explain sulindac sulfide induced gastric cancer cell apoptosis. Carcinogenesis 2004;25: 1853 – 8.

33. Blagosklonny MV. P53: an ubiquitous target of anticancer drugs. Int J Cancer 2002;98:161 – 6.

34. Royds JA, Iacopetta B. p53 and disease: when the guardian angel fails. Cell Death Differ 2006;13:1017 – 26.

35. Grossmann J. Molecular mechanisms of ''detachment-induced apoptosis—anoikis.'' Apoptosis 2002;7:247 – 60.

36. Nicholson KM, Anderson NG. The protein kinase B/Akt signalling pathway in human malignancy. Cell Signal 2002;14:381 – 95.

37. Fujiwara Y, Kawada K, Takano D, Tanimura S, Ozaki K, Kohno M. Inhibition of the PI3 kinase/Akt pathway enhances doxorubicin-induced apoptotic cell death in tumor cells in a p53-dependent manner. Biochem Biophys Res Commun 2006;340:560 – 6.

38. Pap M, Cooper GM. Role of glycogen synthase kinase-3 in the phosphatidylinositol 3-kinase/Akt cell survival pathway. J Biol Chem 1998;273:19929 – 32.

39. Sheridan JP, Marsters SA, Pitti RM, et al. Control of TRAIL-induced apoptosis by a family of signaling and decoy receptors. Science 1997; 277:818 – 21.

Capítulo 2.3. Estudio de los mecanismos de inducción del gen regulador del ciclo celular p21$^{WAF1/CIP1}$ en células de cáncer de mama tras el tratamiento con prodigiosina.

(**"**Soto-Cerrato V, Viñals F, Lambert JR, Pérez-Tomás R. The anticancer agent prodigiosin induces p21$^{WAF1/CIP1}$ expression via transforming growth factor-beta receptor pathway. Biochem Pharmacol 2007; doi:10.1016/j.bcp.2007.07.016").

El agente anticanceroso prodigiosina es también un inmunosupresor muy eficaz, ya que induce parada de ciclo celular a concentraciones no citotóxicas. El análisis de la expresión génica de células MCF-7 tratadas con prodigiosina mostró un aumento significativo en la expresión del gen p21$^{WAF1/CIP1}$, un regulador negativo del ciclo celular. Fue por ello que nos propusimos estudiar a fondo los mecanismos por los que prodigiosina provocaba la parada de la proliferación celular. Analizando el mecanismo por el cual prodigiosina inducía p21, demostramos que éste era independiente de la actividad del gen p53, ya que p21 se expresaba de igual forma en células con p53 mutada o células que expresaban un mutante negativo de p53. En cambio, la ruta del factor de crecimiento transformante (TGF-β) era necesaria, aunque no suficiente, para la inducción de p21. Esto fue demostrado ya que al bloquear la ruta de TGF- β con SB431542, un inhibidor específico de ésta, la expresión de p21 se veía anulada. El miembro de la familia del TGF-β, NAG-1, podría estar activando esta ruta en nuestro modelo, ya que esta habilidad le ha sido conferida en otras ocasiones. Además, como ya hemos descrito previamente, NAG-1 se sobreexpresa en respuesta al tratamiento con prodigiosina y colocaliza con el receptor de TGF-β, sugiriendo una posible interacción entre ellos. Estos resultados muestran que la vía del TGF-β es necesaria para la expresión de p21 tras el tratamiento con prodigiosina.

available at www.sciencedirect.com
ScienceDirect
journal homepage: www.elsevier.com/locate/biochempharm

The anticancer agent prodigiosin induces p21$^{WAF1/CIP1}$ expression via transforming growth factor-beta receptor pathway

Vanessa Soto-Cerrato [a], *Francesc Viñals* [b,c], *James R. Lambert* [d], *Ricardo Pérez-Tomás* [a,*]

[a] *Department of Pathology and Experimental Therapeutics, Cancer Cell Biology Research Group, Universitat de Barcelona, Barcelona, Spain*
[b] *Laboratori de Recerca Translacional, ICO-IDIBELL, L'Hospitalet de Llobregat, Barcelona, Spain*
[c] *Departament de Ciències Fisiològiques II, Campus de Bellvitge, Universitat de Barcelona, Barcelona, Spain*
[d] *Department of Pathology, University of Colorado Denver and Health Science Center, Aurora, CO, USA*

ARTICLE INFO

Article history:
Received 25 April 2007
Accepted 5 July 2007

Keywords:
Prodigiosin
p21
Cell cycle arrest
TGF-β
NAG-1
Breast cancer

ABSTRACT

The anticancer agent prodigiosin has been shown to act as an efficient immunosuppressant, eliciting cell cycle arrest at non-cytotoxic concentrations, and potent proapoptotic and antimetastatic effects at higher concentrations. Gene expression profiling of MCF-7 cells after treatment with a non-cytotoxic concentration of prodigiosin showed that expression of the p21$^{WAF1/CIP1}$ gene, a negative cell cycle regulator was induced. In this study, we show that prodigiosin induces p21 expression leading to cell cycle blockade. Subsequently, we attempted to elucidate the molecular mechanisms involved in prodigiosin-mediated p21 gene expression. We demonstrate that prodigiosin induces p21 in a p53-independent manner as prodigiosin induced p21 in cells with both mutated and dominant negative p53. Conversely, the transforming growth factor-beta (TGF-β) pathway has been found to be necessary for p21 induction. Prodigiosin-mediated p21 expression was blocked by SB431542, a TGF-β receptor inhibitor. Nevertheless, this pathway alone is not enough to induce p21 expression. The TGF-β family member (nonsteroidal anti-inflammatory drug)-activated gene 1/growth differentiation factor 15 (NAG-1) may activate this pathway, as it has previously been suggested to signal through the TGF-β pathway and is overexpressed in response to prodigiosin treatment. We show that NAG-1 colocalizes with TGF-β receptor type I, suggesting a possible interaction between them. Taken together, these results suggest the TGF-β pathway is required for induction of p21 expression after prodigiosin treatment of MCF-7 cells.

1. Introduction

The bioactive secondary metabolite prodigiosin (2-methyl-3-pentyl-6-methoxyprodiginine) belongs to a family of tripyrrole red pigments produced by both Gram-negative and Gram-positive bacteria [1]. Prodigiosin is effective as an immunosuppressant at non-cytotoxic concentrations [2]. Higher levels lead to anticancer and antimetastatic effects [3,4]. Prodigiosin

* *Corresponding author at*: Department of Pathology and Experimental Therapeutics, Cancer Cell Biology Research Group, Universitat de Barcelona. Pavelló Central, 5a planta, LR 5101C/Feixa Llarga s/n, E 08907 L'Hospitalet de Llobregat, Barcelona, Spain. Tel.: +34 934024288; fax: +34 934029082.
E-mail address: rperez@ub.edu (R. Pérez-Tomás).

Abbreviations: GSK-3β, glycogen synthase kinase-3 beta; FBS, fetal bovine serum; IC_{25}, inhibitory concentration 25; MAPK, mitogen-activated protein kinase; MTT, methyl-thiazole-tetrazolium; NAG-1/GDF-15, (nonsteroidal anti-inflammatory drug)-activated gene 1/growth differentiation factor 15; p21, p21$^{WAF1/CIP1}$; PG, prodigiosin; TGF-β, transforming growth factor-beta; TGF-βRI, TGF-β receptor type I.

0006-2952/$ – see front matter
doi:10.1016/j.bcp.2007.07.016

provokes cell death in a broad range of human cancer cell lines [5–8]. It induces mitochondria-mediated apoptosis irrespective of multidrug resistance phenotype [9,10]. Resistance is a common phenomenon that reduces the effectiveness of chemotherapy. Interestingly, prodigiosin has multiple mechanisms of action. However, the contribution of each mechanism to the observed effects is still unclear. Prodigiosin reversibly disrupts the pH gradient between lysosomes and cytoplasm [11], induces G_1-S transition arrest [12], causes DNA fragmentation and topoisomerases inhibition [13,14], induces GSK-3β activation [15] and exerts an uncoupling effect on the electron chain transport of protons to mitochondrial ATP synthase [16].

Transforming growth factor-beta (TGF-β) family cytokines regulate many physiological processes such as cell proliferation, differentiation, adhesion, matrix production, motility and apoptosis [17,18]. TGF-β members exert their biological effects by signaling through membrane-bound receptors. The best characterized is the TGF-β/Smad pathway. Binding of TGF-β family members to type II receptors (TβRII) leads to the formation of a heterodimeric cell surface receptor complex together with a type I receptor (TβRI). The latter is phosphorylated by TβRII and thus activated. It subsequently phosphorylates a receptor-regulated Smad, allowing this protein to associate with Smad-4 and translocate into the nucleus. Once in the nucleus, the Smad complex activates transcription of target genes [19]. Other signaling pathways have also been implicated downstream from the TGF-β receptors, including several Smad-independent mitogen-activated protein kinase (MAPK) pathways [20].

The growth-inhibitory effect of TGF-β signaling in epithelial cells is the consequence of the activation of a cytostatic gene response program that includes the down-regulation of the c-Myc and Id family of transcription factors, and the activation of $p15^{INK4b}$ and $p21^{WAF1/CIP1}$ (p21) cyclin-dependent kinase inhibitors [21]. p21 mainly inhibits the activity of cyclin/cdk2 complexes [22] and negatively regulates cell cycle progression after cell exposure to different stimuli such as DNA-damaging agents [23]. Apart from the tumor suppressor p53, a variety of other factors (including Sp1/Sp3, Smads, Ap2, STAT, BRCA1, E2F-1/E2F-3, and CAAT/enhancer binding protein α and β) are known to activate p21 transcription [24].

The TGF-β family member (nonsteroidal anti-inflammatory drug)-activated gene 1/growth differentiation factor 15 (NAG-1/GDF15) is a secreted protein thought to activate the TGF-β signaling pathway inducing cell cycle arrest [25] or apoptosis in many different cell types [26,27]. Many anti-tumorigenic compounds, such as cyclooxygenase inhibitors [28], retinoids [29], genistein [30], resveratrol [31], and vitamin D [32], among others, have been found to up-regulate its expression. Prodigiosin has recently been reported to induce NAG-1 expression, death receptors 4 and 5 and apoptosis in breast cancer cells through glycogen synthase kinase-3 beta (GSK-3β) activation [15].

In this report, we demonstrate p21 induction and subsequent cell cycle arrest in MCF-7 breast cancer cells following prodigiosin treatment. Identification of TGF-β signaling as an essential molecular pathway responsible for prodigiosin-mediated p21 expression is reported and new insights into the role of this pathway on prodigiosin-induced cytostatic effects are provided.

2. Materials and methods

2.1. Drugs and reagents

2-Methyl-3-pentyl-6-methoxyprodigiosene, also called prodigiosin, was purified from *Serratia marcescens* 2170, as previously described [5]. Stock solutions were prepared in methanol and their concentrations were then determined by UV–vis in 95% EtOH–HCl (ε_{535} = 112,000/M cm). SB431542 (Cat# 1614) and AR-A014418 (Cat# 361546) were purchased from Tocris (Ellisville, MO) and Calbiochem (EMD Biosciences, Darmstadt, Germany), respectively.

2.2. Cell lines and culture conditions

Human breast cancer cell lines MCF-7 and MDA-MB-231 were purchased from American Type Culture Collection (Manassas, VA) and cultured in DMEM:HAM F12 (1:1) (Biological Industries, Beit Haemek, Israel) supplemented with 10% heat-inactivated fetal bovine serum (FBS) (GIBCO BRL, Invitrogen life technologies, Carlsbad, CA), 100 U/ml penicillin, 100 μg/ml streptomycin, and 2 mM L-glutamine, all from Biological Industries. C2C12 mouse cells were cultured in DMEM containing 10% FBS, 50 U/ml penicillin, and 50 μg/ml streptomycin sulphate. Cells were grown at 37 °C in a 5% CO_2 atmosphere.

2.3. cDNA array analysis

Gene expression was analyzed by hybridization to cDNA arrays (Atlas™ Human Cancer Array 1.2 from Clontech, BD Biosciences, Palo Alto, CA) as previously described [15]. Briefly, cells (1.5×10^7 in 30 ml) were untreated (control) or treated with 0.5 μM prodigiosin for 24 h. An Atlas™ Pure Total RNA Labeling kit (Clontech, BD Biosciences) was used for total RNA isolation, poly A^+ RNA enrichment and probe synthesis. Hybridization to cDNA arrays was performed, films were scanned and image analysis was carried out with BD AtlasImage™ 2.7 (Clontech, BD Biosciences).

2.4. Quantitative real-time RT-PCR

Cells (5×10^5 cells/ml) were exposed to 0.5 μM prodigiosin for 24 h. When the inhibitors AR-A014418 (50 μM) and SB431542 (20 μM) were used, they were added 30 min before prodigiosin treatment. Total RNA extraction was performed using TRIzol® Reagent (Invitrogen life technologies). The RNA pellet was washed in 75% ethanol, dissolved in H_2O, and cDNA synthesis (1 μg RNA/50 μl) was performed using random hexamers and MuLV RT, according to the manufacturer's instructions (Applied Biosystems, Warrington, UK). Each cDNA sample was analyzed for the expression of several genes using the fluorescent TaqMan 5′ nuclease assay. Oligonucleotide primers p21 (CDKN1A, Cat# Hs00355782_m1), death receptor (DR) 4 (TNFRSF10A, Cat# Hs00269492_m1), DR-5 (TNFRSF10B, Cat# Hs00187196_m1), beta actin (ACTB, Cat# Hs99999903_m1) and probes were purchased as Assay-on-Demand Gene Expression Products (Applied Biosystems). The 5′ nuclease assay PCRs were performed using the ABI PRISM 7700 Sequence Detection System for thermal cycling and real-time fluorescence measurements (Applied Biosystems). Each 50 μl reaction

Please cite this article in press as: Soto-Cerrato V, et al., The anticancer agent prodigiosin induces $p21^{WAF1/CIP1}$ expression via transforming growth factor-beta receptor pathway, Biochem Pharmacol (2007), doi:10.1016/j.bcp.2007.07.016

consisted of 1X TaqMan Universal PCR MasterMix (PE Biosystems); 1X Assay-on-Demand mix containing forward primer, reverse primer, and a TaqMan quantification probe (Applied Biosystems); and a 100 ng cDNA template. Reaction conditions consisted of an initial step at 92 °C for 10 min, then 40 cycles at 95 °C for 15 s and 60 °C for 1 min. The gene expression levels obtained were normalized by mRNA expression of actin. The relative mRNA expression was then presented in relation to the control. Data were analyzed using ''Sequence Detector Software'' (SDS Version 1.9, Applied Biosystems) and were presented as the mean ± S.D. of three independent experiments. For the statistical analysis among treatment groups, ANOVA and LSD tests were performed with the Statgraphics plus 5.1 statistical package. $P < 0.05$ and $P < 0.01$ were represented with * and **, respectively.

2.5. Western blotting

Cells (5×10^5 cells/ml) were exposed to several prodigiosin concentrations for different times, depending on the experiment. When used, the inhibitors AR-A014418 and SB431542 were added 30 min before prodigiosin treatment. Supernatants, with detached cells were then collected, centrifuged, pooled with the cells on the plate and washed in PBS prior to the addition of a lysis buffer (85 mM Tris–HCl pH 6.8, 2% SDS, 1 μg/ml aprotinin, 1 μg/ml leupeptin, and 0.1 mM phenylmethanesulfonyl fluoride). The protein concentration was determined by BCA protein assay (Pierce, Rockford, IL) using bovine serum albumin (BSA) as a standard. Fifty micrograms of protein extracts were separated by 12% SDS-polyacrylamide gel electrophoresis and transferred to Immobilon-P membranes (Millipore, Bedford, MA). Membranes were blocked in 5% dry milk diluted in TBS–Tween (50 mM Tris–HCl pH 7.5, 150 mM NaCl, 0.1% Tween 20) for 1 h and then incubated overnight with primary antibodies, according to the manufacturer's instructions. Antibodies were obtained from the following sources: anti-actin (Cat# sc-1616) was from Santa Cruz Biotechnology, (Santa Cruz, CA); anti-p21 (Cat#OP-64) was from Calbiochem (La Jolla, CA); anti-p53 (Cat# MS-186-P1) was from Neomarkers (Fremont, CA); phospho-smad-2 Ser465/467 (Cat# 3101) was from Cell Signaling Technology (Beverly, MA); anti-vinculin (Cat# V-4505) was from Sigma (St Louis, MO). Antibody binding was detected with goat anti-rabbit, goat anti-mouse (Bio-Rad Laboratories, Hercules, CA) or donkey anti-goat (Santa Cruz Biotechnology) immunoglobulin G (IgG) secondary antibodies conjugated to horseradish peroxidase and the ECL detection kit (Amersham, Buckinghamshire, UK). Actin or vinculin were used as gel loading controls. The results shown are representative of Western blot data obtained from at least three independent experiments with identical observations.

2.6. [^{3}H]-Thymidine incorporation assay

MCF-7 cells (5×10^5 cells/ml) were seeded in a 24-well plate. Cells were incubated in complete medium in the absence or presence of the indicated concentrations of prodigiosin and with 1 μCi of [^{3}H] thymidine ([6-^{3}H] thymidine) (0.5 Ci/mmol, Amersham Pharmacia Biotech) for 24 h. Cells were washed twice in cold 5% TCA and lysed with 0.1 M NaOH. The lysates were mixed with 5 ml scintillation buffer. Radioactivite counts were then measured using a scintillation counter (Beckman). The mean of triplicate experiments and standard deviations are shown.

2.7. Flow cytometry

MCF-7 cells (1×10^6) were plated in 10 cm dishes 16 h prior to treatment with prodigiosin or methanol control. After a 24 h-treatment, cells were trypsinized, collected and centrifuged at 1500 rpm for 5 min. Then, cells were resuspended in 1.5 ml saponin/PI solution (0.3% saponin (w/v), 2.5% PI (w/v), 0.1 mM EDTA, 10 μg/ml RNase in PBS) and incubated overnight in the dark. FACS analysis was performed using a Beckman Coulter FC500 flow cytometer. ModFit LT software (Verity Software House, Topsham, ME) was used for doublet exclusion and cell cycle analysis.

2.8. Dominant negative p53 MCF-7 cells

Dominant negative p53 retrovirus production and infection of MCF-7 were performed as previously described [15].

2.9. Immunocytochemistry

Cells cultured in a 24-well plate containing glass coverslips (1.25×10^5 cells in 250 μl) were incubated with 0.5 μM prodigiosin for 24 h. When using the inhibitor SB431542, a concentration of 20 μM was added 30 min before prodigiosin treatment. Cells were then washed twice with PBS and fixed with 4% paraformaldehyde for 20 min. Fixed cells were permeabilized with 0.2% Triton X-100 and then blocked with 3% bovine serum albumin (BSA) in PBS for 1 h. Cells were incubated overnight at 4 °C with anti-NAG-1/PTGF-β (1:50 dilution, Cat# sc-10603) and anti-TGF-β Receptor I (1:50 dilution, Cat# sc-398) antibodies, both from Santa Cruz Biotechnology or 1 h at room temperature with Smad 2/3 (1:50 dilution, Cat#610843) from Pharmingen, BD Biosciences, Palo Alto, CA. The cells were washed with PBS containing 3% BSA and incubated with Alexa Fluor® 488-conjugated donkey anti-goat (Cat# A11055, Molecular Probes, Invitrogen) and/or Fluorolink™ Cy™ 3-labelled goat anti-rabbit (Cat# PA43004, Amersham Biosciences, Buckinghamshire, UK) IgGs at 1:400 dilution for 1 hour. Finally, a 15-min incubation with TO-PRO®-3 iodide (1:6000 dilution, Cat# T3605, Molecular Probes, Invitrogen) was performed and coverslips were placed on the slides using Immunofluore mounting medium (MD Biomedicals, Aurora, OH). The immunofluorescent images were captured using a Leica TCS SL spectral confocal microscope. Representative images from three independent experiments are shown.

2.10. Cell viability assay

Cell viability was determined using the methyl-thiazole-tetrazolium (MTT) assay [33]. Cells were plated in triplicate wells (2.5×10^4 cells/well) in 100 μl of growth medium in 96-well plates and allowed to grow for 24 h. Cells were pre-treated for 30 min with 20 μM SB431542 prior to 1.4 μM prodigiosin treatment. After 24 h incubation, 10 μM of MTT (Sigma

Please cite this article in press as: Soto-Cerrato V, et al., The anticancer agent prodigiosin induces p21$^{WAF1/CIP1}$ expression via transforming growth factor-beta receptor pathway, Biochem Pharmacol (2007), doi:10.1016/j.bcp.2007.07.016

Chemical Co., St. Louis, MO) was added to each well for an additional 4 h. The blue MTT formazan precipitate was dissolved in 100 μl of isopropanol: 1N HCl (24:1). The absorbance at 570 nm was measured on a multiwell plate reader. Cell viability was expressed as a percentage of the control and data are shown as the mean value ±S.D. of three independent experiments. Statistical analysis (ANOVA and LSD tests) was carried out with the Statgraphics plus 5.1. statistical package. $P < 0.05$ and $P < 0.01$ were represented with * and **, respectively.

3. Results

3.1. *Cell cycle arrest and p21 induction after prodigiosin treatment*

cDNA array experiments analyzing differential gene expression after prodigiosin treatment were performed in our laboratory in order to identify the molecular targets of this anticancer drug [15]. MCF-7 cells were treated with 0.5 μM prodigiosin (IC_{25} at 24 h, the drug concentration that caused a cell viability decrease of 25% in the cell population [9]). The cell-cycle regulator protein p21 was identified among the most modulated genes. It was then selected for validation by more accurate methods, including quantitative real time RT-PCR and Western blot assays (Fig. 1). MCF-7 cells were treated with 0.5 μM prodigiosin for different time periods. p21 mRNA levels significantly increased, especially after 24 h of treatment (levels were 35-fold higher than in non-treated cells) (Fig. 1A). We also observed a time-dependent increase in p21 protein levels, which was significant from 16 h of drug treatment (Fig. 1B).

Because p21 is a cyclin dependent kinase inhibitors, we investigated the effect of prodigiosin on cell proliferation and cell cycle in MCF-7 cells. To determine the effect of prodigiosin on MCF-7 cell proliferation, ^{3}H-thymidine incorporation experiments were assessed. Different doses of prodigiosin

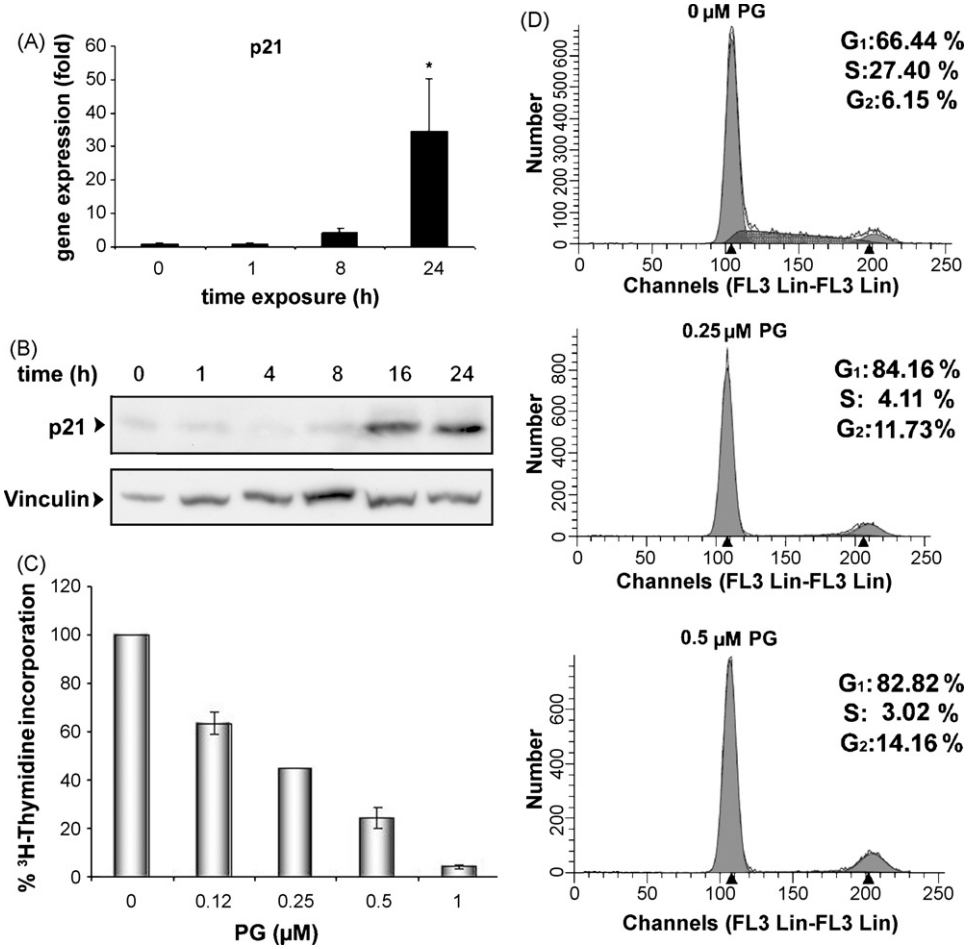

Fig. 1 – The effect of prodigiosin treatment on p21 expression and the cell cycle regulation of MCF-7 cells. (A) MCF-7 cells were treated for 1, 8 and 24 h with 0.5 μM of prodigiosin, and fold changes in gene expression with respect to control cells were determined by quantitative real time reverse transcription-PCR. The values are expressed as the mean ± S.D. (triplicates). Values were normalized using actin mRNA expression. Statistical significance among groups is represented by *$P < 0.05$. (B) Time-course analysis of protein levels in 0.5 μM prodigiosin-treated MCF-7 cells subjected to immunobloting with p21 antibody. Vinculin is shown as a loading control and representative blots of independent experiments are shown. (C) [^{3}H]-thymidine incorporation after 24 h-exposure of MCF-7 cells to different doses of prodigiosin. Triplicate experiments were performed and the S.D. is shown. (D) Cell cycle analysis of MCF-7 cells treated with 0.25 and 0.5 μM of prodigiosin.

Please cite this article in press as: Soto-Cerrato V, et al., The anticancer agent prodigiosin induces p21$^{WAF1/CIP1}$ expression via transforming growth factor-beta receptor pathway, Biochem Pharmacol (2007), doi:10.1016/j.bcp.2007.07.016

were analyzed (Fig. 1C). We used low cytotoxic doses of prodigiosin in order to differentiate between cell death and cell cycle blockade. The dose that caused a cell viability decrease of 25% of the cell population (IC_{25} = 0.5 μM) caused 70% ^{3}H-thymidine incorporation, suggesting that this antiproliferative effect was due to cell cycle blockade. In general, a marked dose-dependent decrease in [^{3}H]-thymidine incorporation was found. Cell cycle progression was analyzed by flow cytometry using propidium iodide in MCF-7 cells exposed to 0.25 and 0.5 μM of prodigiosin for 24 h. Fig. 1D shows a marked accumulation of treated cells in G_0/G_1 (from 66.44% to 84.16% and 82.82%) at both doses exposed. Additionally, the percentage of cells in S phase decreased sharply following prodigiosin treatment thus indicating a significant cell cycle arrest provoked by prodigiosin.

3.2. *p21 induced by prodigiosin is not dependent on p53 accumulation*

The tumor suppressor protein p53 regulates the expression of 21 [23]. To identify whether p53 was responsible for p21 expression after prodigiosin treatment, MCF-7, MCF-7 cells expressing a dominant negative p53 and MDA-MB-231 cells were used. The latter is a human breast cancer cell line that lacks functional p53. Western blot analysis showed that p21 expression correlates with p53 accumulation in the p53 wild-type cell line MCF-7. However, p21 is also induced in MDA-MB-231 cells, while mutated p53 is not accumulated in response to the treatment (Fig. 2A). To further analyze the relationship between p21 and p53, we expressed a dominant negative p53 in MCF-7 cells and analyzed p21 protein levels. We compared p21 levels in MCF-7 cells infected with a dominant negative-expressing retrovirus and cells infected with empty virus as a control. Dominant negative p53 in MCF-7 cells had no effect on p21 expression (Fig. 2B). The blot was stripped and reprobed for an indicator of the efficiency of dominant negative p53 function: stabilization of p53. Infection of cells with pMSCV-IRES-GFP-p53dd results in stabilization of p53, indicating strong dominant negative p53 function in these cells. These results suggest prodigiosin-induced p21 expression is not dependent on p53.

3.3. *Prodigiosin-mediated p21 expression is dependent on TGF-β pathway*

The TGF-β pathway has been reported to induce p21 expression [34]. To determine if prodigiosin induces p21 through a TGF-β dependent mechanism, the levels of p21 mRNA and protein were measured following prodigiosin treatment of MCF-7 cells in the absence or presence of the specific TGF-β receptor type I (TGF-βRI) inhibitor, SB431542 [35]. We observed prodigiosin-induced increase in the amount of p21 mRNA and protein sharply decreased in cells that were pretreated with 20 μM SB431542 (Fig. 3A and B).

Smad-2 is phosphorylated when the TGF-β pathway is activated [17]. The presence of phospho-Smad-2 in non-treated cells (Fig. 3B) indicates that this pathway is already active in MCF-7 cells. This could be due to the fact that they are TGF-β producing cells [36]. The TGF-β receptor smad-dependent pathway remains activated at the onset of

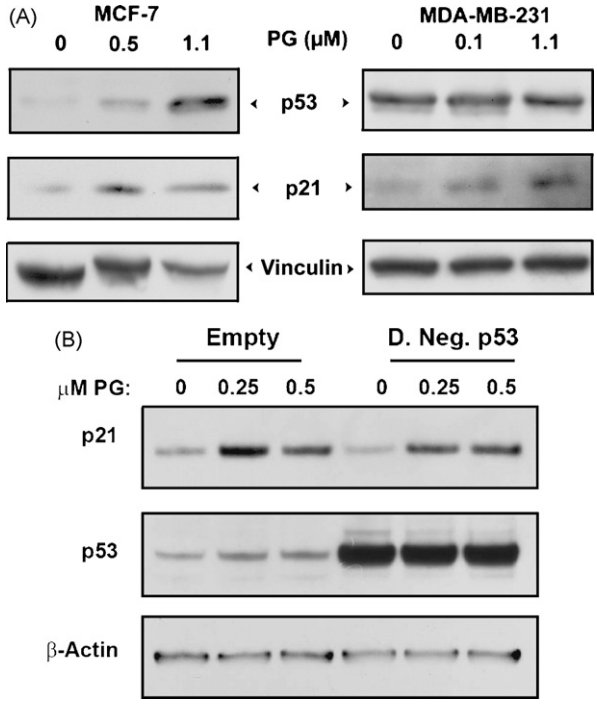

Fig. 2 – Analysis of p21 expression in wild-type p53 and mutated p53 cells after prodigiosin exposure. (A) MCF-7 and MDA-MB-231 cells were incubated with different prodigiosin doses corresponding to their respective IC_{25}, IC_{50} and IC_{75} values at 24 h and then subjected to immunoblot for p53 and p21 detection. Vinculin is shown as a loading control and representative blots of independent experiments are shown. (B) MCF-7 cells were infected with a retrovirus expressing a dominant negative p53 (D.Neg.p53). A pool of infected cells was analyzed for p21 and p53 protein levels after prodigiosin treatment (0.5 μM). β-Actin is shown as a loading control.

prodigiosin treatment. When SB431542 was added phospho-Smad-2 disappeared, indicating that this pathway was inhibited. Therefore, p21 expression seems to depend on the TGF-β pathway. Taken together, these findings suggest that prodigiosin interacts with the TGF-β receptor pathway and TGF-β receptor activity is necessary for p21 induction, as p21 is not expressed when the pathway is inhibited. However, the smad-dependent TGF-β receptor pathway alone is not enough to induce p21 expression, as phospho-Smad-2 is already found in non-treated cells and they do not express p21.

3.4. *Prodigiosin-induced NAG-1 interferes with TGF-β receptor type I*

To further investigate p21 induction, we tried to elucidate which molecule was activating the TGF-β pathway. One possible candidate ligand was NAG-1, a TGF-β family protein that signals through the TGF-β pathway [25]. The gene expression of NAG-1 was up-regulated 79-fold after prodigiosin treatment [15]. Cells were subjected to immunofluorescence after treatment with 0.5 μM of prodigiosin for 24 h, and

Please cite this article in press as: Soto-Cerrato V, et al., The anticancer agent prodigiosin induces p21$^{WAF1/CIP1}$ expression via transforming growth factor-beta receptor pathway, Biochem Pharmacol (2007), doi:10.1016/j.bcp.2007.07.016

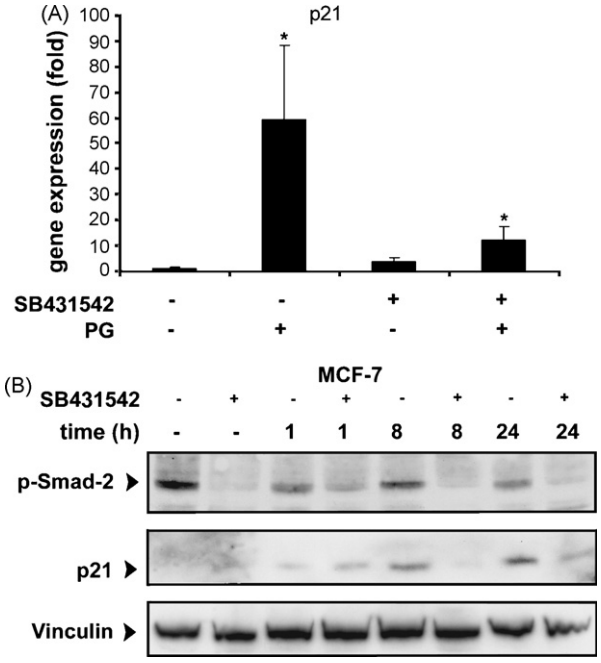

Fig. 3 – p21 regulation by the TGF-β signalling pathway. (A) Cells were incubated with 0.5 μM prodigiosin for 24 h either alone or with 20 μM SB431542. Changes in mRNA levels were analyzed by quantitative real-time RT-PCR. Data were expressed as the mean (columns) ± S.D. (bars) of triplicate experiments and values were normalized using actin mRNA expression (Statistical significance: *P < 0.05). (B) Representative Western blot images of phospho-smad-2, p21 and vinculin (gel loading control) proteins of MCF-7 cells treated for different time periods with 0.5 μM prodigiosin in the absence or presence of 20 μM SB431542.

the NAG-1 protein was seen to accumulate in vesicles throughout the cytoplasm of cells (Fig. 4A, PG). However, cells pre-incubated with 20 μM of the TGF-β pathway inhibitor SB431542 prior to prodigiosin exposure (Fig. 4A, PG + SB431542) showed a similar NAG-1 distribution to those treated solely with prodigiosin. Therefore, inhibition of this pathway does not interfere with prodigiosin-induced NAG-1 expression and cytoplasmic vesicle accumulation. To determine whether prodigiosin-induced NAG-1 could be interacting with the TGF-β pathway, simultaneous incubation with TGF-β receptor type I (TGF-βRI) and NAG-1 antibodies was performed. Co-localization of both proteins in prodigiosin-treated cells was observed, particularly at the membrane surface, suggesting an interaction between NAG-1 and the TGF-β pathway (Fig. 4B). Moreover, since the smad-dependent TGF-β pathway is already activated in MCF-7 cells, we wanted to determine whether prodigiosin had any effect on smad cellular localization. In Figure 4C, we can observe how the majority of smad-2/3 protein in non-treated MCF-7 cells is located in the nucleus. After 4 h of prodigiosin treatment smad-2/3 was still in the nucleus but it was translocated to the cytoplasm after 24 h of treatment. This agrees with our previous results on p-smad protein levels (Fig. 3B).

3.5. *Activation of GSK-3β is required for p21 induction*

GSK-3β is activated by prodigiosin treatment and its activation is necessary for NAG-1 expression induced by prodigiosin [15]. Experiments using a specific inhibitor of this kinase (AR-A014418) were performed. MCF-7 cells were pre-incubated with 50 μM AR-A014418 30 min before treating cells with 0.5 μM prodigiosin for 24 h. We could then observe how p21 gene expression induced by prodigiosin was totally blocked when GSK-3β was inactivated by the inhibitor (Fig. 5A). At the protein level (Fig. 5B), we also observed that p21 accumulation following prodigiosin treatment was blocked by increasing AR-A014418 concentrations. This suggests that GSK-3β activation and p21 expression are dependent. This might be due to GSK-3β induction of NAG-1 expression after prodigiosin treatment, which could lead to TGF-β receptor pathway activation and thus to p21 induction. However, we observed that the AR-A014418 inhibitor induces a dose-dependent increase in p53 protein, which does not induce p21 expression. This corroborates with our previous findings showing that p21 gene induction is independent from p53 protein accumulation (Fig. 2).

3.6. *The TGF-β pathway is not implicated in prodigiosin-induced apoptosis*

Cell viability experiments were performed in order to find out whether the TGF-β pathway also contributes to the apoptotic phenotype induced by prodigiosin (Fig. 6A). MCF-7 cells were pre-treated with 20 μM SB431542. An apoptotic concentration of prodigiosin (IC_{75}) was then added. A 70% decrease in cell viability was observed in MCF-7 cells treated with prodigiosin. No recovery in cell viability was observed when pre-treating cells with 20 μM SB431542. Hence, the TGF-β pathway is not involved in prodigiosin-induced apoptosis. Moreover, death receptor proteins 4 and 5 have been related to NAG-1 overexpression [37]. Prodigiosin treatment also up-regulates the expression of these death receptor proteins [15]. Gene expression quantification experiments were performed to analyze whether the expression of death receptors could be regulated through the TGF-β pathway. Fig. 6B shows a significant increase in DR-4 and DR-5 mRNAs (5- and 14-fold higher than the control, respectively) after 24 h-prodigiosin treatment. No significant modifications occurred when adding 20 μM SB431542 (3 and 11).

4. Discussion

The negative cell-cycle regulator p21 has previously been reported as one of the most significantly up-regulated genes in breast cancer cells after treatment with the anticancer drug prodigiosin [15]. The aim of the present study was to identify the molecular mechanisms that triggered prodigiosin-induced p21 expression. Here we demonstrate that p21 expression is independent of the tumor suppressor protein p53, but dependent on the activation of the TGF-β signaling pathway and on GSK-3β kinase activity. We also suggest that this pathway might be activated by the interaction between the cytokine NAG-1 and the TGF-β pathway receptors. Finally, we

Please cite this article in press as: Soto-Cerrato V, et al., The anticancer agent prodigiosin induces $p21^{WAF1/CIP1}$ expression via transforming growth factor-beta receptor pathway, Biochem Pharmacol (2007), doi:10.1016/j.bcp.2007.07.016

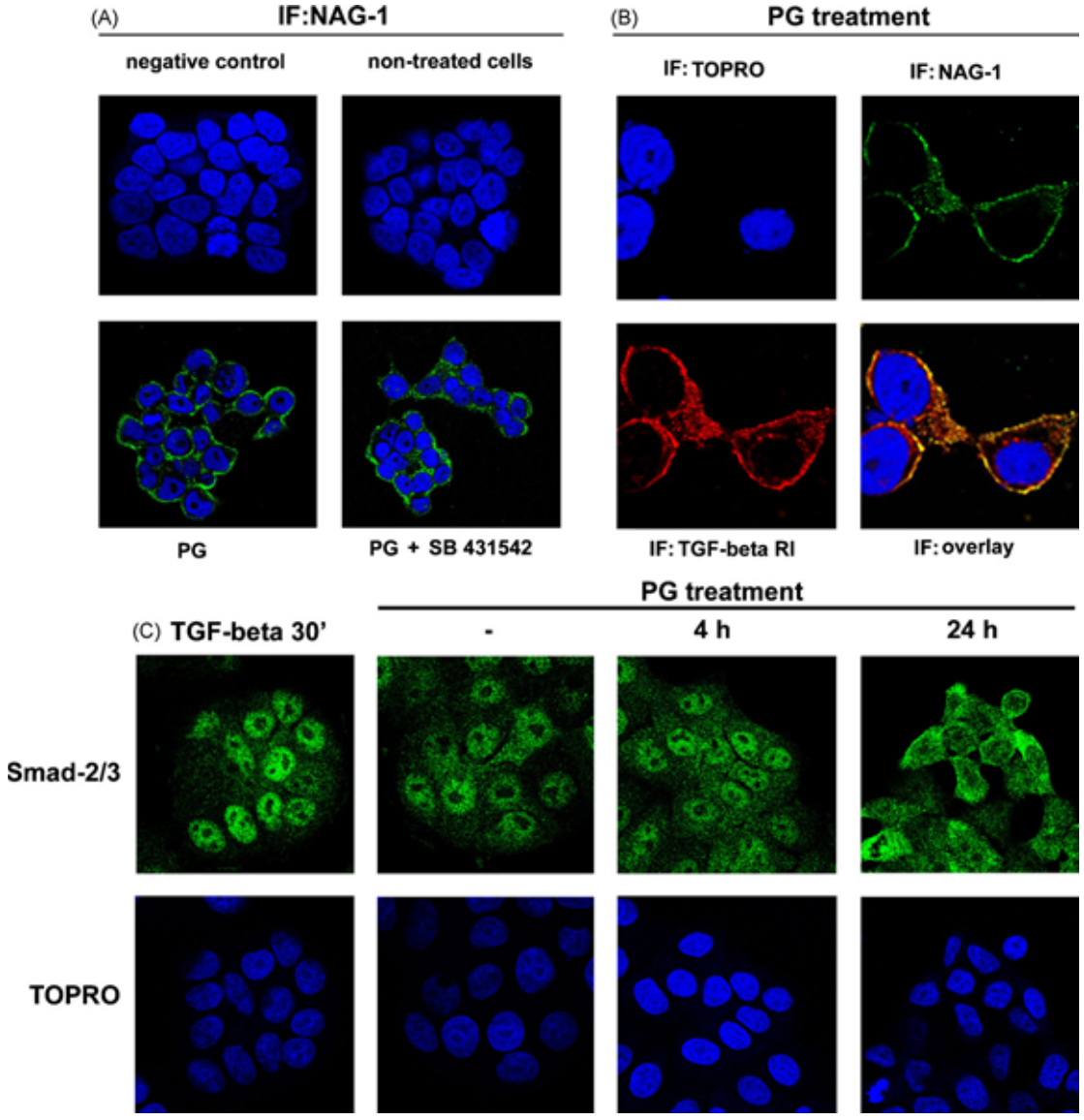

Fig. 4 – Cellular localization of NAG-1, TGF-βRI and smad-2/3. (A) Immunocytochemistry for NAG-1 detection was performed in MCF-7 cells ("negative control" [incubated without NAG-1 antibody] and "non-treated cells") and in cells treated with 0.5 μM prodigiosin for 24 h in the absence ("PG") or presence of 20 μM SB431542 ("PG + SB431542"). (B) MCF-7 cells exposed to 0.5 μM prodigiosin for 24 h were incubated with NAG-1 and TGF-βRI antibodies simultaneously; nuclear staining with TO-PRO®-3 iodide (TOPRO) was also performed. Representative immunofluorescent images from three independent experiments are shown. (C) MCF-7 cells were exposed to 0.5 μM prodigiosin for different time periods and then were incubated with smad-2/3 antibody; nuclear staining with TO-PRO®-3 iodide (TOPRO) was also performed. Representative immunofluorescent images from three independent experiments are shown.

observe that this pathway is not involved in prodigiosin cytotoxicity, although it might contribute to prodigiosin's cytostatic properties.

p21 is a cyclin-dependent kinase (CDK) inhibitor that belongs to the Cip/Kip family of CDK inhibitors. Cell cycle progression is blocked when the catalytic activity of (CDK)-cyclin complexes is inhibited by the binding of a CDK inhibitor molecule, such as p21 [22]. Cells exposed to stress signals, such as DNA-damaging agents, induce p21 expression, which leads to cell cycle arrest [23]. It has also been shown that overexpression of p21 results in G_1 and G_2 arrest [38]. Here we observe that prodigiosin treatment provokes cell cycle arrest as well as p21 induction. Likewise, the blockade of cell-cycle progression in response to prodigiosin was previously described in hematopoietic cancer cells [12]. Altogether, these results suggest that p21 might be involved in cell cycle arrest induced by prodigiosin treatment.

p21 gene expression can be transcriptionally regulated by a wide variety of different molecules [24]. It has been extensively described that p21 is a target gene of the tumor suppresor protein p53 [39]. After prodigiosin treatment, p21 gene expression was more than 34-fold higher than in non-treated

Please cite this article in press as: Soto-Cerrato V, et al., The anticancer agent prodigiosin induces $p21^{WAF1/CIP1}$ expression via transforming growth factor-beta receptor pathway, Biochem Pharmacol (2007), doi:10.1016/j.bcp.2007.07.016

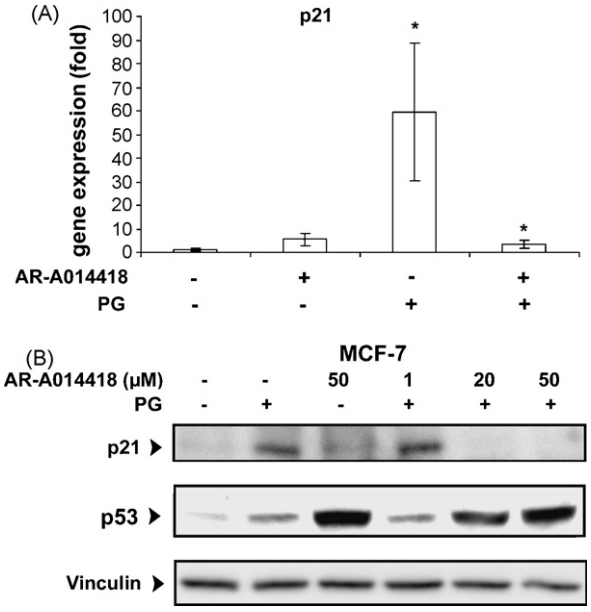

Fig. 5 – p21 regulation by GSK-3β. (A) MCF-7 cells were exposed to 0.5 μM prodigiosin for 24 h in the absence or presence of 50 μM AR-A014418 and changes in gene expression (fold changes with respect to control cells) were evaluated by quantitative real time RT-PCR. Columns are expressed as the means of three independent experiments, bars are S.D. Significant ($P < 0.05$) induction by prodigiosin or inhibition when combined with AR-A014418 is indicated by *. (B) After treating cells with 0.5 μM prodigiosin for 24 h with or without 1, 20 or 50 μM AR-A014418, cell lysates were collected for Western blot analysis using p21, p53 and vinculin antibodies. The latter is shown as a gel loading control. Representative blots from independent experiments are shown.

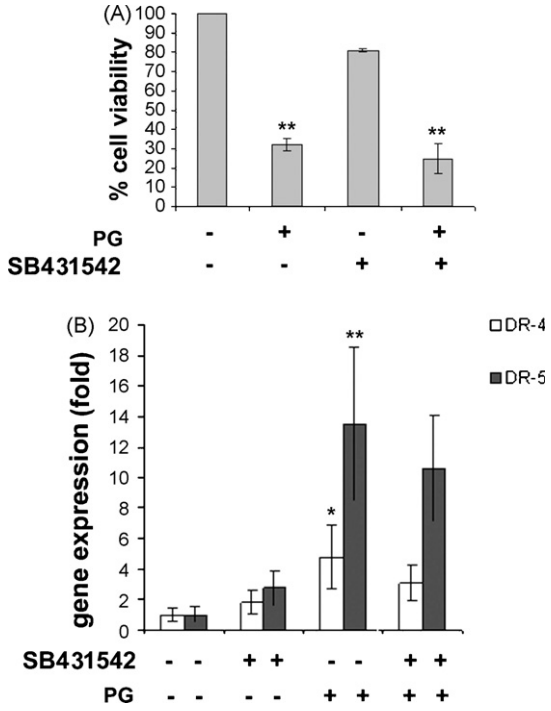

Fig. 6 – Analysis of the role of the TGF-β pathway in prodigiosin-induced apoptosis. (A) Cells were incubated with 1.4 μM prodigiosin for 24 h alone or in the presence of 20 μM SB431542 and cell viability was measured by the MTT assay. Data are expressed as the percentage of non-treated cells and shown as the mean (triplicate experiments) ± S.D. and statistical significance is indicated by *$P < 0.05$; **$P < 0.01$. (B) mRNA from MCF-7 cells that were either not treated or treated with 20 μM SB431542 (prior to 0.5 μM prodigiosin treatment for 24 h) was extracted and DR-4 and DR-5 levels were quantified by quantitative real-time RT-PCR. Data are presented as the mean of triplicate experiments (columns) ± S.D. (bars). Statistical significance is indicated by *$P < 0.05$; **$P < 0.01$.

cells. We observed that p21 gene expression was induced in a p53-independent way. This might represent an advantage in the clinical treatment of tumors, as the p53 protein is mutated in most human tumors. This mutation prevents cancer cells from suffering the cytostatic and/or cytotoxic effects of anticancer drugs [40].

The TGF-β pathway can also induce p21 expression [41] and this pathway is already activated in MCF-7 cells. The cytostatic and apoptotic functions of this pathway help control the homeostasis of normal tissues. The loss of these effects leads to hyperproliferative disorders [18]. Late stage human carcinomas, especially advanced breast cancers [42], often become resistant to TGF-β growth inhibition. They also overproduce this cytokine, probably to create a local immunosuppressive environment that promotes tumor growth and intensifies the invasive and metastatic behaviour of the tumor cells themselves [43]. Both features have been described in MCF-7 cells [36,42] and might explain why MCF-7 cells continue proliferating even when the TGF-β pathway is already active. The Smad-dependent pathway has previously been related to pro-metastatic properties and tumor cell invasiveness [44], hence this might be one advantage that its continuous activation may give to MCF-7 cells.

TGF-β pathway activation mediated by a TGF-β type I receptor has been shown to be necessary for p21 induction after prodigiosin treatment, but smad phosphorylation and translocation to the nucleus are not enough to induce p21 expression, as shown in MCF-7 cells. Other molecular pathways, which are or are not dependent on TGF-β pathway activation, also seem to interact with the p21 promoter. TGF-β family members also signal through a smad-independent TGF-β pathway. These include as downstream effectors the extracellular signal-regulated kinase (ERK), c-Jun NH2-terminal kinase (JNK), p38 MAPK, phosphatidylinositol-3 kinase (PI3K), TGF-β-activated kinase 1 (TAK1), protein phosphatase 2A (PP2A) and Rho GTPases [20]. In particular, it has been shown that the TGF-β family member NAG-1 activates the smad-dependent TGF-β pathway [25] but also some MAPK signaling pathways [45]. In addition, after prodigiosin cell exposure, NAG-1 is over expressed [15] and colocalizes with the TGF-β type I receptor. Therefore, it might bind to its receptor and activate some other molecule that is different than smads. This molecule, in collaboration or not with

Please cite this article in press as: Soto-Cerrato V, et al., The anticancer agent prodigiosin induces $p21^{WAF1/CIP1}$ expression via transforming growth factor-beta receptor pathway, Biochem Pharmacol (2007), doi:10.1016/j.bcp.2007.07.016

smads, may be responsible for p21 induction after prodigiosin treatment. In this regard, prodigiosin is known to activate the p38 MAPK kinase after 15 min of treatment in jurkat cells [46]. The p38 MAPK classes of protein kinases are activated by stress signals and mediate cellular responses, including steps in the apoptosis and maturation of some cell types [47]. Therefore, one possibility is that NAG-1 may bind to the TGF-β receptor, which in turn activates p38 inducing p21 expression through the sp1 transcription factor. This mechanism of action has previously been described in other compounds, such as benzyl isothiocyanate [48]. Besides this, NAG-1 is also capable of inducing cell-cycle arrest through p21 induction in ovarian cancer cells [49]. This fits with our proposed mode of prodigiosin-induced cell cycle arrest via the TGF-β pathway activated by the cytokine NAG-1.

However, an additional molecular pathway necessary for p21 induction could be independent of the TGF-β pathway. Prodigiosin provokes GSK-3β activation through AKT dephosphorylation [15]. This kinase is a negative regulator of p21 expression. The negative regulation occurs by exporting a transcription factor, called FoxO, necessary for TGF-β-stimulated p21 promoter activation [50] to the cytoplasm. Therefore, prodigiosin could be inducing AKT dephosphorylation, thus enabling FoxO to collaborate with the smads that still remain in the nucleus at early times of prodigiosin treatment in order to induce p21 expression.

In conclusion, among the molecular mechanisms of action of the anticancer agent prodigiosin, induction of the p21 cell cycle inhibitor through activation of the TGF-β pathway has been observed. This process might lead to cell-cycle arrest but it is not involved in the cytotoxic properties of this molecule. Altogether, these results shed light on the molecular mechanism of the action of prodigiosin and might explain its well-documented pharmacological effects as an immunosuppressor.

Acknowledgements

This work was supported by a research grant from Ministerio de Sanidad and the European Union (FIS-PI061226, R. Pérez-Tomás) and a research scholar award from the American Cancer Society (RSG-04-170-01-CNE, J.R. Lambert). The authors thank Julie A. Kelly for technical assistance and Esther Castaño and Benjamín Torrejón from Serveis Cientificotècnics (Campus de Bellvitge, Universitat de Barcelona) for their technical support.

REFERENCES

[1] Williamson NR, Fineran PC, Leeper FJ, Salmond GPC. The biosynthesis and regulation of bacterial prodiginines. Nat Rev Microbiol 2006;4(12):887–99.
[2] Han SB, Kim HM, Kim YH, Lee CW, Jang ES, Son KH, et al. T-cell specific immunosuppression by prodigiosin isolated from *Serratia marcescens*. Int J Immunopharmacol 1998;20(1–3):1–13.
[3] Perez-Tomas R, Montaner B, Llagostera E, Soto-Cerrato V. The prodigiosins, proapoptotic drugs with anticancer properties. Biochem Pharmacol 2003;66(8):1447–52.
[4] Zang J, Shen Y, Liu J, Wei D. Antimetastatic effect of prodigiosin through inhibition of tumor invasion. Biochem Pharmacol 2005;69(3):407–14.
[5] Montaner B, Navarro S, Pique M, Vilaseca M, Martinell M, Giralt E, et al. Prodigiosin from the supernatant of *Serratia marcescens* induces apoptosis in haematopoietic cancer cell lines. Br J Pharmacol 2000;131:585–93.
[6] Campas C, Dalmau M, Montaner B, Barragan M, Bellosillo B, Colomer D, et al. Prodigiosin induces apoptosis of B and T cells from B-cell chronic lymphocytic leukemia. Leukemia 2003;17(4):746–50.
[7] Diaz-Ruiz C, Montaner B, Perez-Tomas R. Prodigiosin induces cell death and morphological changes indicative of apoptosis in gastric cancer cell line HGT-1. Histol Histopathol 2001;16(2):415–21.
[8] Montaner B, Perez-Tomas R. Prodigiosin-induced apoptosis in human colon cancer cells. Life Sci 2001;68(17):2025–36.
[9] Soto-Cerrato V, Llagostera E, Montaner B, Perez-Tomas R. Mitochondria-mediated apoptosis operating irrespective of multidrug resistance in breast cancer cells by the anticancer agent prodigiosin. Biochem Pharmacol 2004;68(7):1345–52.
[10] Llagostera E, Soto-Cerrato V, Joshi R, Montaner B, Gimenez-Bonafe P, Perez-Tomas R. High cytotoxic sensitivity of the human small cell lung doxorubicin-resistant carcinoma (GLC4/ADR) cell line to prodigiosin through apoptosis activation. Anticancer Drugs 2005;16(4):393–9.
[11] Castillo-Avila W, Abal M, Robine S, Perez-Tomas R. Non-apoptotic concentrations of prodigiosin (H^+/Cl^- symporter) inhibit the acidification of lysosomes and induce cell cycle blockage in colon cancer cells. Life Sci 2005;78(2):121–7.
[12] Perez-Tomas R, Montaner B. Effects of the proapoptotic drug prodigiosin on cell cycle-related proteins in Jurkat T cells. Histol Histopathol 2003;18(2):379–85.
[13] Melvin MS, Wooton KE, Rich CC, Saluta GR, Kucera GL, Lindquist N, et al. Copper-nuclease efficiency correlates with cytotoxicity for the 4-methoxypyrrolic natural products. J Inorg Biochem 2001;87(3):129–35.
[14] Montaner B, Castillo-Avila W, Martinell M, Ollinger R, Aymami J, Giralt E, et al. DNA interaction and dual topoisomerase I and II inhibition properties of the anti-tumor drug prodigiosin. Toxicol Sci 2005;85(2):870–9.
[15] Soto-Cerrato V, Viñals F, Lambert JR, Kelly JA, Pérez-Tomás R. Prodigiosin induces the proapoptotic gene NAG-1 via glycogen synthase kinase-3β activity in human breast cancer cells. Mol Cancer Ther 2007;6(1):362–9.
[16] Francisco R, Perez-Tomas R, Gimenez-Bonafe P, Soto-Cerrato V, Gimenez-Xavier P, Ambrosio S. Mechanisms of prodigiosin cytotoxicity in human neuroblastoma cell lines. Eur J Pharmacol 2007; doi:10.1016/j.ejphar.2007.06.054.
[17] Massague J. TGF-beta signal transduction. Annu Rev Biochem 1998;67:753–91.
[18] Massague J, Blain SW, Lo RS. TGF-β signalling in growth control, cancer, and heritable disorders. Cell 2000;103:295–309.
[19] Shi Y, Massague J. Mechanisms of TGF-beta signaling from cell membrane to the nucleus. Cell 2003;113(6):685–700.
[20] Derynck R, Zhang YE. Smad-dependent and Smad-independent pathways in TGF-beta family signalling. Nature 2003;425(6958):577–84.
[21] Kang Y, Chen CR, Massague J. A self-enabling TGF-beta response coupled to stress signaling: Smad engages stress response factor ATF3 for Id1 repression in epithelial cells. Mol Cell 2003;11(4):915–26.
[22] Gartel AL, Serfas MS. Tyner AL. p21-negative regulator of the cell cycle. Proc Soc Exp Biol Med 1996;213:138–49.
[23] El-Deiry WS, Harper JW, O'Connor PM, Velculescu VE, Canman CE, Jackman J, et al. WAF1/CIP1 is induced

Please cite this article in press as: Soto-Cerrato V, et al., The anticancer agent prodigiosin induces $p21^{WAF1/CIP1}$ expression via transforming growth factor-beta receptor pathway, Biochem Pharmacol (2007), doi:10.1016/j.bcp.2007.07.016

in p53-mediated G1 arrest and apoptosis. Cancer Res 1994;54(5):1169–74.
[24] Gartel AL, Tyner AL. Transcriptional regulation of the p21 (WAF1/CIP1) gene. Exp Cell Res 1999;246:280–9.
[25] Tan M, Wang Y, Guan K, Sun Y. PTGF-β, a type β transforming growth factor (TGF- β) superfamily member, is a p53 target gene that inhibits tumor cell growth via TGF-β signalling pathway. Proc Natl Acad Sci USA 2000;97(1):109–14.
[26] Liu T, Bauskin AR, Zaunders J, Brown DA, Pankhurst S, Russell PJ, et al. Macrophage inhibitory cytokine 1 reduces cell adhesion and induces apoptosis in prostate cancer cells. Cancer Res 2003;63(16):5034–40.
[27] Li PX, Wong J, Ayed A, Ngo D, Brade AM, Arrowsmith C, et al. Placental transforming growth factor- β is a downstream mediator of the growth arrest and apoptotic response of tumor cells to DNA damage and p53 overexpression. J Biol Chem 2000;275(26):20127–35.
[28] Baek SJ, Kim KS, Nixon JB, Wilson LC, Eling TE. Cyclooxygenase inhibitors regulate the expression of a TGF-β superfamily member that has proapoptotic and antitumorigenic activities. Mol Pharmacol 2001;59(4):901–8.
[29] Newman D, Sakaue M, Koo JS, Kim KS, Baek SJ, Eling T, et al. Differential regulation of nonsteroidal anti-inflammatory drug-activated gene in normal human tracheobronchial epithelial and lung carcinoma cells by retinoids. Mol Pharmacol 2003;63(3):557–64.
[30] Wilson LC, Baek SJ, Call A, Eling TE. Nonsteroidal anti-inflammatory drug-activated gene (NAG-1) is induced by genistein through the expression of p53 in colorectal cancer cells. Int J Cancer 2003;105(6):747–53.
[31] Baek SJ, Wilson LC, Eling TE. Resveratrol enhances the expression of non-steroidal anti-inflammatory drug-activated gene (NAG-1) by increasing the expression of p53. Carcinogenesis 2002;23(3):425–34.
[32] Lambert JR, Kelly JA, Shim M, Huffer WE, Nordeen SK, Baek SJ, et al. Prostate derived factor in human prostate cancer cells: gene induction by vitamin D via a p53-dependent mechanism and inhibition of prostate cancer cell growth. J Cell Physiol 2006;208(3):566–74.
[33] Mosmann T. Rapid colorimetric assay for cellular growth and survival: application to proliferation and cytotoxicity assays. J Immunol Methods 1983;65:55–63.
[34] Datto MB, Li Y, Panus JF, Howe DJ, Xiong Y, Wang XF. Transforming growth factor beta induces the cyclin-dependent kinase inhibitor p21 through a p53-independent mechanism. Proc Natl Acad Sci USA 1995;92(12):5545–9.
[35] Inman GJ, Nicolas FJ, Callahan JF, Harling JD, Gaster LM, Reith AD, et al. SB-431542 is a potent and specific inhibitor of transforming growth factor-beta superfamily type I activin receptor-like kinase (ALK) receptors ALK4, ALK5, and ALK7. Mol Pharmacol 2002;62(1):65–74.
[36] Danforth Jr DN. All trans-retinoic acid acts synergistically with hydroxytamoxifen and transforming-growth factor beta to stimulate apoptosis in MCF-7 breast cancer cells. J Endocrinol 2004;183(2):395–404.
[37] Jang TJ, Kang HJ, Kim JR, Yang CH. Non-steroidal anti-inflammatory drug activated gene (NAG-1) expression is closely related to death receptor-4 and -5 induction, which may explain sulindac sulfide induced gastric cancer cell apoptosis. Carcinogenesis 2004;25(10):1853–8.
[38] Niculescu III AB, Chen X, Smeets M, Hengst L, Prives C, Reed SI. Effects of p21(Cip1/Waf1) at both the G1/S and the G2/M cell cycle transitions: pRb is a critical determinant in blocking DNA replication and in preventing endoreduplication. Mol Cell Biol 1998;18(1):629–43.
[39] el-Deiry WS, Tokino T, Velculescu VE, Levy DB, Parsons R, Trent JM. WAF1, a potential mediator of p53 tumor suppression. Cell 1993;75(4):817–25.
[40] Royds JA, Iacopetta B. p53 and disease: when the guardian angel fails. Cell Death Differ 2006;13(6):1017–26.
[41] Pardali K, Kurisaki A, Moren A, ten Dijke P, Kardassis D, Moustakas A. Role of Smad proteins and transcription factor Sp1 in p21 (Waf1/Cip1) regulation by transforming growth factor-beta. J Biol Chem 2000;275(38):29244–56.
[42] Reiss M, Barcellos-Hoff MH. Transforming growth factor-beta in breast cancer: a working hypothesis. Breast Cancer Res Treat 1997;45(1):81–95.
[43] Derynck R, Akhurst RJ, Balmain A. TGF-beta signaling in tumor suppression and cancer progression. Nat Genet 2001;29(2):117–29.
[44] Kang Y. Pro-metastasis function of TGFbeta mediated by the Smad pathway. J Cell Biochem 2006;98(6):1380–90.
[45] Nazarova N, Qiao S, Golovko O, Lou YR, Tuohimaa P. Calcitriol-induced prostate-derived factor: autocrine control of prostate cancer cell growth. Int J Cancer 2004;112(6):951–8.
[46] Montaner B, Perez-Tomas R. The cytotoxic prodigiosin induces phosphorylation of p38-MAPK but not of SAPK/JNK. Toxicol Lett 2002;129(1-2):93–8.
[47] Tibbles LA, Woodgett JR. The stress-activated protein kinase pathways. Cell Mol Life Sci 1999;55(10):1230–54.
[48] Moon SK, Choi YH, Kim CH, Choi WS. p38MAPK mediates benzyl isothiocyanate-induced p21WAF1 expression in vascular smooth muscle cells via the regulation of Sp1. Biochem Biophys Res Commun 2006;350(3):662–8.
[49] Kim JS, Baek SJ, Sali T, Eling TE. The conventional nonsteroidal anti-inflammatory drug sulindac sulphide arrests ovarian cancer cell growth via the expression of NAG-1/MIC-1/GDF-15. Mol Cancer Ther 2005;4(3):487–93.
[50] Seoane J, Le HV, Shen L, Anderson SA, Massague J. Integration of Smad and forkhead pathways in the control of neuroepithelial and glioblastoma cell proliferation. Cell 2004;117(2):211–23.

Please cite this article in press as: Soto-Cerrato V, et al., The anticancer agent prodigiosin induces $p21^{WAF1/CIP1}$ expression via transforming growth factor-beta receptor pathway, Biochem Pharmacol (2007), doi:10.1016/j.bcp.2007.07.016

Capítulo 2.4. Análisis proteómico de la apoptosis inducida por prodigiosina.

(**"**Monge M, Vilaseca M, Soto-Cerrato V, Montaner B, Giralt E, Pérez-Tomás R. Proteomic analysis of prodigiosin-induced apoptosis in a breast cancer mitoxantrone-resistant (MCF-7 MR) cell line. Invest New Drugs 2007;25(1):21-9").

En la misma línea de investigación, siguiendo con el propósito de entender mejor el mecanismo de acción del agente citotóxico prodigiosina en células de cáncer de mama, se realizó una nueva aproximación en nuestro grupo. Se llevó a cabo un estudio para identificar proteínas inducidas tras el tratamiento con dicha sustancia. Para ello se examinó, mediante electroforesis bidimensional de alta resolución, la variación en la expresión proteica causada tras la exposición a prodigiosina en células de cáncer de mama con fenotipo de resistencia a múltiples fármacos (MCF-7 MR). Seis proteínas asociadas al proceso de apoptosis fueron caracterizadas en profundidad mediante un espectrómetro de masas MALDI-TOF/TOF. Las proteínas identificadas estaban involucradas en varias funciones celulares, las cuales incluyen mecanismos de defensa celular, reparación del ADN y organización celular. Estos resultados muestran nueva información acerca de los mecanismos moleculares de respuesta al tratamiento con prodigiosina.

(Estudio llevado a cabo por nuestro grupo de investigación en el que he contribuido de forma parcial).

Invest New Drugs (2006) 25:21–29
DOI 10.1007/s10637-006-7774-8

PRECLINICAL STUDIES

Proteomic analysis of prodigiosin-induced apoptosis in a breast cancer mitoxantrone-resistant (MCF-7 MR) cell line

Marta Monge · Marta Vilaseca · Vanessa Soto-Cerrato · Beatriz Montaner · Ernest Giralt · Ricardo Pérez-Tomás

Published online: 5 April 2006

Summary Prodigiosin (PG) is a bacterial, red-pigmented antibiotic with immunosuppressive and apoptotic activities. To better understand its mechanisms of action, we tried to identify proteins associated with apoptosis induced by PG. For this purpose, the variation of protein expression on exposure to apoptotic concentrations of PG was examined, by high-resolution two-dimensional gel electrophoresis (2D-E), in the MCF-7 cancer cell line resistant to mitoxantrone (MCF-7-MR). Six PG apoptosis-associated protein spots were further characterized by complementary peptide mass fingerprinting and tandem mass spectrometry data obtained on a matrix-assisted laser desorption ionization-time-of-flight/time-of-flight (MALDI-TOF/TOF) mass spectrometer. The proteins identified were involved in various cellular functions, including cell defence, DNA repair and cellular organization. Our data provide novel information on cell response to PG, a new apoptotic drug with interesting anticancer activity.

Keywords Apoptosis · Prodigiosin · Proteomics · Breast cancer

M. Monge · V. Soto-Cerrato · B. Montaner · R. Pérez-Tomás
Department of Pathology and Experimental Therapeutic,
Cancer Cell Biology Research Group, University of Barcelona,
Barcelona, Spain

M. Vilaseca
Servei Espectrometria de Masses-Serveis Cientificotècnics,
University of Barcelona, Barcelona,
Spain

E. Giralt
Departament de Química Orgànica, IRBB-PCB,
University of Barcelona, Barcelona,
Spain

R. Pérez-Tomás (✉)
Dept. Patologia i Terapèutica Experimental. CCBR Group,
Pavelló Central, 5ªplanta. LR 5101, C/Feixa Llarga s/n,
E-08907 L'Hospitalet, Barcelona, Spain
Tel.: 34-93-402-4288
Fax: 34-93-402-9082

Abbreviations

CK: Cytokeratin; FA: formic acid; GST: glutathione S-transferase; IFs: intermediate filaments; IEF: Isoelectric focusing; pI: isoelectric point; MALDI-TOF/TOF: matrix-assisted laser desorption ionization-time-of-flight/time-of-flight; MCF-7-MR: MCF-7 breast cancer cell line resistant to mitoxantrone; MAPK: mitogen-activated protein kinase; MDR: multidrug resistance; MRP: multidrug resistance protein; PG: prodigiosin; TFA: trifluoroacetic acid; 2D-E: two-dimensional gel electrophoresis; V-ATPase: vacuolar H^+-ATPase; CHCA: α-cyano-4-hydroxycinnamic acid; DHB: 2,5-dihydroxybenzoic acid.

Introduction

Prodigiosins (PGs) are a family of naturally occurring polypyrrole red pigments produced by a small group of microorganisms, including *Streptomyces* and *Serratia* strains, characterized by a common pyrrolyldipyrrolylmethene skeleton.

PG has potent antimicrobial, antimalarial and cytotoxic action (for a review, see [1]). PG rapidly and potently triggers apoptosis in hematopoietic, gastrointestinal and lung cancer cell lines, whilst not being markedly toxic to non-malignant cell lines [2–5]. PG also triggers the reorganization of the actin cytoskeleton and may promote the breakdown of actin

microfilaments, which might be involved in apoptotic cell death [5].

Four possible mechanisms of action for these molecules have been suggested: (i) PGs as pH modulators; (ii) PGs as cell cycle inhibitors; (iii) PGs as DNA cleavage agents; (iv) PGs as mitogen-activated protein kinase (MAPK) regulators. Part of the action of PGs depends on their ability to uncouple vacuolar H^+-ATPase (V-ATPase) through promotion of the H^+/Cl^- symporter and to induce neutralisation of the acid compartment of cells, so bringing about cytosol acidification and eventual apoptosis [6, 7]. PG inhibits the proliferation of human Jurkat T cells mainly *via* G1-S transition arrest [8]. Moreover, PG-induced apoptosis is p53-independent, which may represent an advantage over other chemotherapeutic drugs [3]. In addition, PG is a DNA-interacting agent with a preference for alternating base pairs, that induces DNA single- and double-strand breaks *via* poisoning topoisomerases and through copper-promoted oxidative DNA damage [9]. Finally, PG-induced cytotoxicity is mediated by phosphorylation of p38-MAPK, but not of SAPK/JNK [10].

In this study, we characterized the PG up-regulated proteins in MCF-7 parental and MCF-7-MR breast cancer cell lines. We examined, by High-resolution 2D-E, the variation in protein expression on the exposure of both cell lines to apoptotic concentrations of PG. The protein expression pattern of both cell lines were similar so we focused on MCF-7-MR cells. This cell line has the multidrug resistance (MDR) phenotype characterized by high levels of the ABCG2 transporter [11], which confers on these cells a very high degree of resistance to mitoxantrone [12]. The importance of doing the study in this cell line is that, despite this phenotype, the transporter cannot expel PG from the cell. Thus, the cell is sensitive to PG's apoptotic effect [13].

Comparison of the 2D-E protein pattern in non-treated and PG-treated cells showed differences in 6 proteins, which were analysed/identified by complementary peptide mass fingerprinting and tandem mass spectrometry, using a MALDI-TOF/TOF mass spectrometer. Of these proteins, one was related to cell detoxification (Glutathione S-transferase M3), another to DNA repair (Ribosomal Potein P0) and the others to cell structure (Cytokeratin -19, -18 and -8). Our data support the view that cells, during the apoptosis induced by PG, suffer important structural cytoskeleton changes and try to defend themselves in response to PG and to repair the cell damage induced by the drug.

Methods

Isolation and purification of PG

2-Methyl-3-pentyl-6-methoxyprodigiosene (PG) was purified from a culture of *S. marcescens* 2170, as previously described [3]. It was then solubilized and its concentration determined by UV–vis in 95% EtOH–HCl (ε_{535} = 112 000/$M^{-1}cm^{-1}$).

Cell culture

The human breast carcinoma cell line MCF-7-MR was a generous gift from Dr. Scheffer (Pathology Dept., Free University, Amsterdam). The cells were cultured in DMEM: HAMF-12 (1:1) (Biological Industries), 10% fetal bovine serum (FBS) (Gibco BRL), 2 mM L-glutamine, 100 U/ml penicillin, 100 μg/ml streptomycin, 50 μM sodium pyruvate, 10 μg/ml insulin and 50 μg/ml gentamycin at 37°C and 5% CO_2.

Preparation of protein samples

After cells (5×10^5/ml) were exposed to 1 μM of PG for 1/4, 1/2, 1, 3, 6, 12, 16 and 24 h, they were then washed in PBS and a lysis buffer was added (85 mM Tris pH 6.8, 2% SDS, 1 μg/ml aprotinin, 1 μg/ml leupeptin and 0.1 mM PMSF). Protein extracts were quantified using Pierce's BCA Assay Kit (Bio Rad Lab, CA).

High-resolution two-dimensional gel electrophoresis

The method used is based on the one described by O'Farrell [14], but with some modifications. Isoelectric focusing (IEF) electrophoresis was used to separate the proteins according to isoelectric point (pI) in the first dimension. IEF gels (120 mm) were made in glass tubing (160 × 4-mm inside diameter) and contained 10.3 g urea, 7.125 ml distilled water, 2.44 ml acrylamide (28.38% acrylamide, 1.62% bis-acrylamide), 0.750 ml carrier ampholytes 3/10, 0.375 ml NP-40, 34.625 μl PSA 15% and 12.5 μl TEMED (all chemicals are from Bio-Rad Lab, CA). After half an hour's polymerisation, a pre-run for focusing the ampholytes was performed by loading 30 μl lysis solution [9.8 M urea, 2% NP-40 (10% in distilled water), 2% carrier ampholytes 7/9, 100 mM DTT] and over 30 μl overlay solution (8 M urea, 1% carrier ampholytes 7/9, 5% NP-40, 100 mM DTT). Upper running buffer (20 mM NaOH) was degassed for 10 min, but the lower one (10 mM H_3PO_4) was not. The electrophoretic conditions of the rod gels during the IEF were: 200 V for 1/4 h, 300 V for 1/2 h and 400 V for 1 h. Then, solutions were removed from the top of the gels and 300 μg of the samples were prepared by adding lysis solution in a 1:2 proportion and then heating for 2 min at 100°C, before loading. 30 μl of overlay solution was added above every sample, which was then run at 400 V for 16 h. After focusing, IEF gels were maintained in equilibrating buffer (0.06 M Tris-HCl Ph 6.8, 2% SDS, 5% BME, 10% Glycerol) for 30 min and could then be frozen at –80°C. After thawing, the rod gels were equili-

brated again for 15 min in an SDS-DTT equilibrating buffer containing 100 mg DTT in 10 ml SDS-buffer (50 mM Tris pH 8.8, 6 M urea, 30% glycerol, 2% SDS, 0.002% bromophenol blue). The SDS-DTT equilibrating buffer was removed and a second one, containing 250 mg Iodoacetamyde in 10 ml SDS buffer, added. Then, the IEF rod gels were immediately applied to an SDS-polyacrylamide gel that contained 10.5% or 12% acrylamide, but the stacking gel was replaced by IEC rod gels fixed to the SDS-PAGE gel with an agarose solution (1% agarose, 0.002% bromophenol blue in the first equilibrating buffer). For analytical gels, proteins were silver-stained following an MS-compatible protocol [15].

Enzymatic in-gel digestion, extraction of peptides from the gel

Protein spots were isolated in small pieces and subjected to in-gel tryptic digestion overnight at 37°C (Sequencing Grade Modified Trypsin, Promega). Peptides were extracted from the gel with 50 μl of 50% CH_3CN/50%, 5% Trifluoroacetic acid (TFA) [16].

Sample preparation for MALDI-MS and MALDI-MS/MS

Peptide mixtures were prepared freshly by dissolving again the lyophilised tryptic digests in 7 μl CH_3CN/5% TFA (1:1, vol/vol). A combination of α-cyano-4-hydroxycinnamic acid (CHCA) and 2,5-dihydroxybenzoic acid (DHB) was used as a matrix. The mixture was prepared by making separate solutions of the two matrices, each in its specific solvent. (a) CHCA: 5 mg/ml in CH_3CN/5% formic acid (FA) (70:30, vol/vol); (b) DHB: 5 mg/ml in CH_3CN/0.1% TFA (70:30, vol/vol)]. The solutions were then combined in a 1:1 volume ratio. The resulting mixture was used as the matrix solution in a dried-droplet preparation [17]: 0.5 μl peptide solution and 0.5 μl matrix were mixed in a clean Eppendorf and then applied to the MALDI sample plate and allowed to dry.

Mass spectrometry and database searching

All experiments were performed on an Applied Biosystems MALDI-TOF/TOF mass spectrometer (4700 Proteomics Analyzer, Framingham, MA, USA).

1. *Protein identification using peptide maps*: to obtain the peptide mass maps, positively charged ions were analysed in the reflector mode using delayed extraction over a m/z range 300–4,000. Usually 1,000 shots were averaged to improve the signal-to-noise ratio with a laser power of 5,000–6,000. All spectra were analysed using the 4.4 version Data Explorer software. The measured monoisotopic masses of peptides produced by MALDI-MS were automatically compared with a m/z peak list in the Peak Erazor Program (1.45 version) to remove m/z peaks from keratin contaminants, trypsin autolysis products and other blank products or unknowns. Protein from the resultant peak lists was identified by searching in a protein sequence database (NCBInr), using the Peptide Mass Fingerprint Mascot program (http://www.matrixscience.com).
2. *Protein identification using tandem mass spectra*: peptide ions from each sample were selected to obtain the MS/MS data. Laser power and collision energy were adjusted manually to obtain desirable fragmentation patterns. Positively charged ions were analysed in the reflector mode, using delayed extraction over a mass range from 0 to the m/z of the precursor ion selected. The Mascot Sequence Query Program identified proteins with MS/MS data.
3. *Protein identification by combination of peptide maps and MS/MS results:* data peak lists obtained by MS and MS/MS analysis were sent together to the Mascot Sequence Query program, giving protein identification with higher scores.

Western blot analysis

50 μg of protein extracts were separated by SDS–PAGE on a 10% or 12% polyacrylamide gel and transferred to immobilon-P membranes (Millipore, MA, USA). Blots were blocked in 5% dry milk diluted in TBS-T (50 mM Tris–HCl, pH 7.5, 150 mM NaCl, 0.1% Tween-20) for 1% and then incubated overnight at 4°C or 3 h at room temperature with polyclonal antibodies against cleaved caspase-7 (Cell Signalling Technology, New England Biolabs), caspase-8 (PharMingen BD Biosciences), anti-PARP (New England Biolabs), actin (Sta Cruz Biotechnology, Inc.) and with the monoclonal antibodies, anti-caspase-9 (Upstate), anti-Keratin-8 (Oncogene) and anti-keratin-19 (NeoMarkers), according to the manufacturer's instructions. Antibody binding was detected with goat anti-rabbit or goat anti-mouse IgG secondary antibodies conjugated to HRP (BioRad Lab, CA) and the ECL detection kit (Amersham).

Alternatively, after 2D-gel electrophoresis, the separated proteins were transferred according to the above procedures and incubated with monoclonal antibodies against α, μ-Glutathione S-transferase (GST) (Sta Cruz Biotechnology), according to the manufacturer's recommendations.

Results

PG induces apoptosis in MCF-7-MR cell line

To identify proteins associated with PG-induced apoptosis, we first characterised the conditions under which PG triggered significantly apoptosis in the MCF-7-MR cell line. For

this purpose, we analysed the time-dependent activation of the main proteases that execute apoptosis, such as the initiator caspases-9 and -8 and also the effector caspase-7, as well as cleavage of the caspase substrate PARP. We used 1 μM concentrations of the drug as the dose that induces 25% apoptosis in this cell line [13]. Processing of caspase-9 and -8 was evident in MCF-7-MR cells incubated for 24 h with 1 μM PG, as shown by the disappearance of their inactive forms of 45 and 55/50 kDa, respectively (Fig. 1). Furthermore, PG promoted the appearance of the caspase-7 active form of 20 kDa between 12–24 h of incubation (Fig. 1). Finally, with an antibody which recognises both the 116 kDa parent PARP and the 89 kDa cleaved product, PARP processing increased at 12 to 24 h in response to PG treatment (Fig. 1). These results demonstrate the effective induction of apoptosis by 1 μM PG in a time-dependent manner in MCF-7-MR cells, with a maximum effect at 24 h of PG incubation.

Protein expression pattern associated with apoptosis in the PG-treated MCF-7-MR cell line

We compared 2D-E patterns of non-treated MCF-7-MR cells *versus* 24 h PG-treated MCF-7-MR cells, as apoptosis induction was found relevant at this time. We analysed the appearance or increase in intensity of protein spots as a surrogate of protein induction associated with PG-related apoptosis. Six main areas containing up-regulated proteins came up in 2D-E comparison of 24 h-treated *versus* control non-treated cells (Fig. 2).

A more detailed analysis of each area is illustrated in Fig. 3; where both MCF-7 parental (Fig. 3A) and MCF-7-MR cell line (Fig. 3B) showed similar protein pattern expression. Area P1 shows a protein (arrow) with an approximate molecular weight of 27 kDa and pI 6.5–7.0 (see Fig. 2). This spot increased significantly more at 24 h of PG treatment than control non-treated cells. A protein of approximately 36 kDa and pI 6.8–6.9 emerged in the P2 area during PG treatment. Interestingly, two spots were visible at 16 h of PG treatment, with a shift to neutral pH as apoptosis increased at 24 h. In the P3 area, a protein of approximately 26 kDa and pI 5.5–6.0 emerged in PG-induced apoptotic cells, while the P4 area showed the increased levels of a protein of approximately 28 kDa and pI 6.8–6.9 in PG treated for 24 h *versus* control non-treated cells. A similar effect occurred in the P5 and P6 areas, in which two proteins of approximately 44 kDa and pI 5.7–5.9 and 44 kDa and pI 5.9–6.0, respectively, increased in expression as apoptosis was induced by PG treatment for 24 h. All the proteins above mentioned were obtained from at least three independent experiments that showed high reproducibility. In order to identify the selected protein spots, next experiments were focused to the PG-treated and untreated MCF-7-MR cell line.

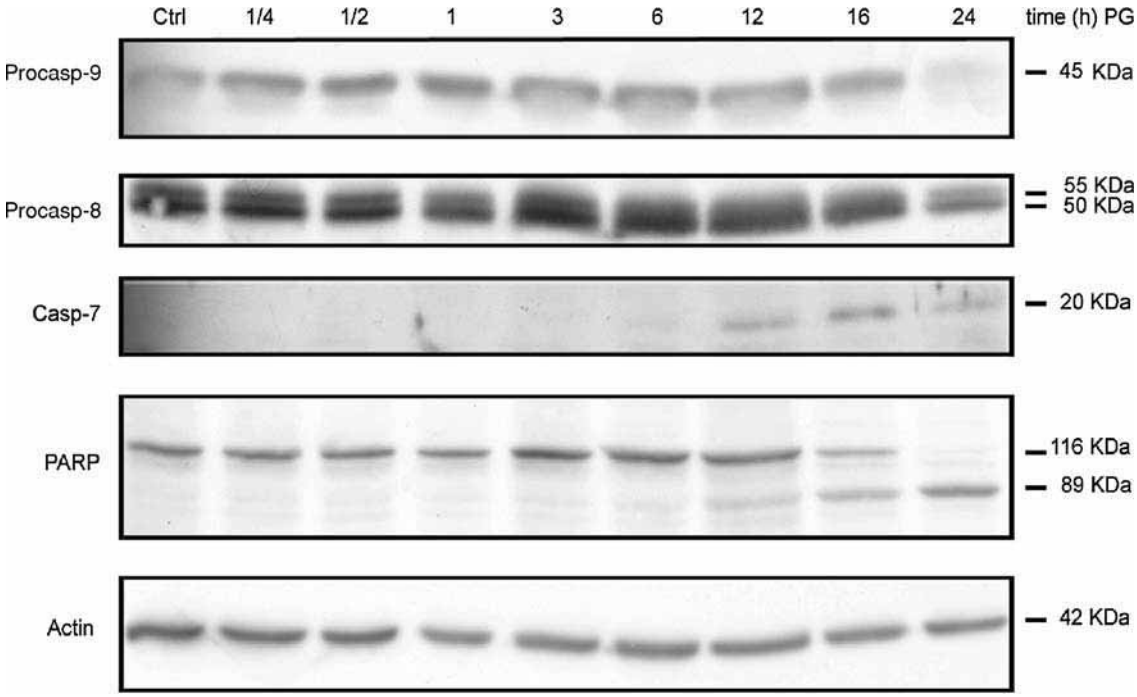

Fig. 1 PG-induced apoptosis in MCF-7-MR cell line. Cells were exposed to 1 μM of PG for 1/4, 1/2, 1, 3, 6, 12, 16 and 24 h and processed for Western Blot analysis of cleavage products of procaspase-9, -8; caspase-7, and PARP cleavage. Actin levels were used as load controls

Table 1 Identification of PG-induced apoptosis proteins as determined by MALDI-TOF and MALDI-TOF/TOF-MS and by Edman degradation

Data base protein identification	MW	Spot number	Spot regulation	m/z of sequenced peptides	Internal sequence
Glutathion S-transferase M3 protein	26998	P1	Up-regulation	1972	LTFVDFLTYDQNR
				1655	LKPQYLEELPGQL
Ribosomal protein, large, PO	34424	P2	Appearance	1895.90	VLALSVETDYTFPLAK
Keratin 18 protein, type I cytoskeletal 18 (Cytokeratin 18)	47897	P3	Appearance	1419.91	QAQEYEALLNIK
				1506.90	TVQSLEIDLDSMR
Keratin 19, type I, cytoskeletal	44065	P4	Up-regulation	850.58	FGPGVAFR
				1041.75	IVLQIDNAR
				1675.01	DYSHYYTTIQDLR
Keratin 19, type I cytoskeletal 19	44079	P5	Up-regulation	1674.76	DYSHYYTTIQDLR
Cytokeratin 8	53529	P6	Up-regulation	1419.74	LEGLTDEINFLR
				1762.99	SYTSGPGSRISSSSFSR

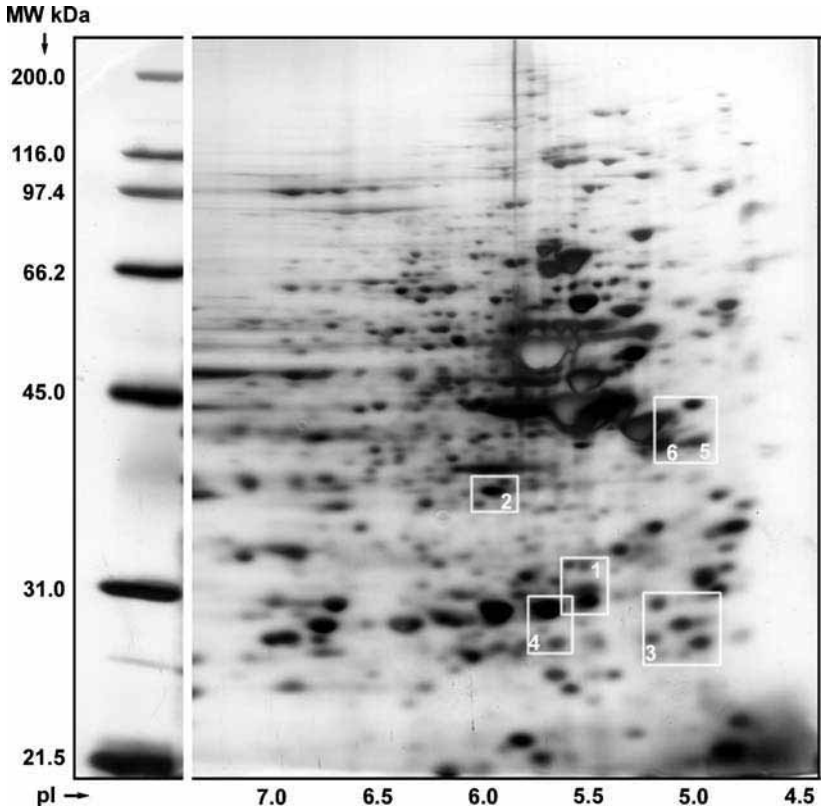

Fig. 2 Protein expression pattern associated with the PG-treated MCF-7-MR cell line. 2D-E pattern of total cell extract from 24 h PG-treated MCF-7-MR cells. The gel size was 16 × 12 × 0.016 cm. Proteins were detected by silver staining. The inserts enclose those up-regulated proteins (numbered 1 to 6) that were further analysed by peptide mass fingerprinting and tandem mass spectrometry using a MALDI-TOF/TOF mass spectrometer

Identification of up-regulated proteins in the PG-treated MCF-7-MR cell line

To identify the spots described in the 2D-E comparison of PG-treated and untreated MCF-7-MR cells, we analysed them by complementary peptide mass fingerprinting and tandem mass spectrometry, using a MALDI-TOF/TOF mass spectrometer (Table 1).

The peptide mass map of the tryptic digest of the P1 protein did not identify any protein with a significant score. Additionally, two tandem TOF/TOF mass spectra were acquired from the peptide precursor ions, with m/z 1972.85 and 1655.93. The subsequent database search from the product ion results identified the two fragments as LKPQYLEELPGQL and LTFVDFLTYDQNR, respectively, from glutathione S-Transferase M3 protein (MW 26 998) with scores of 33 and 61 (Fig. 4). By combining the peptide mass map and the MS/MS results, the protein was identified more specifically as Chain B, Ligand-Free Heterodimeric Human Glutathione S-Transferase M2-3 (MW 26 867) with a score of 71. 16 peptide ions matched the masses of the protein with a 58% sequence coverage.

The peptide mass map results of the tryptic digest of P2 protein were combined with the results of a tandem mass

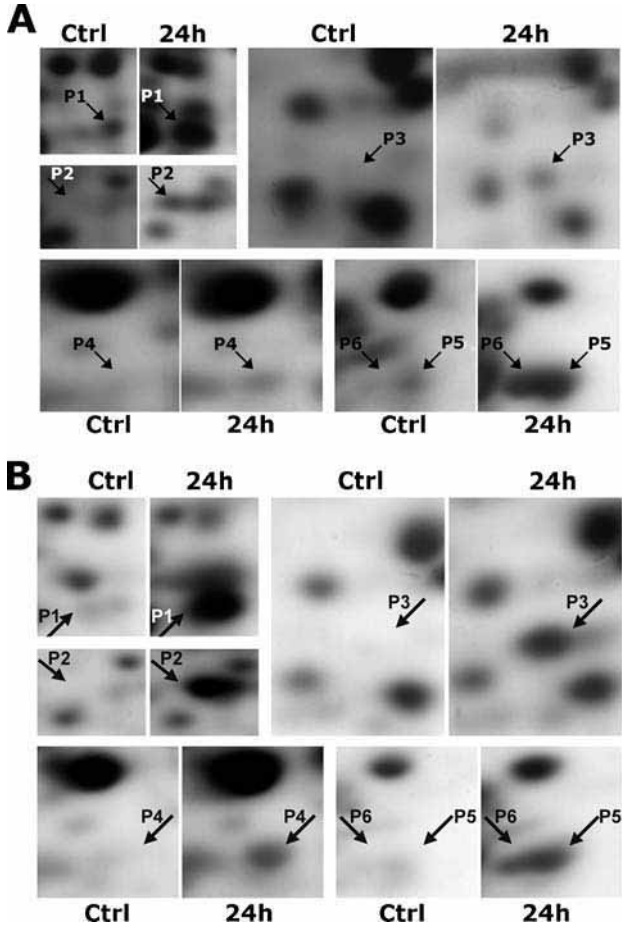

Fig. 3 Enlargement of the 2D-E areas containing the up-regulated proteins (P1, P2, P3, P4, P5, P6) that came up in the 2D-E comparison of control non-treated *versus* 24 h-treated in both MCF-7 parental cells (A) and MCF-7-MR cells (B). Altered proteins are marked with arrows. Results are representative of three independent experiments

experiment on the same sample acquired from a peptide precursor ion with m/z 1895.90. The database search in the Mascot program matched the peptide fragment with the sequence VLALSVETDYTFPLAK of the Ribosomal protein, large, PO (MW 34 424) with a total score of 65 and 12% sequence coverage.

In a peptide mass map of the tryptic digest of P3 protein, masses of 8 peptide ions matched the masses of cytokeratin 18 (CK-18) (calculated MW 47 897), with an average accuracy of 50 ppm. In addition, two tandem TOF/TOF mass spectra were acquired from the peptide precursor ions with m/z 1419.91 and 1506.90. The following database search from the product ion results identified the two fragments as QAQEYEALLNIK and TVQSLEIDLDSMR, respectively, from the Keratin 18 protein, type-I cytoskeletal 18 (CK-18). By combining the peptide mass map and the MS/MS results, this protein was identified with a score of 70.

In the case of P4 protein, 11 peptide fragments matched the masses of cytokeratin 19 (CK-19) tryptic peptides with an average accuracy of <30 ppm and 47% sequence coverage. MS/MS experiments on three peptide ion precursors, with m/z 850.58, 1041.75 and 1675.01, matched the following sequences, respectively: FGPGVAFR, IVLQIDNAR and DYSHYYTTIQDLR, with scores from 65–75. CK-19 (MW 44 065) matched the results with a score of 72. AF20231 NID protein also matched the same set of peptides with the same score.

Protein 5 was also identified as CK-19 (MW 44 079), with a score of 76, by combination of the peptide mass map results and the tandem experiment results acquired on the peptide precursor ion m/z 1674.76. The sequence identified for the latest fragment was DYSHYYTTIQDLR and 10 more peptides could be matched with 27% sequence coverage.

Protein 6 was identified as cytokeratin 8 (CK-8) (MW 53 529), with a score of 71, by the corresponding peptide mass map results, matching the masses of 12 peptide ions. Two peptide precursor ions with m/z 1419.74 and 1762.99 were matched with the sequences LEGLTDEINFLR and SYTSGPGSRISSSSFSR, respectively, by tandem mass experiments. The combined results of the MS/MS and MS experiments confirmed CK-8 as the most likely protein, with a very high score of 153 and 15 peptide ions matched with 32% sequence coverage.

MS and MS/MS experiments were repeated 3 times for each protein analysed, with different sample digests coming from different gel runs. Results given here were perfectly reproduced.

PG induces up-regulation of Glutathione S-Transferase

To validate the results given here, we blotted a 2D-E membrane with antibodies recognising the isoforms α and μ of the GST protein. These antibodies specifically recognised three spots. The most basic one, visible at 24 h of PG treatment (Fig. 5B) but not in the control membrane (Fig. 5A), corresponded to the spot identified in the P1 area as the glutathion S-Transferase M3. This result validates the mass spectrometry identification of the proteins associated with PG-induced apoptosis.

Discussion

Apoptosis has become one of the most extensively studied biomedical events of the last two decades. Dysfunctional apoptosis has an impact on major human diseases like cancer and neurodegenerative or infectious diseases [18]. The basic mechanism of apoptosis undoubtedly involves the modification of proteins. Proteomic analysis is an excellent tool for understanding these alterations during apoptosis. In the last few years, proteome analyses have been performed with some apoptotic agents that are currently un-

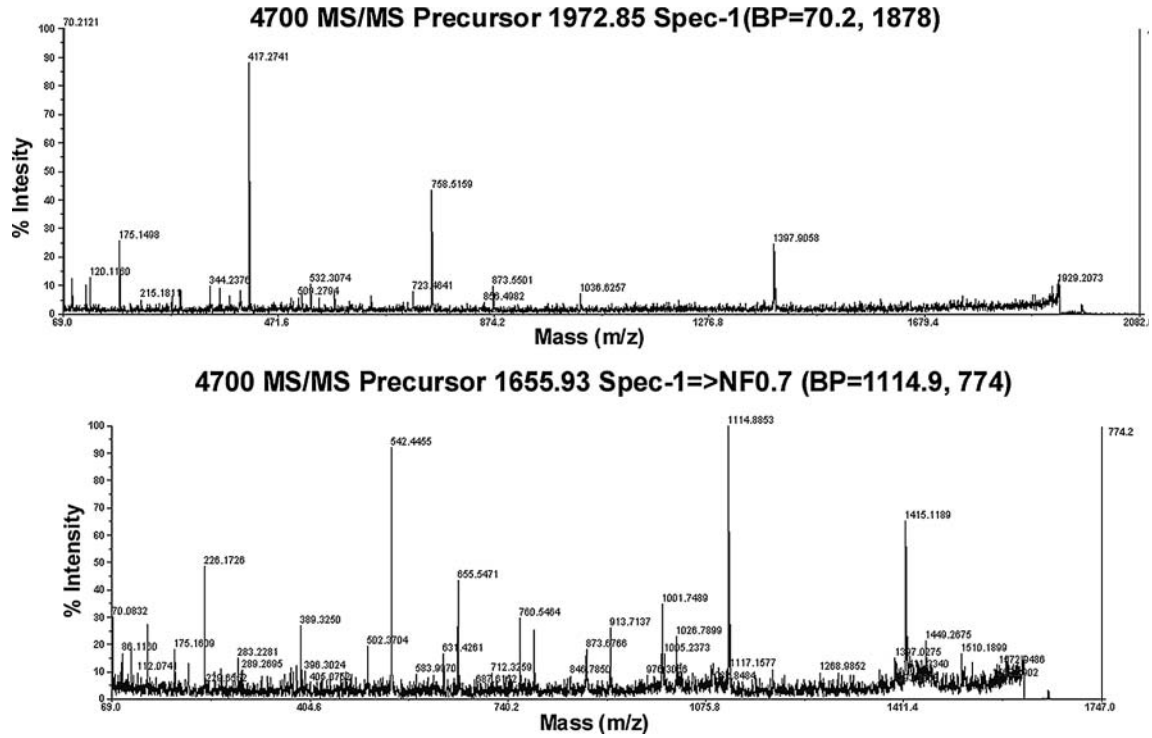

Fig. 4 Chain B, Ligand-Free Heterodimeric Human Glutathione S-Transferase M2-3 spot identification: MALDI-TOF/TOF-MS of the tryptic digestion mixture. Two tandem TOF/TOF mass spectra were acquired from the peptide precursor ions with m/z 1655.93 (lower spectrum) and 1972.85 (upper spectrum)

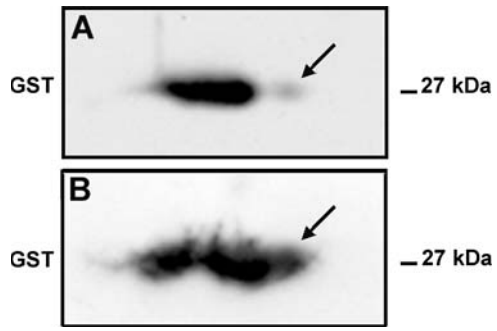

Fig. 5 PG induces up-regulation of Glutathione S-Transferase. (A) P1 area of the 2D-E membrane corresponding to non-treated MCF-7-MR cells blotted with antibodies recognizing the isoforms α and μ of the glutathion S-Transferase protein (GST). (B) P1 area of the 2D-E membrane corresponding to PG-treated MCF-7-MR cells blotted as above. The Glutathione S-Transferase M2-3 isoform is indicated by arrows

der active pre-clinical research or being used clinically for cancer [19, 20].

Prodigiosins are an emerging group of natural agents with promising anti-cancer properties [21]. Recently we demonstrated that PG is effective, regardless of the presence of MDR transporter molecules [13]. To better understand the molecular events triggered by PG, in the present study we analysed up-regulated proteins in the PG-treated MCF-7 cancer cell line resistant to mitoxantrone.

Our experiments demonstrated that Glutathion S-transferase M3 (P1), a protein involved in protective and drug metabolism functions, was up-regulated during PG-induced apoptosis. Increased expression of certain GST isoenzymes has often been associated with the development of resistance to alkylating agents and other classes of anti-neoplasm drugs in drug-selected cell lines [22–24]. Furthermore, the over-expression of GST can operate in synergy with efflux transporters such as multidrug resistance proteins (MRPs), and thus confer resistance to several carcinogens, mutagens and anticancer drugs. For example, over-expression of GSTM1 alone in melanoma is involved in resistance to chlorambucil, whereas it can act in synergy with MRP1 to protect cells from the toxic effects of vincristine [25]. Using MCF-7-MR cells (cell line with MDR phenotype), high levels of the ABCG2 transporter have been reported [12]. Furthermore, we recently demonstrated that PG induces apoptosis in these cells, overcoming the ABCG2 transporter [13]. The increase of GSTM3 in the PG MCF-7-MR-treated cell line may be a consequence of a detoxification reaction in the presence of PG rather than a cause/effect relationship between GST over-expression and resistance mechanisms.

The ribosomal stalk structure is a distinct lateral protuberance composed of acidic ribosomal P proteins, forming two heterodimers (P1/P2) attached to the ribosome through the P0 protein [26]. Here we demonstrated the appearance of the P0 ribosomal protein after 24 h exposure to PG in the MCF-7-MR cell line. Similar effect on the P0 ribosomal protein was

observed in a proteomic study using the Burkitt lymphoma cell line (BL60-2) treated with anti-IgM antibody-mediated apoptosis [27]. Furthermore, the P0 gene was induced (30- to 50-fold) by some DNA-damaging agents, commonly used as chemotherapeutic anti-tumour agents, in various human cancer cell lines that lack 0^6-methylguanine methyltransferase activity (Mer^-). These agents are DNA repair-defective for 0^6-alkyguanine lesions [28]. These results lead to the conclusion that P0 is somehow linked to DNA repair and has been over-expressed in the Mer^- cell lines to compensate for decreased MGMT activity. PG intercalates itself into the DNA and induces single- and double-strand DNA cleavage [29]. Presumably, the increase in the P0 ribosomal protein observed here is a consequence of the DNA repair activity associated with this ribosomal protein; another anti-tumour agent, cisplatin, causes modest increases in the transcription of P0 [28]. Another possible role for P0 protein was postulated by Nishida et al., who found that several ribosomal proteins including P0 move to the surface of apoptotic cells during apoptosis and suggested that such molecules serve as markers for recognition of apoptotic cells by phagocytic cells [30].

Cytokeratins are also major structural proteins in epithelial cells. They comprise the intermediate filaments (IFs) of cytoskeletons and are expressed in various combinations, depending on the epithelial type and the degree of differentiation [31]. Cytokeratins-18 and -8 are the main components of IFs. During apoptosis these cytoskeleton proteins are reorganized by caspases leading to dramatic structural cell changes [32]. As has been previously reported, CK-18 but not CK-8 is cleaved by caspase-6 into NH_2 –terminal, 26 kDa and COOH-terminal, 22 kDa fragments during drug- and UV light–induced apoptosis [33]. This processing of CK-18 probably occurs under the experimental conditions used in the present paper, in which in the presence of PG we obtain a 26 kDa protein fragment, called P3, identified as CK-18. In contrast, CK-8 is resistant to proteolysis during the apoptosis induced by PG in MCF-7-MR, which is similar to what Caulin et al. (1997) and Ku et al. (1997) observed when using different cell lines and apoptosis conditions.

In addition, we observed a fragment of 28 kDa, called P5, identified as CK-19. This processing of CK-19 by caspases was also described in colon cancer cells exposed to anisomycin, generating two fragments of 28 and 20 kDa [34].

In summary, apoptosis induced by PG in the MCF-7-MR cell line generates stable fragments of human type-I (CK-18 and CK-19) but not type-II (CK-8) cytokeratins, which indicates that type-I cytokeratins are targets of apoptosis-activated caspases. This is probably a general feature of cytokeratins in most if not all epithelial cells undergoing apoptosis. Furthermore, these cytokeratins were released by the cell using an unknown mechanism and provide useful serum markers for evaluating the clinical progress of patients with epithelial malignancies [35, 36]. In addition, the up-regulation of GSTM3 protein and the appearance of P0 protein, observed in this study, provide evidence that cells try to defend themselves in response to PG and to repair the cell damage induced by this cytotoxic drug.

Altogether, these findings explain the molecular events triggered by PG and help to understand the response of cancer cell line to the exposure of antitumoral drugs.

Acknowledgments We want to thank Miguel Abal for critical and comprehensive reading of the manuscript. We also want to thank Dr. Eliandre de Oliveira and David Bellido from "Plataforma de Proteòmica" University of Barcelona for technical support. M. Monge was a recipient of a fellowship from the University of Barcelona.

References

1. Montaner B, Perez-Tomas R (2003) The prodigiosins: A new family of anticancer drugs. Curr Cancer Drug Targets 3:57–65
2. Llagostera E, Soto-Cerrato V, Joshi R, Montaner B, Gimenez-Bonafe P, Perez-Tomas R (2005) High cytotoxic sensitivity of the human small cell lung doxorubicin-resistant carcinoma (GLC4/ADR) cell line to prodigiosin through apoptosis activation. Anticancer Drugs 16:393–399
3. Montaner B, Navarro S, Pique M, Vilaseca M, Martinell M, Giralt E, Gil J, Perez-Tomas R (2000) Prodigiosin from the supernatant of Serratia marcescens induces apoptosis in haematopoietic cancer cell lines. Br J Pharmacol 131:585–593
4. Montaner B, Perez-Tomas R (2001) Prodigiosin-induced apoptosis in human colon cancer cells. Life Sci 68:2025–2036
5. Diaz-Ruiz C, Montaner B, Perez-Tomas R (2001) Prodigiosin induces cell death and morphological changes indicative of apoptosis in gastric cancer cell line HGT-1. Histol Histopathol 16:415–421
6. Sato T, Konno H, Tanaka Y, Kataoka T, Nagai K, Wasserman HH, Ohkuma S (1998) Prodigiosins as a new group of H + /Cl- symporters that uncouple proton translocators. J Biol Chem 273:21455–21462
7. Yamamoto C, Takemoto H, Kuno K, Yamamoto D, Tsubura A, Kamata K, Hirata H, Yamamoto A, Kano H, Seki T, Inoue K (1999) Cycloprodigiosin hydrochloride, a new H(+)/Cl(-) symporter, induces apoptosis in human and rat hepatocellular cancer cell lines *in vitro* and inhibits the growth of hepatocellular carcinoma xenografts in nude mice. Hepatology 30:894–902
8. Perez-Tomas R, Montaner B (2003) Effects of the proapoptotic drug prodigiosin on cell cycle-related proteins in Jurkat T cells. Histol Histopathol 18:379–385
9. Melvin MS, Wooton KE, Rich CC, Saluta GR, Kucera GL, Lindquist N, Manderville RA (2001) Copper-nuclease efficiency correlates with cytotoxicity for the 4-methoxypyrrolic natural products. J Inorg Biochem 87:129–135
10. Montaner B, Perez-Tomas R (2002) The cytotoxic prodigiosin induces phosphorylation of p38-MAPK but not of SAPK/JNK. Toxicol Lett 129:93–98
11. Ross DD, Yang W, Abruzzo LV, Dalton WS, Schneider E, Lage H, Dietel M, Greenberger L, Cole SP, Doyle LA (1999) A typical multidrug resistance: Breast cancer resistance protein messenger RNA expression in mitoxantrone-selected cell lines. J Natl Cancer Inst 91:429–433
12. Taylor CW, Dalton WS, Parrish PR, Gleason MC, Bellamy WT, Thompson FH, Roe DJ, Trent JM (1991) Different mechanisms of decreased drug accumulation in doxorubicin and mitoxantrone

resistant variants of the MCF7 human breast cancer cell line. Br J Cancer 63:923–929
13. Soto-Cerrato V, Llagostera E, Montaner B, Scheffer GL, Perez-Tomas R (2004) Mitochondria-mediated apoptosis operating irrespective of multidrug resistance in breast cancer cells by the anticancer agent prodigiosin. Biochem Pharmacol 68:1345–1352
14. O'Farrell PH (1975) High resolution two-dimensional electrophoresis of proteins. J Biol Chem 250:4007–4021
15. Heukeshoven J, Dernick R (1988) Improved silver staining procedure for fast staining in PhastSystem Development Unit. I. Staining of sodium dodecyl sulfate gels. Electrophoresis 9:28–32
16. Erdjument-Bromage H, Lui M, Lacomis L, Grewal A, Annan RS, McNulty DE, Carr SA, Tempst P (1998) Examination of micro-tip reversed-phase liquid chromatographic extraction of peptide pools for mass spectrometric analysis. J Chromatogr A 826:167–181
17. Laugesen S, Roepstorff P (2003) Combination of two matrices results in improved performance of MALDI MS for peptide mass mapping and protein analysis. J Am Soc Mass Spectrom 14:992–1002
18. Reed JC, Tomaselli KJ (2000) Drug discovery opportunities from apoptosis research. Curr Opin Biotechnol 11:586–592
19. He QY, Chiu JF (2003) Proteomics in biomarker discovery and drug development. J Cell Biochem 89:868–886
20. Thiede B, Rudel T (2004) Proteome analysis of apoptotic cells. Mass Spectrom Rev 23:333–349
21. Perez-Tomas R, Montaner B, Llagostera E, Soto-Cerrato V (2003) The prodigiosins, proapoptotic drugs with anticancer properties. Biochem Pharmacol 66:1447–1452
22. Morrow CS, Smitherman PK, Townsend AJ (2000) Role of multidrug-resistance protein 2 in glutathione S-transferase P1-1-mediated resistance to 4-nitroquinoline 1-oxide toxicities in HepG2 cells. Mol Carcinog 29:170–178
23. Cullen KJ, Newkirk KA, Schumaker LM, Aldosari N, Rone JD, Haddad BR (2003) Glutathione S-transferase pi amplification is associated with cisplatin resistance in head and neck squamous cell carcinoma cell lines and primary tumors. Cancer Res 63:8097–8102
24. Harbottle A, Daly AK, Atherton K, Campbell FC (2001) Role of glutathione S-transferase P1, P-glycoprotein and multidrug resistance-associated protein 1 in acquired doxorubicin resistance. Int J Cancer 92:777–783
25. Depeille P, Cuq P, Mary S, Passagne I, Evrard A, Cupissol D, Vian L (2004) Glutathione S-transferase M1 and multidrug resistance protein 1 act in synergy to protect melanoma cells from vincristine effects. Mol Pharmacol 65:897–905
26. Tchorzewski M, Krokowski D, Rzeski W, Issinger OG, Grankowski N (2003) The subcellular distribution of the human ribosomal "stalk" components: P1, P2 and P0 proteins. Int J Biochem Cell Biol 35:203–211
27. Brockstedt E, Rickers A, Kostka S, Laubersheimer A, Dorken B, Wittmann-Liebold B, Bommert K, Otto A (1998) Identification of apoptosis-associated proteins in a human Burkitt lymphoma cell line. Cleavage of heterogeneous nuclear ribonucleoprotein A1 by caspase 3. J Biol Chem 273:28057–28064
28. Grabowski DT, Pieper RO, Futscher BW, Deutsch WA, Erickson LC, Kelley MR (1992) Expression of ribosomal phosphoprotein PO is induced by antitumor agents and increased in Mer- human tumor cell lines. Carcinogenesis 13:259–263
29. Montaner B, Castillo-Avila W, Martinell M, Ollinger R, Aymami J, Giralt E, Perez-Tomas R (2005) DNA interaction and dual topoisomerase I and II inhibition properties of the anti-tumor drug prodigiosin. Toxicol Sci 85:870–879
30. Nishida J, Shiratsuchi A, Nadano D, Sato TA, Nakanishi Y (2002) Structural change of ribosomes during apoptosis: Degradation and externalization of ribosomal proteins in doxorubicin-treated Jurkat cells. J Biochem (Tokyo) 131:485–493
31. Steinert PM, Roop DR (1988) Molecular and cellular biology of intermediate filaments. Annu Rev Biochem 57:593–625
32. Oshima RG (2002) Apoptosis and keratin intermediate filaments. Cell Death Differ 9:486–492
33. Caulin C, Salvesen GS, Oshima RG (1997) Caspase cleavage of keratin 18 and reorganization of intermediate filaments during epithelial cell apoptosis. J Cell Biol 138:1379–1394
34. Ku NO, Liao J, Omary MB (1997) Apoptosis generates stable fragments of human type I keratins. J Biol Chem 272:33197–33203
35. Kramer G, Erdal H, Mertens HJ, Nap M, Mauermann J, Steiner G, Marberger M, Biven K, Shoshan MC, Linder S (2004) Differentiation between cell death modes using measurements of different soluble forms of extracellular cytokeratin 18. Cancer Res 64:1751–1756
36. Stigbrand T (2001) The versatility of cytokeratins as tumor markers. Tumour Biol 22:1–3

3. CARACTERIZACIÓN DEL EFECTO ANTICANCEROSO DEL TRIPIRROL PRODIGIOSINA EN OTROS MODELOS DE CÁNCER HUMANOS

Capítulo 3.1. Caracterización de la apoptosis inducida por prodigiosina en células de cáncer de pulmón.

("Llagostera E, Soto-Cerrato V, Montaner B, Pérez-Tomás R. Prodigiosin induces apoptosis by acting on mitochondria in human lung cancer cells. Ann N Y Acad Sci 2003;1010:178-81").

El cáncer de pulmón es la primera causa de muerte por esta enfermedad en las sociedades occidentales. Fue por ello que en nuestro grupo se planteó evaluar la actividad de prodigiosina en la línea cancerosa GLC4 de carcinoma de pulmón de célula pequeña. Las dosis necesarias para inducir apoptosis fueron del orden de nanomolar, identificando este proceso por la condensación de la cromatina. Posteriormente se quiso evaluar el papel de la mitocondria en la apoptosis inducida por prodigiosina. Para ello se analizó la salida de sustancias apoptogénicas de este compartimento celular. Tanto citocromo c como AIF incrementaban considerablemente en la fracción citoplasmática. Esta salida fue provocada de forma dependiente del tiempo, siendo el citocromo c el primero que se liberó. Estos resultados muestran como la apoptosis inducida por prodigiosina provoca la permeabilización de la membrana externa mitocondrial y con ello la salida de sustancias apoptogénicas.

(Estudio llevado a cabo por nuestro grupo de investigación en el que he contribuido de forma parcial).

Prodigiosin Induces Apoptosis by Acting on Mitochondria in Human Lung Cancer Cells

ESTHER LLAGOSTERA, VANESSA SOTO-CERRATO, BEATRIZ MONTANER, AND RICARDO PÉREZ-TOMÁS

Departament de Biologia Cellular i Anatomia Patològica, Cancer Cell Biology Research Group, Universitat de Barcelona, Barcelona, Spain

ABSTRACT: Prodigiosin (PG) is a secondary metabolite, isolated from a culture of *Serratia marcescens*, which has shown potent cytotoxicity against various human cancer cell lines as well as immunosuppressive activity. The purpose of this study was to evaluate the role of mitochondria in PG-induced apoptosis. Therefore, we evaluated the apoptotic action of PG in GLC4 small cell lung cancer cell line by Hoechst 33342 staining. In these cells, we examined mitochondrial apoptosis-inducing factor (AIF) and cytochrome *c* (cyt *c*) release to the cytosol in PG time-response studies. These findings suggest that PG induces apoptosis in both caspase-dependent and caspase-independent pathways.

KEYWORDS: AIF; apoptosis; cytochrome *c*; mitochondria; prodigiosin

INTRODUCTION

Prodigiosin (PG) belongs to a family of tripyrrole red pigments produced by a restricted group of *Streptomyces* and *Serratia* strains, which exhibit promising antitumor and immunosuppressive activities. PG has shown useful cytotoxicity against various human cancer cell lines[1,2] as well as immunosuppressive activity.[3]

The caspase family of proteins is one of the main effectors of apoptosis. However, they are not required for cell death to occur in many systems. For example, apoptosis-inducing factor (AIF) is a caspase-independent death effector which, upon apoptosis induction, translocates from mitochondrial intermembrane to the nucleus and causes chromatin condensation and fragmentation of DNA into 50 kb fragments.[4] In contrast to cytochrome *c*, AIF does not appear to require the presence of further cytosolic factors to induce apoptotic features in nuclei.

On the basis of previous results that showed the activation of caspase-9, -8, and -3 in PG-treated Jurkat cells,[5] we pursued the characterization of the role of mitochondria in PG-induced apoptosis in GLC4 cells.

Address for correspondence: Ricardo Pérez-Tomás, Departament de Biologia Cellular i Anatomia Patològica, Cancer Cell Biology Research Group, Universitat de Barcelona, Ed. Pavelló Central, LR 5101, C/ Feixa Llarga s/n, E-08907 L'Hospitalet (Barcelona), Spain. Voice: 34-93 4024288; fax: 34-93 4029082.
rperez@bell.ub.es

Ann. N.Y. Acad. Sci. 1010: 178–181 (2003).
doi: 10.1196/annals.1299.030

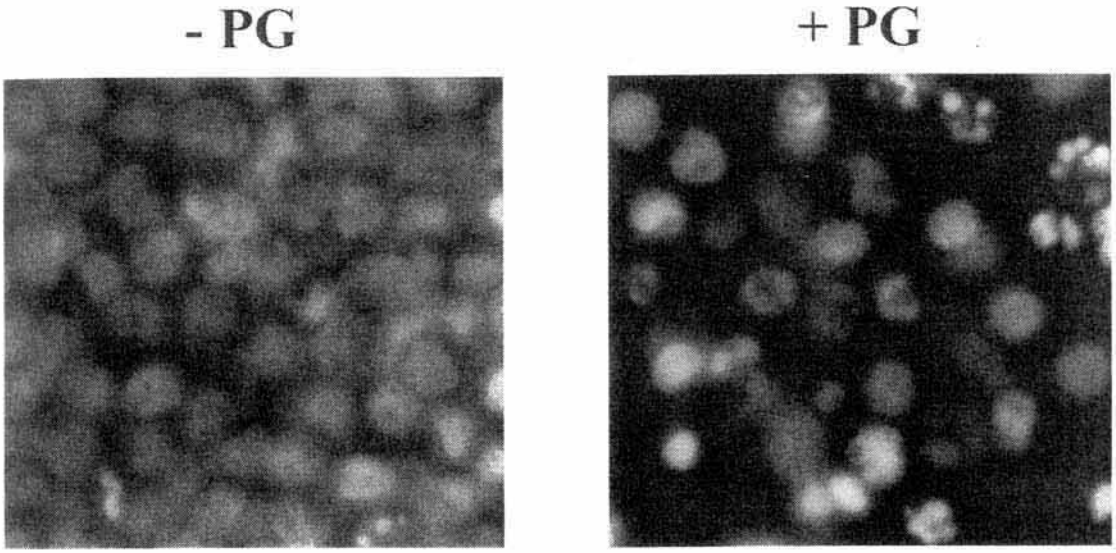

FIGURE 1. Fluorescence microscopic analysis of GLC4 nuclei with Hoechst 33342 staining. Cells were untreated (–PG) or treated (+PG) with 200 nM PG for 16 hours.

MATERIAL AND METHODS

Cell Culture

GLC4 small cell lung cancer cell lines were cultured in RPMI 1640 medium supplemented with 10% fetal calf serum, 100 U/mL penicillin, 100 µg/mL streptomycin, and 4 mM L-glutamine, at 37°C, 5% CO_2 in air.

Isolation and Purification of PG

PG was isolated from a culture of *S. marcescens* 2170 as described previously.[1]

Hoechst Staining

For cell morphology evaluation, cells (5×10^5/mL) were untreated or treated with 200 nM PG for 16 h, washed with PBS, and incubated with 2 µg/mL Hoechst 33342 (Sigma, USA) for 30 min, at 37°C in the dark. The sections were examined with a Leitz Diaplan microscope and photographed with a Wild MPS 45 Photoautomat system.

AIF and Cyt c *Release Analysis*

AIF and cyt *c* release from mitochondria to cytosol were measured by Western blot. After cells (5×10^6) were treated with 200 nM PG for 15 to 720 min, they were lysed in ice-cold lysis buffer (250 mM sucrose, 1 mM EDTA, 0.05% digitonin, 25 mM Tris pH 6.8, 1 mM DTT, 1 µg/mL aprotinin, 1 µg/mL leupeptin, 1 µg/mL pepstatin, and 0.1 mM PMSF), for 30 sec, then centrifuged at 13,000×*g* at 4°C for 3 min. Supernatants (cytosolic extracts) were electrophoresed on 12% polyacrylamide gels and transferred to Immobilon-P membranes (Millipore, USA). Then they were incubated overnight with a polyclonal antibody against AIF (Oncogen Research prod-

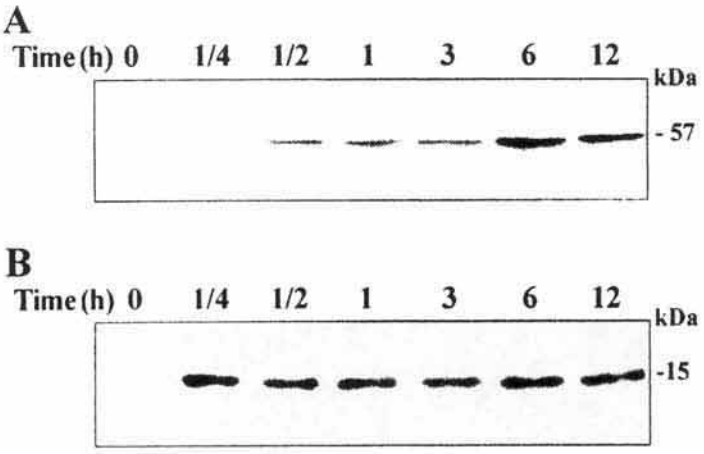

FIGURE 2. Effect of PG on mitochondrial AIF and cyt *c* release. (**A**) Analysis of AIF in cytosolic extracts. Time-dependent release of AIF into the cytosol upon exposure to PG (200 nM) is observed. (**B**) Time-course of cyt *c* release to the cytosol in response to PG treatment (200 nM).

ucts, USA) or with a monoclonal antibody against cyt *c* (Pharmingen International). Secondary antibodies conjugated to HRP were goat anti-rabbit IgG or goat anti-mouse IgG (BioRad, UK). Peroxidase was developed using the enhanced chemiluminescence (ECL) detection kit (Amersham, UK).

RESULTS AND DISCUSSION

The exceptional cytotoxic potency of PG in GLC4 cells (IC_{50} 129 and 143 nM at 16 and 24 h, respectively) prompted us to determine the apoptotic effect of PG in GLC4 cells. We characterized several morphological nuclear changes at microscopic level using Hoechst 33342 staining (FIG. 1). In contrast to untreated cells, chromatin condensation and nuclear fragmentation were observed in PG-treated cells, which are the hallmarks of apoptosis. These changes were triggered by apoptogenic factors harbored by mitochondria. To determine the role of mitochondria in PG-induced apoptosis, we studied its effect on some of these molecules. We found that PG induced mitochondrial release of AIF (FIG. 2A) and also demonstrated the release of cyt *c* into the cytosol (FIG. 2B). Both phenomena occur promptly upon exposure to PG.

These findings suggest that PG causes apoptosis to use the mitochondrial pathway and that PG apoptosis induction occurs in both caspase-dependent and -independent manner to ensure efficient DNA breakdown. Altogether, PG induces the release of cyt *c* and AIF into the cytoplasm. Cyt *c* binds to the adaptor Apaf-1 and the complex recruits and activates caspase 9. This initiates a caspase cascade responsible for the hydrolysis of key cytoplasmic proteins, for cleavage among genomic DNA nucleosomes into 180 bp fragments via the caspase-activated DNase (CAD). On the other hand, AIF migrates to the nucleus and induces high-molecular-mass DNA fragmentation and marginal chromatin condensation. The combined action of caspases and AIF causes the apoptotic phenotype observed in GLC4 cells and cell death.

ACKNOWLEDGMENTS

This work was supported by a grant from the Ministry of Science and Technology and the European Union (SAF2001-3545), and by a "Marató de TV3" grant (Ref. # 001510).

REFERENCES

1. MONTANER, B., S. NAVARRO, M. PIQUÉ, *et al.* 2000. Prodigiosin from the supernatant of *Serratia marcescens* induces apoptosis in haematopoietic cancer cell lines. Br. J. Pharmacol. **131:** 585–593.
2. MONTANER, B. & R. PÉREZ-TOMÁS. 2001. Prodigiosin-induced apoptosis in human colon cancer cells. Life Sci. **68:** 2025–2036.
3. CAMPÀS, C., M. DALMAU, B. MONTANER, *et al.* 2003. Prodigiosin induces apoptosis of B and T cells from B-cell chronic lymphocytic leukemia. Leukemia **17:** in press.
4. LORENZO, H.K., S.A. SUSIN, J. PENNINGER & G. KROEMER. 1999. Apoptosis inducing factor (AIF): a phylogenetically old, caspase-independent effector of cell death. Cell Death Differ. **6:** 516–524.
5. MONTANER, B. & R. PÉREZ-TOMÁS. 2002. Prodigiosin induces caspase-9 and caspase-8 activation and cytochrome *c* release in Jurkat T cells. Ann. N.Y. Acad. Sci. **973:** 246–249.

Capítulo 3.2. Estudio de la sensibilidad al tratamiento con prodigiosina de células de cáncer de pulmón resistentes a doxorrubicina.

(**"**Llagostera E, Soto-Cerrato V, Joshi R, Montaner B, Giménez-Bonafé P, Pérez-Tomás R. High cytotoxic sensitivity of the human small cell lung doxorubicin-resistant carcinoma (GLC4/ADR) cell line to prodigiosin through apoptosis activation. Anticancer Drugs 2005;16(4):393-9").

Como hemos visto anteriormente, prodigiosina puede ejercer su efecto antitumoral en células de mama que sobreexpresan la proteína de resistencia a múltiples fármacos ABCG2. Para ampliar los conocimientos del efecto de prodigiosina sobre células con fenotipo MDR, se utilizó una línea celular de cáncer de pulmón resistente a doxorrubicina llamada GLC4/ADR. Dichas células sobreexpresan la proteína ABC MRP-1, la cual confiere resistencia a diferentes fármacos que ABCG2. En primer lugar se analizó el efecto de prodigiosina sobre la viabilidad celular de GLC4/ADR, viendo que no existían diferencias significativas en la toxicidad inducida por prodigiosina respecto a la que inducía en su línea parental GLC4/S. Además, prodigiosina provocó muerte por apoptosis en las dos líneas celulares, pudiendo observar activación de caspasas, rotura de la PARP y salida de citocromo c en ambas. Estos resultados corroboran los ya descritos acerca de la capacidad de prodigiosina de actuar en células resistentes a múltiples fármacos y amplía esta cualidad a células que sobreexpresen la proteína MRP-1.

(Estudio llevado a cabo por nuestro grupo de investigación en el que he contribuido de forma parcial).

Fe de Erratas

La versión del artículo que se presenta a continuación es la prueba de imprenta provisional. En la publicación definitiva aparecen las siguientes correcciones.

- AQ1: reemplazar "Location" por "Lausen, Switzerland" y siguiente "Location" por "Hercules, CA"
- AQ2: reemplazar "Pepita Giménez-Bonafé[a]" por "Pepita Giménez-Bonafé[b]"
- AQ3: insertar "[b] Department of Physiological Sciences II, Physiology Unit, University of Barcelona, Barcelona, Spain."
- AQ4: reemplazar por "Sponsorship: This study was supported by grant SAF2001-3545 from the Ministerio de Ciencia y Tecnología and the European Union and BMC-2002-04081-C02-02 from the Ministerio de Educación y Ciencia and a grant from La Marató de TV3 (001510)."
- AQ5: reemplazar "we" por "In the present study, we"
- AQ6: reemplazar "(perhaps all)" por "(if not all)"
- AQ7: reemplazar "each" por "every"
- AQ8: reemplazar "H_2O" por "DEPC treated water"
- AQ9: reemplazar "The time-course" por "Time-course"
- AQ10: reeplazar "given" por "giving"
- AQ11: reemplazar "play" por "plays"
- AQ12: reemplazar "to the blots" por "of the blots"
- AQ13: reemplazar "show" por "shown"
- AQ14: reemplazar "We draw attention to" por "It is important to note"
- AQ15: reemplazar "in the same" por "at the same"
- AQ16: cambiar orden por "dose-response assay after PG treatment is observed"
- AQ17: reemplazar "describe" por "describes"
- AQ18: reemplazar "to show" por "that shows"
- AQ19: eliminar "As can observe that"
- AQ20: reemplazar "supplied" por "added"

High cytotoxic sensitivity of the human small cell lung doxorubicin-resistant carcinoma (GLC4/ADR) cell line to prodigiosin through apoptosis activation

Esther Llagostera[a], Vanessa Soto-Cerrato[a], Ricky Joshi[a], Beatriz Montaner[a], Pepita Gimenez-Bonafé[a] and Ricardo Pérez-Tomás[a]

We describe the cytotoxicity of the new drug prodigiosin (PG) in two small cell lung carcinoma (SCLC) cell lines, GLC4 and its derived doxorubicin-resistant GLC4/ADR cell line, which overexpresses multidrug-related protein 1 (MRP-1). We observed through Western blot that PG mediated cytochrome *c* release, caspase cascade activation and PARP cleavage, thereby leading to apoptosis in a dose–response manner. MRP-1 expression increased after PG treatment, although that does not lead to protein accumulation. The MTT assay showed no difference in sensitivity to PG between the two cell lines. Our results support PG as a potential drug for the treatment of lung cancer as it overcomes the multidrug resistance phenotype produced by MRP-1 overexpression. *Anti-Cancer Drugs* 16:000–000 © 2005 Lippincott Williams & Wilkins.

Anti-Cancer Drugs 2005, **16**:000–000

Keywords: apoptosis, chemotherapy, lung cancer, multidrug resistance, prodigiosin

[a]Department of Cellular Biology and Pathology, Cancer Cell Biology Research Group, University of Barcelona, Barcelona, Spain.

Sponsorship: This study was supported by grant SAF2001-3545 from the Ministerio de Ciencia y Tecnologacute;a and the European Union, and a grant from La Marató de TV3 (001510).

Correspondence to R. Pérez-Tomás, Dept. Biologia Cellular i Anatomia Patológica. CCBR Group, Pavelló Central, 5a planta, LR 5101 C/ Feixa Llarga s/n, 08907 L'Hospitalet Barcelona, Spain.
Tel: +34 93 4024288; fax: +34 93 4024213;
e-mail: rperez @ ub.edu

Received 28 September 2004 **Revised form accepted** 8 December 2004

Introduction

Apoptosis is involved in the action of many (perhaps all) chemotherapeutic agents. In most cases, apoptosis is accompanied by cytochrome *c* release from the mitochondria into the cytosol. Then caspases can be activated and generate the characteristic apoptotic morphology (chromatin condensation, membrane blebbing, cell shrinkage, DNA cleavage, etc). Resistance to chemotherapy is the main cause of failure in the treatment of human cancer. One major mechanism of resistance is linked to decreased intracellular accumulation of anticancer drugs through enhanced cellular efflux of the antitumor compound [1]. MRP-1 is an efflux pump that belongs to the family of ABC transporters and is frequently overexpressed in clinical samples from patients with small cell lung cancer (SCLC) [2]. Cytotoxic drugs irrespective of their intracellular target cause cell death in sensitive cells by inducing apoptosis [3]. Some members of a family of natural bacterial pigments called prodigiosins (PGs) induce apoptosis in several human cancer cell lines [4–6] and in hepatocellular carcinoma xenografts [7]. The aim of this study is to describe the apoptosis induction by PG treatment in a doxorubicin-resistant SCLC cell line compared to its parental cell line. Here we studied the ability of PG to overcome the multidrug resistance (MDR) phenotype as well as the cytotoxic effect induced in the MRP-1 overexpressing GLC4/ADR cell line, finding interesting parallels with what we have previously described in the doxorubicin-sensitive GLC4 cell line [8].

Methods

Cell lines and culture conditions

The human lung cancer GLC4 cell line and its doxorubicin-resistant subline GLC4/ADR were derived in the laboratory of N. H. Mulder [9]. GLC4/ADR cells were exposed to 1172 nM doxorubicin (Sigma, St Louis, MO) during 48 h once each 15 days to maintain their resistance characteristics. All the experiments using GLC4/ADR were performed after 7 days of non-exposure to doxorubicin treatment. Both cell lines were cultured in RPMI 1640 medium with 10% FCS (Biological Industries, Beit Haemek, Israel) supplemented with 4 mM L-glutamine, 100 IU/ml penicillin and 100 µg/ml (Sigma) at 37°C with 5% CO_2.

Purification of PG

PG was isolated from a culture broth of *Serratia marcescens 2170* as described previously [4]. Stock solutions were prepared in methanol and concentrations were determined by UV/vis in 95% EtOH–HCl ($\epsilon_{535} = 112\,000$ M/cm).

Cell viability assay

Cell viability was determined by the MTT assay [10]. Briefly, 5×10^4 cells were incubated in 96-well microtiter

cell culture plates, in the absence (control cells) or presence of 20–240 nM PG to a final volume of 100 µl. After 4, 8, 16 or 24 h incubation, 10 µl of MTT (diluted in PBS) was added to a final concentration of 10 mM for an additional 4 h. The blue MTT formazan precipitate was dissolved in 100 µl of isopropanol:1 N HCl (24:1) and the absorbance at 550 nm was measured on a multiwell plate reader. Cell viability was expressed as a percentage of control. Data are shown as the mean value ± SD of triplicate cultures.

Western blot analysis

Cells (5×10^5 cells/ml) were exposed to 100, 150 or 200 nM PG for 16 h, except when MRP-1 was analyzed (100, 200 or 300 nM PG for 24 h), they were then washed twice with PBS and lysed with ice-cold lysis buffer (85 mM Tris–HCl, pH 6.8, 0.4% SDS, 0.1 mM PMSF, 1 µg/ml aprotinin and 1 µg/ml leupeptin). Protein concentration was measured using the micro BCA Protein Assay Reagent Kit (Pierce, Rockford, MD). Protein extracts were electrophoresed on a polyacrylamide gel and transferred to Immobilon-P membrane (Millipore, Bedford, MA). Membranes were blocked with 5% dry-milk diluted in TBS-T (50 mM Tris–HCl, pH 7.5, 150 mM NaCl and 0.1% Tween-20) and incubated overnight at 4°C. The rabbit polyclonal antibodies used were as follows: cleaved caspase-3 (Asp175) (New England Biolabs, Beverly, MA), caspase-8 (BD PharMingen, San Diego, CA), cleaved caspase-9 (37 kDa) (New England Biolabs) and PARP (New England Biolabs). Monoclonal antibody to MRP-1 (human) MRPm6 (Alexis Biochemicals, LOCATION?) and purified mouse anti-cytochrome *c* monoclonal antibody (BD PharMingen) were also used.

AQ1

The peroxidase-conjugated secondary antibodies used were goat anti-rabbit IgG (170-6515; Bio-Rad, UK) and goat anti-mouse (170-6516; Bio-Rad, LOCATION?). Peroxidase was then developed by incubating the membrane with the enhanced chemiluminescence (ECL) detection kit (Amersham, Little Chalfont, UK). Protein expression of Western blot images was quantified using the image analysis software program Phoretix 1-D advanced. Results are presented relative to the control densitometry values.

AQ1

Cytochrome *c* detection assay

In time-course cytochrome *c* detection assays, cells were harvested after a 15-min to 12-h exposure to 200 nM PG and prepared as previously described [11], with slight modifications. Briefly, cells were lysed for 30 s in 50 µl ice-cold lysis buffer (250 mM sucrose, 1 mM EDTA, 0.05% digitonin, 25 mM Tris, pH 6.8, 1 mM DTT, 1 µg/ml aprotinin, 1 µg/ml leupeptin, 1 µg/ml pepstatin and 0.1 mM PMSF). Lysates were centrifuged at 13 000 *g* at 4°C for 2 min to obtain the supernatants (cytosolic extracts) and the pellet (fraction with mitochondria).

Analysis of DNA fragmentation

DNA fragmentation was analyzed by agarose gel electrophoresis, as described previously [6]. Briefly, 5×10^6 cells/ml were treated with 100 or 200 nM PG for 16 h or were left untreated (control). DNA preparations were electrophoresed in a 1% agarose gel containing ethidium bromide. Gels were placed in a UV light box to visualize the DNA ladder pattern.

Gene expression analysis

Cells (5×10^5) were treated with 0 (control), 100, 200 or 300 nM PG during 24 h. Total RNA extraction was performed using Ultraspec RNA (Biotex, TX). cDNA synthesis was obtained using random hexamers and MuLV reverse transcriptase after washing the RNA pellet twice in 75% ethanol, dissolved in H_2O, following the manufacturer's instructions. The final concentration of cDNA was 1 µg in 50 µl. Each cDNA sample was analyzed for expression of MRP-1 using the fluorescent TaqMan 5′ nuclease assay. Oligonucleotide primers MRP-1 (Hs00219905) and actin (Hs99999903) and probes were initially designed and synthesized as Assay-on-Demand Gene Expression Products (Applied Biosystems, Warrington, UK). The 5′ nuclease assay PCRs were performed using the ABI Prism 7700 sequence detection system for thermal cycling and real-time fluorescence measurements (Applied Biosystems). Each 50-µl reaction consisted of 1 × TaqMan Universal PCR MasterMix (PE Biosystems), 1 × Assay-on-Demand mix containing forward primer, reverse primer and TaqMan quantification probe (Applied Biosystems), and 100 ng cDNA template. Reaction conditions comprised an initial step of 92°C for 10 min, then 40 cycles of 95°C for 15 s and 60°C for 1 min. The levels of MRP-1 obtained were normalized by mRNA expression of actin. The relative mRNA expression for MRP-1 was thus presented as relative to the control. Data were analyzed using The Sequence Detector Software (SDS version 1.9; Applied Biosystems).

AQ8

Statistical comparison of mean values was performed using Student's *t*-test.

Results

PG decreases the viability of GLC4 and GLC4/ADR cells

First at all, we proved the doxorubicin sensitivity and resistance phenotypes of both cell lines (Fig. 1). Then, the effect of PG on the viability of human SCLC cell lines (GLC4, GLC4/ADR) was studied. Cell lines were incubated for 4, 8, 16 or 24 h with several doses of PG, ranging from 20 to 200 nM, and cell viability was then determined by the MTT assay. A significant dose-dependent decrease in the number of viable cells was observed in GLC4 and GLC4/ADR cells and no marked

differences were detected between them (Fig. 2A and B). The time-course experiments showed a marked decrease in the IC_{50} value as incubation time increased. GLC4 IC_{50} was 129.40 ± 17.10 and 104.59 ± 5.72 nM at 16 and 24 h of PG incubation, respectively. In contrast, GLC4/ADR presented an IC_{50} value of 143.16 ± 24.57 nM at 16 h, which decreased to 111.40 ± 4.27 nM at 24 h. Therefore, we can conclude that there is no significant difference between the viability of GLC4 and GLC4/ADR cells when given the same PG treatment.

Apoptotic features

Fig. 1

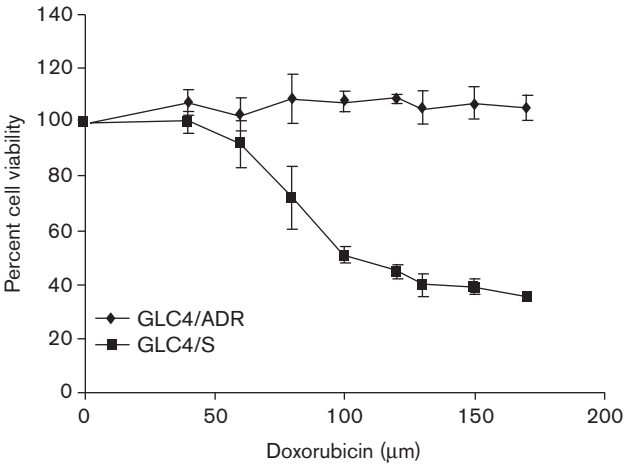

Doxorubicin resistance. Samples of 2×10^6 cells per condition were incubated for 24 h in a 96-well plate at the indicated doxorubicin concentrations. As expected, resistance to doxorubicin was proved in GLC4/ADR, but not in its parental cell line. Results depicted represent the mean of three independent experiments. Error bars represent SD.

One of the main biochemical features associated with apoptosis is caspase activation. PG induced the processing of caspases, as shown by the appearance of the active cleavage products of caspases-8 (23 kDa) and -3 (17 kDa) (Fig. 3). The appearance of the caspase-9 intermediate cleaved product (37 kDa) and the disappearance of the precursor form were also determined by Western blot in whole-cell extracts (Fig. 3).

PARP cleavage, as a result of caspase-3 activation, was analyzed on protein extracts from cells incubated with 100, 150 and 200 nM of PG by immunoblotting as a specific marker of caspase activity. In PG-treated cells, both the native PARP (116 kDa) and the cleavage product (85 kDa) were observed (Fig. 4A). Agarose gel electrophoresis showed the characteristic DNA ladder pattern induced in the apoptotic process in the two cell lines when incubated for 16 h in the presence of 100 and 200 nM PG (Fig. 4B).

Cytochrome *c* involvement

There is evidence that mitochondria play an essential role in many forms of apoptosis by releasing apoptogenic factors as cytochrome *c*. To analyze the involvement of cytochrome *c* release in PG-induced apoptosis, cytosolic and mitochondrial fractions were obtained and analyzed for the presence of cytochrome *c* by Western blot. Cell lines were incubated for 16 h with three doses of PG (100, 150 and 200 nM). PG induced the appearance of cytochrome *c* in the cytosolic fractions in a dose–response manner in both cell lines (Fig. 5A). In time-course experiments (Fig. 5B), we demonstrated that PG induced the appearance of cytochrome *c* in these fractions after 15 min of drug exposure in both cell lines.

Fig. 2

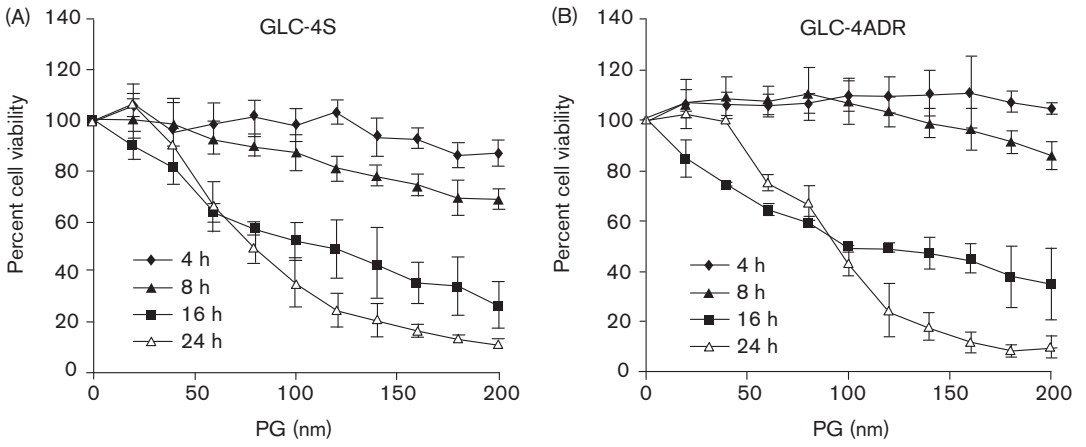

Effect of PG treatment on the viability of GLC4 (A) and GLC4/ADR (B) cell lines by the MTT assay. Cell viability decreases in a dose–response manner, and no significant differences between sensitive and resistant cell lines are observed. The results represent the mean of three independent experiments. Error bars show SD.

Fig. 3

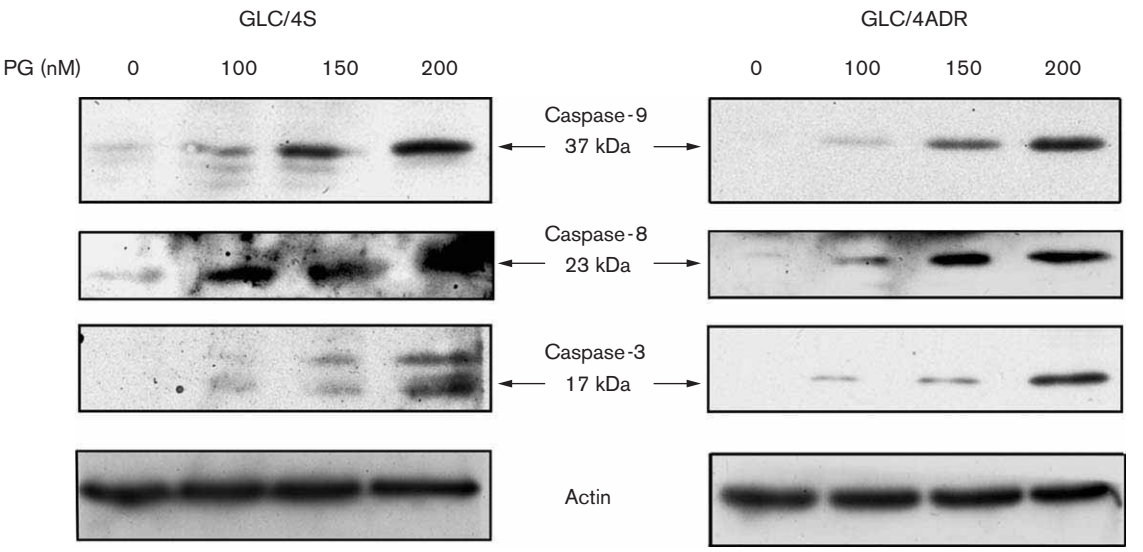

PG induces the activation of caspases. Western Blotting of 50 μg of whole-cell protein extract was used. Cleavage of caspase-9, caspase-8 and caspase-3 was observed after 16 h of PG treatment in a dose–response manner. A representative result from three independent experiments is shown. Control of protein loading by actin is shown in the bottom panel.

AQ12 Densitometric analysis to the blots corresponding to Figs 3, 4(A) and 5 to quantify the intensity of the bands confirmed no differences between both cell lines (data not shown).

Quantification of MRP-1 mRNA and MRP-1 protein

Our study demonstrates that PG circumvents the MDR phenotype acquired by the GLC4/ADR cell line (mainly caused by MRP-1 overexpression) as PG treatment induces similar cell viability loss and biochemical apoptotic features in both sensitive and resistant cell lines. The PG treatment effect in MRP-1 mRNA expression was measured by quantitative PCR (Q-PCR). The relative levels of MRP-1 mRNA expression in GLC-4/ADR cells (Fig. 6A) increased slightly after PG exposure. However, at the protein level, MRP-1 decreased in a dose–response fashion after the first dose (Fig. 6B and C) and it was hardly detectable at the highest dose of PG ($p < 0.05$). The levels of MRP-1 mRNA and protein were also studied for GLC4, but no effect of PG was observed in this cell line (data not AQ13 show).

Discussion

PG exerts its cytotoxic effect in the MDR phenotype GLC4/ADR cell line and its parental GLC4 cell line in a dose-dependent manner. GLC4 and GLC4/ADR have been used as a model to study the effect of several novel or established lung cancer chemotherapy agents [12,13]. The resistant cell line shows cross-resistance not only to doxorubicin, but also to topotecan and paclitaxel [14]. However, PG treatment results in an equivalent decrease in cell viability for both cell lines. We draw attention to AQ14 the low IC_{50} concentration obtained for PG in these cell lines when compared with cisplatin which is one of the most commonly used drugs in SCLC treatment in the US [15], i.e. the IC_{50} values of cisplatin at 72 h are 2000 and 3000 nM in GLC4 and GLC4/ADR, respectively [14].

PG induces apoptosis in hematopoietic, colon and gastric cancer cell lines [4–6]. Cycloprodigiosin hydrochloride, another member of the PG family, also has a pro-apoptotic effect in hepatocarcinoma cells *in vitro* and *in vivo* [7]. Moreover, an apoptotic effect has also been described in human primary cancer cells [16]. However, the mechanism by which PG induces apoptosis remains unclear, although several pathways have recently been hypothesized [17].

Here, we have confirmed the activation of the apoptotic process by analyzing biochemical events such as caspase activation, PARP cleavage and DNA ladder pattern formation as well as the cytochrome *c* release involvement in a doxorubicin-resistant SCLC model. We observed a slight delay in caspase-8 activation in GLC4/ADR, but the final apoptosis execution is performed by caspase-3, AQ15 which is activated in the same way in both sensitive and resistant cell lines.

Our study demonstrates that PG circumvents the MDR phenotype acquired by the GLC4/ADR cell line (mainly caused by MRP-1 overexpression) as PG treatment

Fig. 4

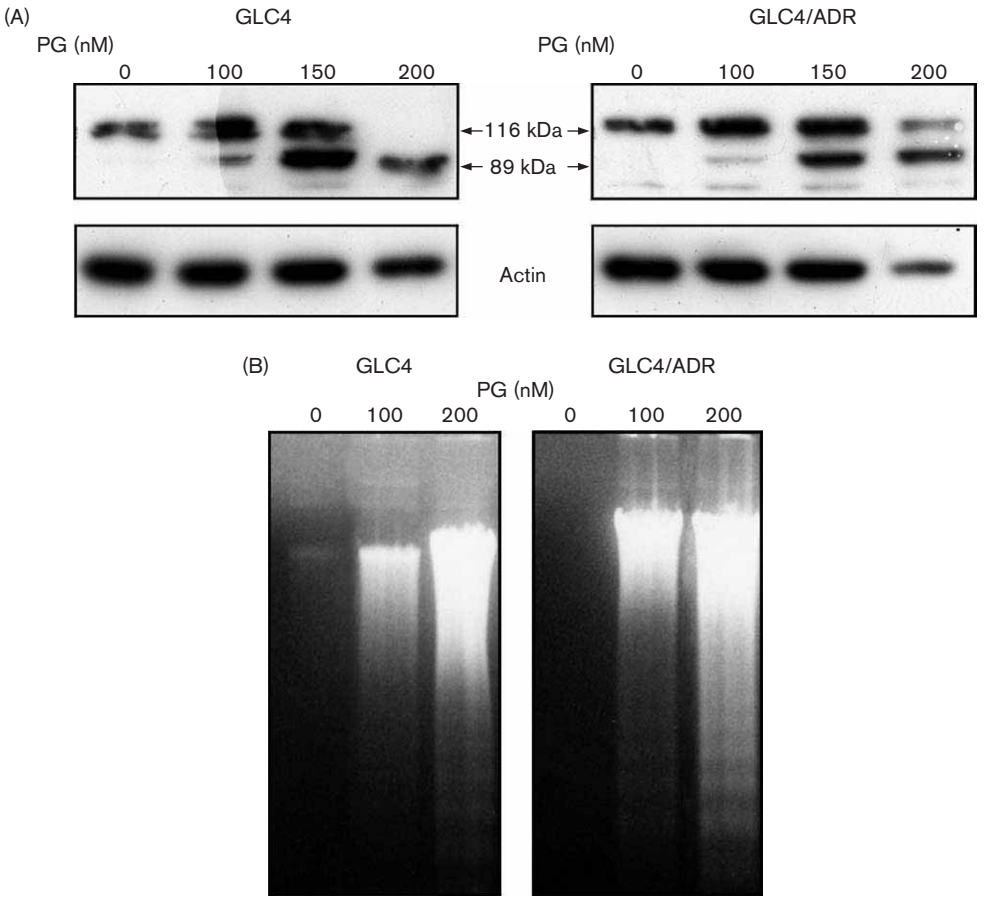

AQ16 PG apoptotic induction. (A) PARP cleavage in a dose–response assay is observed by Western blot after PG treatment. The bottom shows actin as a loading control. (B) DNA fragmentation induced by PG is detected in agarose gel electrophoresis.

Fig. 5

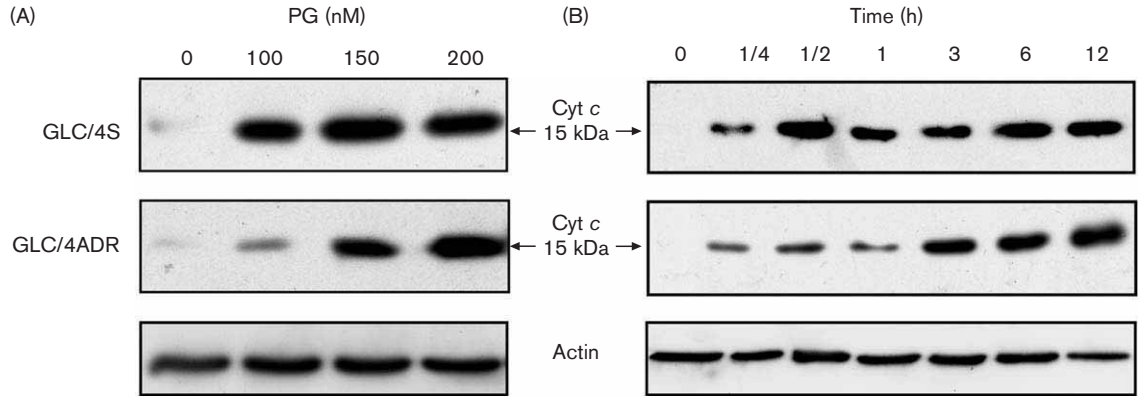

Western blot analysis of cytochrome *c* release from mitochondria in PG-treated cells. Samples of 30 μg of protein from the cytosolic fraction were used. (A) PG induces the appearance of cytochrome *c* in the cytosolic fraction in a concentration–response manner. (B) Time-course assay shows release of cytochrome *c* after 15 min of 200 nM PG treatment. A representative study of three independent experiments is shown. Bottom shows actin as a loading control.

Fig. 6

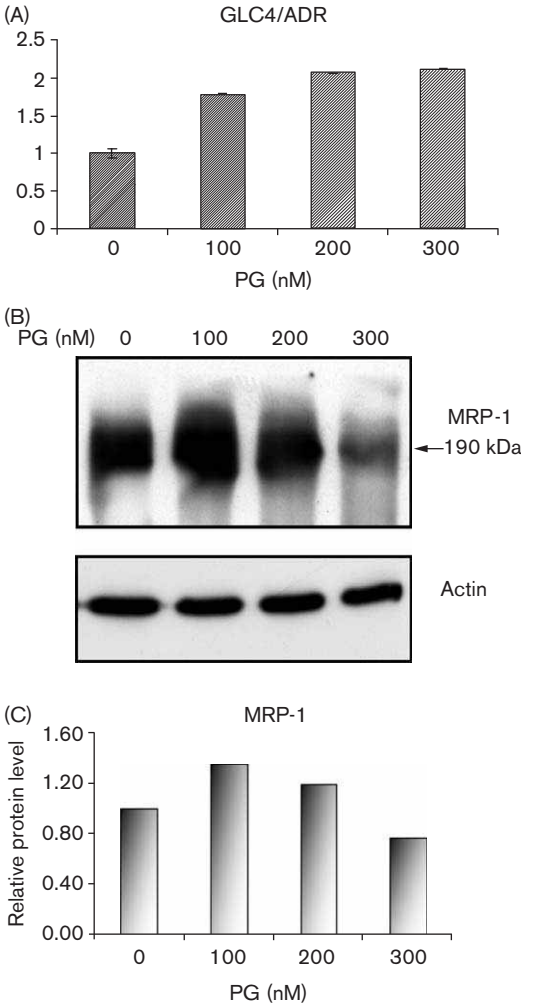

PG effect in MRP-1 (A). The results are shown as the relative expression of MRP-1 mRNA after cell treatment with PG normalized by actin mRNA. A slight increase in the resistance protein is observed. Error bars represent SD. (B) MRP-1 protein detected by Western blot. Samples of 30 μg of protein were electrophoresed. MRP-1 slightly decreases after PG treatment. Figures show a representative result from three independent experiments. (C) Western blot quantification is represented by bars. As can observe that MRP-1 protein increases at low PG concentration (100 nM), but decreases when higher doses are supplied.

induces similar cell viability loss and biochemical apoptotic features in both sensitive and resistant cell lines. We have previously reported that PG is not a substrate for another ABC transporter family member [BCRP (breast cancer resistance protein)] [18]. Results presented here indicate that PG might not be a substrate for MRP-1. The relative levels of MRP-1 mRNA expression in GLC-4/ADR cells increased slightly after PG exposure although MRP-1 protein decreased in a dose–response fashion after dose 1. This finding indicates that PG could have a novel and useful activity in this aspect, as the increase in MRP-1 has been reported in most SCLC patients, and in leukemia, esophageal carcinoma and non-SCLC [19]. Interestingly, Versantvoort and collaborators hypothesized that the GLC4 cell line, probably like most cell lines *in vitro*, reacts to low chemical selective pressure by increasing the MRP-1 detoxifying protein [20], thereby allowing the cell to pump chemotherapy agents such as doxorubicin, epirubicin, etoposide, vincristine and methotrexate [21]. We have also observed an increase of MRP-1 protein at the lower dose followed by decrease when higher doses of PG were used. Here we report that PG blocks the increase in MRP-1 protein levels, an effect that supports its use in combined therapy as well as describe a new property that could be added to those of PG already described [17].

To our knowledge, this is the first study to show the cytotoxic activity of a member of the PG family in a doxorubicin-resistant SCLC cell line. Given the high sensitivity of the GLC4 and GLC4/ADR cell lines to PG compared with other commonly used drugs, we conclude that PG is a potential novel chemotherapy agent for lung cancer, particularly for SCLC.

Acknowledgements

The authors thank the technical assistance of the Serveis Cientificotècnics (Unitat de Bellvitge, Universitat de Barcelona) and Robin Rycroft for reviewing the English.

References

1 Hayes JD, Wolf CR. Molecular mechanisms of drug resistance. *Biochem J* 1990; **272**:281–295.
2 Campling BG, Young LC, Baer KA, Lam Y, Deeley RG, Cole SPC, *et al.* Expression of the MRP and MDR1 multidrug resistance genes in small cell lung cancer. *Clin Cancer Res* 1997; **3**:115–122.
3 Hannun YA. Apoptosis and the dilemma of cancer chemotherapy. *Blood* 1997; **89**:1845–1853.
4 Montaner B, Navarro S, Pique M, Vilaseca M, Martinell M, Giralt E, *et al.* Prodigiosin from the supernatant of *Serratia marcescens* induces apoptosis in haematopoietic cancer cell lines. *Br J Pharmacol* 2000; **131**:585–593.
5 Montaner B, Perez-Tomas R. Prodigiosin-induced apoptosis in human colon cancer cells. *Life Sci* 2001; **68**:2025–2036.
6 Diaz-Ruiz C, Montaner B, Perez-Tomas R. Prodigiosin induces cell death and morphological changes indicative of apoptosis in gastric cancer cell line HGT-1. *Histol Histopathol* 2001; **16**:415–421.
7 Yamamoto C, Takemoto H, Kuno K, Yamamoto D, Tsubura A, Kamata K, *et al.* Cycloprodigiosin hydrochloride, a new H^+/Cl^- symporter, induces apoptosis in human and rat hepatocellular cancer cell lines *in vitro* and inhibits the growth of hepatocellular carcinoma xenografts in nude mice. *Hepatology* 1999; **30**:894–902.
8 Llagostera E, Soto-Cerrato V, Montaner B, Pérez-Tomás R. Prodigiosin induces apoptosis by acting on mitochondria in human lung cancer cells. *Ann NY Acad Sci* 2003; **1010**:178–181.
9 Zijlstra JG, de Vries EGE, Mulder NH. Multifactorial drug resistance in an adriamycin-resistant human small cell lung carcinoma cell line. *Cancer Res* 1987; **47**:1780–1784.
10 Mosmann T. Rapid colorimetric assay for cellular growth and survival: application to proliferation and cytotoxicity assays. *J Immunol Methods* 1983; **65**:55–63.
11 Pique M, Barragan M, Dalmau M, Bellosillo B, Pons G, Gil J. Aspirin induces apoptosis through mitochondrial cytochrome *c* release. *FEBS Lett* 2000; **480**:193–196.
12 Fokkema E, Groen HJM, Helder MNH, de Vries EGE, Meijer C. JM216-, JM118-, and cisplatin-induced cytotoxicity in relation to platinum–DNA adduct formation, glutathione levels and p53 status in human tumour cell

lines with different sensitivities to cisplatin. *Biochem Pharmacol* 2002; **63**:1989–1996.
13 van Gorkom BAP, Timmer-Bosscha H, de Jong S, van der Kolk DM, Keibeuker JH, de Vries EG. Cytotoxicity of rhein, the active metabolite of sennoside laxatives, is reduced by multidrug resistance-associated protein 1. *Br J Cancer* 2002; **86**:1494–1500.
14 Ferreira CG, Tolis C, Span SW, Peters GJ, van Lopik T, Kummer AJ, *et al.* Drug-induced apoptosis in lung cancer cells is not mediated by the Fas/FasL (CD95/APO1) signalling pathway. *Clin Cancer Res* 2000; **6**:203–212.
15 Kelly K. New chemotherapy agents for small cell lung cancer. *Chest* 2000; **117**:156S–162S.
16 Campas C, Dalmau M, Montaner M, Barragán M, Bellosillo B, Colomer D, *et al.* Prodigiosin induces apoptosis of B and T cells from B-cell chronic lymphocytic leukaemia. *Leukemia* 2003; **17**:746–770.
17 Perez-Tomas R, Montaner B, Llagostera E, Soto-Cerrato V. The prodigiosins, proapoptotic drugs with anticancer properties. *Biochem Pharmacol* 2003; **66**:447–452.
18 Soto-Cerrato V, Llagostera E, Montaner B, Scheffer GL, Pérez-Tomás R. Mitochondria-mediated apoptosis operating irrespective of multidrug resistance in breast cancer cells by the anticancer agent prodigiosin. *Biochem Pharmacol* 2004; **68**:1345–1352.
19 Nooter K, Westerman AM, Flens MJ, Zaman GJ, Scheper RJ, van Wingerden KE, *et al.* Expresssion of the multidrug resistance protein (MRP-1) gene in human cancers. *Clin Cancer Res* 1995; **1**:1301–1310.
20 Versantvoort CHM, Withoff S, Broxterman HJ, Kuiper CM, Scheper RJ, Mulder NH, *et al.* Resistance-associated factors in human small-cell lung-carcinoma GLC4 sub-lines with increasing adriamycin resistance. *Int J Cancer* 1995; **61**:375–380.
21 Gottesman MM, Flojo T, Bates SE. Multidrug resistance in cancer: role of ATP-dependent transporters. *Nat Rev* 2002; **2**:48–58.

Capítulo 3.3. Identificación de los mecanismos de toxicidad inducidos por prodigiosina en células de neuroblastoma.

("Francisco R, Pérez-Tomás R, Giménez-Bonafé P, Soto-Cerrato V, Giménez-Xavier P, Ambrosio S. Mechanisms of prodigiosin cytotoxicity in human neuroblastoma cell lines. Eur J Pharmacol 2007; doi:10.1016/j.ejphar.2007.06.054").

Más recientemente hemos ampliado la caracterización del efecto de prodigiosina a células de neuroblastoma, profundizando en el estudio de la localización subcelular y acción de prodigiosina una vez internalizada. Prodigiosina mostró una marcada toxicidad en células de neuroblastoma, llegando a ser hasta treinta veces superior a la de cisplatino, quimioterapéutico en uso clínico. Respecto al mecanismo de acción, se describió cómo prodigiosina actuaba como un agente secuestrador de protones en la mitocondria, orgánulo en el que se observaba acumulación, destruyendo así el gradiente de pH. Allí provocó un efecto desacoplador de la cadena respiratoria de la actividad ATP sintasa. Como resultado, la producción de ATP se vio disminuida sin alterar la tasa de consumo de oxígeno. Este mecanismo de acción es diferente al de los quimioterapéuticos usados actualmente, sugiriendo que prodigiosina podría aumentar el efecto antitumoral de estos en el tratamiento de neuroblastomas.

(Estudio realizado en colaboración con el grupo del Dr. S. Ambrosio en el que he contribuido de forma parcial).

Available online at www.sciencedirect.com
ScienceDirect
ELSEVIER
European Journal of Pharmacology xx (2007) xxx–xxx
ejp
www.elsevier.com/locate/ejphar

Mechanisms of prodigiosin cytotoxicity in human neuroblastoma cell lines

Roser Francisco [a], Ricardo Pérez-Tomás [b], Pepita Gimènez-Bonafé [c], Vanessa Soto-Cerrato [b], Pol Giménez-Xavier [a], Santiago Ambrosio [a,*]

[a] *Unitat de Bioquímica, Departament de Cincies Fisiolgiques II, Campus de Bellvitgte, IDIBELL-Universitat de Barcelona, Spain*
[b] *Unitat de Biologia Cel·lular, Departament de Patologia i Terapèutica Experimental, Campus de Bellvitgte, IDIBELL-Universitat de Barcelona, Spain*
[c] *i Fisiologia, Departament de Cincies Fisiolgiques II, Campus de Bellvitgte, IDIBELL-Universitat de Barcelona, Spain*

Received 26 February 2007; received in revised form 11 June 2007; accepted 12 June 2007

Abstract

Prodigiosin is a bacterial red pigment with cytotoxic properties and potential antitumor activity that has been tested against different cancerous cells. In this study we report the effect and mechanisms of action of prodigiosin against different human neuroblastoma cell lines: SH-SY5Y, LAN-1, IMR-32 (N-type) and SK-N-AS (S-type). We compare the anticancerous effect of prodigiosin with that of cisplatin at different concentrations during 24 h of exposure. Prodigiosin is more potent, with IC_{50} values lower than 1.5 μM in N-type neuroblastoma cells and around 7 μM in the S-type neuroblastoma cell line. We describe prodigiosin as a proton sequestering agent that destroys the intracellular pH gradient, and propose that its main cytotoxic effect could be related to its action on mitochondria, where it exerts an uncoupling effect on the electronic chain transport of protons to mitochondrial ATP synthase. As a result of this action, ATP production is reduced but without decreasing in oxygen consumption. This mechanism of action differs from those induced by conventional chemotherapeutic drugs, suggesting a possible role for prodigiosin to enhance the effect of antitumor agents in the treatment of neuroblastoma.

Keywords: Neuroblastoma; Prodigiosin; Cisplatin; Apoptosis

1. Introduction

Prodigiosins are a family of naturally occurring polypyrrole red pigments produced by a small group of microorganisms, including *Serratia* spp. and *Actinomycetes* (for example, *Streptomyces coelicor A3* and various marine bacteria), characterized by a common pyrrolyl–dipyrrolyl–methene skeleton. The physiology and regulation of prodigiosin production in these bacteria are now well understood (Williamson et al., 2006).

Prodigiosin has antibacterial, antifungical, antimalarial and cytotoxic properties (for a review, see Montaner and Perez-Tomas, 2003), and it has been suggested for the treatment of autoimmune diabetes and collagen-induced arthritis (Han et al., 2001). However, prodigiosin has mainly been studied for its potential as a chemotherapeutic drug. Prodigiosin has been tested *in vitro* against a variety of tumor cell lines and primary cultures (Yamamoto et al., 1999; Yamamoto et al., 2002; Pérez-Tomás et al., 2003), and its antimetastatic effect has been reported in lung cancer cells (Zhang et al., 2005). Prodigiosin triggers apoptosis in haematopoietic, gastrointestinal, breast and lung cancer cell lines, not being markedly toxic to non-malignant cell lines (Montaner et al., 2000; Diaz-Ruiz et al., 2001; Montaner and Pérez-Tomás, 2001; Soto-Cerrato, 2004; Llagostera et al., 2005). The apoptosis induced by prodigiosin is p53 independent and overcomes multidrug resistance, both representing an advantage over other antitumor drugs (Montaner et al., 2000; Soto-Cerrato, 2004). The molecular mechanism of action of prodigiosin is not yet fully understood, but it seems to differ from those of other common chemotherapeutic agents. *In vitro*, prodigiosin is a DNA-interacting agent, which induces DNA single- and double-strand breaks *via* poisoning topoisomerases and through copper-promoted oxidative DNA damage (Melvin et al., 2001; Montaner et al., 2005). Some compounds of the prodigiosin family have been reported to

* Corresponding author. Unitat de Bioquímica, Departament de Cincies Fisiolgiques II, Campus de Bellvitge, Universitat de Barcelona, c/Feixa Llarga s/n, E-08907-L'Hospitalet del Llobregat, Barcelona, Spain. Tel.: +93 403 90 94; fax: +93 402 42 68.
E-mail address: sambrosio@ub.edu (S. Ambrosio).

0014-2999/$ - see front matter © 2007 Elsevier B.V. All rights reserved.
doi:10.1016/j.ejphar.2007.06.054

promote H^+/Cl^- symport transport and to induce neutralization of the acid compartments (Sato et al., 1998; Yamamoto et al., 1999; Castillo-Avila et al., 2005), although the involvement of these mechanisms in the initiation of a programmed cell death is still unknown.

Prodigiosin has not been assayed against neuroblastoma or neuroblastoma cell lines. Neuroblastoma is the most common solid tumor in children and the second most frequent malignancy in infancy after lymphoblastic leukemia. It arises from the neural crest cell precursors of the sympathetic nervous system failing to complete differentiation. Neuroblastoma is one of the most challenging malignant tumors because of its heterogeneity, variety of clinical behavior and high recurrence. At the present, there is no effective or specific chemotherapy against neuroblastoma and new treatment strategies are urgently needed to improve the survival rate and the quality of life of children suffering from this illness (Berthold and Hero, 2000; Broudeur, 2003).

In the present work we examine the mechanisms of action of prodigiosin against tumor cells using distinct human neuroblastoma cell lines. We describe the anti-proliferative activity of prodigiosin, inducing cell death and/or differentiation in a way that involves the disruption of intracellular proton gradients, mainly the mitochondrial gradient needed to couple respiration to ATP production.

2. Materials and methods

2.1. Reagents

Prodigiosin was kindly provided by Dr. R. J. Schultz of the National Cancer Drug Synthesis and Chemistry Branch Chemotherapeutic Agents Repository (Bethesda, MD). Stock solutions were prepared in methanol and concentrations were determined by UV–Vis in 95% EtOH–HCl (19:1) (Melvin et al., 1999). Cisplatin (*cis*-diammine-dichloroplatinum) was purchased from Sigma (Madrid, Spain), dissolved in water and stored at 4 °C from light. 3-(4,5-dimethylthiazol-2-yl)-2,5-diphenyltetrazolium bromide (MTT) was purchased from Sigma. Z-Val-Ala-DL-Asp-fluoromethylketone (zVAD.fmk) was obtained from Bachem (Weil, Germany).

2.2. Cell lines and growth conditions

Three N-type (neuronal lineage), LAN-1, IMR-2 (both highly expressing the bad prognostic factor N-Myc, Zaizen et al., 1998) and SH-SY5Y (not over-expressing N-Myc), and one S-type (stromal), SK-N-AS, human neuroblastoma cell lines were used. The cell lines LAN-1 and SK-N-AS were kindly donated by Dr. J. Mora (Hospital St. Joan de Déu, Barcelona, Spain). SH-SY5Y and IMR-32 were purchased from ATCC (American Type Culture Collection, Manassas, VA). A second SH-SY5Y clone, which we named "high proliferation SH-SY5Y" (SH-SY5Yhp, Boix et al., 1997; Encinas et al., 2000), was provided by Dr. J. Comella (University of Lleida, Spain). Cells were grown in Dulbecco's Modified Eagle's Medium (DMEM), supplemented with 10% decomplemented fetal bovine serum, 2 mM L-glutamine, 100 U/ml penicillin and 100 μg/ml streptomycin. In the IMR-32 medium, 1 mM pyruvate was also added (all the products were purchased from Biological Industries; Kibbutz Beit Haemek, Israel). The cells were maintained at 37 °C in a humidified atmosphere with 10% CO_2.

2.3. Cell viability assay

Cell survival was evaluated using the MTT colorimetric assay. 10^4 cells were incubated in 96 well microtiter cell culture plates, in the absence (control cells) or presence of prodigiosin or cisplatin, in a final volume of 100 μl. After the indicated treatment, cells were incubated for 3 h at 37 °C in DMEM containing 10 μM MTT (diluted in PBS). The blue MTT formazan precipitate was then dissolved in 100 μl of isopropanol and the absorbance was measured at 570 nm on a multiwell plate reader. The absorbance measured was related to the protein content (BCA (bicinchoninic acid) Protein Assays, Pierce, Rockford, USA) and considered proportional to the number of viable cells. Cell viability was expressed as a percentage of these values in treated cells in comparison with the non-treated control cells. Data are shown as the mean ± standard error media of triplicate cultures. Cell viability was also assessed by counting the adherent cells with or without treatment. In that case 2×10^5 cells were cultured in 6 well plates, 24 h after treatment cells were washed twice in phosphate buffer solution (PBS) and counted with a Neubauer cell counting chamber.

The cell-permeable pan-caspase inhibitor zVAD.fmk was used prior to prodigiosin treatment. Cells were incubated for 90 min at 37 °C with or without 100 μM zVAD.fmk and cell survival was evaluated with the MTT colorimetric assay.

2.4. Thymidine incorporation assays

The effect of prodigiosin on cell proliferation was determined using different concentrations of this compound. 10^5 cells were plated in 6-well plates in a final volume of 2 ml. After 24 h, the medium was removed and changed for fresh one containing 1 μCi/ml of [^{3}H]-thymidine and different concentrations of prodigiosin. After 6, 12, 24 and 48 h of incubation, cells were washed twice in cold PBS and 1 ml of 5% trichloroacetic acid (TCA) was added for 20 min at 4 °C. The samples were then washed once with 1 ml of TCA followed by 2 ml of 70% ethanol, and dried out at 37 °C. Finally 0.6 ml of lysis buffer (2% Na_2CO_3, 0.1 M NaOH, 1% sodium dodecyl sulphate (SDS)) was added to each well for 20 min at 37 °C. The radioactivity was counted in a scintillation counter (Beckman LS5000TA, USA) using 0.5 ml of each sample to which 0.5 ml of scintillation liquid was added.

2.5. DNA fragmentation

Analysis of DNA fragmentation was performed as described by Bellosillo et al. (1998). 10^5 cells were cultured on 12 well plates and treated with or without prodigiosin. Cell extracts were run on a 1% agarose gel electrophoresis. Gels were stained with ethidium bromide and viewed under ultraviolet light.

Please cite this article as: Francisco, R. et al. Mechanisms of prodigiosin cytotoxicity in human neuroblastoma cell lines. Eur. J. Pharmacol. (2007), doi:10.1016/j.ejphar.2007.06.054

2.6. Cell staining

Cells were grown over cover slips on 6-well plates and were allowed to attach overnight. For nuclear staining, cells were labeled with 2 μg/ml of the DNA dye Hoechst-33342 (bisbenzimide; Sigma) for 30 min at 37 °C.

Mitochondrial staining was realized with Mitotracker Deep Red 633 (Molecular Probes, Eugene, OR). Cells were incubated in a medium containing 250 nM of Mitotracker Deep Red for 30 min at 37 °C, and washed in PBS three times for 5 min. For vital staining, the living cultured cells were washed twice in PBS and stained with 5 μg/ml acridine orange (Sigma) for 30 min (Castillo-Avila et al., 2005). After incubation, cells were washed three times in PBS containing 10% of fetal bovine serum for 5 min. Finally, cells were examined on a Nikon microscope (E800) equipped with a diagnostic instruments photo automat system (Spot JR).

2.7. Western blotting

Experiments were performed with adherent and floating cells. Protein concentration was determined by the BCA assay. Equal amounts of protein were loaded onto each lane and electrophoresed on SDS-polyacrylamide gels with Tris-glycine running buffer. They were then transferred to nitrocellulose membranes (Millipore, Bredford, MA) by using a semidry electrotransfer for 50 min at 40 V. Membranes were incubated with antibodies to procaspase-2 (rabbit polyclonal, Sta. Cruz Biotech., Sta. Cruz, CA, 1:500), procaspase-3 (rabbit polyclonal, BD Biosci., San Jose, CA, 1:500), procaspase-7 (monoclonal antibody, Cell Signalling, Danvers, MA, 1:1000), procaspase-9 (rabbit polyclonal, New Engl. Biolabs, Beverly, MA, 1:250), PARP (H-250 rabbit polyclonal, Sta. Cruz Biotech., Sta. Cruz, CA, 1:200), and tubulin (Sigma, St. Louis, MO, 1:4000). After washing, the membranes were incubated with biotinylated secondary antibody labeled with horseradish peroxidase (Amersham, Little Chalfont Buckinghamshire, UK) for 1 h at room temperature, washed again, and developed with the electro chemiluminescence ECL-Western blotting system (Amersham, Little Chalfont Buckinghamshire, UK), followed by exposure of the membranes to autoradiographic films (Kodak Medical X-ray film, Windsor, CO).

Antibodies to cytochrome *c* (monoclonal, Pharmingen, San Diego, CA, 1:500), smac/DIABLO (rabbit polyclonal, BD Biosci., St. Louis, MO, 1:200), and AIF (monoclonal, Sigma-Aldrich, Cambridge, UK, 1:100) were used in western blotting to study the release of these compounds from mitochondria to cytosol in mitochondrial and cytosolic fractions respectively. Cells (10^6) were treated during 3 h with prodigiosin, then harvested, washed once, and gently lysed in 150 μl of ice-cold lysis buffer (250 mM sucrose, 1 mM EDTA, 0.1% digitonin, 25 mM Tris, pH 6.8, 1 mM dithiothreitol, 1 μg/ml leupeptine, 1 μg/ml pepstatin, 1 μg/ml aproptin, 1 mM benzamidine and 0.1 mM phenylmethylsulfonyl fluoride). Lysates were centrifuged at 13,000 ×*g* at 4 °C for 3 min to obtain the pelleted fractions. Mitochondrial and cytosolic fractions were lysed with sample buffer and electrophoresed on a 15% polyacrylamide gel and then analyzed by Western blotting as described above.

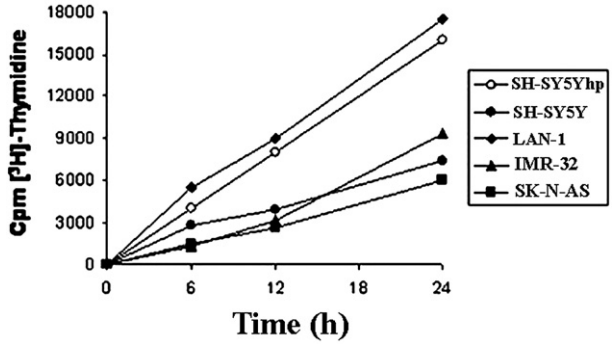

Fig. 1. Analysis of cell proliferation of the different cell lines. [^{3}H]-Thymidine incorporation up to 24 h in 5 distinct human neuroblastoma cell lines. 5×10^3 cells were seeded at the time 0 in their respective culture media.

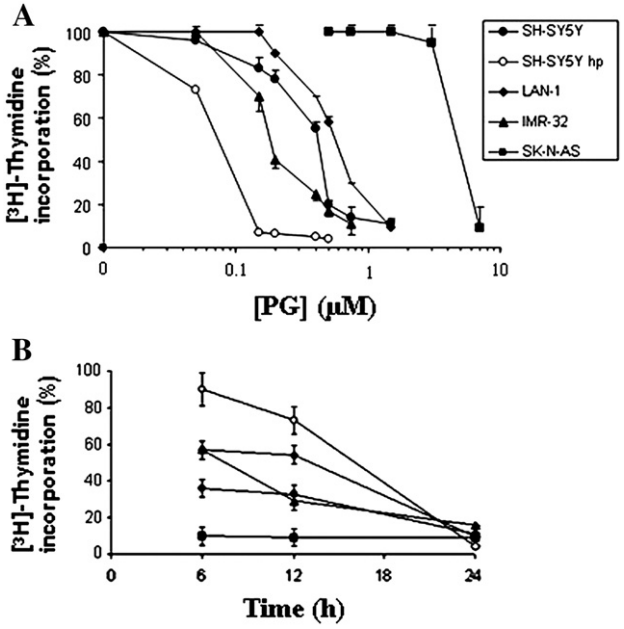

Fig. 2. Reduction of cell proliferation by prodigiosin. A) [^{3}H]-Thymidine incorporation 24 h after the incubation of the distinct human neuroblastoma cell lines with different concentrations of prodigiosin (PG) indicated in logarithmic scale. B) Time course for [^{3}H]-thymidine incorporation with prodigiosin concentrations corresponding to the IC_{50} (see Fig. 4) for each cell line. Values are given as % of tritium incorporation related to non-treated control cells at each time.

2.8. High-resolution respirometry

The function of the respiratory chain was analyzed by high-resolution respirometry in a two-channel titration injection respirometer at 37 °C (Oroboros Oxygraph, Innsbruck, Austria) as described (Giménez-Xavier et al., 2006). Briefly, cells were washed and resuspended in DMEM medium to a final concentration of 5×10^5 cells/ml. Oxygen flux was measured in untreated cells (control) and with 1.5 μM prodigiosin. In both cases, 10 μM oligomycin, an inhibitor of the mitochondrial ATP synthase, was added after 30 min of incubation.

2.9. ATP measurements

ATP content was measured in cell extracts from control cultures and cultures treated for 3 or 24 h with 1.5 μM prodigiosin.

Please cite this article as: Francisco, R. et al. Mechanisms of prodigiosin cytotoxicity in human neuroblastoma cell lines. Eur. J. Pharmacol. (2007), doi:10.1016/j.ejphar.2007.06.054

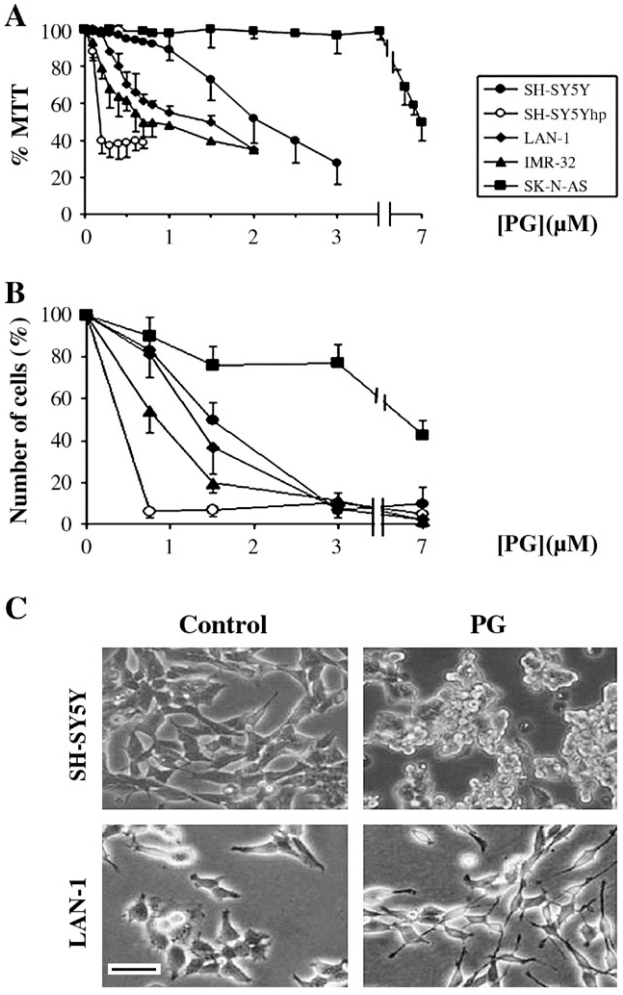

Fig. 3. A) Viability of the distinct cell lines by MTT reduction after 24 h of incubation with different prodigiosin (PG) concentrations. Results are expressed as % compared with non-treated controls after 24 h of incubation. B) Number of adherent cells after 24 h of incubation with different prodigiosin concentrations. Results are expressed as % of cells compared with non-treated controls after 24 h of incubation. The results are the mean ± S.E.M. for three distinct experiments in both cases. C) Morphology of SH-SY5Y and LAN-1 cells 24 h after the treatment with 1.5 μM prodigiosin (IC_{50} dose). LAN-1 cells clearly show a marked differentiation with neurite-like structures after prodigiosin treatment. SH-SY5Y cells are shown as representative of morphological changes observed in the other neuroblastoma cell lines: no or little differentiation and swelling feature. Scale bar 50 μm.

An ATP assay kit based on the luciferin–luciferase procedure was used following the instructions of the manufacturer (Calbiochem, Beeston/Notthingham, UK). The light emission was measured in a luminometer plate (Fluostar optima Microtiter Plate Reader). ATP concentrations were calculated with a standard curve generated using the ATP standard provided by the kit.

3. Results

3.1. Cell proliferation assays

The rate of proliferation, measured by [^{3}H]-thymidine incorporation, was similar in IMR-32, SK-N-AS and SH-SY5Y ATCC-clone, and markedly higher in LAN-1 and the second SH-SY5Y (SH-SY5Yhp) (Fig. 1). No morphological differences were observed between the two SH-SY5Y clones. Proliferation was reduced to less than 50% after 24 h exposure to prodigiosin at concentrations lower than 1 μM in all cell lines except for SK-N-AS, which needed 3.5 μM prodigiosin to reduce the proliferation rate to half (Fig. 2A). The time-course of [^{3}H]-thymidine incorporation using the prodigiosin concentrations corresponding to the IC_{50} for each cell line (see Fig. 4) showed that cell proliferation mechanisms were almost completely blocked in SK-N-AS cells after 6 h, whereas for the other cell lines progressively decreased [^{3}H]-thymidine incorporation until 10–20% of non-treated cells after 24 h (Fig. 2B).

3.2. Cell viability

The arrest of cell proliferation could initiate a program of cell death or lead to cell differentiation. The viability of most of the cell lines (with the exception of SK-N-AS), measured by cell counting and by MTT, was dramatically reduced after 24 h of exposure to prodigiosin concentrations lower than 3 μM. The SH-SY5Yhp was the most sensitive cell line, reducing its viability to 50% (by MTT) with 150 nM prodigiosin (Fig. 3A). Similar curve profiles were found by MTT and the adherent cells number counting. The values obtained by cell counting were however lower, indicating that some of the floating washed cells were still able to reduce MTT (Fig. 3A and B). SK-N-AS was the most resistant cell line, its viability being reduced to 50% with 7 μM prodigiosin after 24 h, and with 3 μM after 48 h (data not shown), values that approached the sensitivity of these kind of cells to those of non-tumoral cells (Montaner and Pérez-Tomás, 2003). The content of protein per cell was established in non-treated cells as: 1.0 ± 0.1 (SH-SY5Yhp), 1.8 ± 0.2 (SH-SY5Y), 2.2 ± 0.2 (LAN-1), 1.8 ± 0.1 (IMR-32), 2.6 ± 0.3 (SK-N-AS) (μg prot. × 10^{-4}/cell). No significant differences were found in this relationship in any prodigiosin-treated cell line, therefore the

Cell line	IC50 Prodigiosin μM ± S.E.M.	IC50 Cisplatin μM ± S.E.M.
SH-SY5Yhp	0.15 ± 0.01	50 ± 5
SH-SY5Y	1.5 ± 0.2	50 ± 5
LAN-1	1.5 ± 0.2	100 ± 8
IMR-32	0.7 ± 0.1	0.7 ± 0.1
SK-N-AS	7.0 ± 0.5	85 ± 8

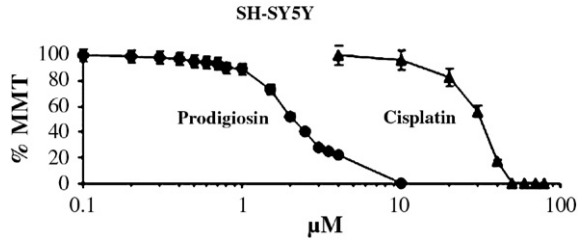

Fig. 4. IC_{50} ± S.E.M. concentrations of the different cell lines for prodigiosin and cisplatin determined by MTT at 24 h of incubation. Viability of SH-SY5Y cells at 24 h of treatment with different concentrations of prodigiosin or cisplatin (in logarithmic scale) is shown as indicative of the results obtained in the distinct cell lines.

Please cite this article as: Francisco, R. et al. Mechanisms of prodigiosin cytotoxicity in human neuroblastoma cell lines. Eur. J. Pharmacol. (2007), doi:10.1016/j.ejphar.2007.06.054

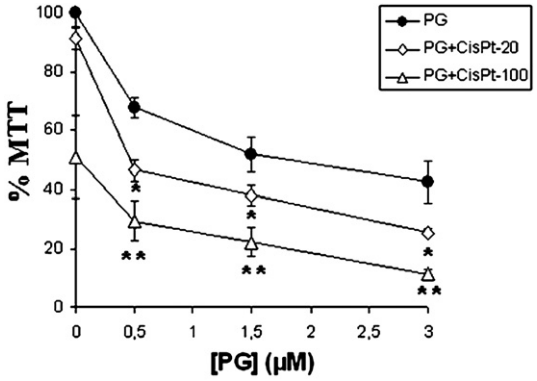

Fig. 5. Cell viability, measured with MTT, after treatment with different concentrations of prodigiosin alone (PG) or in combination with 20 or 100 μM cisplatin (CisPt-20, CisPt-100) in LAN-1 neuroblastoma cells. Results are the mean±S.E:M. for three distinct experiments. *$P<0.05$, **$P<0.01$ compared with prodigiosin treatment (Anova+Duncan test).

values of MTT could be assumed as lineal with the protein content and cell number.

The effect of prodigiosin was compared with the effect of a conventional chemotherapeutic drug such as cisplatin. Fig. 4 shows the values of IC_{50} (24 h) of prodigiosin and cisplatin for each cell line. Only for IMR-32 were the effects of prodigiosin and cisplatin of similar magnitude. SH-SY5Y, LAN-1 and even SK-N-AS cells were much more sensitive to prodigiosin than to cisplatin. A prodigiosin and cisplatin combined treatment was assayed in LAN-1 cells. The results showed a significantly increased effect on the loss of cell viability compared to one-drug treatments, even at a dose of cisplatin ineffective by itself (Fig. 5).

Regarding the possibility of cell differentiation after the arrest of cell proliferation, LAN-1 showed a marked differentiation after 24 h exposure to 1.5 μM prodigiosin, showing neurite-like structures (Fig. 3C), whereas this behavior was very poorly expressed in the other cell lines, in the order LAN-1 > SH-SY5Y > IMR-32 > SK-N-AS. Most of the neuroblastoma cell lines, when incubated with prodigiosin concentrations corresponding to their respective IC_{50}, acquired a shrunken and rounded morphology, characteristic of non-viable cells. Between 48 and 72 h at the IC_{50} (24 h) prodigiosin dose, the viability of the cell lines (with the exception of SK-N-AS) was practically reduced to zero.

3.3. Cell death

Taking these results into consideration, we proceeded to study the induction of apoptosis or other forms of cell death, and their relationship with cell proliferation, after prodigiosin treatment. The most characteristic parameters of apoptosis were observed only in SH-SY5Yhp cells when they were incubated

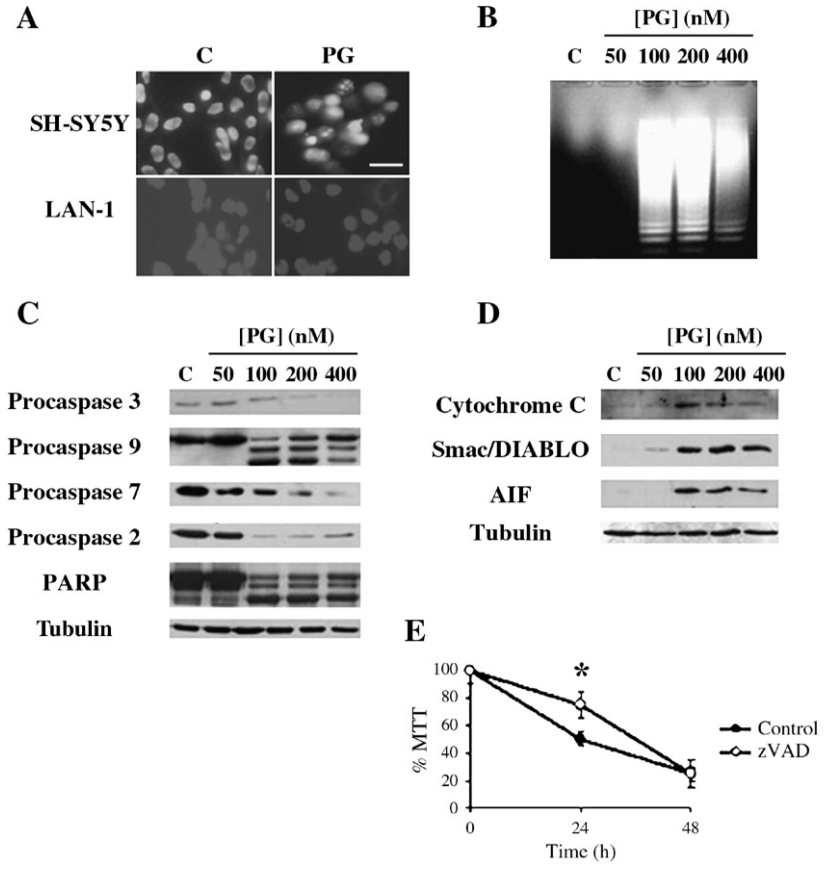

Fig. 6. A) Fluorescent Hoescht staining in SH-SY5Yhp and LAN-1 cells after treatment for 24 h with prodigiosin at the IC_{50} concentration. Scale bar 50 μm. B) DNA laddering of SH-SY5Yhp cells in the same conditions than above. C) Western blot of caspases and PARP in SH-SY5Yhp cells. D) Western blot of mitochondrial factors in the cytosolic fraction of SH-SY5Yhp cells. E) Effect of zVAD.fmk on the viability of the different cell lines after prodigiosin treatment (24 h at their respective IC_{50} doses). Values are the mean±S.E.M. for the viabilities of the different cell lines, *$P<0.05$ compared with controls at 24 h (t-Student).

Please cite this article as: Francisco, R. et al. Mechanisms of prodigiosin cytotoxicity in human neuroblastoma cell lines. Eur. J. Pharmacol. (2007), doi:10.1016/j.ejphar.2007.06.054

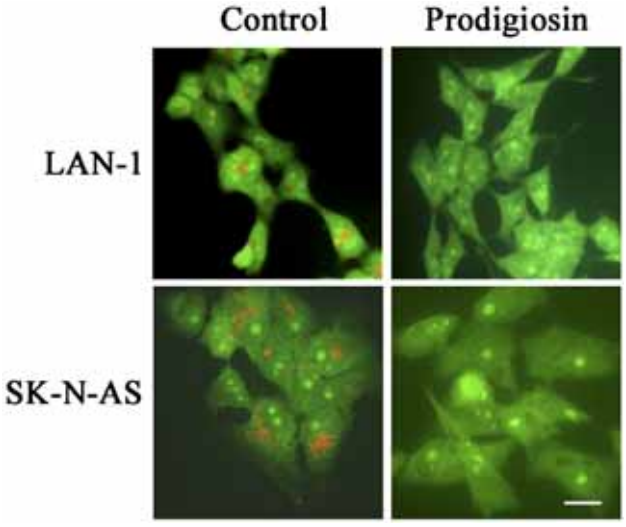

Fig. 7. Intracellular acidic pH detection by orange acridine. Orange fluorescence disappears after the treatment of the distinct cell lines with 1.5 μM prodigiosin for 6 h. The figure shows the results in LAN-1 and SK-N-AS as representative. Scale bar 10 μm.

for 24 h with prodigiosin at the IC_{50}: condensed and fragmented nuclei with the fluorescent Hoescht staining (Fig. 6A); DNA laddering (Fig. 6B); activation of the pro-caspases-2, -9, -3 and -7 (Fig. 6C); activation of poly(ADP-ribose) polymerase (PARP; Fig. 6C); release of mitochondrial factors to the cytoplasm, including cytochrome *c*, apoptosis inducing factor (AIF) and smac/Diablo (Fig. 6D). The other cell lines showed condensed nuclei (Fig. 6A) but not DNA fragmentation or caspase activation. With regard to mitochondrial factors, no release of cytochrome *c* was observed in any of the other cell lines, and only IMR-32 cells showed smac/Diablo release to cytoplasm (data not shown). The non-specific caspase inhibitor zVAD.fmk partially protected the prodigiosin effect at 24 h in all the cell lines, but not at 48 h (Fig. 6E).

3.4. Intracellular pH

According to previously published results (Castillo-Ávila et al., 2005), the loss of acidic pH in intracellular compartments could play an important role in prodigiosin toxicity. Also, in all the neuroblastoma cell lines studied, the acidic intracellular compartments were neutralized after treatment with IC_{50} (24 h) prodigiosin or by a 1.5 μM prodigiosin (a toxic dose for all the cell lines except for SK-N-AS), as it could be seen by the disappearing of the orange colour in orange acridine treated cells (Fig. 7).

3.5. Mitochondrial localization

Prodigiosin is a fluorescent red compound, whose distribution inside the cell can be assessed under a fluorescence microscope. Shortly after 1.5 μM treatment, prodigiosin was seen throughout the cytoplasm and accumulated in mitochondria in all but SK-N-AS cell lines. Prodigiosin and Mitotracker co-localization staining was observed by confocal microscopy (Fig. 8). The cell nucleus was preserved from prodigiosin access in all the cases.

3.6. Oxygen consumption and ATP content

The intramitochondrial accumulation of prodigiosin could impair the mitochondrial function. The analysis of oxygen

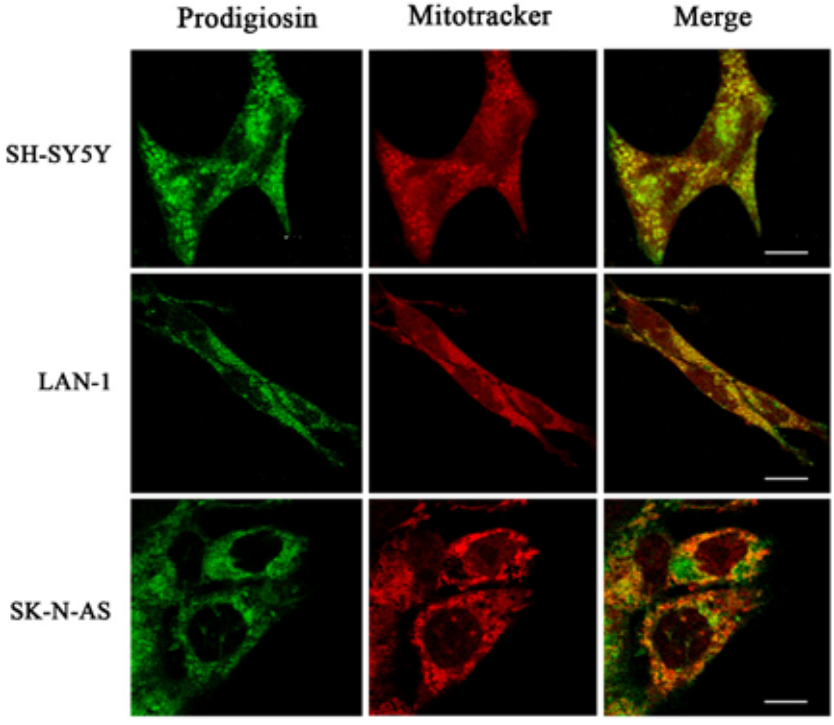

Fig. 8. Confocal fluorescence of prodigiosin (λem = 543 nm) and Mitotracker (λem = 633 nm) in LAN-1, SH-SY5Y and SK-N-AS cells 3 h after 1.5 μM prodigiosin treatment. Prodigiosin fluorescence is shown in green, Mitotracker fluorescence in red and the co-localization (merge) in yellow. Scale bar 10 μm.

Please cite this article as: Francisco, R. et al. Mechanisms of prodigiosin cytotoxicity in human neuroblastoma cell lines. Eur. J. Pharmacol. (2007), doi:10.1016/j.ejphar.2007.06.054

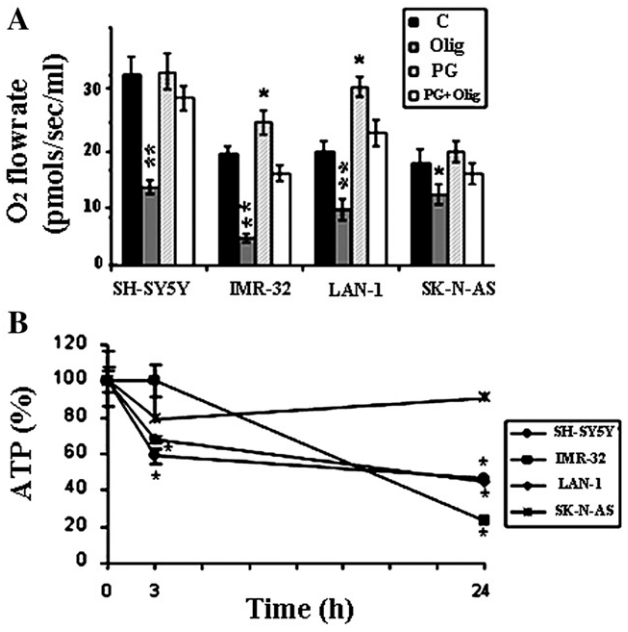

Fig. 9. A) Oxygen flow in culture media measured by respirometry and expressed as pmol of oxygen per second and ml of medium in non-treated cells (C) and 2 h after 1.5 μM prodigiosin (PG) treatment. In both cases the decrease of oxygen consumption after the addition of oligomycin (Olig) is shown. The oxygen concentration was 200 μM at the beginning of the measurements and about 175 μM at the end of the experiment. Oxygen flow in control cells was: 30±1 (SH-SY5Y and SH-SY5Yhp), 18±0.5 (IMR-32), 18±0.7 (LAN-1), 14±1 (SK-N-AS) pmol/s/10^6 cells. The results are the mean±S.E.M. of ten readings over 10 min. *$P<0.05$, **$P<0.01$ compared with the corresponding control (Anova+Duncan test). B) ATP relative concentrations 3 and 24 h after the treatment of different neuroblastoma cell lines with 1.5 μM prodigiosin. The results are the mean of three measures±S.E.M. *$P<0.05$, **$P<0.01$. The basal ATP concentrations were: $[ATP]_{SH\text{-}SY5Y}=0.97\pm0.16$; $[ATP]_{LAN\text{-}1}=0.84\pm0.14$; $[ATP]_{IMR\text{-}32}=0.74\pm0.07$; $[ATP]_{SK\text{-}N\text{-}A}S=0.84\pm0.08$ nmol/10^6 cells, determined as the mean±S.E.M. of three samples. *$P<0.05$, compared with time 0 (non-treated cells, Anova+Duncan test).

consumption revealed a rate of about 30 pmol/s/10^6 cells in SH-SY5Y cells and 14 pmol/s/10^6 cells in SK-N-AS cells. This parameter was increased after 3 h treatment with 1.5 μM prodigiosin in LAN-1 and IMR-32 cells and was not altered in SH-SY5Y and SK-N-AS cells. The inhibition of ATP synthesis with oligomycin decreased the oxygen consumption between 50 and 80% in LAN-1, SH-SY5Y and IMR-32 cells (only 30% in SK-N-AS cells). However, oligomycin had no significant effect on oxygen consumption in prodigiosin-treated cells (Fig. 9A). The ATP basal content was about 1 nmol/10^6 cells in all the cell lines used. The ATP concentrations were significantly reduced in SH-SY5Y and LAN-1 cells by 40% and 35% respectively after 3 h of treatment with 1.5 μM prodigiosin, and between 60% and 80% after 24 h in SH-SY5Y, LAN-1 and IMR-32 cell lines. No significant effect was found in ATP content in SK-N-AS cells (Fig. 9B).

4. Discussion

Prodigiosin is strongly cytotoxic for human N-type neuroblastoma cell lines (cells with a potential neuroblastic phenotype), reducing their viability in 24 h to less than 50% at a dose of 1.5 μM or lower, while S-type cells (SK-N-AS, with glial-schwannian phenotype) require a dose of 7 μM prodigiosin to achieve the IC_{50}, at which non-tumor cells could also be affected (Montaner et al., 2000; Campàs et al., 2003). Although prodigiosin and closely related compounds have been described as potent immunosuppressive agents (Campás et al., 2003) and have been studied for their cytotoxic activity in several cancer cells (Pérez-Tomás et al., 2003; Yamamoto et al., 2000), their effect on neuroblastoma cells had not previously been reported. For SH-SY5Y and LAN-1 the IC_{50} of prodigiosin is more than 30 times lower than that of cisplatin, a conventional chemotherapeutic drug. The effect of prodigiosin is, at least in part, linked to cell proliferation: a cell clone of SH-SY5Y cells with a high rate of proliferation (SH-SY5Yhp) is shown to be one order of magnitude more vulnerable to prodigiosin than another clone with a lower rate of proliferation. Prodigiosin markedly decreased cell proliferation in all the lines studied after 24 h of incubation with the concentrations corresponding to the IC_{50}. The loss of viability at 24 h in relation to non-treated cells might be thus in part due to the arrest of the cell cycle. Although the viability decreased after the arresting of the cell cycle, especially in N-type cells, their subsequent behavior differed from one cell line to another, showing in LAN-1 a higher ability to differentiate than the other cell lines studied.

In an attempt to examine the mechanisms leading to cell cycle arrest and death in greater depth, we analyzed the intracellular prodigiosin distribution. We assessed the uptake and cell distribution of prodigiosin taking advantage of its autofluorescence. Prodigiosin spreads throughout the cytoplasm and organelles, but spares the nucleus, which showed little or no fluorescence after prodigiosin treatment.

Although prodigiosin may interact *in vitro* with DNA by binding to the DNA grooves (Melvin et al., 2001), the lack of access of prodigiosin to the nucleus makes it difficult to consider that a direct prodigiosin–DNA interaction could be achieved *in vivo*. The intra-mitochondrial accumulation of prodigiosin was assessed by the co-localization of Mitotracker and prodigiosin. Mitochondrial swelling caused by prodigiosin in rat mitochondrial preparations had been previously reported (Konno et al., 1998) and could be related to mitochondrial prodigiosin accumulation. At the same time, the ATP cell content was reduced by approximately 30% in the N-type cell lines, indicating damage to mitochondrial activity. The loss of ATP reached 60% after 24 h. Interestingly, co-localization of Mitotracker and prodigiosin was very low in the S-type cells, coinciding with the lack of ATP decrease and with the low effect of prodigiosin on cell viability in these cells.

The mitochondrial damage could lead to the release of mitochondrial factors to the cytoplasm that triggers apoptosis with the recruitment of the apoptosome and the activation of effector caspases. However, this was observed only in SH-SY5Yhp cells; no clear signs of apoptosis were seen in the other cell lines. At least for IMR-32 cells (Yuste et al., 2001) a lack of the caspase-activated DNase has been described.

An apoptotic process may be a secondary effect of mitochondrial cell damage, because the death is only partially protected by caspase inhibition, indicating that even when caspases

Please cite this article as: Francisco, R. et al. Mechanisms of prodigiosin cytotoxicity in human neuroblastoma cell lines. Eur. J. Pharmacol. (2007), doi:10.1016/j.ejphar.2007.06.054

participated in neuroblastoma cell death, their inhibition would be not enough to rescue the cells from death. Mitochondrial damage could trigger apoptotic or non-apoptotic mechanisms of death depending on the metabolic status and the expression of apoptosis-regulating factors (Nakashima et al., 2005). The ATP content and the oxygen consumption were assumed to be indices of mitochondrial activity. However, whereas ATP content decreased, the rate of oxygen consumption was not altered, or even increased, by prodigiosin. The rate of oxygen consumption and the ATP content (about 1 mM) were low in all the neuroblastoma cells studied, consistent with immature cells with a metabolism not completely dependent on aerobic conditions. The decrease of ATP levels to less than a half in 24 h seriously compromised cell viability. Other authors have described an effect in hamster kidney cells of prodigiosin 25-C on the proton pump and the H^+-ATPase lysosomal activity without altering the ATP levels (Kataoka et al., 1995). Those measures of ATP were done at short times (1 h) and in cells with a high ATP content (about 5 mM) which could make them more resistant to the mitochondrial effect of prodigiosin.

We suggest that prodigiosin could modify all the H^+-dependent ATPases but, at least in neuroblastoma cells, this effect is particularly determinant for cell viability only when prodigiosin blocks the H^+-mitochondrial gradient. Our results indicate an uncoupling effect between the energy supplied by the mitochondrial chain and the use of this energy for ATP synthesis. This effect would be due to the proton-trapping ability of prodigiosin. The pK_a of prodigiosin is about 7.2 (Rizzo et al., 1998), meaning an equilibrium prodigiosin$+H^+ \Leftrightarrow$ prodigiosin$-H^+$ displaced to the right at a pH lower than 7.2. Protonated and deprotonated prodigiosin forms have, in addition, different main conformations (a linear prodigiosin-α, favored at pH<7 and a folded prodigiosin-β, favored at pH>7; Manderville 2001). The prodigiosin charge and conformation must be determinant for its intracellular distribution and accumulation. The cytosolic pH in cancerous cells tends to be neutral or even slightly alkaline (Yamamoto et al., 1999), so that prodigiosin is there practically at its pK_a. In acidic compartments such as lysosomes or mitochondrial intermembrane space, the major form of prodigiosin would be prodigiosin$-H^+$. It has already been noted that prodigiosins uncouple F-ATPases and V-ATPases, disrupting the proton intracellular gradients and, through H^+/Cl^- symport activity, causing cytoplasm acidification (Kataoka et al., 1995; Sato et al., 1998; Konno et al., 1998; Yamamoto et al., 2000). We observed this effect in conditions in which cells lost their viability (SH-SY5Y, LAN-1, IMR-32) but also in conditions in which cells maintained it (SK-N-AS).

The effect of prodigiosin accumulation in the mitochondria had not been previously reported. The uncoupling-like effect in mitochondria would be due to proton sequestration in the intermembrane space. The lower accumulation of prodigiosin in SK-N-AS mitochondria is determinant for its effect, but the decrease in oxygen consumption induced by oligomycin was also less in these cells, indicating that SK-N-AS have different metabolic characteristics than N-type cells, probably having a relatively low requirement of mitochondrial ATP for survival.

Taking these results together, we conclude that, at least in human N-type neuroblastoma cells, which are considered to be the most proliferative and invasive in children's tumors, low concentrations of prodigiosin have a mitochondrial uncoupling effect, and reduce ATP levels as well as cell viability. This mechanism of action differs from those of conventional chemotherapeutics, suggesting that this compound could be studied as a toxic agent for neuroblastoma, and could be used alone or in combination with other drugs in neuroblastoma treatment.

Acknowledgments

We are grateful to all the members of the Biochemistry and Cell Biology Units (Campus Bellvitge) of the University of Barcelona. We thank Dr. Jaume Mora and Dr. Joan Comella for supplying cell lines and Dr. Jordi Boada for the help in the respirometry analysis. P. Giménez-Xavier is recipient of a FPU grant and this work has been supported by a grant from the Spanish Government, FIS-PI061226.

References

Bellosillo, B., Piqué, M., Barragán, M., Castaño, E., Villamor, N., Colomer, D., Montserrat, E., Pons, G., Gil, J., 1998. Aspirin and salicylate induce apoptosis and activation of caspases in B-cell chronic lymphocytic leukemia cells. Blood 92, 1406–1414.

Berthold, F., Hero, B., 2000. Neuroblastoma — current drug therapy recommendations as a part of the total treatment approach. Drugs 59, 1261–1277.

Boix, J., Llecha, N., Yuste, V.J., Comella, J.X., 1997. Characterization of the cell death process induced by staurosporine in human neuroblastoma cell lines. Neuropharmacology 36, 811–821.

Brodeur, G.M., 2003. Neuroblastoma: biological insights into a clinical enigma. Nat. Rev., Cancer 3, 203–216.

Campàs, C., Dalmau, M., Montaner, B., Barragàn, M., Bellosillo, B., Colomer, D., Pons, G., Pérez-Tomás, R., Gil, J., 2003. Prodigiosin induces apoptosis of B and T cells from B-cell chronic lymphocytic leukemia. Leukemia 17, 746–750.

Castillo-Ávila, W., Abal, M., Robine, S., Pérez-Tomás, R., 2005. Non-apoptotic concentrations of prodigiosin (H^+/Cl^- symporter) inhibit the acidification of lysosomes and induce cell cycle blockage in colon cancer cells. Life Sci. 78, 121–127.

Díaz-Ruiz, C., Montaner, B., Pérez-Tomás, R., 2001. Prodigiosin induces cell death and morphological changes indicative of apoptosis in gastric cancer cell line HGT-1. Histol. Histopathol. 16, 415–421.

Encinas, M., Iglesias, M., Liu, Y., Wang, H., Muhaisen, A., Ceña, V., Gallego, C., Comella, J.X., 2000. Sequential treatment of SH-SY5Y cells with retinoic acid and brain-derived neurotrophic factor gives rise to fully differentiated, neurotrophic factor-dependent, human neuron-like cells. J. Neurochem. 75, 991–1003.

Giménez-Xavier, P., Gómez-Santos, C., Castaño, E., Francisco, R., Boada, J., Unzeta, M., Sanz, E., Ambrosio, S., 2006. The decrease of NAD(P)H has a prominent role in dopamine toxicity. Biochim. Biophys. Acta 1762, 564–574.

Kataoka, T., Muroi, M., Ohkuma, S., Waritani, T., Magae, J., Takatsuki, A., Kondo, S., Yamasaki, M., Nagai, K., 1995. Prodigiosin 25-C uncouples vacuolar type H^+-ATPase, inhibits vacuolar acidification and affects glycoprotein processing. FEBS Lett. 359, 53–59.

Han, S.B., Park, S.H., Jeon, Y.J., Kim, Y.K., Kim, H.M., Yang, K.H., 2001. Prodigiosin blocks T cell activation by inhibiting interleukin-2Ra expression and delays progression of autoimmune diabetes and collagen-induced arthritis. J. Pharmacol. Exp. Ther. 299, 415–425.

Konno, H., Matsuya, H., Okamoto, M., Sato, T., Tanaka, Y., Yokohama, K., Kataoka, T., Nagai, K., Wasserman, H.H., Ohkuma, S., 1998. Prodigiosins uncouple mitochondrial and bacterial F-ATPases: evidence for their H^+/Cl^- symport activity. J. Biochem. 124, 547–556.

Please cite this article as: Francisco, R. et al. Mechanisms of prodigiosin cytotoxicity in human neuroblastoma cell lines. Eur. J. Pharmacol. (2007), doi:10.1016/j.ejphar.2007.06.054

Llagostera, E., Soto-Cerrato, V., Joshi, R., Montaner, B., Giménez-Bonafé, P., Pérez-Tomás, R., 2005. High cytotoxic sensitivity of the human small cell lung doxorubicin-resistant carcinoma (GLC4/ADR) cell line to prodigiosin through apoptosis activation. Anticancer Drugs 16, 393–399.

Manderville, R.A., 2001. Synthesis, proton-affinity and anti-cancer properties of the prodigiosin-group natural products. Curr. Med. Chem. – Anti-Cancer Agents 1, 195–218.

Melvin, M.S, Ferguson, D.C., Lindquist, N., Manderville, R.A., 1999. DNA binding by 4-methoxypyrrolic natural products. Preference for intercalation at AT sites by tambjamine E and prodigiosin. J. Org. Chem. 64, 6861–6869.

Melvin, M.S., Wooton, K.E., Rich, C.C., Saluta, G.R., Kucera, G.L., Lindquist, N., Manderville, R.A., 2001. Copper-nuclease efficiency correlates with cytotoxicity for the 4-methoxypyrrolic natural products. J. Inorg. Biochem. 87, 129–135.

Montaner, B., Pérez-Tomás, R., 2001. Prodigiosin-induced apoptosis in human colon cancer cells. Life Sci. 68, 2025–2036.

Montaner, B., Pérez-Tomás, R., 2003. The prodigiosins: a new family of anticancer drugs. Curr. Cancer Drug Targ. 3, 57–65.

Montaner, B., Navarro, S., Piqué, M., Vilaseca, M., Martinell, M., Giralt, E., Gil, J., Pérez-Tomás, R., 2000. Prodigiosin from the supernatant of *Serratia marcescens* induces apoptosis in haematopoietic cancer cell lines. Br. J. Pharmacol. 131, 585–593.

Montaner, B., Castillo-Ávila, W., Martinell, M., Ollinger, R., Aymami, J., Giralt, E., Pérez-Tomás, R., 2005. DNA interactions and dual topoisomerase I and II inhibition properties of the anti-tumor drug prodigiosin. Toxicol. Sci. 85, 870–879.

Nakashima, T., Tamura, T., Kurachi, M., Yamaguchi, K., Oda, T., 2005. Apoptosis-mediated cytotoxicity of prodigiosin-like red pigment produced by γ-*Proteobacterium* and its multiple bioactivities. Biol. Pharm. Bull. 28, 2289–2295.

Pérez-Tomás, R., Montaner, B., Llagostera, E., Soto-Cerrato, V., 2003. The prodigiosins, proapoptotic drugs with anticancer properties. Biochem. Pharmacol. 66, 1447–1452.

Rizzo, V., Morelli, A., Pinciroli, V., Sciangula, D., D'Alessio, R., 1998. Equilibrium and kinetics of rotamer interconversion in immusuppressant prodigiosin derivatives in solution. J. Pharmacol. Sci. 88, 73–78.

Sato, T., Konno, H., Tanaka, Y., Kataoka, T., Nagai, K., Wasserman, H.H., Ohkuma, S., 1998. Prodigiosins as a new group of H^+/Cl^- symporters that uncouple proton translocators. J. Biol. Chem. 273, 21455–21462.

Soto-Cerrato, V., Llagostera, E., Montaner, B., Scheffer, G.L., Pérez-Tomás, R., 2004. Mitochondria-mediated apoptosis operating irrespective of multidrug resistance in breast cancer cells by the anticancer agent prodigiosin. Biochem. Pharmacol. 68, 1345–1352.

Williamson, N.R., Fineran, P.C., Leeper, F.J., Salmond, G.P.C., 2006. The biosynthesis and regulation of bacterial prodigiosines. Nat. Rev. Microbiol. 4, 887–899.

Yamamoto, C., Takemoto, H., Kuno, K., Yamamoto, D., Tsubura, A., Kamata, K., Hirata, H., Yamamoto, A., Kano, H., Seki, T., Inoue, K., 1999. Cycloprodigiosin hydrochloride, a new H^+/Cl^- symporter, induces apoptosis in human and rat hepatocellular cancer cell lines in vitro and inhibits the growth of hepatocellular carcinoma xenografts in nude mice. Hepatology 30, 894–902.

Yamamoto, D., Uemura, Y., Tanaka, K., Nakai, K., Yamamoto, C., Takemoto, H., Kamata, K., Hirata, H., Hioki, K., 2000. Cycloprodigiosin hydrochloride, H^+/Cl^- symporter, induces apoptosis and differentiation in HL-60 cells. Int. J. Cancer 88, 121–128.

Yamamoto, D., Tanaka, K., Nakai, K., Baden, T., Inoue, K., Yamamoto, C., Takemoto, H., Kamato, K., Hirata, H., Morikawa, S., Inubushi, T., Hioki, K., 2002. Synergistic effects induced by cycloprodigiosin hydrochloride and epirubicin on human breast cancer cells. Breast Cancer Res. Treat. 72, 1–10.

Yuste, V.J., Bayascas, J.R., Llecha, N., Sanchez-Lopez, I., Boix, J., Comella, J.X., 2001. The absence of oligonucleosomal DNA fragmentation during apoptosis of IMR-5 neuroblastoma cells: disappearance of the caspase-activated DNase. J. Biol. Chem. 276, 22323–22331.

Zaizen, Y., Taniguchi, S., Suita, S., 1998. The role of cellular motility in the invasion of human neuroblastoma cells with or without N-myc amplification and expression. J. Pediatr. Surg. 33, 1765–1770.

Zhang, J., Shen, Y., Liu, J., Wei, D., 2005. Antimetastatic effect of prodigiosin through inhibition of tumor invasion. Biochem. Pharmacol. 69, 407–414.

Please cite this article as: Francisco, R. et al. Mechanisms of prodigiosin cytotoxicity in human neuroblastoma cell lines. Eur. J. Pharmacol. (2007), doi:10.1016/j.ejphar.2007.06.054

4. REVISIÓN DE LAS PROPIEDADES ANTICANCEROSAS DE MIEMBROS DE LA FAMILIA DE LAS PRODIGININAS

Las prodigiosinas, drogas proapoptóticas con actividades anticancerosas.

("Pérez-Tomás R, Montaner B, Llagostera E, Soto-Cerrato V. The prodigiosins, proapoptotic drugs with anticancer properties. Biochem Pharmacol 2003;66(8):1447-52").

Durante la realización de esta tesis, nuestro grupo realizó una revisión de las actividades farmacológicas descritas hasta el momento de los miembros de la familia de las prodigininas. Algunos cuentan con propiedades inmunosupresoras, mientras que otros han mostrado efectos apoptóticos *in vitro* a la vez que actividad antitumoral *in vivo*. Conocer a fondo el mecanismo de acción de una droga es esencial para su desarrollo clínico y requiere de la identificación de las dianas moleculares de dicha sustancia. En esta revisión también se hipotetiza acerca del posible mecanismo de acción de las prodigininas y se discute acerca de las dianas moleculares de estas moléculas. Los resultados mostrados en esta revisión sugieren que las prodigininas son una nueva clase de drogas anticancerosas, las cuales poseen actividades potencialmente prometedoras para la industria farmacéutica.

(Revisión llevada a cabo por nuestro grupo de investigación en la que he contribuido de forma parcial).

Available online at www.sciencedirect.com
SCIENCE DIRECT®
Biochemical Pharmacology 66 (2003) 1447–1452
Biochemical Pharmacology
www.elsevier.com/locate/biochempharm

The prodigiosins, proapoptotic drugs with anticancer properties

Ricardo Pérez-Tomás *, Beatriz Montaner, Esther Llagostera, Vanessa Soto-Cerrato

Cancer Cell Biology Research Group, Departament de Biologia Cel.lular i Anatomia Patològica, Universitat de Barcelona. Feixa Llarga s/n. E-08907 L'Hospitalet, Barcelona, Spain

Received 28 February 2003; accepted 31 March 2003

Abstract

The family of natural red pigments, called prodigiosins (PGs), characterised by a common pyrrolylpyrromethene skeleton, are produced by various bacteria. Some members have immunosuppressive properties and apoptotic effects *in vitro* and they have also displayed antitumour activity *in vivo*. Understanding the mechanism of action of PGs is essential for drug development and will require the identification and characterisation of their still unidentified cell target. Four possible mechanisms of action have been suggested for these molecules: (i) PGs as pH modulators; (ii) PGs as cell cycle inhibitors; (iii) PGs as DNA cleavage agents; (iv) PGs as mitogen-activated protein kinase regulators. Here, we review the pharmacological activity of PG and related compounds, including novel synthetic PG derivatives with lower toxicity and discuss the mechanisms of action and the molecular targets of those molecules. The results reported in this review suggest that PGs are a new class of anticancer drugs, which hold out considerable promise for the Pharmacological Industry.

Keywords: Apoptosis; DNA damage; Cancer; Chemotherapy; Prodigiosin

1. Introduction

In 1888, Dr. William B. Coley (1862–1936), a prominent New York surgeon, stumbled across one of the most intriguing findings ever made in cancer research. Dr. Coley combined the cultures of *Streptococcus* sp. and *Bacillus prodigiosus* (called *S. marcescens*), and then sterilised them by either heat or filtration. The mixture was called mixed bacterial vaccines (now called the Coley's toxins). This therapy was used to treat tumours with fascinating results in tumours of mesodermal origin [1,2]. Although the biologically active substance in Coley's toxins is described as tumour necrosis factor (TNF), a cytokine that is induced in response to lipopolysaccharide (LPS) and causes cancer cell death [3,4], PG might be contained in Coley's toxin. In fact, in recent years new interest in PG and its derivatives has emerged among researchers.

PGs are a family of naturally occurring polypyrrole red pigments produced by a restricted group of microorganisms, including some *Streptomyces* and *Serratia* strains, characterised by a common pyrrolyldipyrrolylmethene skeleton (Fig. 1). PG, cycloprodigiosin hydrochloride (cPrG·HCl), metacycloprodigiosin, nonylprodigiosin and undecylprodigiosin (prodigiosin 25-C, UP) are all members of this family. PG was first isolated from *S. marcescens* in pure form in 1929. Its name, used by early researchers, was retained but the pigment was not characterised and its main structural features elucidated until 1934 [5]. As typical secondary metabolites, PG and related materials have no clearly defined physiological functions in the producing organisms. However, PG is a wetting agent that provides ecological advantages in bacteria dispersion [6,7]. PG family members have potent antimicrobial, antimalarial, immunosuppressive and cytotoxic activity [8–33]. Recently, an extensive chemical research programme was undertaken by D'Alessio and co-workers from Pharmacia & Upjohn, in order to obtain synthetic derivatives of PG [34–36] and identify more active and less

* Corresponding author. Tel.: +34-93-4024288; fax: +34-93-4029082.
E-mail address: rperez@bell.ub.es (R. Pérez-Tomás).

Abbreviations: cPrG·HCl, cycloprodigiosin hydrochloride; ds, double strand; ERK, extracellular signal-regulated kinase; IC_{50}, inhibitory concentration 50%; Jak3, janus kinase 3; JNK, c-*jun* N-terminal kinase; MAPK, mitogen-activated protein kinase; PG, prodigiosin; pH_i, intracellular pH; PKC, protein kinase C; SAPK, stress-activated protein kinase; ss, single strand; UP, prodigiosin 25-C (undecylprodigiosin).

0006-2952/$ – see front matter © 2003 Elsevier Inc. All rights reserved.
doi:10.1016/S0006-2952(03)00496-9

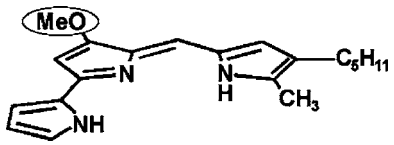

Fig. 1. Side-on view of 2-methyl-3-pentyl-6-methoxyprodigiosene (PG), showing the planar arrangements of the three pyrrole rings. The exceptional cytotoxic potency of PG may be attributed to the presence of the PG C-6 methoxy substituent (circle).

toxic drugs than natural PG compounds. The best compound obtained to date is PNU156804.

2. PGs trigger apoptosis

Apoptosis has become one of the newest areas of cell biology research, possibly because of the belated realisation that cell death is a biochemically regulated process that may be as complex as other fundamental biological processes. It has been linked to such diverse pathophysiologic processes as oncogenesis [36]. The activation of the apoptosis programme is regulated by various signals from both intracellular and extracellular stimuli. Indeed, in recent years evidence is beginning to accumulate that many (and perhaps all) agents of cancer chemotherapy kill tumour cells by launching the mechanisms of apoptosis.

New drugs associated with apoptosis are expected to be most effective against tumours with high proliferation rates and are being screened for use in the treatment of cancer [36]. Microbial pathogens engage or circumvent the host apoptotic programme. Indeed, PGs have been shown to induce apoptosis. Their apoptotic effects have been observed in several human cancer cell lines in tissue culture [19,24,29–33,37–39], in hepatocellular carcinoma xenografts [40] and in human primary cancer cells [33].

cPrG·HCl induces apoptosis in liver cancer cells both *in vitro* and *in vivo*, with high effectiveness on liver cancer and breast cancer cell lines, promyelocytic leukaemia cells and colon cancer cells [37–39], but nominally no toxicity on normal cells [39]. Apoptosis is the mechanism of action suggested for this molecule to exert immunosuppression [19,24]. However, PG rapidly and potently triggers apoptosis in haematopoietic cancer cell lines, including acute T-cell leukaemia, promyelocytic leukaemia, myeloma and Burkitt lymphoma cells [29]. PG also induces apoptosis in cells derived from other human cancers, including gastric [31] and colon [30], with no marked toxicity in non-malignant cell lines [29,31]. It also induces apoptosis of B and T cells in B-cell chronic lymphocytic leukaemia (B-CLL) samples [33].

Understanding the mechanism of action of PGs is essential for drug development and will require the identification and characterisation of their still unidentified cell target. Four possible mechanisms of action for these molecules have been suggested: (i) PGs as pH modulators; (ii) PGs as cell cycle inhibitors; (iii) PGs as DNA cleavage agents; (iv) PGs as mitogen-activated protein kinase (MAPK) regulators.

2.1. PGs as pH modulators

The pH within acidic organelles could be responsible for a wide variety of important cell functions, such as endocytosis, exocytosis and intracellular trafficking, as well as cell differentiation, cell growth and cell death [41]. It has been argued that the apoptotic process is modulated or triggered by changes in intracellular pH (pH_i) [42,43]. A very early event in mitochondria-dependent apoptosis involves a change in cellular pH regulation that is characterised by mitochondrial alkalinization and concomitant cytosol acidification [44]. Alteration of pH regulation precedes cytochrome *c* release from mitochondria and facilitates cytochrome *c* activation of caspases [44]. F-ATPase and V-ATPase inhibitors prevent changes in cytosolic pH and impair caspase activation and thus apoptosis [44]. Part of the action of PGs depends on their ability to uncouple vacuolar H^+-ATPase (V-ATPase) through promotion of the H^+/Cl^- symporter and to induce neutralisation of the acid compartment of cells, so bringing about intracellular acidification and eventually apoptosis (Fig. 2, Route 2) [37,38,40,45].

cPrG·HCl is a protonophore that raises lysosomal pH by inhibiting the proton pump activity of V-ATPase without affecting its ATPase activity [16]. Moreover, in the inhibition of vacuolar acidification by cPrG·HCl, Cl^- is required to collapse the chemical gradient of H^+ across the tonoplast [46]. In human breast cancer cells, which overexpress V-ATPase and maintain a higher pH_i than non-cancerous cells, cPrG·HCl inhibits the acidification of lysosomes, decreases pH_i and causes apoptosis. This suggests that high pH_i is necessary for the maintenance of the function of cancer cells, which are more sensitive to pH changes than normal cells [37]. Other studies in human promyelocytic leukaemia cells (HL-60) and in colon cancer cell lines support this hypothesis [38,39].

PG, metacycloprodigiosin and UP display H^+/Cl^- symport activity on liposomal membranes and uncouple both V- and F-ATPases, although they do not inhibit catalysis or membrane potential formation [45,47]. Additionally, UP induces functional and morphological changes in the Golgi apparatus and swelling of mitochondria [48].

Fürstner *et al.* reported that three pyrrole units are required for PGs to inhibit vacuolar acidification. They used two PG derivatives that essentially affect only one of these two biological responses: the proliferation of murine spleen cells or activity inhibiting vacuolar acidification. Thus, the action of PGs to inhibit proliferation is caused by mechanisms other than the inhibition of vacuolar acidification [26].

It would be useful to explore whether the drugs that modulate pH in cells through their effects on specific

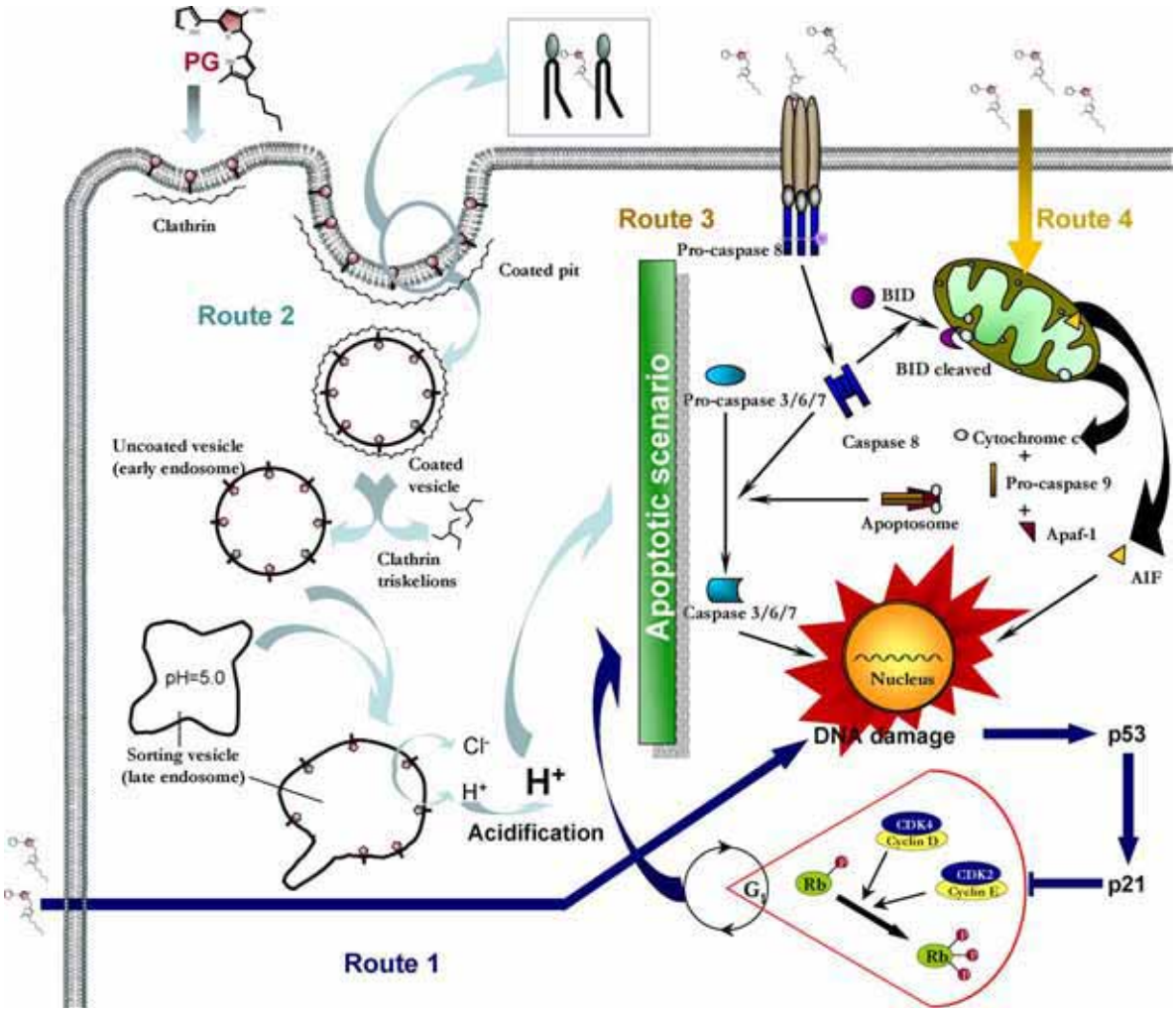

Fig. 2. Scheme for the numerous actions of PG by different pathways. PG could act by simple mechanisms related to its chemical or physical properties. PGs are hydrophobic molecules, very unstable in water solutions, and might diffuse freely through membranes and interact with the DNA with a preference for AT sites from the minor-groove [55] promoting dsDNA cleavage event [59,60]. Cells respond to DNA damage by activating cell cycle arrest [18,22,28,32], DNA repair, and in some circumstances, the triggering of apoptosis (Route 1). PG might be incorporated into the lipids bilayer of the plasmatic membrane, where by endocytosis it reaches the endosome compartment, uncouples vacuolar H^+-ATPase (V-ATPase) through promotion of the H^+/Cl^- symporter, and induces neutralisation of the acid compartment of cells, inducing intracellular acidification and eventually apoptosis (Route 2) [37,38,40,45]. Apoptosis by PG might occur through the activation of an unidentified PG receptor or by the activation of a known death receptor, inducing caspase 8 activation and consequently, apoptosis (Route 3). Finally, PG might diffuse freely through membranes and interact with the mitochondrial outer membrane, uncoupling F_o-F_1-ATPase and therefore, inducing apoptosis (Route 4) [47,48]. In conclusion, the pathway followed by PGs would depend very much on the cell type studied, the drug concentration inside the cell, the hierarchy of the PG targets and the interaction of distinct pathways mentioned above.

membrane transporters could be employed for therapeutic purposes in the modulation of apoptosis pathways *in vivo*.

2.2. PGs as cell cycle inhibitors

Cell cycle-related proteins and cytoplasmic pH homeostasis are connected [49]. In fact, PGs induce cell cycle arrest, although differences exist in the process induced by them, suggesting different mechanisms of action.

UP and PNU156804 induce growth arrest in late G_1 in T and B lymphocytes but not in human Jurkat T [18,22,28]. However, PG inhibits the proliferation of human Jurkat T cells mainly *via* G_1–S transition arrest (Fig. 2, Route 1) [32]. These three molecules abolish the expression of the cyclin-dependent kinase inhibitor p27, suggesting that p27, in their presence, coordinates the final outcome of proliferation or death of the cell [18,22,32]. Furthermore, UP and PNU156804 require the stimulation of Jak3, whereas cPrG·HCl or PG do not need previous stimulation to induce cell cycle arrest in transformed cell lines [18,22,27,28,32,37,44]. cPrG·HCl inhibits proliferation and induces apoptosis in liver carcinoma cell lines [40] and in human breast cancer cell lines [37], and induces differentiation in the human promyelocytic leukaemia cell line HL-60 [38].

Genetic alterations of the p53 tumour suppressor gene are frequently associated with human cancers [50] and give a consistently poor prognosis [51]. The absence of p53 or

aberrant p53 implies that apoptosis does not occur even when the cell suffers genetic damage [52]. PG-induced apoptosis is p53-independent [29], which may represent an advantage over other chemotherapeutic drugs [52,53].

Comparison of the cytotoxic properties of PG (2-methyl-3-pentyl-6-methoxyprodigiosene), prodigiosene and 2-methyl-3-pentylprodigiosene revealed the exceptional cytotoxic potency of PG, which may be attributed to the presence of the PG C-6 methoxy substituent (Fig. 1) [9,29]. Also, differences in the chemical structures of the A-pyrrole rings between PG and UP (2-undecyl-6-methoxyprodigiosene) are key in cytotoxic potency [54]. D'Alessio and co-workers found that the replacement of methoxy by a larger alkoxy steadily reduces activity, which is counterbalanced by a more marked decrease in cytotoxicity, thus favouring selectivity. The best compound with these characteristics obtained by D'Alessio and co-workers was PNU156804, which had a therapeutic index almost 3 times higher than UP [34–36].

2.3. PGs as DNA cleavage agents

DNA-binding molecules regulate mechanisms central to cellular function, including DNA replication and gene expression. The planar PG nucleus binds DNA by intercalation, while the methoxy group and ring nitrogens provide hydrogen-bonding sites to facilitate DNA binding. The cationic nature of PGs at neutral pH also provides electrostatic interaction with the negatively phosphate groups of the DNA helix. PG is a DNA interacting agent, with a preference for AT sites from the minor-groove [55]. In addition, PG facilitates copper-promoted oxidative double strand (ds) DNA cleavage through reductive activation of Cu(II), by oxidation of the electron-rich PG molecule [55,56]. Copper is an essential trace element distributed in all cellular organelles, including nucleus [56,57]. Copper levels are usually high in cancer [58]. In dry non-cancerous breast tissue, the mean concentration of copper is 1.47 ppm, whereas the mean concentration increases to 5.12 ppm in cancerous tissue. Melvin *et al*. predicted that the amount of damage under these conditions would be significant and should be lethal to the cells. They also suggested a correlation between nuclease activity and the cytotoxicity of PG [59].

The A-pyrrole ring of PGs influences the redox properties of pyrromethene. The bipyrrole moiety promotes ssDNA cleavage, while the intact pyrrolylpyrromethene chromophore of PGs is required for the more lethal copper-promoted dsDNA cleavage event [59,60].

Cells respond to DNA damage by activating a complex DNA-damage response pathway that includes cell cycle arrest, DNA repair and, under some circumstances, the triggering of apoptosis (Fig. 2, Route 1) [61,62]. Because PGs bind to DNA, they are capable of disrupting its replication and inducing apoptosis, as we related above, and hence are prospective anticancer drugs.

2.4. PGs as MAPK regulators

Various effects of PGs on MAPK signalling cascades have been described. These cascades include the ERKs, normally associated with proliferation and growth factors, and stress-activated protein kinase (SAPK)/c-*jun* N-terminal kinase (JNK) and p38-MAPK, induced by stress responses and cytokines and a mediator of differentiation and cell death [63].

Protein kinase C (PKC) is involved in many cellular functions, including cell proliferation and differentiation. PKC also participates in the regulation of apoptosis induced by several distinct stimuli, such as TNFα, ionising irradiation and antitumour drugs [64–66]. The activation of PKC by the phorbol ester PMA, which prevents intracellular acidification through PKC-induced activation of the Na^+/H^+ antiport [67], conferred protection against apoptosis induced by PG through an ERK-dependent pathway (Fig. 2, Route 2) [68], whereas the percentage of dead cells increased with cPrG·HCl [19]. The differences in the chemical structures of PG and cPrG·HCl may explain this difference. Moreover, imidazole, a permeable base, prevented intracellular acidification and suppressed cPrG·HCl-induced apoptosis [37].

PGs also activate either or both of the p38-MAPK and SAPK/JNK pathways, so inducing apoptosis. Whereas PG induced phosphorylation of p38 but not of JNK-MAPK [69], cPrG·HCl activated SAPK/JNK to promote apoptosis [38], which suggests that structural or methodological differences account for these discrepancies.

3. Conclusions

The cytotoxic properties of PGs, tripyrrole red pigments, have been recognised for some times. In 1977, Fullan *et al*. observed the antitumour activity of PG in mice [70]. Since then, the results presented above for different cell lines and xenografted nude mice have demonstrated that PG group natural products are promising antineoplastic agents.

Some cancer chemotherapy agents act primarily by causing apoptotic cell death in susceptible cancer cells. Each chemotherapeutic agent interacts with a specific target, causing dysfunction and injury, which is then interpreted by susceptible cancer cells as an instruction to undergo apoptosis [71]. New therapies seek to identify drugs more selectively so as to target more effectively cancer but not normal cells. The identification of novel targets and the development of drugs with greater selectivity towards cancer cells represent the primary goals of cancer therapy research. The *in vitro* 60 human tumour cell panel of the National Cancer Institute Drug Discovery Program (NCI, Bethesda, MD) provides an interesting tool that is available on Internet at www.dtp.nci.nih.gov with the NSC Number: 47147-F. PG has been screened with an average IC_{50} of 2.1 μM.

PGs, therefore, are a new group of molecules with a common mechanism of action to select molecular targets. Although PGs' apoptotic mechanisms are still to be fully determined (additional *in vivo* assays are necessary), current results reported in this review suggest that PGs are a new class of anticancer drugs which hold out considerable promise for the Pharmacological Industry.

Acknowledgments

This study was supported by the Grant SAF2001-3545 from the Ministerio de Ciencia y Tecnología and the Unión Europea and by a grant from the Marató de TV3 (Ref. # 001510). The authors thank Robin Rycroft for linguistic assistance.

References

[1] Bennett JW, Bentley R. Seeing red: the story of prodigiosin. Adv Appl Microbiol 2000;47:1–32.
[2] Rook G. Tumours and Coley's toxins. Nature 1992;357:545.
[3] Carswell EA, Old LJ, Kassel RL, Green S, Fiore N, Williamson B. An endotoxin-induced serum factor that causes necrosis of tumors. Proc Natl Acad Sci USA 1975;72:3666–70.
[4] Pennica D, Nedwin GE, Hayflick JS, Seeburg PH, Derynck R, Palladino MA, Kohr WJ, Aggarwal BB, Goeddel DV. Human tumour necrosis factor: precursor structure, expression and homology to lymphotoxin. Nature 1984;312:724–9.
[5] Wrede F, Rothhass A. Uber das prodigiosin, den roten farbstoff des *Bacillus prodigiosus.* Hoppe Seyler's Z Chem Ber 1934;226:95.
[6] Burger SR, Bennett JW. Droplet enrichment factors of pigmented and nonpigmented *Serratia marcescens*: possible selective function for prodigiosin. Appl Environ Microbiol 1985;50:487–90.
[7] Matsuyama T, Murakami T, Fujita M, Fujita S, Yano I. Extracellular vesicle formation and biosurfactant production by *Serratia marcescens*. J Gen Microbiol 1986;132:865–75.
[8] Castro AJ. Antimalarial activity of prodigiosin. Nature 1967;13:903–4.
[9] Boger DL, Patel M. Total synthesis of prodigiosin, prodigiosene, and desmethoxyprodigiosin: Diels–Alder reactions of heterocyclic azadienes and development of an effective palladium(II)-promoted 2,2′-bipyrrole coupling procedure. J Org Chem 1988;53:1405–15.
[10] Kim HS, Hayashi M, Shibata Y, Wataya Y, Mitamura T, Horii T, Kawauchi K, Hirata H, Tsuboi S, Moriyama Y. Cycloprodigiosin hydrochloride obtained from *Pseudoalteromonas denitrificans* is a potent antimalarial agent. Biol Pharm Bull 1999;22:532–4.
[11] Melo PS, Durán N, Haun M. Cytotoxicity of prodigiosin and benznidazole on V79 cells. Toxicol Lett 2000;116:237–42.
[12] Nakamura A, Nagai K, Ando K, Tamura G. Selective suppression by prodigiosin of the mitogenic response of murine splenocytes. J Antibiot 1986;8:1155–9.
[13] Nakamura A, Magae J, Tsuji RF, Yamasaki M, Nagai K. Suppression of cytotoxic T cell induction *in vivo* by prodigiosin 25-C. Transplantation 1989;47:1013–6.
[14] Tsuji RF, Yamamoto M, Nakamura A, Kataoka T, Magae J, Nagai K, Yamasaki M. Selective immunosuppression of prodigiosin 25-C and FK506 in the murine immune system. J Antibiot 1990;43:1293–301.
[15] Tsuji RF, Magae J, Jamashita M, Nagai K, Yamasaki M. Immunomodulating properties of prodigiosin 25-C, an antibiotic which preferentially suppresses induction of cytotoxic T cells. J Antibiot 1992;45:1295–302.
[16] Lee M, Kataoka T, Magae J, Nagai K. Prodigiosin 25-C suppression of cytotoxic T cells *in vitro* and *in vivo* is similar to that of concanamycin B, a specific inhibitor of vacuolar type H^+-ATPase. Biosci Biotechnol Biochem 1995;59:1417–21.
[17] Magae J, Miller MW, Nagai K, Shearer GM. Effect of metacycloprodigiosin, an inhibitor of killer T cells on murine skin and heart transplants. J Antibiot 1996;49:86–90.
[18] Songia S, Mortellaro A, Taverna S, Fornasiero C, Scheiber EA, Erba E, Colotta F, Mantovani A, Isetta AM, Golay J. Characterization of the new immunosuppressive drug undecylprodigiosin in human lymphocytes. J Immunol 1997;158:3987–95.
[19] Kawauchi K, Shibutani K, Yagisawa H, Kamata H, Nakatsuji S, Anzai H, Yokoyama Y, Ikegami Y, Moriyama Y, Hirata H. A possible immunosuppressant, cycloprodigiosin hydrochloride, obtained from *Pseudoalteromonas denitrificans*. Biochem Biophys Res Commun 1997;237:543–7.
[20] Han SB, Kim HM, Kim YH, Lee CW, Jang ES, Son KH, Kim SU, Kim YK. T-cell specific immunosuppression by prodigiosin isolated from *Serratia marcescens*. Int J Immunopharmacol 1998;20:1–13.
[21] Lee MH, Yamashita M, Tsuji RF, Yamasaki M, Kataoka T, Magae J, Nagai K. Suppression of T cell stimulating function of allogeneic antigen presenting cells by prodigiosin 25-C. J Antibiot 1998;51:92–4.
[22] Mortellaro A, Songia S, Gnocchi P, Ferrari M, Fornasiero C, D'Alessio R, Isetta A, Colotta F, Golay J. New immunosuppressive drug PNU156804 blocks IL-2-dependent proliferation and NF-kappa B and AP-1 activation. J Immunol 1999;162:7102–9.
[23] Lee MH, Kataika T, Honjo N, Magae J, Nagai K. *In vivo* rapid reduction of alloantigen-activated $CD8^+$ mature cytotoxic T cells by inhibitors of acidification of intracellular organelles. Immunology 2000;99:243–8.
[24] Azuma T, Watanabe N, Yagisawa H, Hirata H, Iwamura M, Kobayashi Y. Induction of apoptosis of activated murine splenic T cells by cycloprodigiosin hydrochloride, a novel immunosuppressant. Immunopharmacology 2000;46:29–37.
[25] Nakai K, Hamada Y, Kato Y, Yamamoto D, Hirata H, Hioki K. Cycloprodigiosin hydrochloride as an immunosuppressant in rat small bowel transplantation. Transplant Proc 2000;32:1324–5.
[26] Fürstner A, Grabowski J, Lehmann CW, Kataola T, Nagai K. Synthesis and biological evaluation of nonylprodigiosin and macrocyclic prodigiosin analogues. Chem Biochem 2001;2:60–8.
[27] Han SB, Park SH, Jeon YJ, Kim YK, Kim HM, Yang KH. Prodigiosin blocks T cell activation by inhibiting interleukin-2Rα expression and delays progression of autoimmune diabetes and collagen-induced arthritis. J Pharm Exp Ther 2001;299:415–25.
[28] Stepkowski SM, Erwin-Cohen RA, Behbod F, Wang ME, Qu X, Tejpal N, Nagy ZS, Kahan BD, Kirken RA. Selective inhibitor of janus tyrosine kinase 3 PNU156804 prolongs allograft survival and acts synergistically with cyclosporine but additively with rapamycin. Blood 2002;99:680–9.
[29] Montaner B, Navarro S, Piqué M, Vilaseca M, Martinell M, Giralt E, Gil J, Pérez-Tomás R. Prodigiosin from the supernatant of *Serratia marcescens* induces apoptosis in haematopoietic cancer cell lines. Br J Pharmacol 2000;131:585–93.
[30] Montaner B, Pérez-Tomás R. Prodigiosin-induced apoptosis in human colon cancer cells. Life Sci 2001;68:2025–36.
[31] Díaz-Ruíz C, Montaner B, Pérez-Tomás R. Prodigiosin induces cell death and morphological changes indicative of apoptosis in gastric cancer cell line HGT-1. Histol Histopathol 2001;16:415–21.
[32] Pérez-Tomás R, Montaner B. Effects of the proapoptotic drug prodigiosin on cell cycle-related proteins in Jurkat T cells. Histol Histopathol 2003;18:379–85.
[33] Campàs C, Dalmau M, Montaner B, Barragán M, Bellosillo B, Colomer D, Pons G, Pérez-Tomás R, Gil J. Prodigiosin induces apoptosis of B and T cells from B-cell chronic lymphocytic leukaemia. Leukemia 2003;17:746–50.

[34] D'Alessio R, Rossi A. Short synthesis of undecylprodigiosine. A new route to 2,2′-bipyrrolyl-pyrromethene systems. Synlett 1996;6:513–4.
[35] D'Alessio R, Bargiotti A, Carlini O, Colotta F, Ferrari M, Gnocchi P, Isetta A, Mongelli N, Motta P, Rossi A, Rossi M, Tibolla M, Vanotti E. Synthesis and immunosuppressive activity of novel prodigiosin derivatives. J Med Chem 2000;43:2557–65.
[36] Cameron R, Feuer G. Molecular cellular and tissue reactions of apoptosis and their modulation by drugs. In: Cameron R, Feuer G, editors. Handbook of experimental pharmacology. Berlin: Springer-Verlag; 2000. p. 37–57.
[37] Yamamoto D, Kiyozuka Y, Uemura Y, Yamamoto C, Takemoto H, Hirata H, Tanaka K, Hioki K, Tsubura A. Cycloprodigiosin hydrochloride, a H^+/Cl^- symporter, induces apoptosis in human breast cancer cell lines. J Cancer Res Clin Oncol 2000;126:191–7.
[38] Yamamoto D, Uemura Y, Tanaka K, Nakai K, Yamamoto C, Takemoto H, Kamata K, Hirata H, Hioki K. Cycloprodigiosin hydrochloride H^+/Cl^- symporter induces apoptosis and differentiation in HL-60 cells. Int J Cancer 2000;88:121–8.
[39] Yamamoto C, Takemoto H, Kuno K, Yamamoto D, Nakai K, Baden T, Kamata K, Hirata H, Watanabe T, Inoue K. Cycloprodigiosin hydrochloride, a H^+/Cl^- symporter, induces apoptosis in human colon cancer cell lines in vitro. Oncol Rep 2001;8:821–4.
[40] Yamamoto C, Takemoto H, Kuno K, Yamamoto D, Tsubura A, Kamata K, Hirata H, Yamamoto A, Kano H, Seki T, Inoue K. Cycloprodigiosin hydrochloride, a new H^+/Cl^- symporter, induces apoptosis in human and rat hepatocellular cancer cell lines *in vitro* and inhibits the growth of hepatocellular carcinoma xenografts in nude mice. Hepatology 1999;30:894–902.
[41] Ohkuma S, Sato T, Okamoto M, Matsuya H, Arai K, Kataoka T, Nagai K, Wasserman HH. Prodigiosins uncouple lysosomal vacuolar-type ATPase through promotion of H^+/Cl^- symport. Biochem J 1998;334: 731–41.
[42] Arends MJ, Wyllie AH. Apoptosis: mechanisms and roles in pathology. Int Rev Esp Pathol 1991;32:223–56.
[43] Thangaraju M, Sharma K, Liu D, Shen SH, Srikant CB. Interdependent regulation of intracellular acidification and SHP-1 in apoptosis. Cancer Res 1999;59:1649–54.
[44] Matsuyama S, Llopis J, Deveraux QL, Tsien RY, Reed JC. Changes in intramitochondrial and cytosolic pH: early events that modulate caspase activation during apoptosis. Nat Cell Biol 2000;2:318–25.
[45] Sato T, Konno H, Tanaka Y, Kataoka T, Nagai K, Wasserman HH, Ohkuma S. Prodigiosins as a new group of H^+/Cl^- symporters that uncouple proton translocators. J Biol Chem 1998;273:21455–62.
[46] Nakayasu T, Kawauchi K, Hirata H, Shimmen T. Demonstration of Cl^- requirement for inhibition of vacuolar acidification by cycloprodigiosin in situ. Plant Cell Physiol 2000;41:857–63.
[47] Konno H, Matsuya H, Okamoto M, Sato T, Tanaka Y, Yokoyama K, Kataoka T, Nagai K, Wasserman HH, Ohkuma S. Prodigiosins uncouple mitochondrial and bacterial F-ATPases: evidence for their H^+/Cl^- symport activity. J Biochem 1998;124:547–56.
[48] Kataoka T, Muroi M, Ohkuma S, Waritani T, Magae J, Takatsuki A, Kondo S, Yamasaki M, Nagai K. Prodigiosin 25-C uncouples vacuolar type H^+-ATPase, inhibits vacuolar acidification and effects glycoprotein processing. FEBS Lett 1995;359:53–9.
[49] Shrode LD, Tapper H, Grinstein S. Role of intracellular pH in proliferation transformation and apoptosis. J Bioenerg Biomembr 1997;29:393–9.
[50] Hussain SP, Harris CC. Molecular epidemiology of human cancer: contribution of mutation spectra studies for tumor suppressor genes. Cancer Res 1998;58:4023–37.
[51] Kirsch DG, Kastan MB. Tumor suppressor p53: implications for tumor development and prognosis. J Clin Oncol 1998;16:3158–68.
[52] Brown JM, Wouters BG. Apoptosis p53 and tumor cell sensitivity to anticancer agents. Cancer Res 1999;59:1391–9.
[53] Bunz F, Hwang PM, Torrance C, Waldman T, Zhang Y, Dillehay L, Williams J, Lengauer C, Kinzler KW, Vogelstein B. Disruption of p53 in human cancer cells alters the responses to therapeutic agents. J Clin Invest 1999;104:263–9.
[54] Melvin MS, Tomlinson JT, Saluta GR, Kucera GL, Lindquist N, Manderville RA. Double-strand DNA cleavage by copper·prodigiosin. J Am Chem Soc 2000;122:6333–4.
[55] Melvin MS, Ferguson DC, Lindquist N, Manderville RA. DNA binding by 4-methoxypurrolic natural products. Preference for intercalation at AT sites by tambjamine E and prodigiosin. J Org Chem 1999;64:6861–9.
[56] Linder MC. Biochemistry of copper. In: Frieden E, editor. New York: Plenum Press; 1991.
[57] Sarkar B. Copper transport and its defect in Wilson disease: characterization of the copper-binding domain of Wilson disease ATPase. J Inorg Biochem 2000;79:187–91.
[58] Theophanides T, Anastassopoulou J. Copper and carcinogenesis. Crit Rev Oncol Hematol 2002;42:57–64.
[59] Melvin MS, Wooton KE, Rich CC, Saluta GR, Kucera GL, Lindquist N, Manderville RA. Copper-nuclease efficiency correlates with cytotoxicity for the 4-methoxypyrrolic natural products. J Inorg Biochem 2001;87:129–35.
[60] Melvin MS, Calcutt MW, Noftle RE, Manderville RA. Influence of the a-ring on the redox and nuclease properties of the prodigiosins: importance of the bipyrrole moiety in oxidative DNA cleavage. Chem Res Toxicol 2002;15:742–8.
[61] Fürstner A, Grabowski EJ. Studies on DNA cleavage by cytotoxic pyrrole alkaloids reveal the distinctly different behavior of roseophilin and prodigiosin derivatives. Chem Biochem 2001;9:706–9.
[62] Khanna KK, Jackson SP. DNA double-strand breaks: signaling. Nat Genet 2001;27:247–54.
[63] Cano E, Mahadevan LC. Parallel signal processing among mammalian MAPKs. Trends Biochem Sci 1995;20:117–22.
[64] Mansat V, Laurent G, Levade T, Bettaieb A, Jaffrezou JP. The protein kinase C activators phorbol esters and phosphatidylserine inhibit neutral sphingomyelinase activation, ceramide generation and apoptosis triggered by daunorubicin. Cancer Res 1997;57:5300–4.
[65] Woo KR, Shu WP, Kong L, Liu BC. Tumor necrosis factor mediates apoptosis via Ca^{2+}/Mg^{2+} dependent endonuclease with protein kinase C as a possible mechanism for cytokine resistance in human renal carcinoma cells. J Urol 1996;155:1779–83.
[66] Tomei LD, Kanter P, Wenner CE. Inhibition of radiation-induced apoptosis *in vitro* by tumor promoters. Biochem Biophys Res Commun 1988;155:324–31.
[67] Zanke BW, Lee C, Arab S, Tannock IF. Death of tumor cells after intracellular acidification is dependent on stress-activated protein kinases (SAPK/JNK) pathway activation and cannot be inhibited by bcl-2 expression or interleukin 1B-converting enzyme inhibition. Cancer Res 1998;58:2801–8.
[68] Montaner B, Pérez-Tomás R. Activation of protein kinase C is required for protection of cells against apoptosis induced by the immunossuppresor prodigiosin. Biochem Pharmacol 2002;63:463–9.
[69] Montaner B, Pérez-Tomás R. The cytotoxic prodigiosin induces phosphorylation of p38-MAPK but not of SAPK/JNK. Toxicol Lett 2002;129:93–8.
[70] Fullan NP, Lynch DL, Ostrow DH. Effects of bacterial extracts on Chinese hamster cells and rat neoplasms. Microbiol Lett 1977;5: 157–61.
[71] Hannun YA. Apoptosis and the dilemma of cancer chemotherapy. Blood 1997;89:1845–53.